
Functional *in vivo* characterization of Neprilysin
as a central regulator of insulin signaling and
muscle contraction in *Drosophila melanogaster*

Dissertation

zur Erlangung des akademischen Grades
Doktor der Naturwissenschaften
(Dr. rer. nat.)

vorgelegt am
Fachbereich Biologie/Chemie
der Universität Osnabrück

von
Ronja Thea Schiemann

Osnabrück, April 2022

Abstract

Peptides play pivotal roles in the regulation of various physiological processes. As neuropeptides or peptide hormones, they can bind to a range of receptors and thereby trigger the activation of different pathways, including insulin signaling. Another central functionality is facilitated by the action of the as regulins summarized transmembrane micropeptides. By binding to the sarco/endoplasmic reticulum Ca^{2+} ATPase (SERCA), the regulins control Ca^{2+} homeostasis and muscle contraction. With the ongoing identification of novel modulatory micropeptides encoded by small open reading frames, the urgency to understand peptide-dependent regulatory networks rises. In this regard, especially impact and physiological relevance exerted by the enzymatic inactivation of the mature, biologically active peptides are far from completely understood.

Neprilysins are metalloendopeptidases expressed throughout the animal kingdom. Based on their broad substrate specificity, the activity of neprilysins is crucial for the modulation of multiple peptide-dependent processes. This work aimed to identify new peptide substrates of the *Drosophila melanogaster* Neprilysin 4 (Nep4) and investigate the enzyme's physiological impact on the affected regulatory mechanisms.

The first part of the work could identify 16 novel Nep4 peptide substrates that play essential roles in insulin signaling and the regulation of food intake: allatostatin A1-A4, adipokinetic hormone, corazonin, diuretic hormone 31, drosulfakinin 1 and 2, leucokinin, two short neuropeptide F peptides, and tachykinin 1-4. Thereby, aberrant expression of Nep4 leads to severe phenotypes linked to misregulation of insulin signaling, including reduced body size and weight, compromised food intake, and a characteristic shift in metabolomic composition.

To further investigate and understand the complex functionality of the newly discovered Nep4 substrates, these peptides were tested for their ability to modulate the *Drosophila* heartbeat. A combined *in vitro* *in vivo* screen revealed that the tested substrates exert chronotropic as well as inotropic effects, rendering the peptides as essential novel modulators of the heartbeat in *Drosophila*.

The main project of this thesis was based on the initial finding that animals with Nep4 overexpression exhibit severe impairments of body wall muscle and heart functionality. By applying various experiments, including analyses of muscle and heart contraction, measurement of Ca^{2+} transients, pull-down studies, STED super-resolution microscopy, and mass spectrometry, Neprilysin 4 was identified as a novel modulator of SERCA activity. The molecular underpinning of this regulatory mechanism is the Nep4 mediated

cleavage and inactivation of *Drosophila* SERCA-inhibitory Sarcolamban micropeptides SCLA and SCLB. Strikingly, cleavage experiments using the mammalian neprilysin and apparent colocalization of Neprilysin and SERCA in human heart tissue indicate evolutionary conservation of this mechanism.

In summary, this work could identify a range of so far unknown Nep4 substrates and thereby point out the critical roles these class of enzymes plays in insulin signaling as well as the physiology of muscle and heart contraction.

Table of Contents

Abstract	I
1 Introduction	5
1.1 Peptide signaling networks and their regulation via neprilysins	5
1.1.1 Peptides are critical to insulin signaling in <i>Drosophila melanogaster</i>	8
1.1.2 Neprilysins control diverse processes via cleavage of different peptide substrates	11
1.1.3 <i>Drosophila</i> Neprilysin 4 exhibits dual subcellular localization in muscles	13
1.2 Physiology of muscle contraction and role of regulatory micropeptides	15
1.2.1 The muscle tissue of <i>Drosophila</i>	17
1.2.2 Tightly controlled Ca ²⁺ transients are essential for proper muscle functionality	20
1.2.3 The sarcoplasmic reticulum and SERCA are important for muscle relaxation	27
1.2.4 Activity of SERCA is modulated by binding of regulin peptides	37
1.3 Aim of the thesis	48
2 Results	49
2.1 <i>Drosophila</i> neprilysins control insulin signaling and food intake via cleavage of regulatory peptides	51
2.2 Identification and in vivo characterization of cardioactive peptides in <i>Drosophila melanogaster</i>	73
2.3 Neprilysin 4	88
2.4 Neprilysins regulate muscle contraction and heart function via cleavage of SERCA inhibitory micropeptides	94
3 Discussion	146
3.1 Activity of Nep4 is critical to peptide homeostasis in insulin signaling	147
3.2 Identification of peptides with cardiomodulatory function	152
3.3 Neprilysins control heart and muscle contraction via the inactivation of SERCA-inhibitory micropeptides	154
4 References	163
5 Appendix	CCVI
5.1 Abbreviations	CCVI
5.2 Proteinogenic amino acids and SI units	CCIX

5.3 Index of Figures and tables	CCX
5.4 Publications	CCXI
5.5 Overview of work contributions	CCXII
5.6 Fellowships and awards	CCXIV
6 DVD index	CCXV
7 Curriculum vitae	CCXVI
8 Erklärung über die Eigenständigkeit der erbrachten wissenschaftlichen Leistung	CCXVII
9 Erklärung über frühere etwaige Promotionsversuche	CCXIX
10 Danksagung	CCXX

1 Introduction

1.1 Peptide signaling networks and their regulation via neprilysins

Peptides are critical regulators of many different physiological processes in animals and plants. They are defined as polypeptide chains with a maximal length of 50 amino acids. As a further subdivision, a peptide with less than 20 amino acids is called oligopeptide. There are different possibilities to classify the biologically active peptides. Ribosomal peptides are assembled by ribosomes during translation, whereas nonribosomal peptides are generated by enzymes and are predominately found in fungi, plants, and unicellular organisms. Based on their origin and way of action, ribosomal peptides can be further distinguished in, e.g., neuropeptides, peptide hormones, lipopeptides, antimicrobial, and regulatory transmembrane peptides.

Neuropeptides are produced and released by neurons and act as first messenger at many different sites of the animal or human body (see also section 1.1.1; reviewed by Nässel and Winther, 2010; Schoofs et al., 2017; Nässel and Zandawala, 2019). In contrast to neuropeptides, peptide hormones are signaling molecules that are defined in the first place by their functionality and not by their transcriptional origin. Peptide hormones always act on the endocrine system but can be expressed by a range of endocrine tissues and cells, including neurons. Therefore, some peptides are simultaneously classified as neuropeptides and peptide hormones. Both neuropeptides and peptide hormones are usually generated by processing a so-called prepropeptide that represents a larger precursor encoded by a gene (Figure 1).

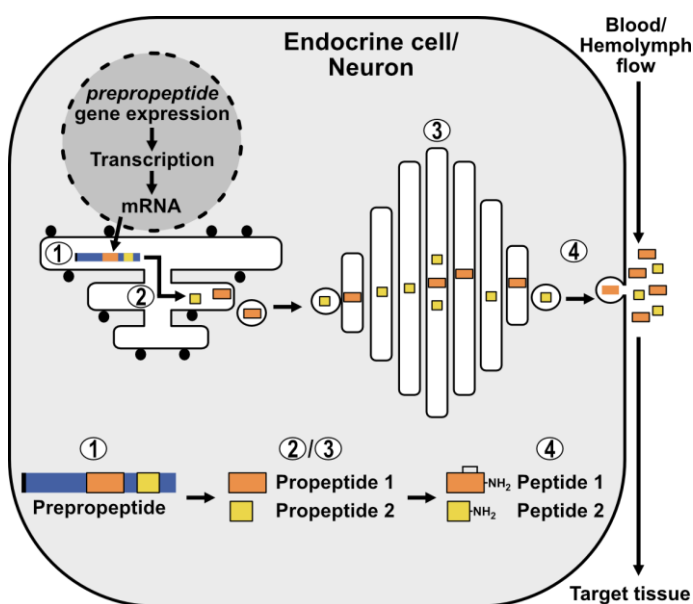


Figure 1 | Maturation and processing of neuropeptides and peptide hormones. (1) The translated prepropeptide harbors spacer regions, propeptides that later give rise to the mature peptides, and a signal sequence guiding the prepropeptide to the secretory pathway. (2)/(3) At the ER and Golgi, the prepropeptide is processed, including protease-mediated propeptide excision. (4) After the addition of posttranslational modifications like amidation of the C-terminus (-NH₂), the mature peptides are released into the extracellular space via secretory vesicles. The bioactive peptides are distributed in the organism via the blood or hemolymph (in insects) flow and finally reach their target tissue/cell, where they often act as first messenger to trigger intracellular signaling pathways.

After translation, the N-terminal signal peptide directs the prepropeptide to the secretory pathway. In the endoplasmic reticulum (ER), the signal sequence is cleaved, and the propeptides are later excised through dibasic or monobasic cleavage mediated by proteases. Finally, the propeptides are processed to mature peptides through the addition of post-translational modifications (PTMs). PTMs are, in many cases, crucial to peptide functionality and stability. For example, bridging of disulfides gives rise to a cyclic peptide, sulfation of tyrosine residues enhances interaction with proteins, and N-terminal or C-terminal blocking via the addition of a pyroglutamate respectively amidation provides stability against degradation. Finally, the mature neuropeptides are released into the extracellular space via secretory vesicles.

Neuropeptides and peptide hormones typically act as first messengers that initiate the release of an intracellular second messenger via activation of plasma membrane-located receptors at the surface of their target cell or tissue (Figure 2). The need to bind to a receptor distinguishes peptide hormones from steroid hormones which are lipid-soluble and can therefore directly pass the plasma membrane. In many cases, the peptide receptors are so-called G protein-coupled receptors (GPCRs, e.g., reviewed in Oldham and Hamm, 2008; Lefkowitz, 2013; Hilger et al., 2018). With nearly 800 representatives in humans and 200 in the fruit fly *Drosophila melanogaster*, the GPCRs constitute the largest superfamily of membrane receptors (Brody and Cravchik, 2000; Bjarnadottir et al., 2006; Hanlon and Andrew, 2015; Liu et al., 2021). Concomitantly with their abundance, GPCRs can trigger different intracellular signaling cascades. The first identified GPCR was the β -adrenergic receptor (Ahlquist, 1948) that is implicated in the regulation of phospholamban (PLN), a very different type of peptide involved in the regulation of heart contraction (see section 1.2.4).

In general, activation of GPCRs through binding of a ligand leads to the exchange of GDP (guanosine diphosphate) by GTP (guanosine triphosphate) at the interacting intracellular located heterotrimeric G protein (guanine nucleotide-binding protein; Figure 2). As a result, the G protein dissociates into the $G\alpha$ and $G\beta\gamma$ subunits, whereby both subunits are capable of regulating different downstream signaling pathways autonomously. Four different $G\alpha$ families with distinct effector targets have been identified so far: $G\alpha_i$, $G\alpha_q$, $G\alpha_s$, and $G\alpha_{12/13}$ (reviewed in Simon et al., 1991; Downes and Gautam, 1999). The α_i and α_s subunits interact with the membrane-bound adenylyl cyclase (AC), hence with different outcomes. The binding of α_s to AC results in ATP-dependent formation of the ubiquitous second messenger cAMP (cyclic adenosine monophosphate), whereas the interaction of α_i inhibits cAMP production. The $G\alpha_q$ subunit mediates activation of the membrane-bound phospholipase that triggers the production of the second messenger inositol-1,4,5-trisphosphate (Ins(1,4,5)P3) and diacylglycerol (DAG) and function of $\alpha_{12/13}$ is to activate RhoGTPases by binding to Rho guanine nucleotide exchange factor proteins (RhoGEFs; Figure 2). GPCR mediated signaling is terminated through hydrolysis of GTP, leading to the reassociation of the G protein subunits.

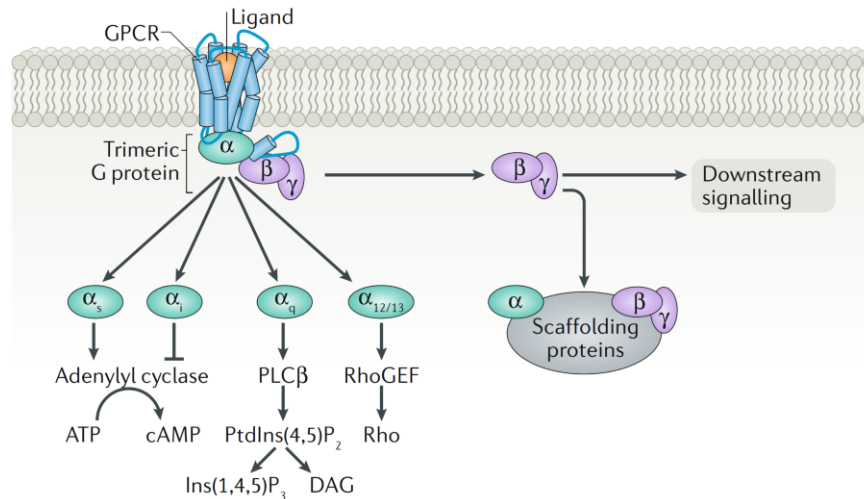


Figure 2 | GPCR-dependent activation of intracellular signaling pathways. The binding of a ligand, for example a neurotransmitter, pheromone, or peptide, induces a conformational change in the GPCR. The conformational change is transmitted to intracellularly bound trimeric G protein resulting in the replacement of the GDP with GTP at the $G\alpha$ subunit. Upon nucleotide exchange, the trimeric G protein dissociates into the $G\alpha$ subunit and $G\beta\gamma$ dimer. Depending on the respective $G\alpha$ family ($G\alpha_i$, $G\alpha_q$, $G\alpha_s$, or $G\alpha_{12/13}$), different downstream effectors are targeted by the dissociated $G\alpha$ subunit. While $G\alpha_i$ and $G\alpha_s$ act through the adenylyl cyclase to affect cAMP production, $G\alpha_q$ activates the membrane-bound phospholipase C β (PLC β). PLC β then hydrolyses the phospholipid phosphatidylinositol-4,5-bisphosphate (PtdIns(4,5)P₂), further leading to formation of Ins(1,4,5)P₃ and DAG. The $G\alpha_{12/13}$ subunit stimulates Rho GTPases (Rho) by binding to RhoGEFs. The $G\beta\gamma$ heterodimer triggers downstream signaling predominately through the interaction with scaffolding proteins. Modified after (Pfleger et al., 2019).

Besides the classical GPCR activation, several novel modes of GPCR mediated signal transduction not depending on G proteins have been identified by now (reviewed in Wang et al., 2018).

In recent years, another type of peptides besides neuropeptides and peptide hormones has gained more and more attention: transmembrane micropeptides regulating proteins localizing to the same membrane (reviewed by Makarewich and Olson, 2017; Makarewich, 2020). The relatively late discovery of many micropeptides is because several of these peptides are encoded by small open reading frames (smORFs/sORFs) of long, formerly “noncoding” annotated RNAs (Hartford and Lal, 2020; Kute et al., 2022). Identifying these peptides was and is therefore challenging and relies on advanced bioinformatic analyses as well as large-scale transcriptomics and proteomics. The most prominent examples are the newly identified members of the “regulin” family (Anderson et al., 2016; reviewed by Rathod et al., 2021). These transmembrane peptides modulate the activity of the Sarco/endoplasmic reticulum Ca²⁺ ATPase (SERCA) to regulate muscle contraction (see section 1.2.4.).

Despite all progress regarding identifying and characterizing the many ways in which peptides modulate different processes, one ‘blind spot’ often remains. Molecular mechanisms targeting the peptides turnover and stipulating how the active peptides themselves are regulated or their activity efficiently terminated, short-termed and in the long run, often remain unclear. Nevertheless, neprilysins represent one important class of enzymes facilitating this necessary functionality (see sections 1.1.2 and 1.1.3).

1.1.1 Peptides are critical to insulin signaling in *Drosophila melanogaster*

Insulin and insulin-like growth factor (IGF) signaling (IIS) is a highly orchestrated interplay of various pathways and effectors. Together, all these processes regulate, e.g., food intake, digestion, metabolism, and physiological homeostasis. In humans, misregulation of insulin signaling can be concomitant with the development of one of the most severe and prevailed diseases of the present age: Diabetes mellitus. Therefore, a mechanistic understanding of all factors implicated in this highly complex system is of extraordinary significance.

Drosophila melanogaster is a model system holding many similarities to vertebrate IIS (reviewed in e.g., Nässel et al., 2013; Rajan and Perrimon, 2013; Nässel et al., 2015; Okamoto and Yamanaka, 2015; Nässel and Vanden Broeck, 2016; Nässel and Zandawala, 2019; Chowanski et al., 2021). However, the open circulatory system of *Drosophila* constitutes one of the main differences in comparison to the vertebrate's closed and subdivided circulatory system concerning the distribution of factors regulating IIS. In flies, the hemolymph called blood-like body fluid is distributed through the pumping action of the heart tube and flows around the inner organs, thereby mediating the transport and exchange of nutrients and signaling factors (reviewed by Rotstein and Paululat, 2016; see also section 1.2.1, Figure 8). Instead of vertebrate insulin and insulin-like growth factor, flies express eight so-called *Drosophila* insulin-like peptides (DILPs) representing the central switches of IIS (Figure 3; Brogiolo et al., 2001; Vanden Broeck, 2001; Grönke et al., 2010; reviewed by Antonova et al., 2012). *dilp2*, 3, and 5 are expressed by IPCs (insulin-producing cells) called neurosecretory cells of the *Drosophila* brain (Brogiolo et al., 2001; Ikeya et al., 2002; Rulifson et al., 2002; Broughton et al., 2005). Regarding their DILP production and release functionality, IPCs are analogous to mammalian insulin-secreting pancreatic β cells. The IPCs are comprised of 14 cells organized as a pair of seven cells each, whereby the cell bodies localize to the pars intercerebralis called region of the central nervous system (CNS). In addition to the release of DILPs, the IPCs also produce and release drosulfakinins, peptides that induce satiety (Söderberg et al., 2012).

In contrast to the DILPs produced by the IPCs, *dilp6* is expressed by adipose cells of the fat body and exhibits structural as well as functional similarities to vertebrate IGF (Slaidina et al., 2009; Okamoto et al., 2009). By binding to IPCs, DILP6 was shown to repress the expression of other *dilps* (Bai et al., 2012). DILP7 is secreted by specific neurons with projections to different sites of the gut and the female reproductive system (Miguel-Aliaga et al., 2008; Yang et al., 2008), while larval imaginal discs produce DILP8 (Colombani 2012; Garelli et al., 2012). The function of DILP8 is to coordinate developmental timing with the growth status of tissues.

In general, IIS can be divided in two parts with the DILPs representing the switch-point (Figure 3; reviewed by e.g., Owusu-Ansah and Perrimon, 2014; Nässel et al., 2015; Nässel and Vanden Broeck, 2016; Nässel and Zandawala, 2019). Upstream of *dilp*

expression, different factors integrate and transmit information like the nutrition state and energy storage to induce DILP production and release. Downstream of the IPCs, the released DILPs translate this information by activating different signaling pathways regulating, e.g., growth, metabolism, reproduction, and lifespan, but also stress resistance, cognitive functions, and behavior (Brogiolo et al., 2001; Clancy et al., 2001; Tatar et al., 2001; Giannakou et al., 2007; Tatar et al., 2014; Itskov and Ribeiro, 2013; Root et al., 2011; Luo et al., 2014; Pool and Scott, 2014; reviewed by Antonova et al., 2012; Nässel and Zandawala, 2019).

Based on their respective secretion site, the peptides and other IPC-binding factors can be distinguished in gut-, fat body-, or neuron-derived (Figure 3). Various neuropeptides and peptide hormones act on the IPCs of *Drosophila*, either directly via binding to their receptor expressed at the surface of the IPCs or indirectly through activation of receptors expressed by other neurons. For example, the gut-derived peptide diuretic hormone 31 (DH₃₁) triggers the release of short neuropeptide F (sNPF) and corazonin from distinct neurons. Upon release, sNPF and corazonin bind to their respective GPCRs at IPCs and thereby induce *dilp* expression (e.g., Johnson et al., 2005; Lee et al., 2008; Veenstra et al., 2008; Kapan et al., 2012). On the contrary, GPCR receptors of the neuropeptides allatostatin A (AstA; Lenz et al., 2001; Hentze et al., 2015), leucokinin (Zandawala et al., 2018; Yurgel et al., 2019), and *Drosophila* tachykinins (Birse et al., 2011) are expressed by IPCs, enabling these group of peptides to trigger *dilp* expression directly. Eventually, these peptides are also expressed by enteroendocrine cells (Yoon and Stay, 1995; Siviter et al., 2000; Veenstra et al., 2008). Additionally, the CCH2amides represent relatively novel peptide hormones with receptors at IPCs (Veenstra and Ida, 2014; Ren et al., 2015; Sano et al., 2015). In contrast to the previously mentioned neuropeptides, the CCH2amides are exclusively produced and released by the fat body and intestine.

Further known factors acting on IPCs are, for example, neurotransmitters, neuromodulators, hormones, glucose (Rulifson et al., 2002; Kreneisz et al., 2010; Park et al., 2014), as well as fat-body derived factors like leptin-like molecule unpaired-2 (Rajan and Perrimon, 2012), and the proteins stunted (Delanoue et al., 2016) and TNF Eiger (Agrawal et al., 2016). Moreover, fat body-derived adiponectin and DILP6 were shown to repress *dilp* expression at IPCs (Kwak et al., 2013; Slaidina et al., 2009; Okamoto et al., 2009). The glucose level in the hemolymph is also sensed by adipokinetic hormone (AKH) secreting cells (APCs; Kim and Rulifson, 2004). The APCs can be found in the corpora cardiaca (CC), a cluster of cells located in the ring gland of *Drosophila*. Upon glucose binding, AKH is secreted by the CC and binds to its receptor, a GPCR present at the surface of IPCs, to induce the expression of *dilp3* (Staubli et al., 2002; Kim and Rulifson, 2004; Kim and Neufeld, 2015). Therefore, the AKH producing CC cells are analogous to mammalian glucagon-secreting pancreatic islet α cells and AKH to mammalian glucagon (Schaffer, 1990; Noyes et al., 1995; Bednarova et al., 2013).

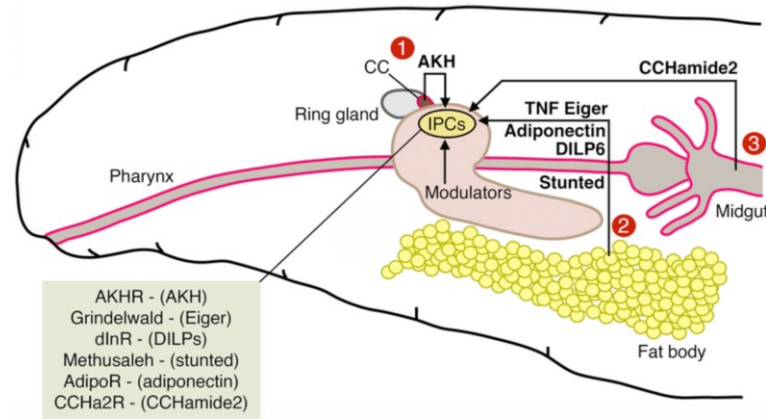


Figure 3 | Factors regulating *dilp* expression at the IPCs of *Drosophila* larvae. Cell bodies of the IPCs localize at the *Drosophila* brain hemispheres, while their axons project to several regions of the body. By binding to their respective receptors present at the surface of the IPC cell bodies (see box), different factors initiate the production and release of DILPs. The factors are predominately derived from three tissues: the CC of the ring gland (1), the fat body (2), or the midgut (3). Thereby, the open circulatory system of *Drosophila* allows for the free distribution of modulating molecules to their target tissue. Some peptides do not directly act on the IPCs, but induce the expression and secretion of other neuropeptides, like corazonin or sNPF, which then activate the IPCs. (1) At the CC, APCs release the peptide AKH that acts on the neighboring IPCs. (2) The fat body is the source of different IPC-regulatory factors. Besides the protein stunted and TF Eiger, the fat body also produces the repressor DILP6 and adiponectin. (3) The midgut secretes, for example, the AstA peptides, DH_{31} , and tachykinins, but also CCHamide is produced by this organ. After their release at different neurohemal sites, the DILPs trigger various downstream insulin signaling pathways. Modified after (Nässel and Zandawala, 2019).

Since APCs also express the AstA receptor, AKH release is as well stimulated by the binding of AstA (Hentze et al., 2015). However, since many of the described factors are restricted to a specific developmental stage, larvae and adult animals exhibit quite distinct mechanisms of IPC activation (see also section 3.1).

The IPCs project axons to different neurohemal areas of the body where the DILPs are released. In flies, the released DILPs bind to one of the two known receptors at the surface of their target tissue: the tyrosine kinase receptor dInR (*Drosophila* insulin receptor) or the GPCR dLgr3 (*Drosophila* Leucine-rich repeat-containing G protein-coupled receptor 3) (Fernandes et al., 1995; Brogiolo et al., 2001; Van Hiel et al., 2015). Different signaling cascades are triggered upon activation of the receptors, for example, the canonical insulin/PI3K/Akt (phosphatidylinositol-3-kinase/protein kinase B) signaling pathway, the with the insulin/PI3K/Akt interrelated target of rapamycin (TOR) pathway, and the mitogen-activated protein kinase (MAPK; extracellular signal-regulated kinase, ERK) pathway, (reviewed, e.g., by Grewal, 2009; Teleanu, 2009; Antonova et al., 2012). This diversity of selectively triggered pathways allows control of the diverse DILP-dependent functions, e.g., growth or life span regulation (see above).

However, the effects exerted by *dilp* expression are relatively well studied, whereas factors that control and effectively govern the different IPC activating pathways remain largely elusive. Especially regulation mechanisms targeting the mature and active peptides that induce *dilp* expression are not known, even though metalloendopeptidases like neprilysins could mediate such a functionality.

1.1.2 Neprilysins control diverse processes via cleavage of different peptide substrates

Neprilysins are M13 zinc-metalloendopeptidases characterized by their broad substrate specificity. Through hydrolysis of various peptide substrates, neprilysins play pivotal roles in several processes, including the regulation of blood pressure and natriuresis, nociception, or the degradation of detrimental peptide species related to Alzheimer's disease (reviewed in, e.g., Erdős and Skidgel, 1989; Turner et al. 2001; Bayes-Genis et al., 2016a). The best-characterized member of the neprilysin M13 family is the mammalian neprilysin (NEP, neutral endopeptidase, EC 3.4.24.11; also known as membrane metalloendopeptidase (MME), common acute lymphoblastic leukemia antigen (CALLA), and enkephalinase). NEP was initially described in 1973 as an enzyme of the rabbit kidney brush border membranes and only shortly after that, purified and classified as neutral endopeptidase (George and Kenny, 1973; Kerr and Kenny, 1974a; Kerr and Kenny, 1974b). In the following years, expression of NEP was detected in many different tissues where the enzyme fulfills versatile gastrointestinal, neurological, renal, pulmonary, and cardiovascular functions (e.g., Malfroy et al., 1978; Roques et al., 1980; Skidgel et al., 1984; Trejdosiewicz et al., 1985; Letarte et al., 1988; Borson, 1991; Kokkonen et al., 1999).

Most of the identified neprilysins are type II integral membrane-bound proteins localizing to the plasma membrane. Though, in urine and blood, the enzyme is present as soluble form resembling other soluble neprilysin species secreted into the extracellular space like the human NEP2 (Erdős and Skidgel, 1989; Whyteside and Turner, 2008). Typically, the membrane-bound neprilysins consist of a short N-terminal intracellular domain, a transmembrane domain, and a C-terminal extracellular domain holding the conserved Neprilysin-like (M13) protease domain (Figure 4). The domain comprises two alpha-helical subdomains connected by a linker (Oefner et al., 2000; Figure 4). Together, these domains build the spherical cavity bearing the active site of neprilysin, whereby the subdomain 2 and the linker domain sterically restrict the binding of peptides with a size of more than ~ 3 kDa (Figure 4B; Tiraboschi et al., 1999; Oefner et al., 2000, Pankow et al., 2009). The active site is located at the larger subdomain 1 and harbors the four sequence motifs critical to catalytic activity: HExxH, ENIAD(xGG), CxxW, and NAY/FY (Oefner et al., 2000; Figure 5A).

The histidine residues of the HExxH consensus sequence and the ENIAD(xGG) glutamate coordinate a zinc atom required for cleavage in a tetrahedral structure (Figure 4C; Oefner et al., 2000; Moss et al., 2018; Moss et al., 2020). Together with the surrounding residues, the coordinated zinc ion builds a small binding pocket with the subsites S1, S1' and S2' (Figure 4C). Besides zinc coordination, the HExxH motif is also accountable for the catalysis of the substrate, which is mediated by its glutamate residue. Consistently, the enzymatic activity of neprilysin is efficiently disrupted by mutation of this residue (Devault et al., 1988; Kubo et al., 1992).

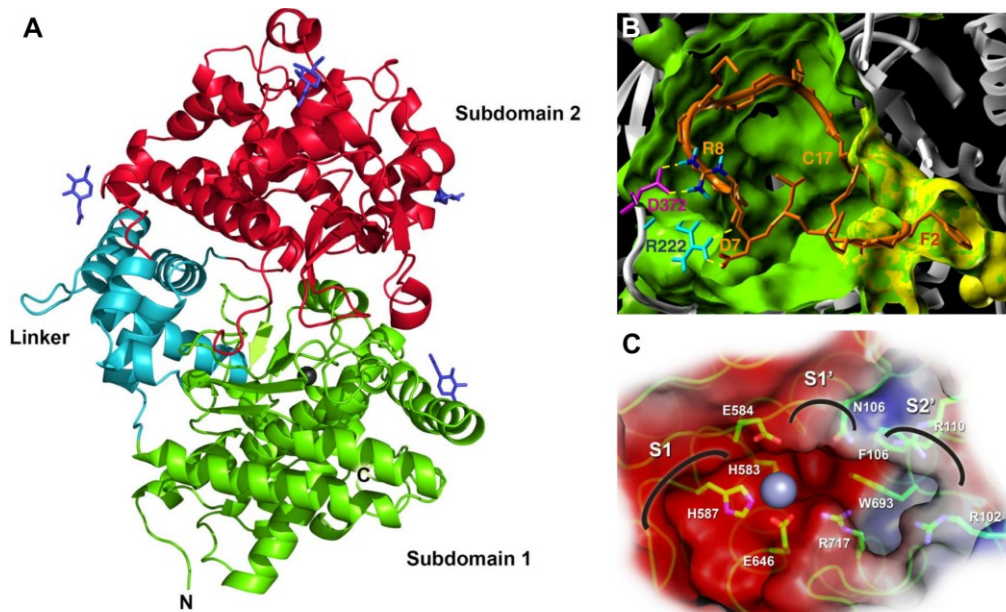


Figure 4 | The extracellular domain of human NEP is critical for catalytic activity. (A) The extracellular domain of human NEP harbors the conserved Neprilysin-like (M13) protease domain composed of the subdomains 1 (green) and 2 (red) and a linker region (cyan) connecting the subdomains. Together, the domains build a spherical cavity that can be entered by small peptides (~ 3 kDa). The zinc ion (black sphere) is crucial for substrate cleavage at the catalytic center. Glycan residues are depicted in blue. Shown is a three-dimensional ribbon diagram based on a crystal structure (Protein Data Bank ID: 6GID). (B) Interior cave of NEP (green) with a bound natriuretic peptide (CNP, C-type natriuretic peptide; orange). NEP residues D372 and R222 interact with CNP residues R8 and D7, respectively, thereby positioning the CNP F2 residue at the catalytic site (yellow). Cleavage of CNP occurs primarily at the amino-terminal bond of the F2 residue. The model is based on crystal structures (Protein Data Bank IDs: 2QPJ; Oefner et al., 2007 and IJDP; He et al., 2001). (C) Detail view of the binding pocket with the subsites S1, S1', and S2' without a bound substrate. The binding pocket is formed by the coordinated zinc atom (grey sphere) and surrounding NEP residues. Coordination of the zinc is mediated by the His583, His587, and Glu646 residues. (A) and (C) were adapted and modified after (Moss et al., 2018), and (B) was adapted and modified after (Pankow et al., 2009).

Additionally, the CxxW motif is critical for protein folding and maturation, and NAY/FY is necessary for substrate binding (Oefner et al., 2000; Turner et al., 2001; Oefner et al., 2004; Sitnik et al., 2014). Neprilysins prefer to cleave the amino-terminal bond at hydrophobic residues of their substrates and are effectively inhibited by phosphoramidon and thiorphan (e.g., Hersh and Morihara, 1986; Tiraboschi et al., 1999; Oefner et al., 2000; Oefner et al., 2004). Among the currently over 50 known NEP substrates are the natriuretic peptides, bradykinin, tachykinins, glucagon, the insulin B-chain, endothelins, and amyloid β -peptides (reviewed, e.g., in Erdős and Skidgel 1989; Bayes-Genis et al., 2016a). Especially because of its role in the cleavage of natriuretic peptides, NEP displays a valuable therapeutic target to treat hypertension and is also used in combination with the blocking of the Angiotensin receptor in the form of so-called vasopeptidase inhibitors to treat patients with systolic heart failure (McMurray et al., 2014; Sharma et al., 2020; e.g., reviewed in Bayes-Genis et al., 2016a; Bayes-Genis et al., 2016b; Singh et al., 2017; Docherty et al., 2020).

Members of the M13 neprilysin family have been identified in many different species ranging from *Hydra vulgaris* or *Drosophila melanogaster* to vertebrates, including mammals (Turner et al., 2001; Bland et al., 2008). Several peptide signaling pathways

are also conserved (see section 1.1.1), emphasizing the comprehensive role of neprilysins in regulating these processes.

1.1.3 *Drosophila* Neprilysin 4 exhibits dual subcellular localization in muscles

Seven neprilysin coding genes have been identified in *Drosophila melanogaster* so far. The corresponding proteins Nep1-Nep7 hold all four conserved sequence motifs critical to catalytic activity (Bland et al., 2008; Sitnik et al., 2014). In contrast to the other *Drosophila* neprilysins, alternative splicing of *nep4* (Nep4) results in the formation of the isoforms Nep4A and Nep4B/C (Meyer et al., 2009; Meyer et al., 2011). The Nep4A isoform holds a transmembrane domain and represents a typical type II integral membrane protein, like the mammalian NEP (Figure 5), whereas Nep4B/C lacks the transmembrane domain (Meyer et al., 2009).

The evolutionary conversation of the protease domain harboring the sequence motifs responsible for the catalytic activity suggests comparable substrate specificity of Nep4 and the other neprilysins (Figure 4; Figure 5). Though, *in vitro* cleavage assays demonstrated that Nep4B efficiently degrades the human peptide substance P but fails to cleave *Locusta migratoria* tachykinin 1 and human bradykinin. In addition, human Angiotensin I and *Drosophila* Pigment Dispersing Factor (PDF) were also cleaved hence with low efficiency. Further experiments using the NEP inhibitors phosphoramidon and thiorphan showed that Nep4 is not susceptible to these inhibitors (Meyer et al., 2009).

The expression of Nep4 is controlled by a neuronal and a mesodermal enhancer element (Panz et al., 2012; Meyer et al., 2011). While the neuronal enhancer mediates the expression of Nep4A in glial cells and neurons of the CNS, the mesodermal enhancer facilitates Nep4 expression in cardiac and muscle cells (Figure 5B-C; Meyer et al., 2009; Meyer et al., 2011; Panz et al., 2012). Furthermore, high Nep4 expression was confirmed in the testes, where the peptidase plays a crucial role in sperm functionality (Meyer et al., 2009; Ohsako et al., 2021). Nevertheless, Nep4 functionality in the different tissues has yet to be fully elucidated. On the one hand, expression of Nep4 in different stages of *Drosophila*, including embryonic tissues, hints at a developmental role of the peptidase.

On the other hand, Nep4 expression in neuronal tissue is related to memory formation, whereas expression in gonads plays a role in reproduction (Sitnik et al., 2014; Turrel et al., 2016). Furthermore, Nep4 was shown to be expressed in larval heart and muscle tissue, where the peptidase is pivotal for muscle integrity (Panz et al., 2012).

Interestingly, in contrast to the typical neprilysin localization at the plasma membrane, Nep4 exhibited dual subcellular localization in muscles (Figure 5B-C; Panz et al., 2012). In addition to surface located Nep4, the enzyme was also detected in membranes of the sarcoplasmic reticulum (SR), an organelle crucial to Ca²⁺ homeostasis during muscle contraction (see section 1.2.3).

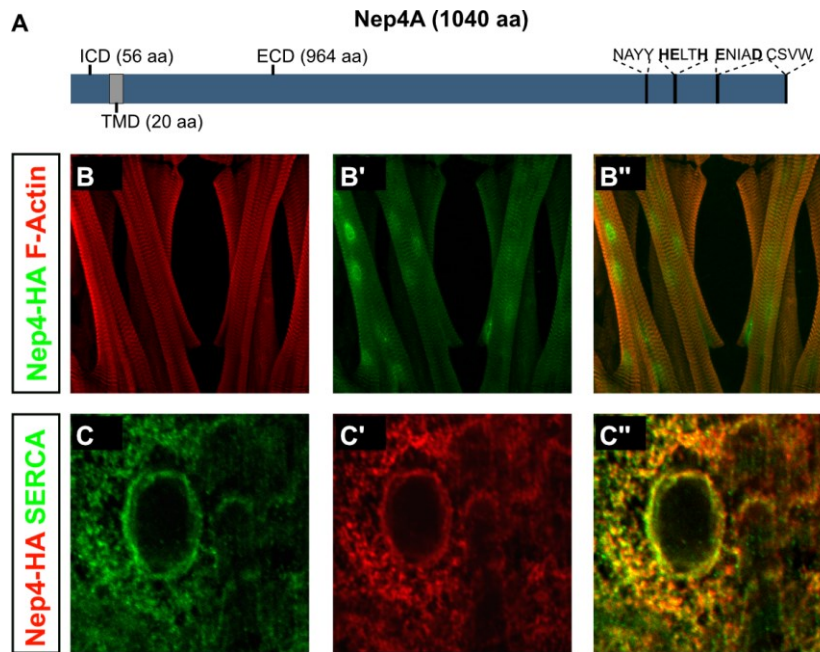


Figure 5 | Nep4A exhibits a dual subcellular localization in *Drosophila* muscles. (A) Primary structure of *Drosophila* Nep4A. The enzyme (1040 aa) consists of a short N-terminal intracellular domain (ICD; 56 aa), a transmembrane domain (TMD; 20 aa), and a large extracellular part (ECD; 964 aa). Catalytic activity is mediated by the four sequence motifs NAYY, HELTH, ENIAD, and CSVW. They are part of the evolutionary conserved Neprilysin-like protease domain at the C-terminal end of the ECD. The motifs HELTH and ENIAD represent zinc-binding domains (bold residues are critical to zinc coordination and catalysis), whereas NAYY mediates substrate binding, and CSVW is important for protein folding and maturation. (B-B'') Expression of HA-tagged Nep4 (Nep4-HA; green) driven by the native mesodermal enhancer results in dual subcellular localization of the peptidase in body wall muscles. While Nep4 signal is apparent at the surface of the myofibers (B', B''); green) and corresponds to F-actin (B, B''); red), a strong Nep4 signal is also detectable around the nuclei. (C-C'') Higher magnification of the nuclear region shows that Nep4 co-localizes with a marker of the SR (SERCA, red). The muscles of third instar larvae were stained with phalloidin-TRITC and an anti-HA/anti-SERCA antibody. (B) and (C) were modified and adapted after (Panz et al., 2012).

While localization at the surface of muscles enables the enzyme to cleave soluble signaling peptides circulating in the hemolymph, the functionality of Nep4 at the SR membrane remains unclear.

1.2 Physiology of muscle contraction and role of regulatory micropeptides

The physiological mechanisms underlying muscle and heart contractions are evolutionary well conserved throughout the animal kingdom. This is due to the fact that the smallest contractile unit of striated muscles, the sarcomere, is highly conserved in different types of muscle tissue and animal taxa (Figure 6; Hanson and Huxley, 1953; reviewed in Clark et al., 2002; Ehler and Gautel, 2008). Consecutively attached sarcomeres build a single myofibril, and several myofibrils are bundled to myofibers covered by the sarcolemma called plasma membrane. Depending on the respective muscle type, a single muscle can be composed of only one myofiber/myofibril or comprises fascicles called muscle fiber bundles.

A molecular sliding mechanism enables sarcomere shortening based on the interaction of thin actin filaments and thick myosin filaments (Huxley and Niedergerke, 1954; Huxley and Hanson, 1954; Burbaum et al., 2021; Wang et al., 2021; see also Figure 9). This interaction generates a mechanical force, further leading to contraction of the whole muscle and subsequently resulting in movement of a structure, organ, or body part. Through various adaptations characterizing the different muscle types, muscles can be optimized to generate maximal forces, like jaw muscles, or to endure long periods of contraction, like the muscles that build up a heart.

In general, muscles can be divided into two major groups, smooth and striated muscles. While the repeated alignment of sarcomeres present in striated muscles results in a typical regular pattern visible under the light microscope, smooth muscles lack this regular composition of thin and thick filaments leading to a more 'smooth' and unregular appearance of the overall muscle tissue (e.g., Gabella, 1984). Smooth muscles are composed of specialized non-syncytial myocytes featuring tapered ends. They typically mediate slow or sustained involuntary contraction, which is, for example, needed for the movement of inner organs in peristaltic waves. In contrast, striated muscles are responsible for precisely controlled rapid movements like the wing stroke of *Drosophila*. This muscle type comprises long, multinucleated cylindrical myocytes and contains many mitochondria due to the high energy requirement. However, invertebrate "hybrid" muscular structures exhibiting molecular composition of both types have been described as well (e.g., Sulbarán et al., 2015; Steinmetz et al., 2012; Kobayashi et al., 1998; Hoyle, 1969; Plesch, 1977). According to the different patterns of striation, the voluntary striated muscles can be further subdivided into transversely/cross-striated (vertebrates and invertebrates) and obliquely/helically striated muscles (invertebrates only) (Hanson, 1957; Paniagua et al., 1996; Royuela et al., 2000). Continuous or discontinuous Z-discs further characterize the transversely striated muscles of invertebrates. With skeletal and cardiac muscles, two different types of cross-striated muscles are present in vertebrates. In contrast to skeletal muscles, cardiac tissue does not exhibit the typical regularly arranged sarcomeres of striated muscles.

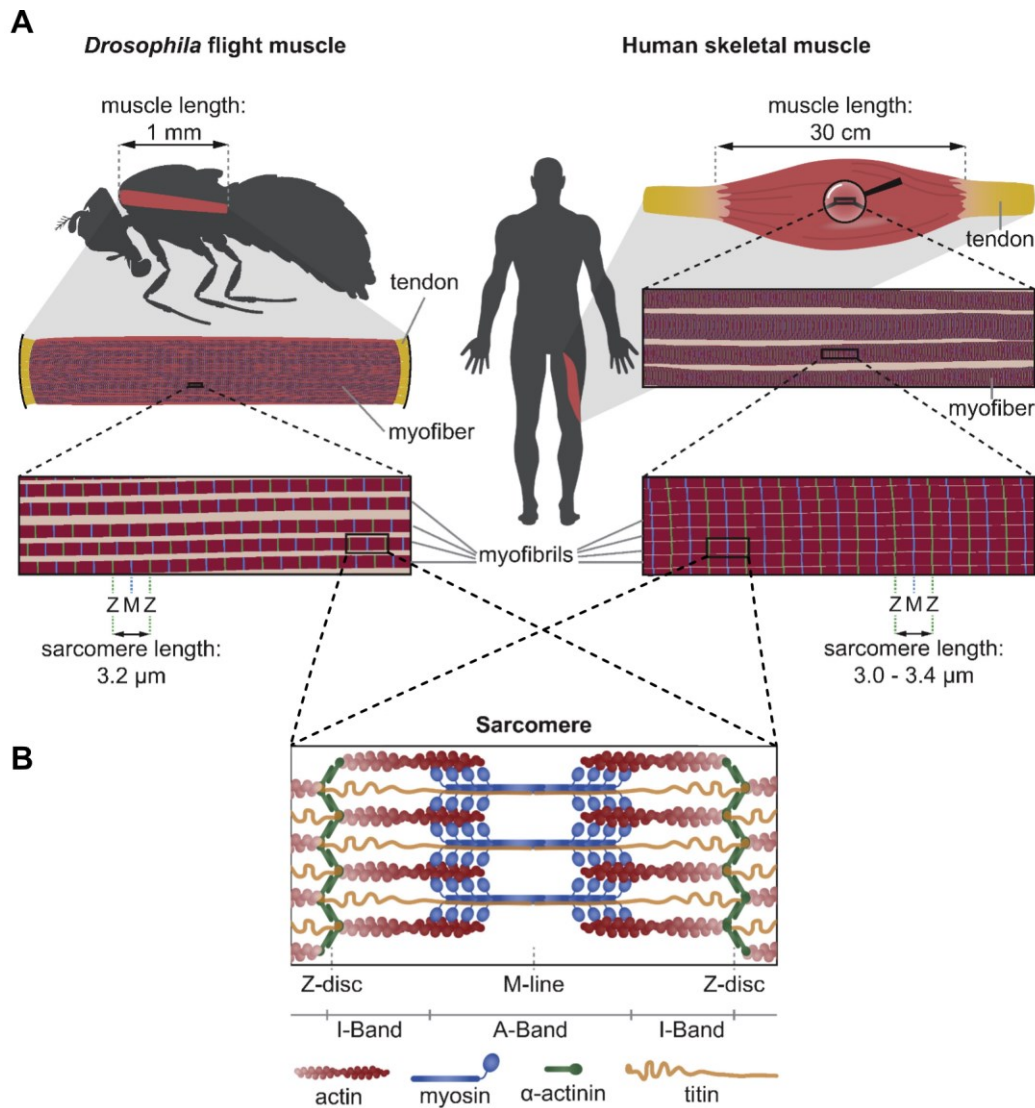


Figure 6 | The sarcomere is the basic contractile unit of muscles. (A) A comparison of a *Drosophila* flight muscle and a human skeletal muscle illustrates the high evolutionary conservation of these tissues. The muscles consist of single myofibers (*Drosophila* flight muscle) or myofiber bundles (human skeletal muscle). In both cases, the myofibers are composed of parallel-assembled myofibrils. One myofibril spans the entire length of one muscle and is built up by end-to-end joined sarcomeres, the contractile units of muscles. Coordinated contraction of all myofibrils of one muscle fiber and transmission of the thereby generated mechanical force via tendons or tendon-like structures results in overall muscle contraction. Even though the size of muscles varies a lot between organisms and yet can be quite variable depending on the muscle type in one animal, the size of the sarcomeres is very consistent. This also applies to the molecular components forming a single sarcomere. (B) The sarcomeric Z-disc consists of α -actinin that serves as an anchor structure for titin and thin actin filaments. By contrast, the M-line is located at the center of a sarcomere, where titin itself serves as the anchor for the thick myosin filaments. Besides the dense Z-discs, the region of thick myosin filaments (A-Band) and the brighter region of thin actin filaments (I-Band) can be distinguished under the light microscope. Modified and adapted after (Lemke and Schnorrer, 2017).

Instead, cardiac tissue is composed of specialized single nucleated cardiomyocytes organized in branched bundles and connected by intercalated discs. As cell-cell adhesion structure, intercalated discs are essential for synchronizing the heartbeat by connecting the cytoplasm of neighboring cardiomyocytes. This distinct architecture of cardiac tissue is causative for the less regular appearance of striation in comparison to skeletal

muscles (e.g., reviewed in Zhao et al., 2019). Two different subgroups of skeletal muscles can be distinguished: slow- and fast-twitch muscles. Slow-twitch or red muscles are specialized for sustained/tonic activity and can be characterized, e.g., by their aerobic respiration (oxidative phosphorylation) in combination with a high content of myoglobin and mitochondria. Fast-twitch fibers (white muscles), on the other hand, use anaerobic metabolism (glycolysis) and exhibit less myoglobin and mitochondria (Schiaffino and Reggiani, 2011; reviewed, e.g., by Calderon et al., 2014; Kuo and Ehrlich, 2015). With these characteristics, fast-twitch fibers are construed for phasic and active activity. Therefore, long-term exercise leads to the conversion of slow-twitch fibers to fast-twitch fibers.

1.2.1 The muscle tissue of *Drosophila*

The fruit fly *Drosophila melanogaster* is a well-established model organism to study muscle functionality, physiology, and myogenesis. In contrast to other invertebrates, only one primary type of muscle tissue is present in arthropods: transversely striated muscles with continuous or discontinuous Z-discs that share many similarities with vertebrate skeletal muscles (Figure 6 and Figure 7; Smith, 1966; Osborne, 1967; Goldstein and Burdette, 1971; Jorgensen and Rice, 1983; Paniagua et al., 1996; Royuela et al., 2000; reviewed in Taylor, 2006). Due to the lack of an internal skeleton, most of the *Drosophila* muscles are connected via myotendinous junctions (MTJs) called tendon-like structures to the cuticular exoskeleton to allow for contractile force transmission (reviewed in, e.g., Volk, 1999; Schnorrer and Dickson, 2004; Schweitzer et al., 2010; Soler et al., 2016).

Like in all holometabolous insects, *Drosophila* muscles undergo two significant rearrangement phases in the course of development: during the embryo to larva transition and during the pupal metamorphosis (reviewed in Poovathumkadavil and Jagla, 2020). In the first phase of the muscle rearrangement, embryonic muscles develop either into larval somatic muscles, also known as body wall muscles, visceral, or cardiac muscle tissue (Figure 7). As a well-orchestrated process, peristaltic contraction waves of the super contractile body wall muscles build the base for the typical larval crawling locomotion. All embryonic and larval muscles have in common that they consist of single myofibrils or single cardiomyocytes, whereas the formation of multifibrillar muscles first takes place in the pupal stage (Miller, 1950; Shafiq, 1963). The resulting thoracic indirect flight muscles (IFMs) of adult flies consist of multiple myofibers and power the wing stroke (Figure 7C). They are composed of dorsoventral muscles (DVMs) and dorsal longitudinal muscles (DLMs), which represent the largest muscles of the adult *Drosophila*. They share their fibrillar organization and many developmental characteristics with vertebrate skeletal muscles, rendering the *Drosophila* DLMs an excellent model system for studying myogenesis and muscle physiology (Shafiq, 1963; reviewed in, e.g., Vigoreaux, 2006; Taylor, 2006). In contrast to the IFMs, all the other

muscle types of adult flies, including direct flight muscles (DFMs), leg, head, abdominal and visceral muscles, and cardiac muscles are only composed of single tubular muscles or cardiomyocytes.

The visceral muscles surround the intestinal system and are responsible for the movement of inner organs in larvae and adult flies. Unlike vertebrate smooth muscles, they exhibit striation to some extent but also show morphological and functional similarities to vertebrate smooth muscles.

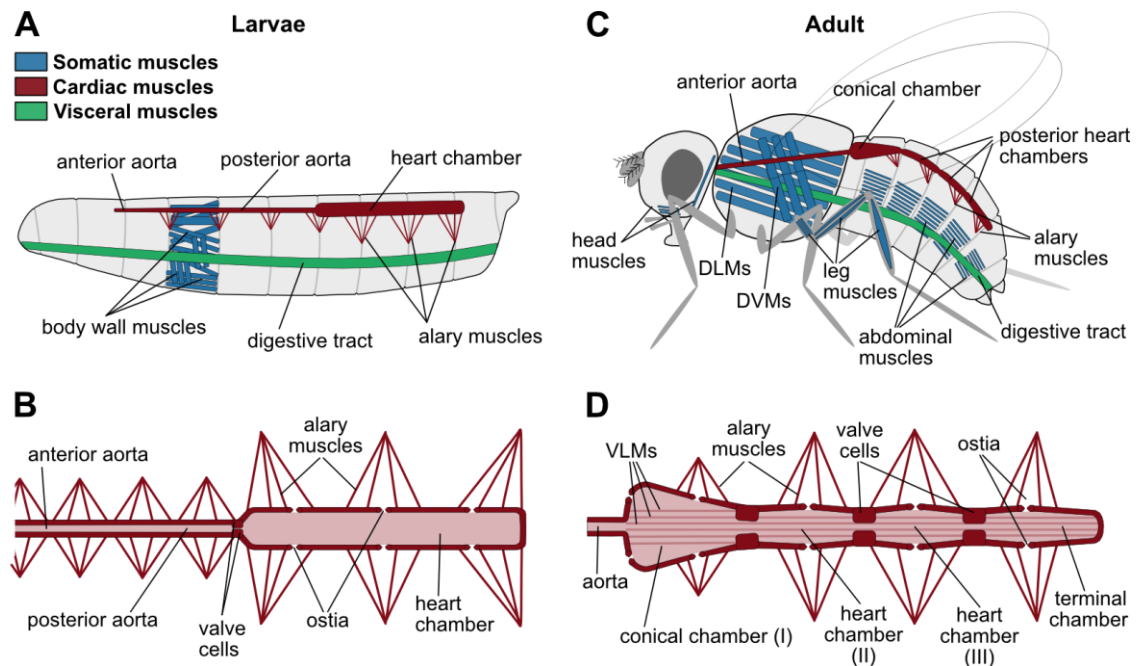


Figure 7 | Muscle tissues present in *Drosophila*. (A) Simplified schematic overview of the main muscle tissues in *Drosophila* third instar larvae. Somatic muscles (blue) are represented by body wall muscles lining the inner cuticle. Body wall muscle contraction is accountable for the locomotion of the animal. Peristaltic contractions of the digestive tract are mediated by the visceral involuntary muscles (green). The cardiac muscles (red) build the dorsal larval heart that can be distinguished in an anterior aorta and a posterior heart chamber. (B) Muscular components of the larval *Drosophila* heart (dorsal view). The cardiac tube is built by cardiomyocytes forming a lumen through which the hemolymph is transported from the posterior end to the anterior part of the animal. Specialized cardiomyocytes, the ostia cells, form six ostia called openings through which the hemolymph enters the heart chamber. One pair of valve cells, located at the transition between the heart chamber and aorta, prevents the backflow of hemolymph during heart contraction. In addition to cardiomyocytes, a second type of cardiac muscle tissue is needed to maintain heart contraction: the alary muscles that position the heart in the open body cavity. (C) Simplified schematic overview of the main muscle tissues present in adult *Drosophila*. Somatic muscles (blue) can, e.g., be found in the head, legs, abdomen, and thorax. The fibrillar thoracic indirect flight muscles, composed of dorsoventral (DVMs) and dorsal longitudinal muscles (DLMs), represent the largest muscles of the fruit fly and power the wing stroke. For digestion of food, contraction of visceral muscles (green) is required. In comparison to the larval stage, the morphology of the adult heart (red) is more complex. (D) Muscular components of the adult *Drosophila* heart (dorsal view). While the posterior larval heart consists of only one chamber, the adult abdominal heart comprises four heart chambers. At the transition of the thorax and abdomen, the narrow aorta merges into the conical heart chamber. Three pairs of adult valves subdivide the following heart sections into a second, third, and terminal chamber. The hemolymph enters the adult heart via five pairs of ostia. Four pairs of alary muscles are attached to the cardiac tube through the ECM and embedded pericardial nephrocytes (not shown). Besides cardiomyocytes and alary muscles, a third muscle group is involved in forming the adult heart: the ventral longitudinal muscles (VLMs) that cover the ventral side of the heart tube.

These are, for example, irregularly aligned filaments, irregular and perforated Z-discs, and an underdeveloped sarcoplasmic reticulum network (Goldstein and Burdette, 1971; reviewed in Lee et al., 2006). Based on their morphology, *Drosophila* visceral muscles can be further distinguished in polynucleated longitudinal and binuclear circular muscles (Goldstein and Burdette, 1971; Klapper, 2000; Klapper et al., 2001; Klapper et al., 2002; reviewed in Lee et al., 2006). In addition to the somatic and visceral muscles, a third type of muscle tissue is initiated during embryonic development: the cardiac muscles (Figure 7). Emerging from embryonic cardioblasts, the cardiomyocytes called mononucleated striated cardiac muscle cells form the tubular contractile heart of *Drosophila* (Miller, 1950; Rizki, 1978; Zaffran et al., 1995; Sellin et al., 2006; reviewed in Medioni et al., 2009; Rotstein and Paululat, 2016; and Bodmer and Frasch, 2010). As an important part of the open circulatory system, the function of the dorsal vessel is to maintain hemolymph flow by pumping the interstitial fluid from the posterior end of the animal to the anterior part (reviewed in Rotstein and Paululat, 2016).

The larval heart tube is built by two opposing rows of 104 cardiomyocytes that are connected via adherens junctions and thereby shape the heart lumen (Rugendorff et al., 1994; Zaffran et al., 1995; Sellin et al., 2006; Lehmacher et al., 2012; reviewed in Medioni et al., 2009). Interestingly, junctions at cardiomyocyte contact sites exhibit similarities to the cardiac intercalated discs of vertebrate cardiac tissue (Lehmacher et al., 2012). The larval heart is further subdivided into a posterior heart chamber comprising the three pairs of ostia called openings allowing the hemolymph to enter the heart lumen and the anterior and more narrow aorta through which the hemolymph emanates into the open body cavity (Figure 7A-B; Miller, 1950; Rizki, 1978; Curtis et al., 1999; Molina and Cripps, 2001; Wasserthal, 2007; Lehmacher et al., 2012; Monier et al., 2005; Sellin et al., 2006; Lehmacher et al., 2012). Thereby, unidirectional flow of the hemolymph is ensured by the action of one pair of intracardiac valve cells present at the transition between the heart chamber and aorta (Rizki, 1978; Zeitouni et al., 2007; Wu and Sato, 2008; Lehmacher et al., 2012; Lammers et al., 2017). Both ostia, as well as valve cells, represent specialized cardiomyocytes. Collective contraction of all cardiomyocytes results in peristaltic movement of the whole heart, whereby contraction is initiated at the end of embryogenesis.

A crucial factor for proper heart functionality is further the cardiac extracellular matrix (ECM) that forms a three-dimensional network surrounding the cardiac tube (Drechsler et al., 2013; Rotstein et al., 2018; reviewed in Volk et al., 2014 and Rotstein and Paululat, 2016). By connecting the heart tube to the seven pairs of so-called alary muscles that position the heart in the body cavity (Miller, 1950; Rizki, 1978; Curtis et al., 1999; LaBeau et al., 2009; Lehmacher et al., 2012; Bataille et al., 2015), the ECM acts as link and force transmitter between the contracting heart and the body wall (Lehmacher et al., 2012; reviewed in Volk et al., 2014; Rotstein and Paululat, 2016). Embedded in the ECM, the pericardial cells accompany the heart in two rows. Besides the expression of ECM compounds (Drechsler et al., 2013), the highly endocytic

pericardial cells filter the hemolymph, rendering these cells an important part of the fly's excretory system (Das et al., 2008; Weavers et al., 2009; Ivy et al., 2015; Dehnen et al., 2020; reviewed in Helmstädter and Simons, 2017).

Like many other organs, *Drosophila's* heart tube also undergoes main remodeling during pupation (Miller, 1950; Rizki, 1978; Curtis et al., 1999; Molina and Cripps, 2001; Monier et al., 2005; Sellin et al., 2006; Lehmacher et al., 2012). As a result, the adult cardiac tube exhibits five pairs of ostia and is connected to four pairs of alary muscles (Figure 7C-D; Curtis et al., 1999; Molina and Cripps, 2001; Wasserthal, 2007, Zeitouni et al., 2007; Shah et al., 2011; Lehmacher et al., 2012). With three pairs, the number of intracardiac valves is also increased in comparison to the larval heart, even though the total number of cardiomyocytes is reduced to 84 in comparison to the 104 cardiomyocytes of the larval heart (Sellin et al., 2006; Zeitouni et al., 2007; Lehmacher et al., 2012; Tang et al., 2014; Lammers et al., 2017). The additional valve cells subdivide the heart chamber into one anterior conical chamber and three posterior chambers (Curtis et al., 1999; Monier et al., 2005; Sellin et al., 2006; Lehmacher et al., 2012). At the transition to the thoracic segment, the conical chamber merges into the aorta extending over the whole length of the thorax.

The rearrangements in the pupal stage also affect the cardiac myofilament organization and orientation. While the circular myofilaments of the larval cardiomyocytes are rather irregular and scattered over the heart tube, adult hearts exhibit a more ordered and condensed cardiac myofilament organization. Moreover, the ventral side of the adult heart is covered by a layer of syncytial ventral longitudinal muscles (VLMs) that are built from larval alary muscles during pupation (Figure 7D; Miller, 1950; Rizki, 1978; Curtis et al., 1999; Molina and Cripps, 2001; Lehmacher et al., 2012; Shah et al., 2011; Schaub et al., 2015). The functionality of this muscle tissue is still not fully understood. However, it was assumed that it could be part of the dorsal diaphragm (Miller 1950; Lehmacher et al., 2012). Unlike in the other cardiomyocytes, the dense reticulated arrangement of myofilaments in cardiac valve cells is not remodeled during pupal development (Lehmacher et al., 2012; Lammers et al., 2017). This also applies to the myofilament organization of ostia cells. Most of the ostial myofilaments resemble typical cardiomyocyte patterns in larvae and adults, while the ostial lips exhibit perpendicular/orthogonally arranged filaments (Lehmacher et al., 2012).

1.2.2 Tightly controlled Ca²⁺ transients are essential for proper muscle functionality

Precisely regulated Ca²⁺ transients are the physiological base for muscle contraction cycles consisting of consecutive phases of contraction (systole) and relaxation (diastole). In memorable experiments from the 19th century, Sydney Ringer could show that calcium is a crucial factor for myocardial function (Ringer, 1882; Ringer, 1883), thus setting the starting point for the rapidly emerging scientific field of Ca²⁺ signaling and

homeostasis (e.g., reviewed by Berridge et al., 2003; Carafoli, 2002; Clapham, 2007; Carafoli and Krebs, 2016). Even though the various muscle types show some differences regarding details of their respective physiological contraction mechanisms, the cycling of Ca^{2+} is always the central incentive. In all cases, an external signal is transduced into an increase in cytosolic Ca^{2+} concentration [Ca^{2+}] of the myocyte, further leading to the interaction of thin actin and thick myosin filaments that finally results in sarcomere shortening and muscle contraction. Thereby, many different channels, transporters, exchangers, ATPase pumps, and calcium-binding proteins are involved maintaining and regulating this process. The fact that most of these proteins transport or bind Ca^{2+} underlines the importance of this class of ions for muscle and heart physiology.

The previously described muscle types differ especially regarding their mechanism of contraction initiation (reviewed by Kuo and Ehrlich, 2015). As voluntarily controlled tissue, skeletal muscles are not self-stimulating, and contractions are exclusively initiated by signals of the nervous system. In contrast, the involuntary smooth and cardiac muscles receive initiating signals from the endocrine system, neighboring cells, pacemaker cells, or via mechanical forces in addition to the nervous system. The skeletal muscles of vertebrates are innervated by motoneurons that release the neurotransmitter acetylcholine at the neuromuscular junctions (NMJs). By binding to sarcolemma-integral nicotinic acetylcholine receptors (nAChRs), acetylcholine causes the influx of cations leading to the depolarization of the sarcolemma. This depolarization opens voltage-gated sodium channels that thereby propagate the action potential along the sarcolemma. On the contrary, the motoneurons of *Drosophila* muscle tissue are glutamatergic, and depolarization of the sarcolemma is accomplished by binding of the neurotransmitter glutamate to ionotropic glutamate receptors (Jan and Jan, 1976a; Jan and Jan, 1976b; Ormerod et al., 2020; reviewed, e.g., by Menon et al., 2013; Harris and Littleton, 2015). One exception is the myogenic larval heart, whose contraction is not dependent on extrinsic neuronal signals (Rizki, 1978; Dowse et al., 1995; Johnson et al., 1997; Johnson et al., 1998; Johnson et al., 2002). Interestingly, the adult *Drosophila* heart is not myogenic but innervated by glutamatergic motoneurons (Rizki, 1978; Dulcis and Levine 2003; Dulcis and Levine, 2005).

At the beginning of a new muscle contraction-relaxation cycle, an incoming action potential originating from an innervating motoneuron (in case of skeletal/somatic muscles) or a pacemaker (in case of cardiomyocytes/cardiac tissue) leads to depolarization of the sarcolemma (Figure 8). Thereby, depolarization constitutes the first step of excitation-contraction coupling (ECC). ECC describes the coupling of sarcolemmal depolarization to the release of the intracellular Ca^{2+} storage that subsequently triggers muscle contraction (Kahn and Sandow, 1950; Sandow, 1952; reviewed, e.g., by Ríos et al., 1990; Lamb, 2000; Bers, 2002 and Calderon et al., 2014). In the first step of cardiac ECC, depolarization of the sarcolemma induces the opening of the sarcolemma-integral voltage-gated L-type calcium channels (LTCCs; also known as dihydropyridine receptors: DHPRs), resulting in an influx of extracellular Ca^{2+} into the cytosol of the myocyte.

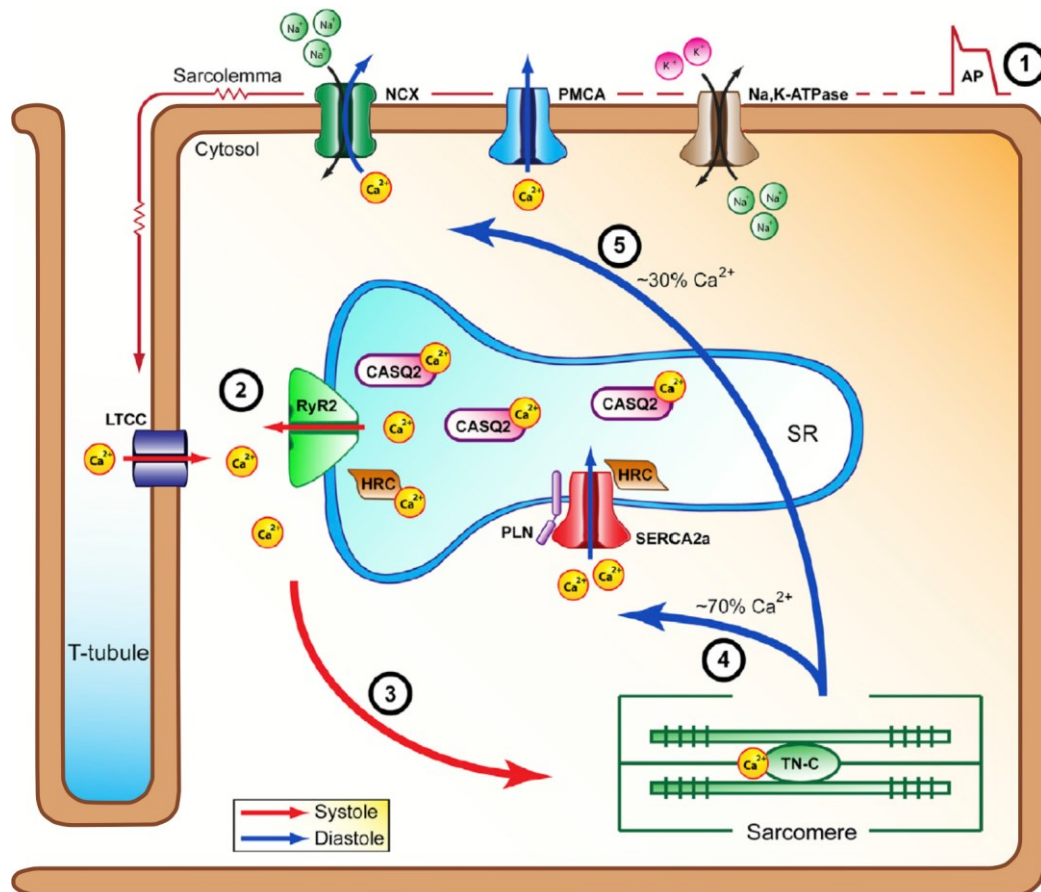


Figure 8 | Ca^{2+} cycling in vertebrate cardiomyocytes. (1) The beginning of a new systolic phase (related processes marked by red arrows) is characterized by an incoming action potential (AP) spreading along the sarcolemma. Depolarization of the membrane induces the opening of the L-type calcium channels (LTCCs), which predominantly localize at T-tubule called invaginations of the sarcolemma, leading to an influx of extracellular Ca^{2+} into the cytoplasm of the myocyte. (2) This influx provokes the fast release of Ca^{2+} , which is stored in the sarcoplasmic reticulum (SR) via the opening of the SR membrane integral ryanodine receptor (RyR2). (3) By binding to troponin's calcium receptor subunit (Tn-C), Ca^{2+} initiates sarcomere shortening and subsequently cardiomyocyte contraction. (4) The diastolic phase (related processes marked by blue arrows) is characterized by reducing the cytosolic Ca^{2+} concentration [Ca^{2+}] resulting in restoration of the tropomyosin-mediated inhibition of actin and myosin interaction at the sarcomeric level. Depletion of cytoplasmic Ca^{2+} is predominately ($\sim 70\%$ in cardiomyocytes) fulfilled by the activity of the Sarco/Endoplasmic Ca^{2+} -ATPase (SERCA2a) enzyme that actively transports cytoplasmic Ca^{2+} back into the SR. Thereby, the SR Ca^{2+} store gets recovered for the next systolic phase. (5) About 30% of the cytoplasmic Ca^{2+} is depleted by the $\text{Na}^+/\text{Ca}^{2+}$ exchanger (NCX) and the plasma membrane Ca^{2+} ATPase (PMCA), though the activity of NCX is dependent on the pumping action of the sodium-potassium ATPase (Na^+/K^+ -ATPase) that builds up the required Na^+ gradient. The action of different proteins also modulates Ca^{2+} cycling. Calsequestrin (CASQ2) and the histidine-rich calcium-binding protein (HRC) localize to the SR lumen and directly bind Ca^{2+} , whereby they help to build up the extremely high diastolic Ca^{2+} concentration in the SR lumen. Additionally, HRC can also directly affect SERCA and RyR. SR-membrane integral peptides like Phospholamban (PLN) are further important regulators of Ca^{2+} -transients and muscle contraction. By binding to SERCA, this class of peptides affects the activity of the ATPase and therefore modulates the rate of cytosolic Ca^{2+} depletion. Abbreviations of proteins and peptides correspond to isoforms found in human cardiomyocytes. Adapted and modified after (Gorski et al., 2015a).

LTCCs represent a subgroup of voltage-gated calcium channels (VGCCs), a protein family that localizes to the plasma membrane of excitable cell types. When the [Ca^{2+}] exceeds a distinct threshold level, it triggers the fast release of Ca^{2+} ions stored in the sarcoplasmic reticulum (SR), which constitutes the specialized endoplasmic reticulum

(ER) of muscle cells (see section 1.2.3). This fast release of the stored Ca^{2+} is induced by the interaction of cytosolic Ca^{2+} with the SR membrane integral ryanodine receptor channels (RyR). The homotetrameric RyR (Fleischer et al., 1985; Kawamoto et al., 1986; Inui et al., 1987) represents a huge P-type channel protein complex that consists of four 560 kDa subunits and harbors numerous functional domains (e.g., reviewed by Hwang et al., 2012; Meissner, 2017; Zalk and Marks, 2017; Santulli et al., 2018). The N-terminal cytoplasmic part of the receptor accounts for most of the receptor's mass and represents the primary target for its regulation. The activity of RyR is modulated by various factors, including $[\text{Ca}^{2+}]$, interacting proteins, nucleotides, divalent cations, the phosphorylation state, or reactive oxygen species (reviewed, e.g., in Lanner et al., 2010; Reddish et al., 2017; Kushnir et al., 2018; Kobayashi et al., 2021). The transmembrane domain is assembled by six α -helices which build the ion-conducting receptor channel with a core formed by the C-terminal domain (des Georges et al., 2016; reviewed by Zalk and Marks, 2017). The C-terminal domain holds binding sites for the channel activators Ca^{2+} , ATP, caffeine, and the plant alkaloid ryanodine at interdomain interfaces (des Georges et al., 2016).

The previously described mechanism of RyR opening triggered by the binding of Ca^{2+} that entered the cell through the DHPR is called calcium-induced calcium release (CICR) and is a characteristic of cardiac tissue (Endo et al., 1970; Ford and Podolsky, 1970; Fabiato and Fabiato, 1972; Fabiato and Fabiato, 1978; reviewed, e.g., by Bers, 2002; Ríos, 2018). By contrast, the opening of the skeletal muscle RyR1 relies predominately on the conformational change of DHPR provoked by depolarization of the sarcolemma (reviewed, e.g., in Calderon et al., 2014; Kobayashi et al., 2021), a process also known as DICR (Depolarization-induced Ca^{2+} release). The direct interaction of DHPR and RyR1 as part of the Ca^{2+} release complex (CRC) (also known as Ca^{2+} release unit (CRU) or “couplon”) allows for the transduction of sarcolemma depolarization into the release of the SR-luminal Ca^{2+} store (e.g., Marty et al., 1994; Franzini-Armstrong et al., 1999; Cheng et al., 2005; reviewed, e.g., in Marty, 2015; Dulhunty et al., 2017). The CRC is the core of a specialized membrane structure: the triad junction (Figure 10; see also section 1.2.3). In addition to DICR, also CICR can play a role in skeletal muscles contraction, especially in non-mammals (Endo et al., 1970; Ford and Podolsky, 1970; reviewed, e.g., in Endo, 2009; Calderon et al., 2014; and Ríos, 2018). However, different studies emphasize that CICR is the primary mechanism for ECC in invertebrate muscles (Takekura and Franzini-Armstrong, 2002; Collet, 2019), including *Drosophila* (Feng et al., 2019; Hsu et al., 2020).

In summary, both described modes of ECC lead to the release of the SR Ca^{2+} storage into the cytoplasm. Here, the released Ca^{2+} can interact with sarcomere components to provoke sarcomere shortening, as initially described by the sliding filament theory (Figure 9; Huxley and Niedergerke, 1954; Huxley and Hanson, 1954). At the molecular level, the filamentous molecule tropomyosin blocks myosin-binding sites of the thin actin filaments at low $[\text{Ca}^{2+}]$ prevalent during diastole, so that thin and thick filaments

interaction is inhibited at this state (Figure 9A-B). At high $[Ca^{2+}]$, Ca^{2+} binds to the calcium receptor subunit (Tn-C) of troponin, thereby inducing a conformational change that is further transmitted to the inhibitory (Tn-I) and tropomyosin-binding/thin filament-anchoring subunits (TnT) of troponin. Due to the close association of troponin and tropomyosin, the conformational change of troponin causes the steric rearrangement of tropomyosin, subsequently resulting in exposure of the myosin-binding sites of actin (e.g., Lehman et al., 1994; Vibert et al., 1997; Lehman et al., 2000). The myosin heads of the thick filaments can now bind to actin to initiate ATP-dependent myosin-actin cycling (Lymn and Taylor, 1971; Hynes et al., 1987; e.g., reviewed in Huxley, 1969; Geeves, 1991; Spudich, 2001; Goody, 2003). Thereby, the release of inorganic phosphate (Pi) after ATP hydrolysis provokes the power stroke in the form of a myosin lever arm swing, also known as swinging cross-bridges. Thus, myosin generates a pulling force by applying tension to the thin filaments so that the thin filaments are pulled in the direction of the M-line (Figure 9C-D). Even though understanding of the exact actin-myosin interaction dynamics has been of great scientific interest since the 1950s, many structural aspects are topics of current investigations or still remain to be resolved (e.g., Irving, 2017; Reconditi et al., 2017; Robert-Paganin et al., 2019; Pospich et al., 2021; Smith et al., 2021).

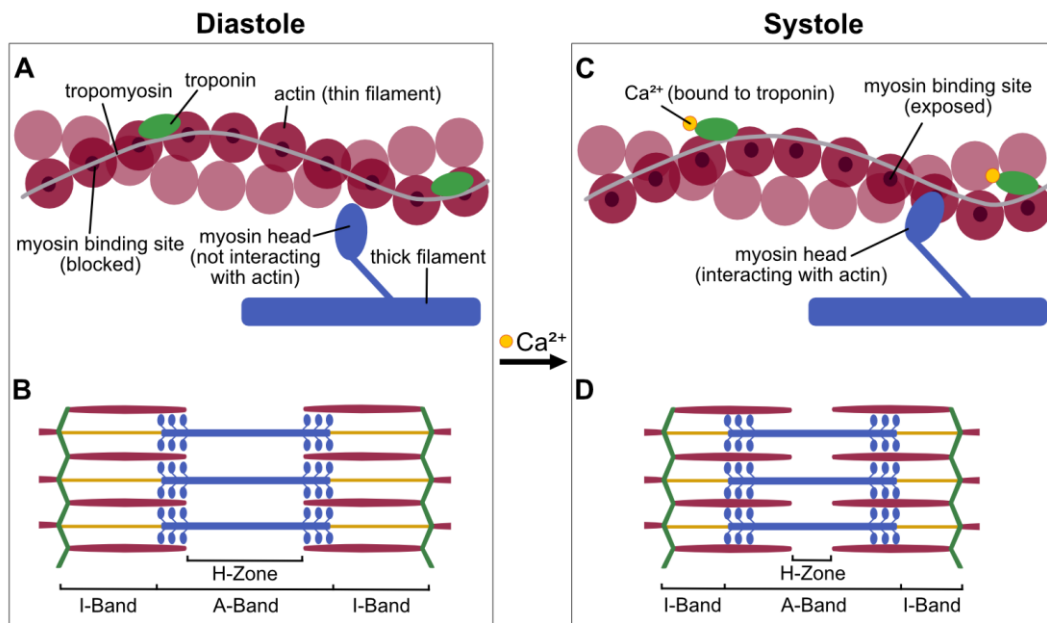


Figure 9 | Sarcomere shortening is Ca^{2+} - and ATP-dependent. The sarcomeric molecular composition allows Ca^{2+} and ATP-dependent spatial interaction of myosin heads and actin filaments resulting in muscle contraction. (A) At low $[Ca^{2+}]$ prevalent during diastole, tropomyosin blocks the myosin-binding sites of actin so that interaction of the thick and thin filaments is inhibited at this state. (B) The sarcomere exhibits its maximal length without myosin (blue) and actin (red) interaction. (C) During systole, the binding of Ca^{2+} to troponin leads to tropomyosin rearrangement and subsequently to the exposure of the myosin binding sites. This enables the myosin heads of the thick filaments to interact with the actin of thin filaments. During a process known as myosin-actin cycling, myosin consecutively binds and releases actin, whereby the release is dependent on ATP hydrolysis. (D) Myosin-actin cycling results in sarcomere shortening according to the early described sliding filament theory and produces contractile force. In the contracted form, the lengths of the sarcomeric I-Bands and H-Zone are reduced, while the size of the A-Band stays constant. The flexible titin filaments (yellow) that connect thick myosin filaments to α -actinin (green) are also crucial for the sliding mechanism.

However, the sarcomere shortens due to the actin-myosin interaction and synchronized shortening of all muscle sarcomeres generates contractile force.

The diastolic or relaxation phase is initiated by alleviating the cytosolic Ca^{2+} concentration mediated by different proteins (Figure 8). The Sarco/Endoplasmic calcium ATPase (SERCA) transports the cytosolic Ca^{2+} back into the SR, restoring the SR Ca^{2+} load, which is needed for the next systole (see section 1.2.3). About 70 % of the systolic, cytosolic Ca^{2+} is replaced by SERCA activity (Bers, 2008). Furthermore, the sarcolemma-integral sodium-calcium exchanger (NCX), the plasma membrane calcium ATPase (PMCA), and mitochondria play notable roles in depleting the cytosolic Ca^{2+} levels, although to a much lower extent than SERCA. During diastole, the antiporter NCX uses the electrochemical gradient of sodium for the extrusion of Ca^{2+} into the extracellular space (first described in Reuter and Seitz, 1968; e.g., reviewed by Blaustein and Lederer, 1999; Philipson and Nicoll, 2000; Khananshvil, 2014). Thereby, the import of three sodium ions enables the export of one calcium ion. The required electrochemical gradient of sodium is established by the action of the sodium-potassium ATPase (Na^+/K^+ -ATPase) (Skou, 1957; e.g., reviewed by Shattock et al., 2015; Hilgemann, 2020). Besides NCX, also PMCA removes calcium from the myocytic cytoplasm into the extracellular space (Dunham and Glynn, 1961; Schatzmann, 1966). Under hydrolysis of one molecule ATP, PMCA removes one calcium ion from the cytosol. In contrast to NCX, PMCA exhibits a relatively high affinity for Ca^{2+} , though with a lower translocation efficiency.

In addition to the mentioned Ca^{2+} -transporting proteins, Ca^{2+} -binding proteins like calsequestrin, triadin, HRC (see section 1.3.3), and calmodulin are critical to ensure and modulate excitation-contraction coupling. Calsequestrin (CASQ) represents a calcium-binding protein localizing to the SR lumen of vertebrates (MacLennan and Wong, 1971; Ikemoto et al., 1972; Wang et al., 2020, e.g., reviewed in Knollmann, 2009; Györke et al., 2009; Royer and Rios, 2009; Woo et al., 2020). The ability of one CASQ protein to bind up to 80 Ca^{2+} ions renders this protein an essential factor to build up the very high SR-luminal Ca^{2+} level prior to systole in vertebrate myocytes (Park et al., 2004). In addition, calsequestrin confers luminal Ca^{2+} sensitivity of the RyR either directly or via the intermediate proteins junctin and triadin (e.g., Szegedi et al., 1999; Zhang et al., 1997; reviewed in Marty, 2015). Both junctin and triadin are only transcribed in mammals, span the SR membrane, and build the Ca^{2+} release complex (CRC) together with calsequestrin, RyR, and other proteins (see section 1.2.3).

A highly conserved Ca^{2+} -binding protein in vertebrates and invertebrates is calmodulin (CaM; Cheung, 1970; Kakiuchi and Yamazaki, 1970; Copley et al., 1999). As a tremendously versatile calcium sensor that gets activated upon binding of Ca^{2+} , it can interact with hundreds of different proteins (Yap et al., 2000; Ikura, 2006; Andrews et al., 2020). Besides its function of modulating the activity of the LTCCs (Peterson et al., 1999; reviewed, e.g., in Ben-Jhony and Yue, 2014), it was also shown that calmodulin affects the Ca^{2+} sensitivity of the RyR (e.g., Seiler et al., 1984; Tripathy et al., 1995; Fruen et al., 2000; Rodney et al., 2000; Gong et al., 2019). Moreover, CaM is an activator

of the Ca^{2+} -calmodulin-dependent protein kinase CaMK, which plays a role in β -adrenergic signaling (e. g., reviewed in Bers, 2008; Mattiazzi and Kranias, 2014; see also section 1.2.4).

In contrast to the previously described contraction initiation mechanism of striated muscles, vertebrate smooth muscles exhibit some differences especially regarding ECC. Thus, smooth muscles contraction is not exclusively triggered by signals of the nervous system. Instead, also activation of GPCRs coupled to inositol 1, 4, 5-trisphosphate receptor (IP_3R)–mediated Ca^{2+} release and stretch-activated conductances are capable of initiating contraction (Figure 2; Lin et al., 2016; Sanders and Koh, 2007). As in striated muscles, depolarization of the smooth muscle sarcolemma leads to a cytosolic Ca^{2+} -influx via LTCCs, but the Ca^{2+} causes not primarily opening of RyR but binds to cytosolic calmodulin. In its Ca^{2+} -bound state, calmodulin activates the myosin light-chain kinase (MLCK), which then phosphorylates the myosin of thick filaments, resulting in smooth muscle contraction (reviewed, e.g., by Kuo and Ehrlich, 2015). Stretch activation (SA) is not exclusively restricted to smooth muscles; one type of SA also plays a crucial role in other muscles with rhythmic activity, especially in insect flight muscles or, to some extent, in the human heart (e.g., Pringle, 1949; Steiger 1971; Bullard and Pastore, 2019; reviewed by Campbell and Chandra, 2006). Up to now, the exact functional mechanism of SA is not fully understood. However, SA can be characterized, i.a., by the occurrence of enhanced actin-myosin cross-bridges associated with a delayed boost in force as a reaction to an increase of the sarcomere length (e.g., Wu et al., 2010; Perz-Edwards et al., 2011; Sanfelice et al., 2016).

Numerous human myopathies and cardiomyopathies are related to the impairment of sarcomere structure or mishandling of calcium during muscle or heart contraction (e.g., reviewed by Hasenfuss and Pieske, 2002; Gorski et al., 2015a). Familial hypertrophic cardiomyopathy (familial HCM or FHC), for example, is also known as the “disease of the sarcomere” (Thierfelder et al., 1994) because various mutations in several genes encoding for different sarcomeric components have been identified as elicitors for FHC (e.g., reviewed by Clark et al., 2002; Geske et al., 2018). Nevertheless, not only FHC but many other myopathies and different forms of muscular dystrophy (e.g., Limb-Girdle MD, Duchenne MD, Beckers MD) can be related to such mutations. Moreover, the complete loss of one of the central ECC components is usually associated with human perinatal death.

With respect to their abundance, skeletal muscle myopathies that are associated with malfunction of the RyR or the Calcium release complex (CRC)/couplon are summarized as “triadopathies” or “couplonopathies” (Dowling et al., 2014; Rios et al., 2015; Dulhunty et al., 2017), though the complete loss of RyR1 or specific subunits of DHPR is lethal. Up to now, hundreds of different mutations of the skeletal muscle *ryr1* gene or the cardiac *ryr2* have been identified as the cause of several congenital myopathies or cardiomyopathies, for example, malignant hyperthermia (MH), the RyR1-related myopathies (RyR1-RM) formerly known as central core disease (CCD), multi-minicore

disease (MmD) and centronuclear myopathy (CNM), catecholaminergic polymorphic ventricular tachycardia (CPVT), arrhythmogenic right ventricular dysplasia type 2 (ARVD2), and idiopathic ventricular fibrillation in cardiac muscle (George et al., 2007; Treves et al., 2008; Leenhardt et al., 2012; reviewed, e.g., in Meissner, 2017; Kushnir et al., 2018). Some of the causative *ryr* mutations result in a Ca^{2+} leakage from the lumen of the SR into the cytosol. SR Ca^{2+} leak via RyR is not only related to muscle and cardiac malfunction (reviewed, e.g., in Hernandez-Ochoa et al., 2015; Kushnir et al., 2018; Jungbluth et al., 2018) but can be as well a factor in the onset of Alzheimer's disease (Oules et al., 2021), cancer (Waning et al., 2015), and diabetes (Santulli et al., 2015).

In comparison to the fatal consequences of RyR loss, the knockout of other Ca^{2+} handling proteins like CSQ, triadin, junctin, or FKBP12 is normally not related to those severe effects. However, mutations in their encoding genes can as well result in the development of a myopathy or cardiomyopathy (e.g., Leenhardt et al., 2012; Beghi et al., 2020; Titus et al., 2020; Wang et al., 2020). In addition to SR Ca^{2+} leak and reduced or elevated cytosolic Ca^{2+} content, defects in SR Ca^{2+} uptake and reduced SR calcium load are often associated with impaired calcium cycling/ECC in heart failure (reviewed by Gorski et al., 2015a). The latter are typically based on malfunctions of SERCA or regulators of the ATPase, underlining their importance for proper heart and muscle contraction.

1.2.3 The sarcoplasmic reticulum and SERCA are important for muscle relaxation

The sarcoplasmic reticulum functionality is crucial for successful ECC and muscle contraction (reviewed by Rossi and Dirksen, 2006; Sorrentino, 2011; Reddish et al., 2017). Thereby, several structural adaptations, including the formation of distinct SR subcompartments, ensure optimal translation of sarcolemmal depolarization into proper cycling of Ca^{2+} between the SR lumen and the cytosol (Figure 8-11). As transversely protruding and interconnected invaginations of the sarcolemma, the T-tubules (transverse tubules) allow for the fast and extensive transmission of sarcolemmal depolarization from the muscle surface to the interior of the three-dimensional muscle fibers where the LTCCs predominately localize to the so-called triad or junctional complex (Figure 10; Franzini-Armstrong and Porter, 1964; Franzini-Armstrong et al., 1999; Edwards et al. 2012). At the muscle triad, the T-tubule membrane localizes adjacent to a subcompartment of the SR network: the terminal cisternae of the junctional SR (Porter and Palade, 1957; Franzini-Armstrong and Porter, 1964; Peachey, 1965; Mitchell et al., 1983; reviewed, e.g., by Rossi et al., 2008; Barone et al., 2015). Generally, the SR forms a network surrounding each myofibril and can be distinguished in longitudinal regions (L-SR), terminal cisternae, and the junctional (jSR), all regularly aligned to the underlying sarcomeres (Figure 11; reviewed in Rossi and Dirksen, 2006; Sorrentino, 2011; Reddish et al., 2017). The L-SR is specialized for Ca^{2+} uptake to

terminate muscle contraction and builds a sarcotubular network surrounding the myofibrils, whereas the terminal cisternae are adapted for Ca^{2+} release to initiate contraction. This is mediated by RyRs, which are enriched at the terminal cisternae membrane facing the T-Tubule. This membrane is referred to as jSR. The triad junction is formed by a T-tubule and two associated SR junctional terminal cisternae, whereby junctophilin called proteins primarily mediate bridging (Takeshima et al., 2000). Close spatial proximity of LTCCs, RyRs, and the previously described CRC proteins (see also section 1.2.2) at the triad allows for efficient translation of sarcolemmal depolarization into Ca^{2+} release from the SR lumen (Figure 8; Figure 10).

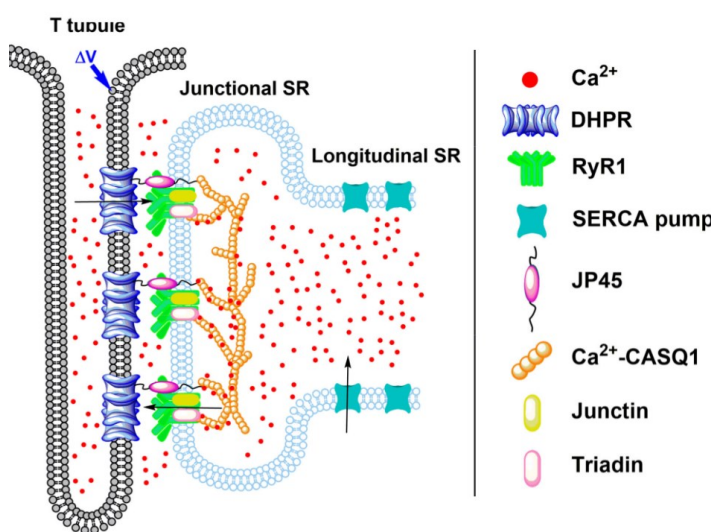


Figure 10 | Triadic junctions of skeletal muscles. DHPRs predominately localize at T-tubules, where they build a triad/junctional complex together with RYR1 present at the junctional SR. Besides RYR and DHPR, the bridging protein junctophilin (JP45) and the SR proteins junctin, triadin, and calsequestrin (Ca^{2+} -CASQ1) are also part of the triad. Triadic junctions allow for fast transmission of sarcolemmal depolarization into muscle contraction during DICR, while muscle relaxation is predominately achieved through the SERCA-mediated Ca^{2+} uptake into the longitudinal SR. Modified and adapted after (Reddish et al., 2017).

The architecture of the SR varies in different muscle types to meet the tissue's individual requirements. Junctions between sarcolemma and SR can be found in skeletal muscles and in cardiac cells of mammals, but they are more less absent in smooth muscles (reviewed in Wray and Burdyga, 2010) that also lack the elaborate T-Tubule network due to their alternative contraction initiation mechanism (see 1.2.2). In mammalian cardiac tissue, the junctional microdomain consisting of a T-tubule membrane and the contiguous jSR is referred to as a “dyad” or “dyadic junction” (Franzini-Armstrong et al., 1999; reviewed in Eisner et al., 2017; Lu and Pu, 2020), whereas LTCCs localizing at the muscle surface build so-called “peripheral couplings” with the jSR (Franzini-Armstrong et al., 1999; Scriven et al., 2000; Takeshima, 2002). In contrast to the skeletal muscle triads, dyads and peripheral couplings are characterized by only one jSR cisternae per dyad and CICR as the facilitated contraction initiation mechanism (and not DICR as in skeletal muscles).

Drosophila muscles also exhibit varying SR architecture. For example, the indirect flight muscles of arthropods are characterized by a less extensive SR network (e.g., Syme and Josephson, 2002) and the absence of triads, whereas the other somatic muscles possess triadic or dyadic junctions (Medioni et al., 2009; Lehmacher et al., 2012). This can be explained by the fact that contraction initiation in flight muscles is mostly triggered by

SA and does not rely on CICR. Therefore, close LTCC/RyR proximity is not required in this tissue.

The Sarco/Endoplasmic Ca^{2+} -ATPase SERCA predominately localizes to the membranes of the L-SR in accordance with the Z-disks and, though with less coverage, with the M-lines (Figure 11B; e.g., Sanyal et al., 2006; Rossi et al., 2008; Sorrentino et al., 2011). Accountable for the majority of the cytosolic Ca^{2+} removal after contraction, SERCA is the most critical protein responsible for the muscle relaxation phase initiation (Bers, 2008). The fact that the L-SR represents the largest part of the organelle, together with the high abundance of SERCA at its membranes, emphasizes the central significance of Ca^{2+} translocation into the lumen of the L-SR during muscle contraction cycles. Though the Ca^{2+} sequestering function of the SR has already been linked to contraction relaxation initiation by Setsuro Ebashi (Ebashi, 1961, Ebashi and Lippmann, 1962) and Annemarie Weber (Weber and Herz, 1961; Weber et al., 1963), the causative SERCA protein was first discovered by Wilhelm Hasselbach in 1961 (Hasselbach and Makinose, 1961; Hasselbach and Makinose, 1963, reviewed by Rüegg, 2016)

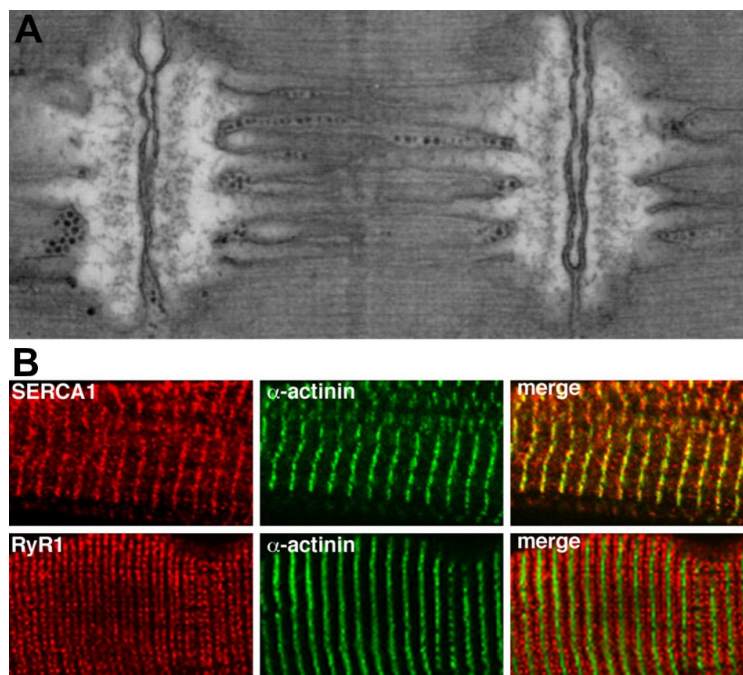


Figure 11 | The sarcoplasmic reticulum is subdivided into junctional and longitudinal domains. (A) In ground-breaking EM studies of fish muscles conducted in 1964 by Franzini-Armstrong and Porter, distinct SR domains can be distinguished: the longitudinal SR (L-SR) that spans the distance between two terminal cisternae and the junctional SR (jSR) adjacent to the T-tubules. SR domains are nicely aligned to the sarcomeric composition, with triads especially being present at the borders of A- and I-bands. **(B)** SERCA localizes to the L-SR surrounding the myofilaments at A- and I-bands. Due to the high density of the L-SR at Z-discs (marked by α -actinin), SERCA and α -actinin exhibit extensive colocalization. As a marker of the jSR, RyR1 predominately localizes at the borders of A- and I-bands, resulting in the alternation of RyR- and α -actinin signal. Shown are antibody stainings of longitudinal cryosections derived from skeletal muscle fibers. **(A)** is adapted and modified after (Franzini-Armstrong and Porter, 1964), and **(B)** is modified after (Sorrentino et al., 2011).

In the following years and decades, Hasselbach and many others further elucidated the exact molecular mechanism by which SERCA mediates muscle relaxation. However, the

fact that Ca^{2+} transport into the SR is coupled to ATP hydrolysis was also a finding of the early years (Hasselbach and Makinose, 1962).

SERCA belongs to the superfamily of P-type ATPases whose general function is the ATP-powered transport of cations across membranes. P-type ATPases can be divided into five subfamilies (P1-P5). Besides SERCA (P2A-ATPases), the subfamily of P2-ATPases further includes the calmodulin-binding Ca^{2+} -ATPases (P2B-ATPases), Na^+/K^+ - and H^+/K^+ -ATPases of animals (P2C-ATPases), and Na^+ -pumps of fungi (P2D-ATPases) (reviewed, e.g., by Kühlbrandt, 2004; Palmgren and Nissen, 2011; Dyla et al., 2020). SERCA is an asymmetrically oriented 110 kDa transmembrane protein that consists of a single polypeptide distributed over five domains: the cytosolic A (actuator)-, N (nucleotide-binding)-, and P (phosphorylation)-domains, and the transmembrane T (transport)-, and S (support)-domains (Figure 12A).

The catalytic mechanism of SERCA-mediated Ca^{2+} transport is characterized by ATP-hydrolysis, associated with autophosphorylation of the cytoplasmic part of the ATPase and cycling between a high (E1) and low (E2) affinity state (Figure 13; reviewed, e.g., by Apell, 2003; Kühlbrandt, 2004; Olesen et al., 2007; Møller et al., 2010; Palmgren and Nissen, 2011; Dyla et al., 2020; Aguayo-Ortiz and Espinoza-Fonseca, 2020a). Based on the findings elucidating the Na^+/K^+ -ATPase catalytic mechanism, cycling between the E1 and E2 state is also known as the Post-Albers cycle (Albers, 1967; Post et al., 1969; Post et al., 1972; Jorgensen, 1975). In general, phosphorylation state and bound ligands determine conformational changes of the P-type ATPases. Thereby, the tight coupling of the transmembrane and cytoplasmic domains allows ion translocation against steep concentration gradients (Geurts et al., 2020; reviewed in Inesi and Tadini-Buoninsegni, 2014). At the E1 state, the two ion binding sites residing at the transmembrane domains of SERCA are accessible from the cytosol and exhibit a high affinity for Ca^{2+} (K_{Ca}). The binding of two Ca^{2+} ions enables interaction of Mg^{2+} -ATP and the N-domain (E1-ATP state) followed by ATP hydrolysis coupled to autophosphorylation of a conserved aspartate at the DKTG motif of the P-domain and occlusion of the binding sites (Jensen et al., 2006; Sørensen et al., 2004; Toyoshima and Mizutani, 2004). This conformation is referred to as the E1P-ADP state.

Extensive structural rearrangements including an $\sim 120^\circ$ rotation of the A-domain (Olesen et al., 2007; Dyla et al., 2020) together with ADP release during a putative intermediate state (E2P-ADP and/or $[\text{Ca}_2]\text{E2P}$) finally lead to the reduction of Ca^{2+} affinity of the ion binding sites. Because the binding sites are now accessible through the SR lumen, the liberation of the two bound Ca^{2+} ions into the SR lumen can occur in the so-called luminal/extracellular or outward ion exchange pathway of the E2P state (Clausen and Andersen, 2010; Dyla et al., 2017).

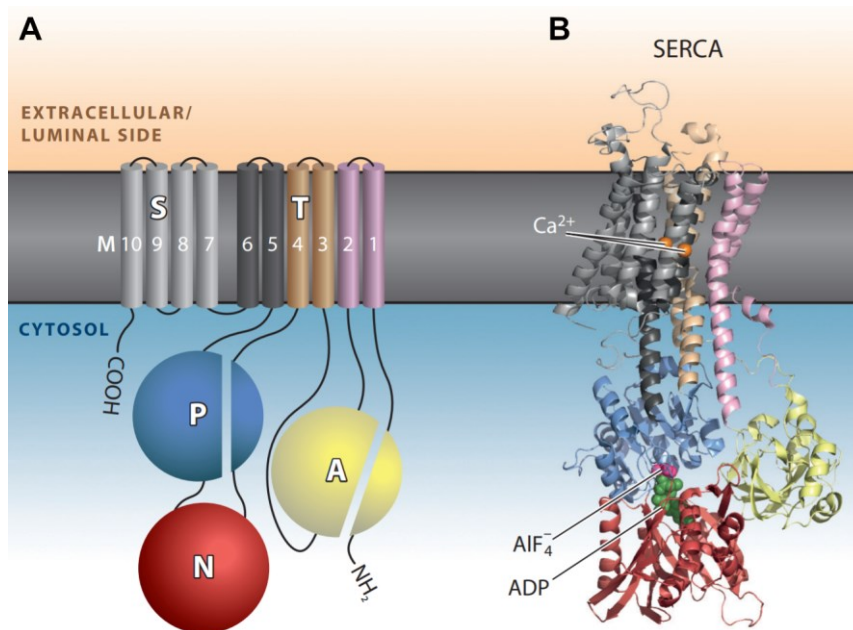


Figure 12 | Functional domains of SERCA. (A) Simplified scheme of the SERCA domain architecture. The transmembrane part of the ATPase comprises ten membrane-spanning helices building two domains and localizing to the SR membrane. Functions of the transmembrane support-domain (S) consisting of four helices (M7-M10, grey) and the transport-domain (T, M1-2, purple; M3-4, brown; M6-M5, anthracite) is substrate binding and translocation. Three cytosolic loops, together with an N-terminal part, build the three cytosolic domains: the actuator (A)-, nucleotide-binding (N)-, and phosphorylation (P)-domain. (B) SERCA crystal structure at the E1P-ADP state based on Protein Data Bank ID: 1T5T (Sørensen et al., 2004). Colors correspond to domain assignments in (A). Ca²⁺ ions bound to the substrate-binding sites of the T-domain are depicted as orange spheres. ADP (green) interacts with the N-domain of the cytoplasmic part, and the AIF₄⁻ (dark pink; phosphoryl transfer analog) mimics autophosphorylation of the P-domain. Modified and adapted after (Dyla et al., 2020).

In the next step of E1/E2 cycling (E2-Pi state), two or three counterions (H⁺), localized at the SR lumen in high abundance, access the binding sites of the transmembrane domain, thereby initiating dephosphorylation of the N-domain (Olesen et al., 2004; Lewis et al., 2012; Toyoshima et al., 2004). Finally, Pi is released (E2 state), and SERCA transforms into the E1 state resulting in the extrusion of the counterions into the cytosol (Figure 13). This part of the catalytic cycle is also known as the inward ion exchange/N-terminal pathway (reviewed by Bublitz et al., 2013). Both the luminal/extracellular and the inward ion exchange pathway are Mg²⁺-dependent. By interacting with the transmembrane binding sites, which also represent low-affinity Mg²⁺ sites, Mg²⁺ stabilizes the inward-open and outward-open conformations (Peinelt and Apell, 2002; Inesi et al., 2004; Olesen et al., 2007; Clausen and Andersen, 2010). In addition to the E1 state, SERCA can also transform into a Ca²⁺-free E1 state upon binding to the regulatory micropeptides sarcolipin and phospholamban (see section 1.2.4). At this state, E1/E2 cycling is inhibited. Under most conditions, E1/E2 cycling exhibits a distinct directionality (clockwise with respect to Figure 13) with two transported Ca²⁺ ions for each hydrolyzed ATP. However, partial reactions can be reversed under certain conditions, even though *in vivo* relevance of these findings remains unclear (e.g., Makinose and Hasselbach, 1971; de Meis et al., 1980; Dyla et al., 2017).

The P-type ATP cycling mechanism was predominately derived from structural data since it is possible to trap SERCA at different stages via the addition of ions, ATP analogs, and structural analogs to mimic phosphorylation, phosphoryl transfer, or phosphate release (Karlsen and Bublitz, 2016). Already in the year 1983, two-dimensional SERCA crystals were obtained and analyzed via electron microscopy (EM) by Dux and Martonosi as one of the first structural studies (Dux and Martonosi, 1983). In 2000, Toyoshima et al. determined the first SERCA X-ray crystal structure at 2.6 Å resolution (Toyoshima et al., 2000). This was the starting point for a downright race for higher resolutions, different conformational states, and isoforms (reviewed in Kühlbrandt, 2004; Møller et al., 2010; Toyoshima and Corvelius, 2013; Aguayo-Ortiz and Espinoza-Fonseca, 2020a) finally leading to 94 deposited SERCA crystal structures in the RCSB Protein Data Bank (state of data as of April 2022; Figure 13).

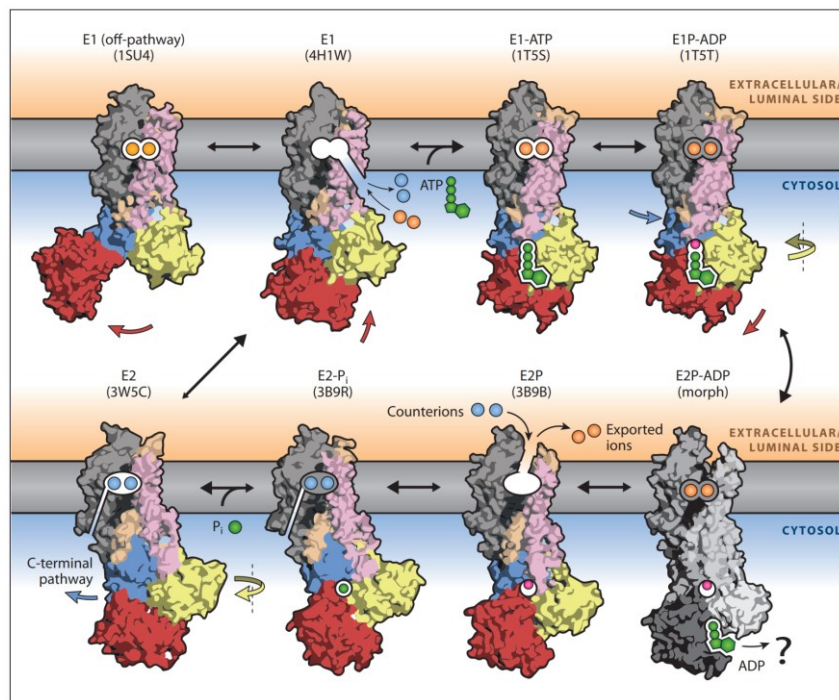


Figure 13 | Catalytic mechanism of SERCA-mediated Ca²⁺ transport. At the beginning of a new catalytic cycle, Ca²⁺ ions bind to the substrate-binding sites of the T-domain, which is accessible from the cytosol during the E1 state. This leads to a conformational movement of the N-domain (red) and subsequent ATP binding, resulting in the E1-ATP state. In the next step, ATP hydrolysis is coupled to autophosphorylation of the P-domain (blue), and the transmembrane substrate binding sites get occluded, resulting in the E1P-ADP state. The E2P-ADP state (greyscale) represents a putative intermediate state, a morph of E1P-ADP and E2P. However, after the release of the ADP, Ca²⁺ is delivered to the SR lumen, and counterions (H⁺) can now bind to the T-domain at the E2P state. During the transition into the E2-Pi state, SERCA gets dephosphorylated, and the release of the Pi finally leads to the conversion into the E1 state in which the counter-transported H⁺ ions are released. The E1 (off-pathway) state is characterized by the N- and P-domain detachment and displays one example of an inactive state. Shown are surface representations of SERCA structures with corresponding Protein Data Bank IDs in parenthesis underneath the names of respective states. The domain colors correspond to domain annotations in Figure 13. Ca²⁺ ions are depicted as orange spheres and H⁺ ions as blue spheres. ATP and bound ADP are shown in green, while the dark pink sphere marks phosphorylation of SERCA. Free Pi is depicted as a green sphere. In contrast to the white background of accessible binding sites, occluded binding sites exhibit a grey background color. Colored arrows indicate upcoming conformational shifts of domains. Background color saturation of the SR lumen (orange) and cytosol (blue) correlate with respective ion (Ca²⁺ or H⁺) excess. Modified after (Dyla et al., 2020).

In more recent years, insights derived from crystallographic data gets completed by advanced biophysical and microscopic data on the atomic level (e.g., Dyla et al., 2017; Raguimova et al., 2018; reviewed by Aguayo-Ortiz and Espinoza-Fonseca, 2020a).

Different ligands like thapsigargin, orthovanadate, or complex peptide toxins such as mastoparan, can bind to SERCA, thereby trapping the enzyme at distinct conformational states and inhibiting further E1/E2 cycling. On the one hand, this was extensively used as a tool to obtain the numerous crystal structures. On the other hand, specific SERCA inhibition could help to elucidate the physiological function of the ATPase (reviewed, e.g., by Michelangeli and East, 2011).

SERCA localizes to the SR/ER membranes of all eukaryotic cells, representing one of the most prevalent proteins. In vertebrates, three SERCA genes (*ATP2A1*, *ATP2A2*, and *ATP2A3*) encode three isoforms of the ATPase: SERCA1, SERCA2, and SERCA3. However, alternative splicing of the genes results in the translation of 12 proteins: SERCA1a/b, SERCA2a/b/c/d, and SERCA3a/b/c/d/e/f (Periasamy and Kalyanasundaram 2007; reviewed by Hovnanian, 2007; Brini and Carafoli, 2009). The different isoforms are expressed in different tissues at different stages, thereby exhibiting functionally distinct properties to meet the unique requirements of their individual expression surrounding (see Table 1). SERCA2b displays some peculiarities regarding its structure and properties. In comparison to SERCA1 and SERCA3, SERCA2 was documented to exhibit the highest affinity for Ca^{2+} (Chandrasekera et al., 2009). In addition, the SERCA2b isoform holds an 11th transmembrane helix, leading to the formation of a C-terminal ER/SR-luminal extension peptide with a high affinity for Ca^{2+} that probably harbors regulatory function (Campbell et al., 1992; Vandecaetsbeek et al., 2009; Gorski et al., 2012; Inoue et al., 2019).

In contrast to the three expressed SERCA genes in vertebrates, invertebrates possess only one gene for the ATPase, with two exceptions. The parasite *Schistosoma mansoni* was shown to have two genes encoding for SERCA, and the leech *Helobdella robusta* even has three SERCA genes (de Mendonça et al., 1995; Talla et al., 1998; Altshuler et al., 2012). Although most invertebrates possess one SERCA gene, some of them exhibit expression of different isoforms due to alternative splicing as in vertebrates. Examples of this are the crustacean *Artemia franciscana* (Escalante and Sastre, 1993; Escalante and Sastre, 1994) and the nematode *Caenorhabditis elegans* (Zwaal et al., 2001). Also splicing of the *Drosophila* SERCA gene gives rise to at least two isoforms (Varadi et al., 1989; Magyar and Varadi, 1990; Magyar et al., 1995).

Tight regulation of P-type ATPase activity on a short timescale is crucial regarding different aspects. On the one hand, these enzymes consume high amounts of ATP, so misregulation would lead to energy dissipation which is not manageable for a healthy organism in the long term (Smith et al., 2013). Moreover, the energy available from ATP would be counteracted by the electrochemical gradient built by a non-regulated P-type ATPase.

Table 1 | SERCA genes and isoforms present in vertebrates (SERCA expression levels are based on respective references and Periasamy and Kalyanasundaram, 2007)

SERCA gene	Isoform	Expression	References	Interacting regulin*
<i>ATP2A1</i>	1a	Adult fast-twitch skeletal muscles (strong expression)	Brandl et al., 1987 Korzak et al., 1988 Zhang et al., 1995	MLN SLN
	1b	Fetal fast-twitch skeletal muscles (strong expression)	Brandl et al., 1986 Zhang et al., 1995	
<i>ATP2A2</i>	2a	Adult cardiac muscles (strong expression) Adult slow-twitch skeletal muscles (strong expression) Fetal slow and fast-twitch skeletal muscle (weak expression) Smooth muscles (weak expression)	MacLennan et al., 1985 Lytton and MacLennan 1988 Lytton et al., 1989 Verboomen et al., 1992 Verboomen et al., 1994 Zarain-Herzberg and Alvarez-Fernandes 2002	PLN DWORF
	2b	Ubiquitous (weak expression)	Gunteski-Hamblin et al., 1988 Lytton and MacLennan 1988 Lytton et al., 1989 Verboomen et al., 1992 Verboomen et al., 1994 Zarain-Herzberg and Alvarez-Fernandes 2002	ALN
	2c	Cardiac muscle (moderate expression) Monocytes and hematopoietic, epithelial, and mesenchymal cell lines (weak expression)	Gelebart et al., 2003 Dally et al., 2006	
	2d	Skeletal muscle (weak expression)	Kimura et al., 2005	
<i>ATP2A3</i>	3a	Ubiquitous (weak expression) Slightly elevated levels in hematopoietic cell lineages, lung, kidney, colon, pancreas and salivary glands trachea	Burk et al., 1989 Anger et al., 1993 Bobe et al., 1994 Wuytack et al., 1994 Wu et al., 1995	ELN
	3b		Dode et al., 1998 Poch et al., 1998 Martin et al., 2002	
	3c		Dode et al., 1998 Martin et al., 2002	
	3d		Martin et al., 2002	
	3e		Martin et al., 2002	
	3f		Bobe et al., 2004	

* see section 1.2.4 for references

On the other hand, the enzyme must maintain the respective resting ion concentration, and an excessive decrease in its activity would have detrimental effects. Therefore, accommodation of the exact activity level can be achieved by a broad range of mechanisms: auto-inhibition, the chemical environment, adjustment of the enzyme

expression, post-translational modifications, or interaction with other proteins or peptides (reviewed by, e.g., Kühlbrandt et al., 2004; Periasamy and Kalyanasundaram, 2007; Calderon et al., 2014; Stammers et al., 2015; Dyla et al., 2020) Since SERCA activity is not regulated via auto-inhibitory mechanisms, the remaining are more critical to ensure proper functionality of the enzyme. Among the factors of the chemical environment that modulate SERCA activity, Ca^{2+} concentration and pH are the most important. If the SR luminal Ca^{2+} exceeds the dissociation constant from the low affinity binding sites of SERCAs transmembrane domain, $\text{Ca}^{2+}/\text{H}^{+}$ exchange is circumvented resulting in uncoupling of ATP hydrolysis and ion transport (reviewed by Inesi et al., 2014). Uncoupling of SERCA is also triggered through a high pH and associated reduction of H^{+} concentration. This phenomenon is known as “slippage of the pump” and probably plays a role in heat production and thermogenesis (de Meis et al., 1997; de Meis et al., 2005; Bal et al., 2012; see also section 1.2.4)

Transcriptional regulation of SERCA expression is mediated by the hormones thyroid and adiponectin (reviewed by Periasamy and Kalyanasundaram, 2007; Stammers et al., 2015). Thyroid hormone was shown to regulate the expression of SERCA2a in cardiac tissue (Rohrer and Dilmann, 1988; Nagai et al., 1989; Zarain-Herzberg et al., 1994; Hartong et al., 1994; Tuyl et al., 2004), but it acts on the SERCA inhibitor phospholamban as well (Kimura et al., 1994; Kiss et al., 1994; see section 1.2.3). This is probably also true for the adipocyte-derived peptide hormone adiponectin, which can restore SERCA2 activity to baseline levels (Guo et al., 2013). Of note, adiponectin is also an important peptide in insulin signaling (Figure 3). Another known factor affecting the expression of SERCA1 and SERCA2 is exercise (reviewed in Stammers et al., 2015). Interestingly, exercise increases SERCA2a protein content (e.g., Wisløff et al., 2002), whereas effect on SERCA1 protein content ranges between reduction and increase, dependent on the respective organism, training, and muscle fiber type (e.g., Green et al., 2003; Morissette et al., 2014).

Besides modulation of SERCA expression, microRNA interference and post-translational modification of the translated protein are documented mechanisms to adjust the activity of the enzyme (Gurha et al., 2012; Wahlquist et al., 2014; Kumarswamy et al., 2012)

Post-translational modifications that directly affect SERCA activity include glutathionylation, SUMOylation, glycosylation, O-glcNAcylation, nitration, and acetylation (reviewed in Stammers et al., 2015). Glutathionylation and SUMOylation of SERCA mRNA increase SERCA2a activity and can rescue SERCA2a function in heart failure (Adachi et al., 2004; Kho et al., 2011).

Several proteins and peptides modulate SERCA activity via direct interaction. The histidine-rich Ca^{2+} -binding protein (HRC; Hofmann et al., 1991), calumenin (Yabe et al., 1997), and sarcalumenin (Leberer et al., 1990; Jiao et al., 2012) are all expressed in mammals, localize to the SR lumen and directly bind to SERCA and thereby affect its activity. HRC (see also Figure 8) and calumenin are Ca^{2+} -storage proteins that bind Ca^{2+} with low affinity and inhibit SERCA by interacting with SR luminal loops of the

transmembrane domain (Arvanitis et al., 2007; Sahoo and Kim, 2008; Sahoo et al., 2009). Correspondingly, knockout of HRC leads to muscle hypercontractility caused by elevated SERCA activity (Park et al., 2013). Vice-versa, overexpression of calumenin was shown to result in hyperinhibition of SERCA2 (Sahoo and Kim, 2008). Nevertheless, the principal SERCA-regulatory mechanism is the direct interaction with SR membrane integral peptides, and some of the before-mentioned SERCA regulatory mechanisms also act through phospholamban (see section 1.2.4).

The genetic manipulation of SERCA in different model organisms was crucial for understanding the essential physiological functions of the pump. Phenotypes of animals harboring SERCA mutations provided important insights regarding SERCA functionality and significance in Ca^{2+} cycling. Besides the mouse model, significant work was also done in the *Drosophila* model system (reviewed by Chorna and Gaiti, 2012). By analyzing conditional *Drosophila Ca-P60A/dSERCA* mutants, Sanyal et al. could show that inhibition of the ATPase greatly impacts neuromuscular physiology and can paralyze larvae (Sanyal et al., 2005). Further studies elaborated on effects of SERCA activity on heartbeat frequency and rhythmicity in *Drosophila* (Sanyal et al., 2006; Desai-Shah et al., 2010; Abraham and Wolf, 2013). Furthermore, the implication of SERCA in Notch signaling was investigated in *Drosophila*, thereby identifying the ATPase as a possible therapeutic target to treat cancer (Periz and Fortini, 1999; Roti et al., 2013).

Concomitant with their central role in muscle and heart physiology, dysregulation or aberrant function of SERCA has been implicated in the pathology of several human diseases (e.g., reviewed in Brini and Carafoli, 2009; Hovnanian, 2007; Chemaly et al., 2018). For example, distinct mutations in the SERCA coding genes cause Brody myopathy and the skin disorder Darier's disease. Brody myopathy, or Brody's disease is a rare autosomal genetic disorder elicited by loss-of-function mutations of the *ATP2A1* gene (Brody, 1969; Karpati et al., 1986; Odermatt et al., 1996; Novelli et al., 2004; reviewed by Brini and Carafoli, 2009). The mutations lead to impairments of SERCA1 functionality resulting in heterogeneous symptoms related to delayed skeletal muscle relaxation elicited by a slow-down of the SERCA1 mediated Ca^{2+} uptake into the SR (Benders et al., 1994). Nevertheless, relatively common symptoms of Brody's disease are skeletal muscle cramping and stiffening induced by exercise or low temperatures (Odermatt et al., 1996; Novelli et al., 2004).

The rare autosomal dominant skin disorder Darier's disease (or Darier-White's disease/keratosis follicularis) is caused by mutations in the *ATP2A2* gene (Sakuntabhai et al., 1999; reviewed, e.g., by Foggia and Hovnanian, 2004; Dhitavat et al., 2004; Hovnanian, 2007). Darier's disease is characterized by a loss of cell-to-cell adhesion in the suprabasal epidermis layer resulting in skin lesions, wart-like blemishes, and abnormal keratinization. Up to now, it remains unclear why the disease is restricted to specific cells of the epidermis. However, concerning the crucial importance of SERCA2 in

different muscle types, the presence of compensatory mechanisms for reduced SERCA2 activity in these tissues is very likely (Hovnanian, 2007).

In addition to Brody's and Darier's disease, impairment of SERCA activity has been linked to several other disorder phenotypes. For example, a functionally decreased SERCA pump is often detectable in human heart failure (HF) patients as well as in HF animal models (reviewed by Brini and Carafoli, 2009; Gorski et al., 2015a). In recent years, restoring SERCA2 in failing hearts via gene therapy and other therapies targeting SERCA became a research topic of great interest. Surprising at first glance, SERCA malfunction has also been related to cancer and diabetes (e.g., reviewed in Zarain-Herzberg et al., 2014; Stewart et al., 2015; Chemaly et al., 2018; Pagliaro et al., 2021).

1.2.4 Activity of SERCA is modulated by binding of regulin peptides

The most important mechanism to modulate SERCA activity is the reversible direct binding of SR transmembrane micropeptides, also called "regulins" or "regulin peptides". Up to now, six regulins have been identified in vertebrates. Phospholamban (PLN), sarcolipin (SLN), myoregulin (MLN), another-regulin (ALN), and endoregulin (ELN) represent inhibitors of the Ca²⁺-ATPase, whereas DWORF was shown to enhance SERCA activity (Figure 14; reviewed by Payre and Desplan, 2016; Primeau et al., 2018; Rathod et al., 2021). The peptides are generally expressed in a tissue-specific manner, localize to the SR/ER membrane, and preferentially interact with the SERCA isoform of the respective tissue (see Table 1). However, by far the best characterized regulatory peptide happens to be phospholamban. The structural base of SERCA/PLN interaction has been studied extensively, making it one of the best understood transporter-peptide interactions (e.g., reviewed in MacLennan and Kranias, 2003; Primeau et al., 2018; Rathod et al., 2021). Initially described in 1975 (Kirchberger et al., 1975; reviewed in Katz, 1998), PLN consists of 52 amino acids and has a size of 6.1 kDa. The peptide is composed of an N-terminal cytoplasmic helix (~aa 1-20; domain Ia) holding with Ser¹⁶ and Thr¹⁷ two potential phosphorylation sites, a flexible linker (~aa 21-30; domain Ib), and a highly conserved single transmembrane helix (~aa 31-52; domain II) harboring the SERCA-interaction sites (Figure 14; Simmerman et al., 1986; Verardi et al., 2011; reviewed by MacLennan and Kranias 2003). The linker enables the peptide to switch between two configurations depending on the phosphorylation of the cytoplasmic domain: the tilted T-state or the more elongated R-state (e.g., Traaseth et al., 2009; Gopinath et al., 2021).

Like the other regulins, PLN binds to SERCAs inhibitory cleft that is built by the transmembrane helices M2, M6, and M9 (Figure 14C) at E2 states and thereby decreases Ca²⁺ affinity (K_{Ca}) of the ATPase (Reddy et al., 1995; Akin et al., 2013). The Thr⁸⁰⁵ residue of SERCAs M6 helix (Toyoshima et al., 2003) and the PLN

transmembrane residue Asn³⁴ are the most critical residues for inhibition since mutation of Asn³⁴ is concomitant with a loss of inhibitory function (Kimura et al., 1997; Trieber et al., 2005; Trieber et al., 2009). Usually, PLN interacts with the Ca²⁺-free SERCA conformation, holding the ATPase in a metal ion-free E1-like state, also known as E1-Like-PLN (Figure 13; Figure 14; Akin et al., 2013; Espinoza-Fonseca et al., 2015). In this state, SERCA affinity for Ca²⁺ is markedly reduced. Nevertheless, it was shown that PLN also binds to Ca²⁺-bound SERCA conformations, though with lower affinity (Bidwell et al., 2011). PLN can occur as a monomer or as an oligomer, whereby the pentamer represents the most abundant oligomeric form (Simmerman et al., 1986). Since the monomeric PLN is preferentially bound to SERCAs inhibitory groove, monomeric PLN represents the inhibitory form (Autry and Jones, 1997; Kimura et al., 1997; Thomas et al., 1998). Additionally, more recent data finally explain the early finding that PLN pentamers could not only represent inactive storage forms (Chu et al., 1998).

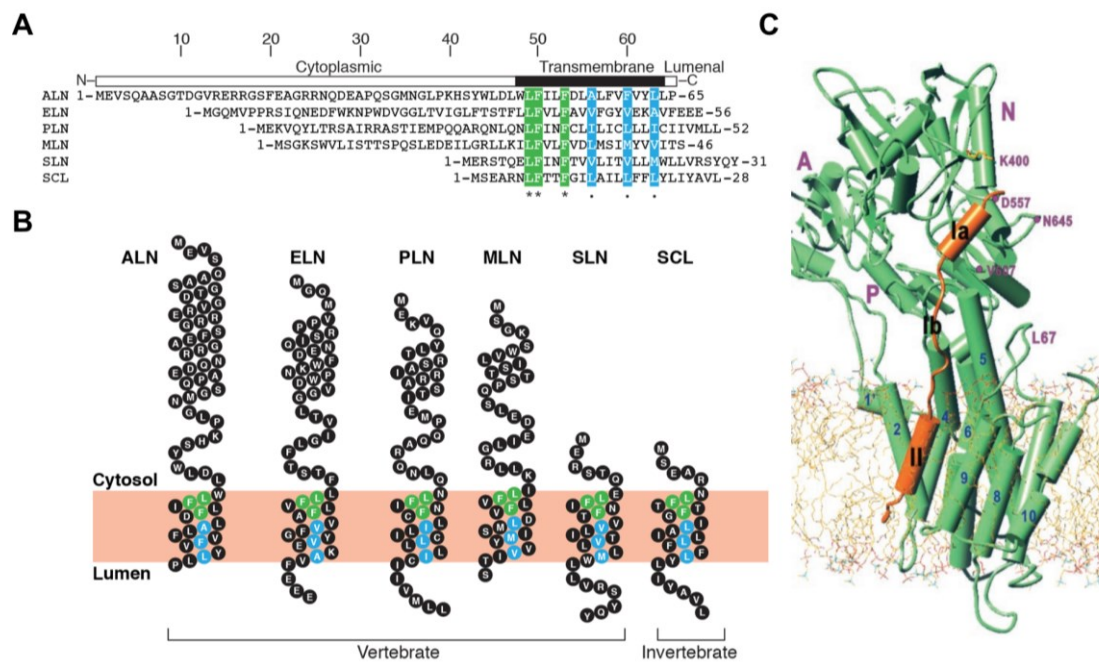


Figure 14 | Comparison of SERCA-inhibitory peptides. (A) Sequence alignments of the SR membrane integral regulins another-regulin (ALN), endoregulin (ELN), phospholamban (PLN), myoregulin (MLN), sarcolipin (SLN), and sarcolamban A (SCLA) are shown. All peptides consist of a cytoplasmic domain of variable length, a transmembrane domain, and a rather short SR-luminal domain. Identical conserved transmembrane residues are marked in green (*), and transmembrane residues with similar properties are depicted in blue (.). (B) While ALN, ELN, PLN, and MLN exhibit rather large cytoplasmic parts, SLN and SCL harbor minor cytoplasmic domains. Additionally, SLN and PLN also possess a luminal domain of comparable size. The peptide's well-conserved transmembrane domains form the canonical interaction face with SERCA within the SR membrane. The depicted SCL protein corresponds to SCLA from *Drosophila*. Despite the SCLA sequence, shown amino acid sequences are derived from mouse. (C) Atomic model of PLN (orange) bound to SERCA1a (green) in a lipid bilayer. Coupled via a linker region (Ib) to the TM helix, the PLN cytoplasmic helix (Ia) interacts with SERCAs N-domain. The model of SERCA is based on a rabbit SERCA1a crystal structure at the E2 state (Protein Data Bank ID: 1IWO; Toyoshima and Nomura, 2002), and the PLN model was derived from two NMR structures (Protein Data Bank IDs: 1FJK and 1PLP) refined with molecular dynamics and energy minimization. SERCAs cytoplasmic domains are indicated as violet letters (A- N-, and P-domain), and TM helices are highlighted with blue numbers. (A) and (B) are modified and adapted after (Anderson et al., 2016), (C) is modified after (Toyoshima et al., 2003).

Instead of binding to the canonical inhibitory groove, the pentamer was indeed found to bind to an accessory site of the Ca^{2+} -ATPase (Glaves et al., 2019; Alford et al., 2020). Interestingly, these experiments and molecular dynamics simulation propose an activating role for this non-canonical interaction (Glaves et al., 2019; Glaves et al., 2011; Stokes et al., 2006). In this manner, the PLN pentamer interacts with SERCA's M3 helix inducing repositioning of the PLN cytoplasmic domain. Nevertheless, the physiological relevance of this probably activating interaction has to be proved.

Critical for the inhibitory effect exerted by PLN are different factors: the molar ratio of PLN and SERCA, the Ca^{2+} concentration [Ca^{2+}], as well as the oligomerization and phosphorylation state of the peptide. The fact that all these aspects are linked to each other renders this system rather complex. PLN-dependent modulation of SERCA activity is terminated at high cytosolic Ca^{2+} concentrations and through phosphorylation of PLN's cytoplasmic helix (Tada et al., 1975; James et al., 1989). At low calcium concentrations (~ 0.1 to $1.0 \mu\text{M}$), inhibition through PLN reaches its maximum, whereas SERCA exhibits maximal activity (V_{max}) at high Ca^{2+} concentrations (~ 1.0 to $10 \mu\text{M}$) if bound to PLN (Figure 17; Cantilina et al., 1993; Asahi et al., 2000; Fernandez-de Gortai and Espinoza-Fonseca, 2018; Raguimova et al., 2020).

At one-to-one molar stoichiometry, PLN monomers bind to SERCA, and the elicited inhibitory effect is maximal (e.g., Glaves et al., 2019). At higher PLN concentrations, the peptide tends to organize in oligomers, thereby reducing inhibition through monomers or even activating the ATPase through interaction with PLN pentamers (see above; Glaves et al., 2019; Trieber et al., 2005; Trieber et al., 2009). On the one hand, phosphorylation of PLN Ser¹⁶ and/or Thr¹⁷ directly affects the equilibrium of PLN monomer/oligomer dynamics (Cornea et al., 1997). On the other hand, phosphorylation results in the reorganization of the PLN N-terminal cytoplasmic domain into the R-state so that it can interact with SERCA's cytoplasmic domain, probably inducing relief of inhibition (Karim et al., 2006; Sugita et al., 2006; Gustavsson et al., 2013; Aguayo-Ortiz and Espinoza-Fonseca, 2020b). However, up to now, it remains unclear whether PLN dissociates from SERCA as a result of phosphorylation (dissociation model) or if the SERCA-PLN complex is instead maintained, hence allowing for Ca^{2+} translocation due to conformational change of the transmembrane domain induced by phosphorylation (subunit model; see also Primeau et al., 2018; Alford et al., 2020).

The functionality of PLN dependent regulation of SERCA is to modulate cardiac contractility. By phosphorylation of PLN in response to β -adrenergic stimulation, inhibition of SERCA is relieved, resulting in enhanced SR Ca^{2+} load and faster rates of contraction and relaxation (Figure 15). Therefore, the β -adrenergic system is crucial to rapidly increase physical performance as part of the fight-or flight response.

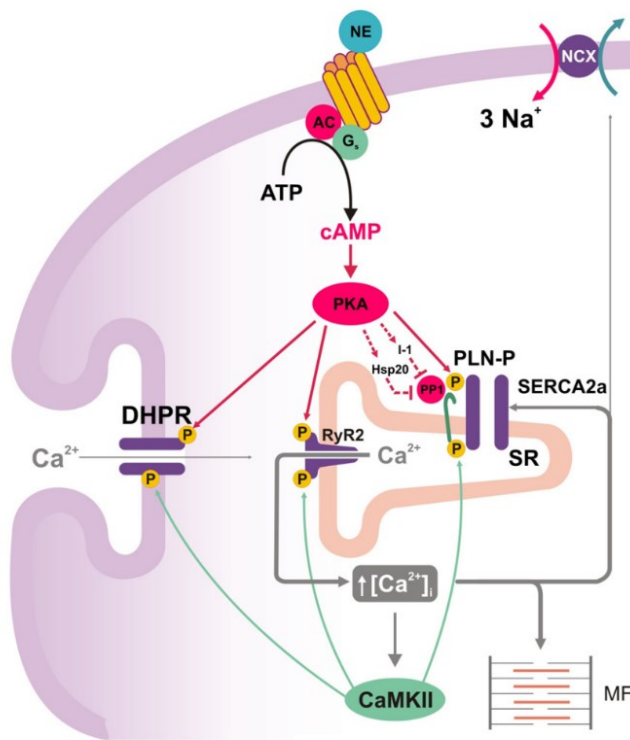


Figure 15 | Phospholamban is phosphorylated through the β -adrenergic pathway. Scheme of β -adrenergic stimulation and CaMKII (calcium/calmodulin-dependent protein kinase II) induced phosphorylation at cardiac myocytes. The binding of noradrenaline (NE) to the β -adrenergic receptor (yellow) results in cyclic AMP (cAMP) production mediated by the adenylate cyclase (AC) and G protein (G). cAMP activates protein kinase A (PKA), leading to phosphorylation of different targets like DHPR, RyR2, and the main target PLN. Phosphorylation of the latter relieves SERCA2a inhibition. Dephosphorylation of PLN is mediated by PP1 (protein phosphatase 1), itself inhibited by phosphorylated I-1 (inhibitor-1) and Hsp20 (heat shock protein 20). Another consequence of PKA activation is the rise in cytoplasmic Ca^{2+} concentration that initiates further phosphorylation of Ca^{2+} handling proteins through CaMKII. In summary, relief of PLN mediated SERCA inhibition combined with the activation of different Ca^{2+} handling proteins results in faster cardiac contraction/relaxation rates. Modified after (Mattiuzzi and Kranias, 2014).

As a central target of β -adrenergic signaling, PLN is phosphorylated by the protein kinase A (PKA; e.g., Tada et al., 1974; Kranias and Solaro, 1982; Chen et al., 2007; reviewed by MacLennan and Kranias, 2003), protein kinase B (PKB/Akt; Catalucci et al., 2009) and calcium/calmodulin-dependent protein kinase II (CaMKII; see also section 1.2.2; e.g., Kirchberger et al., 1982; Movsesian et al., 1984; Simmerman et al., 1986). The β -adrenergic pathway is triggered by sympathetic nervous system activation. As a result, catecholamines, such as adrenaline or noradrenaline, bind to the β -adrenergic receptor, a GPCR localizing at the surface of the muscles. Activation of the GPCR (see also Figure 2) initiates the production of the second messenger cyclic AMP (cAMP) through the adenylate cyclase (Kirchberger et al., 1972). The cAMP then stimulates PKA that in turn phosphorylates several cardiac proteins, like LTCC (e.g., reviewed by Kamp and Hell, 2000), troponin I (e.g., Li et al., 2000), RyR (see 1.2.2) or PLN. Besides targeting PLN monomers at the Ser¹⁶ residue of the cytoplasmic domain, it was shown that PKA could also phosphorylate PLN bound to SERCA or PLN organized in pentamers or even support PLN pentamerization (Cornea et al., 1997; Ceholski et al., 2012; Wittmann et al., 2015).

Phosphorylated PLN gets reactivated for SERCA inhibition through dephosphorylation mediated by the protein phosphatase 1 (PP1; Kranias, 1985; MacDougall et al., 1991; Steenaert et al., 1992). PP1 is organized in a regulatory complex residing at the SR membrane. Besides PP1, PLN, PKA, and SERCA, this complex was shown to include further a kinase anchoring protein, inhibitor-1 (I-1), small heat shock protein 20 (Hsp-20), the HS-1 associated protein X-1 (HAX-1), small ubiquitin-related modifier (SUMO-

1), and phosphodiesterase (Figure 15; reviewed in, e.g., Kranias and Hajjar, 2012; Mattiazzi and Kranias, 2014). In addition, the phosphorylation of the different Ca^{2+} -handling proteins also leads to an increase in the cytosolic $[\text{Ca}^{2+}]$. Elevated $[\text{Ca}^{2+}]$, in turn, activates CaMKII that further amplifies the phosphorylation effect by targeting the Thr¹⁷ residue of PLN (reviewed e.g., by Mattiazzi and Kranias, 2014). Dephosphorylation of Thr17 is facilitated by the SR-luminal localized protein phosphatase 2Ce (PP2Ce; Akaike et al., 2017). In summary, PLN phosphorylation is the main determinant of the β -adrenergic response and therefore represents the key mediator for eliciting positive cardiac chronotropic, inotropic, and lusitropic/relaxant effects.

In accordance with the expression of the SERCA2a isoform as the primary interaction target (see table 1), PLN can be found in cardiac (at ventricles and in lower amounts in atrial tissue), slow-twitch skeletal and smooth muscles (e.g., Bokník et al., 1999; Vangheluwe et al., 2005). Interestingly, expression with other regulins like sarcolipin is apparent in some tissues, perhaps conciliating SERCA superinhibition (Asahi et al., 2003; Vangheluwe et al., 2005; Fajardo et al., 2013). In contrast to PLN, SLN is predominately expressed in fast-twitch skeletal muscles, with lower amounts of the peptide being present in slow-twitch skeletal and atrial muscles of vertebrates (e.g., Odermatt et al., 1997; Odermatt et al., 1998; Minamisawa et al., 2003; Babu et al., 2007; Fajardo et al., 2013). Agreeing with its expression pattern, SLN is the primary regulator of the SERCA1a isoform. In 1972, SLN was discovered as a proteolipid that coprecipitates with SERCA (MacLennan, 1974). It was not until 1992 that the amino acid sequence of this proteolipid was determined and named sarcolipin (Wawrzynow et al., 1992). Even though the authors speculated that sarcolipin could be “a modulator of the ATPase”, first extensive characterization as SERCA-inhibitory peptide happened to be in the year 1998 (Odermatt et al., 1998). As a homolog of PLN, the SLN peptide exhibits some structural similarities to the first described regulin but substantial differences regarding the mechanism of SERCA inhibition as well (reviewed in Bhupathy et al., 2007; Primeau et al., 2018; Rathod et al., 2021). With 31 amino acids and a molecular weight of 3.8 kDa, SLN is considerably smaller than PLN (Figure 14; Figure 17). The single-span TM helix of SLN (~ aa 7-26) is highly conserved and accounts for most of the peptide size. Structural data revealed binding of the transmembrane domain to SERCA's inhibitory cleft formed by helices M2, M6, and M9 to build a 1:1 heterodimeric complex as it was also publicized for PLN (Figure 14C; Figure 16C; Toyoshima et al., 2013; Winther et al., 2013). With only six residues, the unstructured N-terminal cytoplasmic domain is relatively small and holds with Thr⁵ a possible phosphorylation site. Though remaining unclear for a long period, it was finally shown that SLN can get phosphorylated at this residue by CaMKII (Bhupathy et al., 2009) as well as serine/threonine kinase 16 (STK16; Gramolini et al., 2006). Even though phosphorylation seems to play a role in alleviating SLN mediated inhibition, the exact mechanism and physiological relevance are unsolved.

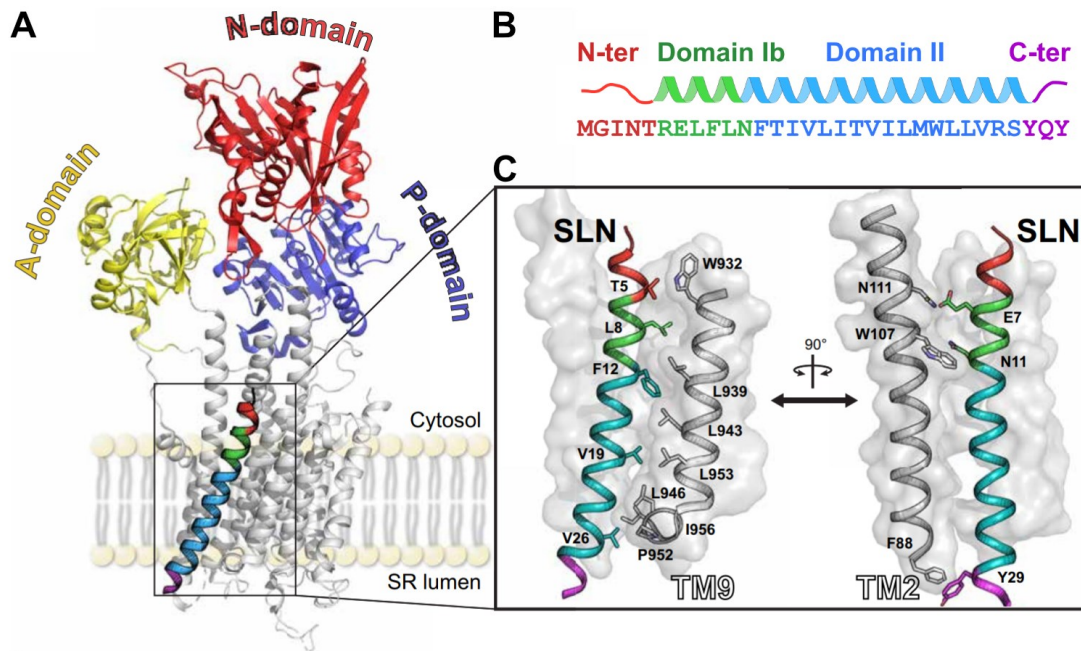


Figure 16 | Interaction of SLN and SERCA. (A) SLN interacts with SERCA's canonical binding groove built by the transmembrane helices M2, M6, and M9. Shown is a model based on an X-ray structure of rabbit SLN bound to SERCA1a at E1-state (Protein Data Bank ID: 4H1W; Winther et al., 2013). The colors of SLN correspond to the colors in (B) and (C). (B) The SLN peptide is composed of a short N-terminal cytoplasmic domain (red), a helical transmembrane domain that can be further distinguished in a more N-terminal (Ib; green) and a more C-terminal part (II; blue), and a cytoplasmic tail (purple). (C) The detailed view of the transmembrane region depicted in (A) reveals the interaction of SLN residues with residues of SERCA's TM9 and TM2. Modified and adapted after (Wang et al., 2021).

Even though phosphorylation seems to play a role in alleviating SLN mediated inhibition, the exact mechanism and physiological relevance are unclear. The short C-terminal tail of SLN (~aa Arg²⁷-Ser²⁸-Tyr²⁹-Gln³⁰-Tyr³¹) localizes to the SR lumen and is highly conserved. Unlike PLN, SLN probably inhibits SERCA not only through the interaction of the transmembrane domain with the inhibitory groove of the ATPase; instead, the luminal tail also facilitates SERCA inhibition (e.g., Hughes et al., 2007; Gorski et al., 2013; Wang et al., 2021; see section 3.3. for further discussion). However, as a result, both PLN and SLN decrease SERCA's apparent Ca^{2+} affinity K_{Ca} at low $[\text{Ca}^{2+}]$, thereby holding the ATPase in a Ca^{2+} - and metal ion-free intermediate state (Espinoza-Fonesca et al., 2015), but the exerted effect on SERCA's V_{max} at high $[\text{Ca}^{2+}]$ is quite contrary (Figure 17). Under this condition, V_{max} of PLN bound SERCA exceeds the value of SERCA alone, whereas binding of SLN at high molar ratios (~4 SLN to 1 SERCA) reduces V_{max} of the ATPase (e.g., Gorski et al., 2013; Sahoo et al., 2013; reviewed in Rathod et al., 2021). Due to the lack of structural and functional studies, as well as some inconclusive data, the exact interaction mechanism of SLN-mediated SERCA inhibition has yet to be fully elucidated.

Like PLN, the SLN peptide can form oligomers, whereby the monomeric peptide and dimers display the most abundant species (Hellstern et al., 2001; Autry et al., 2011; Graves et al., 2020). Interestingly, like PLN, SLN was shown to bind to the M3 accessory site of SERCA *in vitro*, hence not only as a pentamer but also as a monomeric peptide

(Glaves et al., 2020). However, *in vivo* physiology and the relevance of this interaction is unclear.

Besides inhibition of SERCA activity, the role of SLN in non-shivering thermogenesis of fast-twitch skeletal muscles and its implication in energy metabolism displays a unique functionality of SLN in comparison to the other regulins (Bal et al., 2012; reviewed by Gamu et al., 2014; Maurya and Periasamy, 2015). SLN-mediated muscle-based thermogenesis is achieved by uncoupling of SERCA through separation of ATP hydrolysis and calcium transport resulting in futile enzymatic cycles (Smith et al., 2002; Mall et al., 2006). In that way, the excess ATP hydrolysis contributes to heat production. Uncoupling of SERCA is already known to occur at very high Ca^{2+} concentrations present inside and outside the cytosol and high pH (e.g., reviewed by de Meis et al., 2005; Periasamy et al., 2017). Different theories have been proposed regarding the molecular underpinnings of this phenomenon. Structural studies could show that SLN remains associated with Ca^{2+} bound SERCA conformations throughout the kinetic cycle (Sahoo et al., 2013; Wang et al., 2021). It is assumed that this maintained interaction facilitates uncoupling predominantly through the action of distinct residues of the transmembrane helix and the C-terminus (Figure 16C; Wang et al., 2021; see section 3.3 for further discussion). Another theory is that uncoupling is mediated by the SLN cytoplasmic domain (Autry et al., 2016). Experiments using SLN-null mice demonstrated that these animals could not maintain their body core temperature in cold surroundings, which promotes *in vivo* relevance of SLN mediated thermogenesis (Bal et al., 2012; Rowland et al., 2015). However, incongruent data and many outstanding questions concerning a physiologically meaningful impact of SLN contribution to thermogenesis outline this research field as a subject of ongoing debate (reviewed in Campbell and Dicke, 2018).

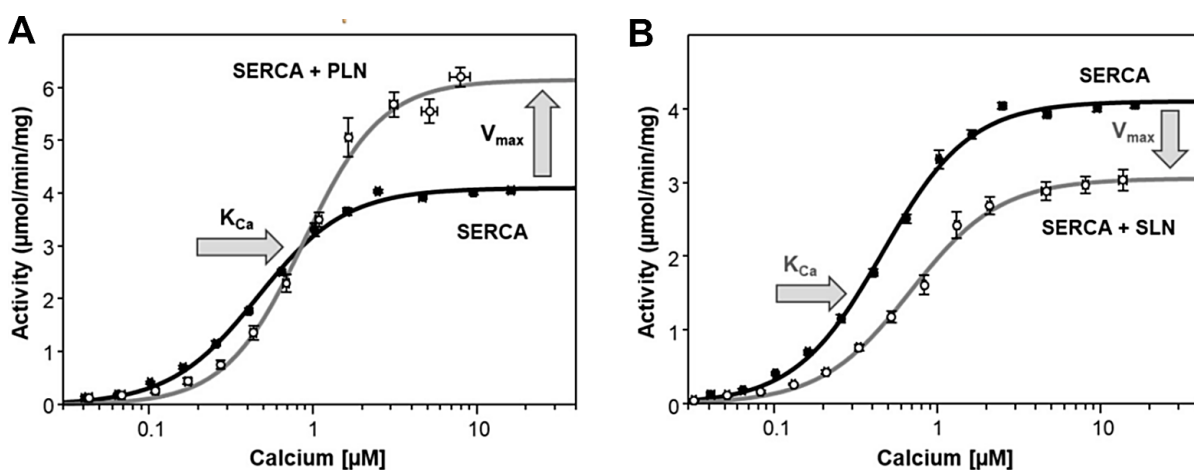


Figure 17 | Comparison of SERCA-modulating effects exerted by PLN and SLN. Measurement of Ca^{2+} -dependant SERCA1a activity in the absence (black) or presence (grey) of the regulins PLN and SLN. (A) At low cytosolic Ca^{2+} concentrations, SERCAs apparent affinity for Ca^{2+} (K_{Ca}) is slightly reduced in the presence of PLN. At higher Ca^{2+} concentrations ($> 1.0 \mu\text{M}$), PLN facilitates an increase of SERCAs maximal activity (V_{max}). (B) The SLN-mediated inhibitory effect on SERCA activity is not reliant on the $[\text{Ca}^{2+}]$. Even at high $[\text{Ca}^{2+}]$, K_{Ca} and V_{max} are markedly reduced. Modified and adapted after (Rathod et al., 2021).

In summary, despite their structural and functional similarities, PLN and SLN exhibit quite distinct differences regarding the details of their SERCA-regulatory mechanisms. Different factors with the power to terminate PLN's inhibitory impact on SERCA, including $[Ca^{2+}]$, phosphorylation, and oligomerization, have been identified for PLN. In contrast, an *in vivo* mechanism to alleviate or end SLN-mediated SERCA inhibition has not been identified yet.

Aberrant PLN functionality is implicated in several diseases like general contractile dysfunction, dilated cardiomyopathy (DCM), and cardiac hypertrophy (e.g., reviewed by Kranias and Bers, 2007; Mattiazzi and Kranias, 2014; Gorski et al., 2015b). Thereby, mutation of residues important for β -adrenergic regulation can cause lethal hereditary DCM (Schmitt et al., 2003). Heart failure can be associated with diminished SR Ca^{2+} uptake related to decreased PLN phosphorylation (e.g., Huang et al., 1999; Schwinger et al., 1999). Since cardiac function is improved by reducing PLN-mediated inhibition, altering PLN levels to restore perturbed SR Ca^{2+} uptake could be a therapeutic tool for the treatment of heart failure (e.g., Stroik et al., 2020; Grote Beverborg et al., 2021). The availability of data regarding the implication of SLN in the development of diseases is reduced compared to PLN. Nevertheless, it was shown that SLN expression is often dysregulated in patients with a cardiovascular disease (Uemura et al., 2004; Zheng et al., 2014), and for the onset of Tako Tsubo cardiomyopathy, ventricular expression of SLN seems to be a significant factor (Nef et al., 2009). In addition, the role of SLN in thermogenesis gives rise to new possibilities to treat metabolic disorders, for example, diabetes or obesity (Maurya et al., 2015; Periasamy et al., 2017).

In comparison to the relatively well-studied regulins PLN and SLN, investigation and understanding of the remaining vertebrate regulins MLN, ELN, ALN, DWORF, and the arthropod SCL peptides is still in the fledgling stages (reviewed by Payre and Desplan, 2016; Primeau et al., 2018; Rathod et al., 2021). The peptides are encoded by smORFs that were previously assumed to be noncoding (see also section 1.1). Through bioinformatic screening of so far uncharacterized muscle RNA transcripts, different groups could identify several smORFs encoding for the peptides (Magny et al., 2013; Anderson et al., 2015; Nelson et al., 2016). The thereby identified myoregulin peptide is expressed in skeletal muscles together with SLN, though MLN seems to be the main regulin in skeletal muscles of adult mice (Anderson et al., 2015; Anderson, 2016). The topology of the 46 amino acid long MLN peptide exhibits broad similarities to PLN (Figure 14A-B). Differences apply predominately to the cytosolic domain and the C-terminus. While the cytosolic domain appears to be closely related to the SR membrane, the C-terminal tail is with only three amino acids rather short and does not extend far into the SR lumen (Anderson et al., 2015; Rathod et al., 2021). A molecular model of MLN/SERCA interaction based on molecular dynamics simulations and molecular modeling revealed that the regulin preferentially interacts with transmembrane helices M2 and M9 if bound to SERCA, whereas interaction with M6 is alleviated in comparison to PLN- or SLN/SERCA interaction (Rathod et al., 2021) So far, functional data

regarding the MLN-mediated effect on SERCA's K_{Ca} remains inconclusive (Anderson et al., 2015; Rathod et al., 2021). However, comparable to the exerted effect of SLN, SERCAs V_{max} seems to be reduced even at high $[Ca^{2+}]$.

Endoregulin localizes to endothelial and epithelial tissue, whereas another-regulin was found to be ubiquitously expressed (Anderson et al., 2016). Therefore, these regulins represent unique non-muscle regulatory subunits of SERCA. Both ELN and ALN, were identified in a bioinformatic screen for DNA sequences exhibiting homologies to the already known regulins (Anderson et al., 2016). The result was the identification of ELN as a regulator of SERCA3a and ALN of SERCA2b (Figure 14A-B). In addition, ALN expression was also detected in skeletal and cardiac muscles. With 65 amino acids, ALN is the largest regulin peptide but seems not to comprise a C-terminal tail (Figure 14A-B; Anderson et al., 2016; Rathod et al., 2021). On the contrary, TMHMM predictions reveal a rather long C-terminus as part of the 56 amino acid ELN peptide (Anderson et al., 2016; Rathod et al., 2021). First interaction studies emphasize, on the one hand, canonical interaction with the inhibitory cleft of SERCA for both peptides (Anderson et al., 2016). On the other hand, molecular dynamics simulations, and molecular modeling revealed the preferred interaction of ALN and SERCAs helix M2 with less extensive contacts to M6 and M9 (Rathod et al., 2021). In addition, ALN seems to reduce both K_{Ca} and V_{max} of SERCA, thereby resembling effects exerted by SLN (Rathod et al., 2021).

Dwarf open reading frame truly stands out of the line of so far identified regulins because it is the only known primary positive modulator of SERCA (Nelson et al., 2016). The fact that many heart diseases are related to diminished SR Ca^{2+} uptake by SERCA outlines DWORF as an attractive therapeutic target for treating cardiomyopathies (Makarewich et al., 2018; Makarewich et al., 2020). With a length of 35 amino acids, DWORF belongs to the rather short representatives of the regulin family. It is expressed in the same tissues as PLN: in the heart muscles (predominately ventricles) and slow-twitch skeletal muscles (Nelson et al., 2016). Also, regarding its overall structure, the peptide exhibits the most similarities to PLN. DWORF is composed of a cytoplasmic helix localizing at the membrane surface, a flexible linker around the Pro¹⁵ residue connecting the cytoplasmic helix to the transmembrane domain, and a relatively short transmembrane helix that lacks, like ALN, the C-terminal tail intruding to the SR lumen (Gopinath et al., 2021; Fisher et al., 2021; Reddy et al., 2022). The DWORF/SERCA interaction increases in SERCA's turnover rate and V_{max} (Fisher et al., 2021; Rathod et al., 2021), but it does not influence K_{Ca} of the ATPase (Nelson et al., 2016; Makarewich et al., 2018). Interestingly, DWORF seems to enhance SERCA activity by two different mechanisms. On the one hand, the congruent expression pattern of PLN and DWORF enables the replacement of PLN as the dominant SERCA interaction subunit. When bound to SERCA, distinct structural characteristics of the activator prevent SERCA inhibition. The linker domain of DWORF replaces a part of the transmembrane helix that is known to be important for SERCA inhibition, even though the peptide binds to SERCAs inhibitory groove (Nelson et al., 2016; Singh et al., 2019;

Fisher et al., 2021). As a result, the binding of DWORF enhances SERCA activity by reducing PLN-mediated interaction. In addition to the displacement of PLN, DWORF was also found to enhance SERCA activity directly, even in the absence of PLN (Li et al., 2021; Fisher et al., 2021; Reddy et al., 2022). This functionality is probably based on the linker region around Pro¹⁵ that introduces a kink in DWORF's topology since mutation of this region relieves activation (Reddy et al., 2022).

The starting point for discovering the new regulins was in 2013 when Magny et al. identified and characterized the *Drosophila* regulin peptides Sarcolamban A and B (Magny et al., 2013). Their finding confirms the conservation of regulins from insects to humans. Besides *Drosophila*, expression of SCL peptides was meanwhile confirmed for other arthropods including further insects and the tadpole shrimp, an early crustacean representative (Bak et al., 2020). The in this course identified SCL peptides either better resembled functional and structural characteristics of SLN or PLN. By using bioinformatic tools, Magny et al. identified *Drosophila* SCLA and SCLB; both encoded by a smORF located on the same formerly annotated non-coding RNA. With 28 respectively 29 amino acids, SCLA and SCLB represent the smallest regulin peptides (Figure 14A-B; Figure 18). Both were found to be expressed in cardiac and somatic muscles of *Drosophila* (Figure 18B), where they co-localize with *Drosophila* SERCA (CaP60A) and regulate calcium homeostasis and muscle contraction by inhibition of the ATPase (Magny et al., 2013).

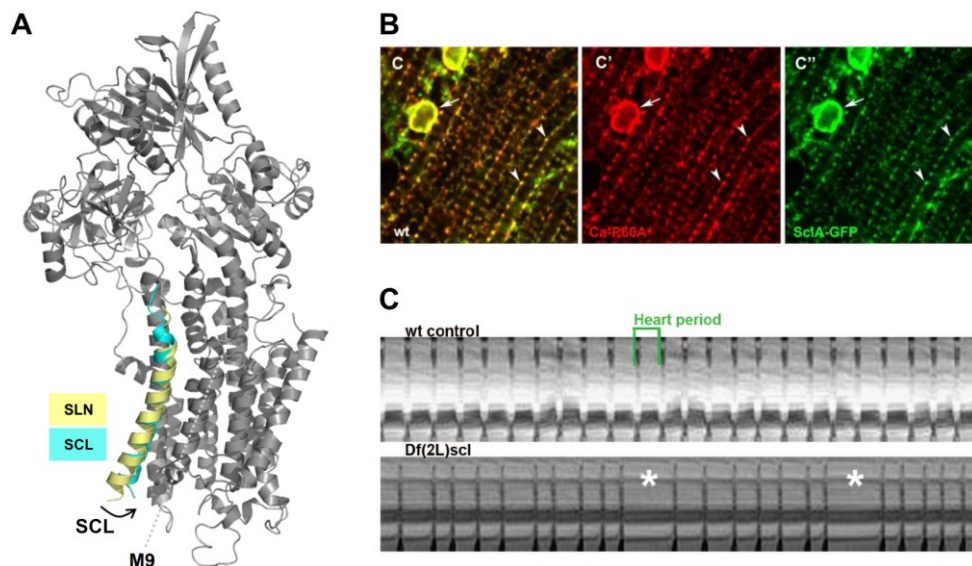


Figure 18 | Insect SCL peptides modulate muscle contraction by inhibiting SERCA activity. (A) Comparison of SLN and *Bombus terrestris* SCL bound to *Drosophila* SERCA. Overlay of SLN and SCLB shows that both peptides are bound to SERCA's canonical inhibitory groove. The model is based on a molecular dynamics simulation using crystal structures of SERCA and SLN as templates (Protein Data Bank IDs: 3AR4 from Toyoshima et al., 2011; and 3W5A from Toyoshima et al., 2013). (B) In indirect flight muscles of *Drosophila*, SCLA (green) and SERCA (red) colocalize at the SR membrane, especially at the dyads (arrowheads) and the dense SR around the nuclei (arrows). Shown is a muscle-specific overexpression of GFP-tagged SCLA and an antibody staining of endogenous SERCA. (C) Adult flies with complete loss of *scl* expression (*Df(2L)scl*) exhibit extensive heart arrhythmia with recurrent heartbeat arrests (*). (A) is modified after (Bak et al., 2020), and (B) and (C) are modified and adapted after (Magny et al., 2013).

Mutant flies with loss of *scl* expression exhibit, e.g., heart arrhythmia and altered Ca^{2+} transients. Structurally, both SCL peptides best resemble the topology of vertebrate SLN (Magny et al., 2013; Bak et al., 2020). They possess a short N-terminal unstructured cytoplasmic domain (~aa 1-6 for SCLA), a highly conserved TM helix (~aa 7-16 for SCLA), and a short C-terminal tail (~aa 23-28 for SCLA) that probably extends into the SR lumen (amino acid predictions based on Anderson et al., 2016). Interestingly, SCLA and SCLB exhibit extensive sequence resemblances, with the biggest differences applying to their C-termini (see also section 3.3).

Evolutionary conservation was underlined by experiments showing that PLN and SLN localize similarly to SCL if ectopically expressed in *Drosophila* muscles (Magny et al., 2013). In modeling studies, the authors could also demonstrate the conserved binding of SLN and PLN to *Drosophila* SERCA and vice versa interaction of insect SCL with vertebrate SERCA, which is further supported by co-immunoprecipitation experiments. This is also corroborated by later co-reconstitution experiments using different arthropod SCLB peptides and rabbit SERCA1a (Bak et al., 2020). All peptides were shown to inhibit the mammalian SERCA. Based on different phylogenetic analyses, Magny et al. propose a common ~30 amino acid ancestral peptide that gave rise to the regulins of the different species. However, the functional role of expressing two distinct regulin peptides in insects remains completely unclear. In addition, no data regarding modulation of the SCL mediated inhibition is available, even though this would be of high interest, especially concerning the complex and still not fully understood regulatory mechanisms affecting and governing the action of the different vertebrate regulins.

1.3 Aim of the thesis

Peptide hormones, neuropeptides, and regulatory membrane integral micropeptides play pivotal roles in various physiological processes, including insulin signaling and the control of muscle contraction. Misregulation of these sensitively balanced, often crosslinked regulatory networks can end in the development of severe diseases like Alzheimer's Disease, diabetes, or heart failure. Therefore, a comprehensive understanding of these regulatory networks is of central meaning and could be the starting point for developing therapeutic strategies for treating the named diseases. As metalloendopeptidases with broad substrate specificity, neprilysins display crucial modulators of peptide-dependent processes. However, mechanistic understanding and physiological relevance of neprilysin-mediated cleavage of peptide substrates are far from being understood.

On the one hand, this work aims to investigate if peptides implicated in the insulin signaling pathway represent novel substrates of the neprilysin and to further elucidate the physiological impact of neprilysin-mediated regulation of insulin signaling. In addition, by applying a combined *in vitro/in vivo* screen, this work aims to test whether these peptides also play another, formerly unknown role by acting on the *Drosophila* heart. On the other hand, the objective of this thesis is to reveal the role of neprilysin in the regulation of muscle and heart contraction. Since it is already known that Nep4 is implicated in muscle functionality, it is of high interest to investigate if the SERCA-inhibitory micropeptides represent novel substrates of the enzyme.

Peptide-dependent regulation of insulin signaling and muscle contraction, as well as neprilysin-mediated inactivation of peptide substrates, are evolutionarily well-conserved mechanisms. Therefore, *Drosophila melanogaster* represents a convenient model system to investigate the mechanistic underpinning and, most importantly, to evaluate the physiological relevance *in vivo*.

2 Results

The results of this thesis are presented in the following research publications and manuscripts:

- 2.1** Hallier, B., Schiemann, R., Cordes, E., Vitos-Faleato, J., Walter, S., Heinisch, J. J., Malmendal, A., Paululat, A., and Meyer, H. (2016). *Drosophila* neprilysins control insulin signaling and food intake via cleavage of regulatory peptides. *eLife*, 5, e19430. doi: 10.7554/eLife.19430. PMID: 27919317; PMCID: PMC5140268.

Status 13.04.22: Published

- 2.2** Schiemann, R., Lammers, K., Janz, M., Lohmann, J., Paululat, A., and Meyer, H. (2018). Identification and In Vivo Characterisation of Cardioactive Peptides in *Drosophila melanogaster*. *International journal of molecular sciences*, 20(1), 2. doi: 10.3390/ijms20010002. PMID: 30577424; PMCID: PMC6337577.

Status 13.04.22: Published

- 2.3.** Schiemann, R. and Meyer, H. (2022). Neprilysin 4. Chapter in „Rawlings - Vol. 1 - Handbook of Proteolytic Enzymes: Metallopeptidases, 4th Edition”, ISBN: 9780128235874

Status 13.04.22: Manuscript accepted for publication

- 2.4.** Schiemann, R., Buhr, A., Cordes, E., Walter, S., Heinisch, J. J., Ferrero, P., Milting, H., Paululat, A., and Meyer, H. Neprilysins regulate muscle contraction and heart function via cleavage of SERCA-inhibitory micropeptides.

Status 13.04.22: Manuscript in revision at Nature communications

Updated status 29.07.22: The revised and adapted manuscript was published by Nature communications:

Schiemann, R., Buhr, A., Cordes, E., Walter, S., Heinisch, J. J., Ferrero, P., Milting, H., Paululat, A., and Meyer, H. (2022). Neprilysins regulate muscle contraction and heart function via cleavage of SERCA-inhibitory micropeptides. *Nature communications*, 13(1):4420. doi: 10.1038/s41467-022-31974-1. PMID: 35906206; PMCID: PMC9338278.

Further publications:

Meyer, H., Buhr, A., Callaerts, P., Schiemann, R., Wolfner, M. F., and Marygold, S. J. (2021). Identification and bioinformatic analysis of neprilysin and neprilysin-like metalloendopeptidases in *Drosophila melanogaster*. *microPublication biology*, vol 2021. doi: 10.17912/micropub.biology.000410. PMID: 34189422; PMCID: PMC8223033.

Status 13.04.22: Published

Santalla, M., García, A., Schiemann, R., Paululat, A., Mattiazzi, A., Valverde, C., Hernández, G., Meyer, H., Ferrero, P. Interplay between SERCA, 4E-BP and eIF4-E in the *Drosophila* heart

Status 13.04.22: Manuscript accepted for publication at PLOS ONE

Own respective contributions and work shares are listed in Appendix section 5.5.

2.1 *Drosophila* neprilysins control insulin signaling and food intake via cleavage of regulatory peptides

The results of this project are presented in the following research publication:

Hallier, B., Schiemann, R., Cordes, E., Vitos-Faleato, J., Walter, S., Heinisch, J. J., Malmendal, A., Paululat, A., and Meyer, H. (2016). *Drosophila* neprilysins control insulin signaling and food intake via cleavage of regulatory peptides. *eLife*, 5, e19430. doi: 10.7554/eLife.19430. PMID: 27919317; PMCID: PMC5140268.

Link: <https://elifesciences.org/articles/19430>

The published article corresponds to pages 51-72 of the printed version of this thesis.

2.2 Identification and in vivo characterization of cardioactive peptides in *Drosophila melanogaster*

The results of this project are presented in the following research publication:

Schiemann, R., Lammers, K., Janz, M., Lohmann, J., Paululat, A., and Meyer, H. (2018). Identification and In Vivo Characterisation of Cardioactive Peptides in *Drosophila melanogaster*. *International journal of molecular sciences*, 20(1), 2. doi: 10.3390/ijms20010002. PMID: 30577424; PMCID: PMC6337577.

Link:

<https://www.mdpi.com/1422-0067/20/1/2>

The published article corresponds to pages 73-87 of the printed version of this thesis.

2.3 Neprilysin 4

Abstract

Neprilysins are evolutionarily conserved ectoenzymes that cleave and thereby inactivate physiologically relevant peptides in the extracellular space. Members of the neprilysin family typically consist of a short N-terminal cytoplasmic domain, a membrane spanning region, and a larger extracellular domain that holds sequence motifs critical to zinc coordination, catalysis, and substrate or inhibitor binding. In *Drosophila melanogaster*, seven neprilysin genes have been identified. However, up to now only two of the corresponding protein products, Nep2 and Nep4, were characterized in terms of enzymatic activity. This chapter summarizes the current knowledge on Nep4 with a particular focus on cleavage specificity, expression pattern, and physiological relevance.

Keywords

Neprilysin, M13 metallopeptidase, metalloendopeptidase, neuropeptides, peptide hormones, peptide hydrolysis, *Drosophila melanogaster*

Databanks

Name and History

The first characterization of a neprilysin, also known as neutral endopeptidase (NEP) 24.11, endoprotease 24.11, membrane metalloendopeptidase (MME) EC 3.4.24.11, common acute lymphoblastic leukemia antigen (CALLA), and enkephalinase, was reported in 1973. While the enzyme was initially described as a “neutral peptidase” in rabbit kidney brush border membranes (1), further analyses resulted in purification of the enzyme from rabbit kidney and subsequent classification as endopeptidase (2). Later on, the renal enzyme was found to be identical to a clinically relevant brain enkephalinase (3), as well as to the lymphocyte marker CALLA (CD10) (4). In the following years, many additional tissues were reported to express NEP and, based on the concurrently growing number of clinically relevant peptide substrates, today’s research mainly focuses on the potentially critical functions of the endopeptidase in cardiovascular, neurological, renal, pulmonary, and gastrointestinal physiology (5).

Like human NEP, *Drosophila melanogaster* Neprilysin 4 (Nep4) belongs to the M13 family of metalloendopeptidases. In *Drosophila*, 28 genes encoding M13 class metalloendopeptidases have been identified, with 7 of the corresponding protein products holding all four conserved sequence motifs that are critical to catalytic activity in vertebrate neprilysins (HExxH, ENIAD(xGG), CxxW, and NAY/FY, (6,7)). These 7 genes are classified “Neprilysins” (Nep1 - Nep7). The remaining 21 genes display sequence similarity to Neprilysins but lack at least one of the catalytically relevant motifs. The corresponding protein products may thus be catalytically inactive or exhibit non-canonical cleavage-specificities (see **Activity and Specificity**). Members of this group are classified “Neprilysin-like” and characterized by a “NepI” prefix (Nep11 - Nep21, (6)).

Activity and Specificity

Reaction and specificity

Nep4 enzymatic activity is determined by four sequence motifs located within the extracellular domain of the enzyme (see **Structural Chemistry**). In-line with vertebrate neprilysins, *Drosophila* Nep4 is characterized by a rather broad substrate specificity. However, based on structural data for human NEP that indicate sterically restricted active site access (substrates needs to be \leq 3kDa) (8), corresponding restrictions likely apply also to Nep4. Among the 16 Nep4 substrates identified so far (Table 1; (9,10)), DH31 represents the largest (3.15 kDa). Generally, Nep4 substrates are preferentially cleaved next to hydrophobic residues, predominantly with Phe or Leu at P1' (9,10). G#L and X#F cleavage, which are also preferred hydrolysis positions of many mammalian neprilysins (11,12), can be observed in particular.

Assay methods

Cleavage of human Substance P, human Angiotensin I, human Bradykinin, *Drosophila* PDF, and *Locusta migratoria* Tachykinin 1 was assessed using 1 µg of N-terminally GST-tagged Nep4B (expressed in *Escherichia coli*, see **Preparation**). The purified enzyme was incubated with 750 ng of the respective candidate peptide in 50 mM Tris (pH 7), 100 mM NaCl (2h, 35 °C). Resulting cleavage products were characterized via electrospray ionization (ESI) mass spectrometry (10).

Putative Nep4 *in vivo* substrates were identified by using Nep4B expressed and purified from *Sf21* insect cells (C-terminal His-tag, see **Preparation**). To measure enzymatic activity, 25 ng of the purified enzyme were incubated with 150 ng of each respective candidate peptide in 50 mM NaH₂PO₄ (pH 7.9), 300 mM NaCl (5h, 35 °C). Cleavage products were analyzed by ESI mass spectrometry (9).

pH optimum

Optimal catalytic activity requires neutral conditions (pH 7), with a significant decrease in activity being observed above pH 8 and below pH 6 (10).

Inhibitors

Up to now no specific Nep4 inhibitor or activator has been identified. Phosphoramidon and thiorphan, two highly efficient transition-state inhibitors of vertebrate neprilysins (13,14), do not significantly affect Nep4-mediated hydrolysis (10).

Table 1: Neprilysin 4 substrates and hydrolysis positions

Peptide	Sequence	Scissile bonds	Cleavage products
Allatostatin A-1 ⁹	VERYAFGLa	G#L F#G	VERYAFG VERYAF
Allatostatin A-2 ⁹	LPVYNFGLa	G#L F#G N#F	LPVYNFG LPVYNF LPVYN
Allatostatin A-3 ⁹	SRPYSFGLa	P#Y	YSFGLa
Allatostatin A-4 ⁹	TTRPQPFNFGLa	G#L N#F P#F	TTRPQPFNFG TTRPQPFN FNFGLa
AKH ⁹	QLTFSPDWa	L#T T#F	TFSPDWa FSPDWa
Corazonin ⁹	QTFQYSRGWTNa	T#F G#W	FQYSRGWTNa QTFQYSRG
DH31 ⁹	TVDFGLARGYSGTQEAKHR MGLAAANFAGGPa	G#Y; G#L G#Y	YSGTQEAKHRG TVDFGLARG
Drosulfakinin-1 ⁹	FDDYGHMRFa	R#F	FDDYGHMR
Drosulfakinin-2 ⁹	GGDDQFDDYGHMRFa	R#F Q#F	GGDDQFDDYGHMR FDDYGHMRFa
Leucokinin ⁹	NSVVLGKKQRFHSWGa	S#W H#S R#F R#F	NSVVLGKKQRFHS NSVVLGKKQRFH NSVVLGKKQR FHSWGa
sNPF 1 ₁₋₁₁ ⁹	AQRSPSLRLRFa	L#R	AQRSPSLRL
sNPF 1 ₄₋₁₁ ⁹ ; sNPF2 ₁₂₋₁₉ ⁹	SPSLRLRFa	R#F S#L	SPSLRLR LRLRFa
Substance P ¹⁰	RPKPQQFFGLMa	F#G G#L	RPKPQQFF RPKPQQFFG
Tachykinin 1 ⁹	APTSSFIGMRa	G#M S#F	APTSSFIG FIGMRa
Tachykinin 2 ⁹	APLAFVGLRa	P#L G#L A#F F#V	LAFVGLRa APLAFVG FVGLRa APLAF

Tachykinin 4 ⁹	APVNSFVGMRa	G#M	APVNSFVG
Tachykinin 5 ⁹	APNGFLGMRa	G#F	FLGMRa

Superscripts indicate corresponding references.

Drosophila peptides that are resistant to Nep4-mediated hydrolysis include Hugin, NPF, sNPF3, sNPF4, Tachykinin 3 and Tachykinin 6 (9). *Locusta migratoria* Tachykinin 1 and human Bradykinin are also unaffected by Nep4 enzymatic activity, while human Angiotensin I and *Drosophila* Pigment Dispersing Factor (PDF) are hydrolyzed with low efficiency (10).

Structural Chemistry

Primary structure

Nep4 isoform A (1040 aa; 119.577 kDa; pI 7.63) represents a type II integral membrane protein composed of a short N-terminal intracellular domain (56 aa), a transmembrane domain (20 aa), and a large extracellular part (964 aa) that holds the catalytic center (**Fig 1**). In contrast to isoform A, isoforms B and C (978 aa; 113.059 kDa; pI 6.93) lack the intracellular and the transmembrane domain and therefore constitute soluble, secreted peptidases (10). All isoforms share the Peptidase M13 Neprilysin-like protease domain (aa 251 - 1040 for Nep4A; aa 189 - 978 for Nep4B/C) that holds four conserved sequence motifs critical to enzymatic activity and specificity: while HEXxH and ENIAD(xGG) represent zinc-binding domains, CxxW is critical to protein folding and maturation and NAY/FY mediates substrate binding ((6,7,15), **Fig. 1**). A single point mutation within the HEXxH motif (Nep4A: E873Q, Nep4B/C: E811Q) completely disrupts enzymatic activity (9,16).

Secondary structure

Since up to now no experimentally validated secondary or tertiary structure is available for Nep4, corresponding information can be deduced only from sequence comparisons with members of the neprilysin family whose structure has been solved. Such comparisons indicate structural similarity between Nep4A and membrane-bound vertebrate NEP, ECE-1 and ECE-2 (7,8,10,17-19). On the other hand, Nep4B/C exhibit similarities to soluble vertebrate NEP2 (10,20,21).

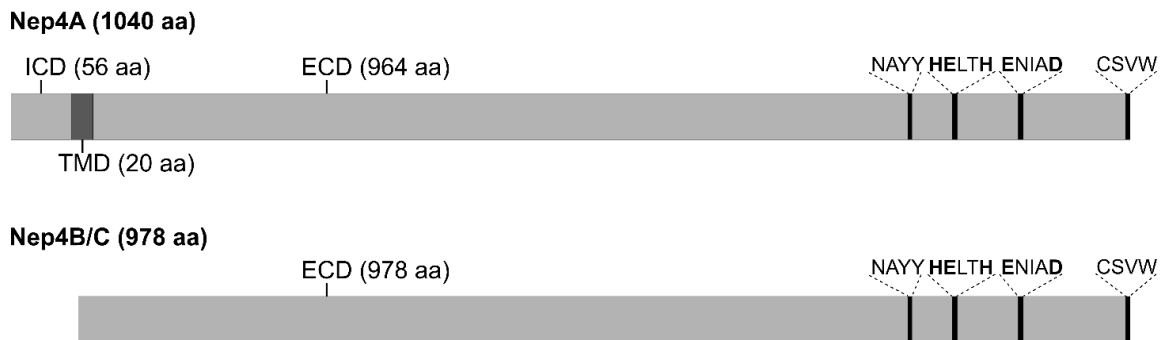


Figure 1: Primary structure of Nep4A and Nep4B/C. All isoforms share a large extracellular domain (ECD) that harbors four conserved sequence motifs critical to catalytic activity (**HExxH**, **ENIAD(xGG)**, CxxW, and NAY/FY). Bold residues are involved in zinc coordination. Nep4A furthermore holds a short N-terminal intracellular domain (ICD) and a transmembrane domain (TMD) that are both absent in Nep4B/C.

Preparation

Source

Commercial sources for Nep4 fly stocks are listed in Table 2. In addition, *nep4* deficiency lines, cDNA clones, and transgenes can be obtained from various sources (Bloomington *Drosophila* Stock Center, *Drosophila* Genomics Resource Center, Vienna *Drosophila* Resource Center, Source BioScience). Finally, tissue-specific *nep4* overexpression and reporter lines have been generated and described (9,10,16,22).

Table 2: Available Nep4 fly stocks

Identifier	Description	Resource	Applied in
BI36979	y[1] w[*]; Mi{y[+mDint2]=MIC}Nep4[MI03765] MiMIC insertion in <i>nep4</i> gene	Bloomington <i>Drosophila</i> Stock Center	
v100189	P{KK104462}VIE-260B <i>nep4</i> RNAi line	Vienna <i>Drosophila</i> Resource Center	(7,9,16,23)
v16669	w[1118]; P{GD5655}v16669 <i>nep4</i> RNAi line	Vienna <i>Drosophila</i> Resource Center	(7,16,23)
v16668	w[1118]; P{GD5655}v16668/TM3 <i>nep4</i> RNAi line, balanced	Vienna <i>Drosophila</i> Resource Center	(7)
4058R-1	<i>nep4</i> RNAi line	National Institute of Genetics (Japan)	
4058R-2	<i>nep4</i> RNAi line	National Institute of Genetics (Japan)	

Expression systems

Catalytically active Nep4B has been expressed in transgenic *Drosophila*, in Sf21 cells, and in *E. coli* Rosetta (DE3) cells (9,10,16). Expression in Sf21 cells was based on the 'Bac-to-Bac' baculovirus expression system (Life Technologies, Carlsbad, CA, USA). Prior to generating recombinant bacmids via site-specific transposition, the *nep4B* coding sequence was cloned in-frame with a C-terminal His-tag into an *E.coli/S.cerevisiae/Baculovirus* triple-shuttle derivative of the pFastBac Dual vector (Life Technologies, Carlsbad, CA, USA) adapted for cloning by homologous recombination *in vivo* (24). Sf21 cells were transfected with the resulting bacmids and grown in 75 cm² flasks for 72 hr. *E. coli* expression was done by inserting the *nep4B* coding sequence in frame with an N-terminal GST-tag into the pGEX-5X-1 vector (Cytiva, Marlborough, MA, USA). Expression was induced by adding 0.2 mM IPTG and cells were incubated at 28°C for 5h.

Isolation, purification

His-tagged Nep4B was isolated from transfected Sf21 cells via gravity-flow based Ni-NTA purification (9).

GST-tagged Nep4B was purified from transformed *E. coli* Rosetta (DE3) cells using glutathione agarose (10).

Biological Aspects

Nep4 is involved in the regulation of numerous physiological processes. These include insulin signaling and food intake (9), memory formation (23), and reproduction (7). Fundamental reasons for the functional diversity are i) a broad substrate specificity (see **Activity and Specificity**) and ii) the multifaceted expression pattern of the enzyme.

Distribution in organisms and tissues

Nep4 expression has been confirmed in embryonic tissues like heart and muscle precursor cells, glial cells, and gonads (7,10). In larval and adult stages, the peptidase is expressed in testes, in cardiac and body wall muscles, in glial cells, and in a few neurons of the central nervous system, including insulin producing cells (IPCs) (9,10,16,23). As shown in (16,22), neuronal expression is controlled by regulatory elements located within the first intron of *nep4* isoform B, while the mesodermal enhancer is located in the 3'-UTR of the *nep4* gene.

Normal function

Tissue-specific regulation of *nep4* expression is accompanied by tissue-specific functions of the peptidase. While neuronal expression appears to be required for proper formation of long-term and middle-term memory (23), gonad-specific expression is essential to

reproduction (7). Control of feeding behavior and proper expression of insulin-like peptides is based mainly on presence of the enzyme at the surface of body wall muscles (9). In addition, Nep4 localizes to the sarcoplasmic reticulum of heart and body wall muscles. Presence in this subcellular compartment may be causally related to impaired muscle integrity that has been observed as a result of altered *nep4* expression (16).

In most cases, hydrolysis of specific neuropeptides or peptide hormones (see **Activity and Specificity**) represents the mechanistic basis of the Nep4 biological significance. In this regard, it has been shown that both, increasing as well as reducing Nep4 activity cause severe physiological impairments and premature lethality (9). This result indicates a need for precisely adjusted neprilysin activity to ensure physiological homeostasis of the individual peptide substrates.

Distinguishing Features

While most neprilysins are expressed in a membrane-bound state with the catalytically active site localizing to the extracellular space, Nep4 is expressed isoform-specifically either as a membrane bound (Nep4A) or as a soluble, secreted enzyme (Nep4B, Nep4C). Isoform expression is stage-dependent, with soluble Nep4 being the predominant variant during development, and membrane-bound Nep4 representing the major isoform in adults (10). Another aspect specific to Nep4 is presence of the peptidase in muscle tissue (9,16). No other *Drosophila* neprilysin shares this particular expression pattern.

Antibodies

A monospecific Nep4 antibody has been generated and described (10).

Related Peptidases

In the *Drosophila* genome 7 Neprilysins have been identified (Nep1 - Nep7). The corresponding protein products share a high structural similarity and are characterized by presence of 4 distinct sequence motifs that are critical to catalytic activity (see **Structural Chemistry**). In addition, 21 Neprilysin-like genes exist in *Drosophila*, with the presumptive protein products lacking at least one of the conserved motifs (6). Related mammalian enzymes include NEP, the endothelin-converting enzymes (ECE-1, ECE-2), the erythrocyte surface antigen KELL (ECE-3) and the PEX peptidase (15).

Further readings

First characterization of Nep4 expression, solubility, subcellular localization, and enzymatic activity was performed in (10). Biological processes regulated by Nep4 were identified in (7,9,16,23). Cleavage and substrate specificity was assessed in detail in (9).

References

1. George, S. G., and Kenny, J. (1973) Studies on the enzymology of purified preparations of brush border from rabbit kidney. *Biochem J* **134**, 43-57
2. Kerr, M. A., and Kenny, A. J. (1974) The purification and specificity of a neutral endopeptidase from rabbit kidney brush border. *Biochem J* **137**, 477-488
3. Malfroy, B., Swerts, J. P., Guyon, A., Roques, B. P., and Schwartz, J. C. (1978) High-affinity enkephalin-degrading peptidase in brain is increased after morphine. *Nature* **276**, 523-526
4. Letarte, M., Vera, S., Tran, R., Addis, J. B., Onizuka, R. J., Quackenbush, E. J., Jongeneel, C. V., and McInnes, R. R. (1988) Common acute lymphocytic leukemia antigen is identical to neutral endopeptidase. *J Exp Med* **168**, 1247-1253
5. Bayes-Genis, A., Barallat, J., and Richards, A. M. (2016) A Test in Context: Neprilysin: Function, Inhibition, and Biomarker. *J Am Coll Cardiol* **68**, 639-653
6. Harten, H., Callaerts, P., Wolfner, M.F., Marygold, S.J. (2018) *D. melanogaster* M13/neprilysin genes. FlyBase, <https://flybase.org/reports/FBrf0239474.html>
7. Sitnik, J. L., Francis, C., Hens, K., Huybrechts, R., Wolfner, M. F., and Callaerts, P. (2014) Neprilysins: an evolutionarily conserved family of metalloproteases that play important roles in reproduction in *Drosophila*. *Genetics* **196**, 781-797

8. Oefner, C., D'Arcy, A., Hennig, M., Winkler, F. K., and Dale, G. E. (2000) Structure of human neutral endopeptidase (Neprilysin) complexed with phosphoramidon. *J Mol Biol* **296**, 341-349
9. Hallier, B., Schiemann, R., Cordes, E., Vitos-Faleato, J., Walter, S., Heinisch, J. J., Malmendal, A., Paululat, A., and Meyer, H. (2016) *Drosophila* neprilysins control insulin signaling and food intake via cleavage of regulatory peptides. *Elife* **5**
10. Meyer, H., Panz, M., Zmojdzian, M., Jagla, K., and Paululat, A. (2009) Neprilysin 4, a novel endopeptidase from *Drosophila melanogaster*, displays distinct substrate specificities and exceptional solubility states. *J Exp Biol* **212**, 3673-3683
11. Gafford, J. T., Skidgel, R. A., Erdos, E. G., and Hersh, L. B. (1983) Human kidney "enkephalinase", a neutral metalloendopeptidase that cleaves active peptides. *Biochemistry* **22**, 3265-3271
12. Rose, C., Voisin, S., Gros, C., Schwartz, J. C., and Ouimet, T. (2002) Cell-specific activity of neprilysin 2 isoforms and enzymic specificity compared with neprilysin. *Biochem J* **363**, 697-705
13. Fulcher, I. S., Matsas, R., Turner, A. J., and Kenny, A. J. (1982) Kidney neutral endopeptidase and the hydrolysis of enkephalin by synaptic membranes show similar sensitivity to inhibitors. *Biochem J* **203**, 519-522
14. Roques, B. P., Fournie-Zaluski, M. C., Soroca, E., Lecomte, J. M., Malfroy, B., Llorens, C., and Schwartz, J. C. (1980) The enkephalinase inhibitor thiorphan shows antinociceptive activity in mice. *Nature* **288**, 286-288
15. Turner, A. J., Isaac, R. E., and Coates, D. (2001) The neprilysin (NEP) family of zinc metalloendopeptidases: genomics and function. *Bioessays* **23**, 261-269
16. Panz, M., Vitos-Faleato, J., Jendretzki, A., Heinisch, J. J., Paululat, A., and Meyer, H. (2012) A novel role for the non-catalytic intracellular domain of Neprilysins in muscle physiology. *Biol Cell* **104**, 553-568
17. Oefner, C., Roques, B. P., Fournie-Zaluski, M. C., and Dale, G. E. (2004) Structural analysis of neprilysin with various specific and potent inhibitors. *Acta Crystallogr D Biol Crystallogr* **60**, 392-396
18. Bur, D., Dale, G. E., and Oefner, C. (2001) A three-dimensional model of endothelin-converting enzyme (ECE) based on the X-ray structure of neutral endopeptidase 24.11 (NEP). *Protein Eng* **14**, 337-341
19. Schulz, H., Dale, G. E., Karimi-Nejad, Y., and Oefner, C. (2009) Structure of human endothelin-converting enzyme I complexed with phosphoramidon. *J Mol Biol* **385**, 178-187
20. Whyteside, A. R., and Turner, A. J. (2008) Human neprilysin-2 (NEP2) and NEP display distinct subcellular localisations and substrate preferences. *FEBS Lett* **582**, 2382-2386
21. Voisin, S., Rognan, D., Gros, C., and Ouimet, T. (2004) A three-dimensional model of the neprilysin 2 active site based on the X-ray structure of neprilysin. Identification of residues involved in substrate hydrolysis and inhibitor binding of neprilysin 2. *J Biol Chem* **279**, 46172-46181
22. Meyer, H., Panz, M., Albrecht, S., Drechsler, M., Wang, S., Husken, M., Lehmacher, C., and Paululat, A. (2011) *Drosophila* metalloproteases in development and differentiation: the role of ADAM proteins and their relatives. *Eur J Cell Biol* **90**, 770-778
23. Turrel, O., Lampin-Saint-Amaux, A., Preat, T., and Goguel, V. (2016) *Drosophila* Neprilysins Are Involved in Middle-Term and Long-Term Memory. *J Neurosci* **36**, 9535-9546
24. Paululat, A., and Heinisch, J. J. (2012) New yeast/*E. coli*/*Drosophila* triple shuttle vectors for efficient generation of *Drosophila* P element transformation constructs. *Gene* **511**, 300-305

2.4 Neprilysins regulate muscle contraction and heart function via cleavage of SERCA-inhibitory micropeptides

Ronja Schiemann^{1#}, Annika Buhr^{1#}, Eva Cordes¹, Stefan Walter⁵, Jürgen J Heinisch^{2, 5}, Paola Ferrero³, Hendrik Milting⁴, Achim Paululat^{1, 5}, and Heiko Meyer^{1, 5*}

¹Department of Zoology & Developmental Biology, Osnabrück University, 49076 Osnabrück, Germany

²Department of Genetics, Osnabrück University, 49076 Osnabrück, Germany

³Center for Cardiovascular Research - CONICET/National University of La Plata, 1900 La Plata, Argentina

⁴Heart & Diabetes Center NRW, University of Bochum, Erich & Hanna Klessmann-Institute for Cardiovascular Research and Development, 32545 Bad Oeynhausen, Germany

⁵Center of Cellular Nanoanalytics Osnabrück - CellNanOs, 49076 Osnabrück, Germany

#These authors contributed equally

*For correspondence: Meyer@biologie.uni-osnabrueck.de

Summary

Muscle contraction depends on strictly controlled Ca²⁺ transients within myocytes. A major player maintaining these transients is the sarcoplasmic/endoplasmic reticulum Ca²⁺ ATPase, SERCA. Activity of SERCA is regulated by binding of micropeptides and impaired expression or function of these peptides results in cardiomyopathy. To date, it is not known how homeostasis or turnover of the micropeptides is regulated. We found that the *Drosophila* endopeptidase Neprilysin 4 hydrolyzes SERCA-inhibitory Sarcolamban peptides in membranes of the sarcoplasmic reticulum, thereby ensuring proper regulation of SERCA. Cleavage was necessary and sufficient to maintain homeostasis and function of the micropeptides. Analyses on human Neprilysin, sarcolipin, and ventricular cardiomyocytes indicated that the regulatory mechanism is evolutionarily conserved. By identifying a neprilysin as essential regulator of SERCA activity and Ca²⁺ homeostasis in cardiomyocytes, these data contribute to a more comprehensive understanding of the complex mechanisms that control muscle contraction and heart function in health and disease.

Keywords: SERCA, Neprilysin, micropeptides, muscle contraction, heart physiology, calcium homeostasis, sarcoplasmic reticulum, cardiomyopathy, *Drosophila melanogaster*

Introduction

The contraction of muscle fibers is governed by well-characterized molecular processes, with the concentration of free cytosolic calcium ions being a crucial parameter. This concentration is largely maintained by the activity of the sarcoplasmic and endoplasmic reticulum Ca^{2+} ATPase (SERCA), an enzyme that transports Ca^{2+} from the cytosol into the sarcoplasmic reticulum (SR). The resulting reduction in cytosolic Ca^{2+} levels initiates the muscle relaxation phase. Accordingly, precise regulation of SERCA activity is essential for the proper function of muscle tissue, and the physiological relevance of SERCA in heart and muscle disease has been extensively studied (see ^{1,2} and references therein). One central result of these studies is that the amount and activity of SERCA are significantly reduced upon aging as well as under pathophysiological conditions, such as congestive heart failure or progressive muscular dystrophy. In addition, an increase in SERCA activity ameliorates corresponding etiopathologies, which provides further evidence for the critical relevance of SERCA to muscle physiology. Moreover, these data emphasize the therapeutic potential of modulating SERCA activity in a directed manner ^{1,3,4,5,6}.

A prerequisite for the development and implementation of appropriate therapies is knowledge of all relevant factors affecting SERCA activity. In this context, the high degree of structural and functional conservation between human and *Drosophila* SERCA renders the fly an ideal model system to identify relevant factors ⁷, especially since also in *Drosophila*, SERCA activity is essential to proper cardiac function ^{8,9}. Both in vertebrates ¹⁰ and in *Drosophila melanogaster* ¹¹, the activity of SERCA is controlled by certain SR membrane integral peptides that bind to the enzyme and inhibit its activity. In vertebrate hearts, Phospholamban (PLN) and Sarcolipin (SLN) have been identified as such regulatory peptides ^{12,13}, with the affinity of PLN for SERCA depending on PLN phosphorylation and oligomerization states ¹⁰. For both micropeptides, alterations in expression or function are associated with severe cardiomyopathy ^{14,15,16,17,18,19}. Recently, two additional micropeptides that bind and regulate SERCA in muscle tissue have been identified: myoregulin (MLN) and dwarf open reading frame (DWORF). MLN shares sequence and structural similarity with PLN and SLN and appears to be a major peptide inhibitor of SERCA activity in fast-type skeletal muscle ²⁰. By contrast, DWORF represents the only SERCA-activating micropeptide identified up to now ^{21,22}. Among these peptide regulators of SERCA activity, MLN, PLN, and SLN share several amino acids within their transmembrane helices that are critical to the interaction with SERCA ²⁰. These residues are also conserved in Sarcolamban A (SCLA) and Sarcolamban B (SCLB), invertebrate SERCA-inhibitory micropeptides present in cardiac and somatic muscles of *Drosophila melanogaster* ^{11,20}. Analogous to human PLN, SLN, and MLN, binding of SCL to *Drosophila* SERCA reduces the activity of the enzyme. Accordingly, SCL loss-of-

function mutants exhibit impaired calcium transients in heart cells, concomitant with heart arrhythmia¹¹. To date, mechanisms that regulate the amount or the turnover of any of the SERCA-regulatory micropeptides are largely unknown.

In this study, we present evidence that the endopeptidase Neprilysin 4 (Nep4) acts as a novel and essential regulator of SCL homeostasis and SERCA activity in *Drosophila*. Increased *nep4* expression in heart cells phenocopied characteristic effects of *scl* knockout, including impaired Ca²⁺ transients, aberrant SERCA activity, and heart arrhythmia. Respective phenotypes strictly depended on the catalytic activity of the enzyme, which identified abnormal peptide cleavage as a critical factor. In a combined *in vitro* and *in vivo* approach we identified Sarcolamban peptides as the phenotype-relevant Nep4 substrate and could show that hydrolysis of the peptides reduces their membrane affinity, thereby releasing them from the SR membrane and precluding further SERCA interaction. In addition, the Nep4-hydrolyzed peptides exhibited a significantly impaired ability to oligomerize. Finally, Nep4, SERCA, and SCL colocalized in SR membranes of heart and body wall muscles, suggesting that spatial proximity between the three factors is of high mechanistic relevance. Initial analyses on corresponding human factors indicated that the regulatory mechanisms identified in *Drosophila* are relevant also in humans.

Results

Modulating nep4 expression affects cardiac function, Ca²⁺ homeostasis, and SERCA activity

In a screen for candidate proteins regulating heart function in adult *Drosophila melanogaster* we identified the metallopeptidase Nep4 as a novel and essential factor. Using semi-automated optical heartbeat analysis (SOHA²³), physiological heart parameters were analyzed in animals exhibiting either increased or reduced expression of the peptidase in heart cells. In addition to the active enzyme, the effects of overexpressing a catalytically inactive Nep4 variant, containing glutamine instead of the essential glutamate within the zinc-binding motif (E873Q^{24, 25}), were assessed (Fig. 1). Animals overexpressing active Nep4 displayed both arrhythmia and prolonged periods of diastolic heart arrest, while increased production of the catalytically inactive variant had no such effects. Cardiomyocyte-specific *nep4* knockdown resulted in a tendency toward arrhythmia, but the effect was not statistically significant (Fig. 1A, D, supplementary videos 1-4). However, compared to controls, abnormally long heart periods (HP) were recurrently observed in knockdown animals, with individual periods lasting up to 4.500 ms (Fig. 1C, supplementary video 4). Prolonged HPs were also characteristic for increased *nep4* expression, yet to an even stronger extent (individual HP > 20.000 ms, Fig. 1C, supplementary video 2). Unlike rhythmicity, heart rate

was not affected by increased or reduced *nep4* expression. Corresponding animals exhibited a median heart rate of about 90-100 beats per minute, which was not significantly different from control hearts (Fig. 1B) and within the range of published data ^{26, 27}. Similar inter-individual Nep4 overexpression levels were confirmed by immunostainings (Fig. S9A, B). To exclude nonspecific effects caused by the upstream activation sequence (UAS) constructs employed or owed to the chromosomal background, all analyzed lines (UAS-Nep4, UAS-Nep4^{E873Q}, and UAS-*nep4* RNAi) were crossed to *w*¹¹¹⁸ flies. None of the control offspring exhibited aberrant heart parameters (Fig. 1A, B).

To evaluate whether the functional impairments were specific to cardiomyocytes or affected muscle cells in general, we analyzed third instar larval body wall muscles for corresponding deficiencies. Endogenous *nep4* expression in cardiac and somatic muscle tissue of all *Drosophila* developmental stages has been confirmed previously ^{24, 25, 28, 29}. Consistent with the effects in heart cells, body wall muscle function was significantly impaired by increased Nep4 levels. Relative to controls, corresponding animals exhibited a reduced crawling speed (Fig. 1E) that was based on a decreased muscle contraction frequency (Fig. 1F), while the magnitude of the individual contractions was not affected (Fig. S9C). Again, the phenotype depended on the enzymatic activity of Nep4; increased expression of the catalytically inactive variant did not affect any of the measured parameters. RNAi-mediated knockdown of the peptidase was also without significant effects (Fig. 1E, F). Equivalent expression levels and wildtype-like subcellular localizations of all Nep4 overexpression constructs, as well as a high *nep4*-specific knockdown capacity of the analyzed RNAi line, were confirmed previously ^{24, 25}.

To assess the physiological basis of the observed phenotypes, we employed a genetically encoded Ca²⁺ indicator (GCaMP3) to analyze Ca²⁺ transients in cardiomyocytes exhibiting altered *nep4* expression. We found that both increasing and reducing *nep4* levels affected cardiac Ca²⁺ handling, namely SR Ca²⁺ load, SERCA activity, and cardiac relaxation constants (Fig. 2). To estimate the SR Ca²⁺ load, we analyzed caffeine-induced Ca²⁺ transients in the corresponding transgenic animals. Caffeine activates ryanodine receptors; thus, measuring caffeine-induced transients allows calculation of the Ca²⁺ content within the SR ^{30, 31}. Interestingly, *nep4* overexpression animals exhibited a significant increase in SR Ca²⁺ load, while animals overproducing the catalytically inactive variant did not (Fig. 2A). Since a major factor determining the degree of the SR Ca²⁺ load is SERCA ², we subsequently calculated the activity of this enzyme. In accordance with the increased Ca²⁺ load, overexpression of active Nep4 increased SERCA activity by about two-fold. Vice versa, cardiac-specific *nep4* knockdown significantly reduced SERCA activity. Again, only the enzymatically active Nep4 affected SERCA activity, while catalytically inactive Nep4 had no such effect (Fig. 2B). Finally, we determined the constant of relaxation (Tau) in the respective

transgenic animals (Fig. 2C). In agreement with reduced SERCA activity, *nep4* knockdown caused a significant increase in Tau, as reflected by prolonged relaxation in corresponding Ca^{2+} traces (Fig. 2D). Conversely, overexpression of catalytically active Nep4 resulted in a tendency toward a reduced Tau. However, the effect was not statistically significant (Fig. 2C). To exclude any influence of variable beating frequencies on the measured Ca^{2+} flux parameters, we analysed a subgroup of *nep4* knockdown flies selected specifically for slower heart rates. For this group, all effects on SR Ca^{2+} load, SERCA activity, and Tau were consistent with the population data of that genotype (Tab. S2, Fig. 2A-C), indicating that variations in heart rate did not significantly affect the measured parameters. The possibility that the observed changes in SERCA activity were based on altered expression of this enzyme was assessed by Western blots using protein extracts isolated from animals of all genotypes tested. SERCA expression levels and protein stability were not affected by altered *nep4* expression (Fig. 2E), indicating a direct regulatory effect of Nep4 on the activity of SERCA.

Nep4 colocalizes and coprecipitates with SERCA

To understand the Nep4 dependent effects on myocytic Ca^{2+} homeostasis in more detail, the subcellular localization of Nep4 in adult cardiomyocytes and heart-associated ventral longitudinal muscles³² was analyzed. We employed the previously established endogenous *nep4* enhancer²⁸ to drive expression of HA-tagged *nep4A* gene product (Nep4A::HA) at near-physiological levels. Identical subcellular localizations of endogenous and tagged versions of the protein were confirmed previously²⁴. As depicted in Fig. 3, within the heart and ventral longitudinal muscles, Nep4 localized to endomembranes, including the nuclear membrane (Fig. 3A', C', D', F', arrowheads). In addition, a punctate repetitive pattern along the muscle fibers was apparent (Fig. 3A', C', D', F', arrows). Identically-treated control crosses lacking the UAS construct (*nep4* > *w*¹¹¹⁸) did not exhibit any signal above background (Fig. 3G-G'). Co-labeling using anti-SERCA antibodies resulted in considerable signal overlap, indicating colocalization of the two enzymes within membranes of the SR compartment (Fig. 3B-C', E-F'). A similar pattern was evident in larval heart and body wall muscles (Fig. S1). This observation, together with the consistent responses to modified *nep4* expression in cardiomyocytes and body wall muscles (Fig. 1), suggests analogous functions of the peptidase in the two contractile tissues and across developmental stages.

To assess whether colocalization of Nep4 and SERCA reflected an interaction at the protein level, we performed pull-down assays using a green fluorescent protein (GFP) tagged Nep4 fusion protein (Nep4::GFP) as bait (Fig. 3I). The construct was expressed in muscles (*mef2-Gal4*) to probe interaction in a tissue with endogenous relevance of SERCA and Nep4.

SERCA efficiently coprecipitated with Nep4::GFP, indicating physical interaction between the two enzymes. Free cytoplasmic GFP (*mef2-Gal4* > GFP, Fig. 3I), as well as SR-luminal GFP (*mef2-Gal4* > GFP.ER, Fig. S9D) were used as individual controls. Coprecipitation of SERCA was absent in either control.

Nep4 colocalizes with SERCA-inhibitory Sarcolamban peptides

As depicted in Fig. 1, all Nep4-mediated effects on cardiac Ca^{2+} homeostasis and SERCA activity depended on the catalytic activity of the peptidase. This result implies that aberrant hydrolysis of certain peptides represents the mechanistic basis of the observed phenotypes. To date, only two SCL peptides have been identified as peptidergic regulators of SERCA activity in *Drosophila*¹¹. We found that Nep4::GFP and FH-tagged SCLA (FH::SCLA) partially colocalized with SERCA in body wall (Fig. S3) as well as in cardiac muscle cells (Fig. 4A-A''', B). In cardiomyocytes, substantial colocalization of all three factors was observed around the nucleus (Fig. 4B, solid arrow). More distant from the nucleus, mainly SERCA and SCLA signals were visible (Fig. 4B, open arrows). A similar localization pattern was observed for SCLB, Nep4, and SERCA (Fig. S2). Correct functionality and localization of the FH-tagged constructs had been confirmed previously¹¹. To analyze the subcellular localization in more detail, we performed stimulated emission depletion (STED)-based super-resolution imaging of corresponding heart preparations (Fig. 4C-C''', D-D'). The results indicated a rather dynamic local distribution of the three factors, with considerable overlap of Nep4, SERCA, and SCLA signals being evident in membranes contiguous with the nuclear membrane (Fig. 4D, solid arrow). In addition, individual colocalization between SCLA and SERCA (Fig. 4D, open arrow), Nep4 and SERCA (Fig. 4D, feathered arrow), or Nep4 and SCLA (Fig. 4D, solid winged arrowhead) was occasionally observed. Finally, we also detected free SERCA (Fig. 4D, open arrowhead), Nep4 (Fig. 4D, open winged arrowhead), and SCLA (Fig. 4D, solid arrowhead). More distant from the nucleus, mainly SERCA and SCLA were detected (Fig. 4D'). Again, a colocalizing portion (Fig. 4D', open arrow), as well as individual SERCA (Fig. 4D', open arrowhead) and SCLA signals (Fig. 4D', solid arrowhead), were present.

Nepilysins hydrolyze the luminal domain of SERCA-inhibitory peptides from flies and humans

Based on their spatial proximity within the SR membrane, we analyzed whether SCL represents a substrate of Nep4. To narrow down possible cleavage sites, we employed a Nep4::roGFP fusion protein to determine whether the catalytic center of Nep4, and thus its

hydrolytic activity, is oriented towards the SR lumen or the cytosol of muscle cells. As shown in a previous study, the excitation spectrum of roGFP is highly redox sensitive^{33, 34}. Accordingly, the steady-state fluorescence intensity ratio (405 nm / 488 nm excitation) of the free roGFP control reflected the reducing conditions present in the cytoplasm (Fig. S4A). By contrast, roGFP fused to the C-terminus of Nep4 exhibited a steady-state fluorescence intensity ratio characteristic of oxidizing conditions (Fig. S4B). This indicates that the C-terminus of Nep4, and thus its catalytic activity, resides in the SR lumen, suggesting that Nep4-mediated hydrolysis of target peptides occurs within this compartment. Of note, most of the SERCA-regulatory peptides identified to date, including the *Drosophila* SCL, harbor a luminal domain at their C-terminus²⁰. For human PLN, a single point mutation within this domain (V49A) completely disrupts the inhibitory effects of PLN on SERCA2a¹², which demonstrates the physiological relevance of the luminal domain.

To analyze whether the Nep4-mediated regulation of SERCA activity involves cleavage of the corresponding SCL peptide domains, we assessed the susceptibility of the luminal termini of SCLA (YLIYAVL, SCLA_{lum}) and SCLB (YAFYEAAF, SCLB_{lum}) to Nep4-mediated hydrolysis. To this end, recombinant Nep4 was purified from transfected *Sf21* insect cells and incubated with the respective peptides. As depicted in Fig. 5, Nep4 hydrolyzed both SCLA_{lum} and SCLB_{lum} at distinct positions. While SCLA_{lum} was mainly cleaved between Ala-5 and Val-6 (Fig. 5A, red chromatogram), SCLB_{lum} was hydrolyzed predominantly between Ala-2 and Phe-3 as well as between Ala-7 and Phe-8 (Fig. 5B, red chromatogram). Identically-treated control preparations lacking Nep4 did not exhibit any hydrolytic activity (Fig. 5A, B, green chromatograms). The observed cleavage specificities agree with the reported preference of Nep4 to cleave next to hydrophobic residues, particularly with Phe or Leu at P1'²⁴. To confirm the mechanistic relevance of the amino acids at P1', and thus the specificity of the Nep4-mediated SCL cleavage, we also analyzed mutated forms of the respective peptides (SCLA_{lum}(V6A); SCLB_{lum}(F8A), SCLB_{lum}(F3A), and SCLB_{lum}(F3A/F8A), Fig. S5). In all cases, the substitution of the P1' residue by Ala resulted in altered cleavage characteristics, ranging from the generation of novel hydrolysis products (Fig. S5A), up to a complete resistance of the corresponding derivative to Nep4 mediated hydrolysis (Fig. S5D). Considering the functional conservation of SERCA-regulatory peptides in metazoa^{35, 36}, we investigated whether the *Drosophila* SCL peptides are also cleaved by human neprilysin (NEP). Interestingly, the human enzyme hydrolyzed the *Drosophila* peptides with the same specificity as Nep4, yielding largely identical cleavage products (Fig. 5C, D). Furthermore, SLN, the vertebrate ortholog of SCL, was also hydrolyzed by both enzymes in a similar manner (Fig. 5E, F). In this regard, the SR-luminal domain of human SLN (WLLVRSYQY, SLN_{lum}) was analyzed for NEP- as well as Nep4-catalyzed hydrolysis. The peptide was selected because of two reasons: (i) it represents a potent inhibitor of SERCA activity and (ii)

it exhibits structural and functional homology to *Drosophila* SCL, including an intraluminal C-terminus of considerable size and mechanistic relevance^{35, 37, 38}. Both human NEP and *Drosophila* Nep4 cleaved SLN_{lum} predominantly between Leu-2 and Leu-3 as well as between Ser-6 and Tyr-7 (Fig. 5E, F), which confirms SLN as a novel NEP substrate *in vitro* and produces initial evidence that homeostasis and turnover of SERCA-regulatory micropeptides are controlled via similar mechanisms in humans and flies. All analyzed peptides, along with the individual Nep4 or NEP specific hydrolysis positions, are depicted in Tab. S1.

Nepilysin-mediated hydrolysis impairs membrane anchoring of SERCA-inhibitory micropeptides in S2 cells

To investigate the physiological significance of Nep4 / NEP-mediated SCL / SLN hydrolysis, we analyzed the consequences of the cleavage events at the molecular level. Therefore, CLIP-tagged full-length SCLA, SCLB, and SLN were expressed in *Drosophila* S2 cells, either with or without co-expression of Nep4 (SCLA, SCLB) or human NEP (SLN) (Fig. 6A-C). Consistent with the localization pattern in heart and body wall muscles (Figs. 3, 4, S1, S2, S3), the full-length peptides localized to the outer nuclear membrane and the ER of the cells (Fig. 6A, arrows), with only minor signals being present in nucleoplasm or cytoplasm. A similar localization pattern of full-length SCLA and SCLB in S2 cells has been reported previously¹¹. Strikingly, co-expression of Nep4 or NEP resulted in partial relocalization of the peptides to the cytoplasm, as indicated by reduced signal overlap with the ER marker Calnexin (Fig. 6A, arrowheads), suggesting a reduced membrane association of the cleaved peptides. To corroborate this indication, we analyzed cytoplasmic and membrane-enriched fractions generated from correspondingly transfected S2 cells by in-gel fluorescence detection and correlated Western blots. In absence of Nep4 or NEP, all peptides were present predominantly in the membrane-enriched fraction, but shifted into the cytoplasmic fraction in response to added expression of the individual peptidases (Fig. 6B). This effect was observed for all three peptides tested, yet the extent of relocalization was peptide-specific. While in case of SCLA, the ratio between membrane-enriched and soluble fraction shifted from 1.54 (-Nep4) to 0.68 (+Nep4, factor 2.3), the respective ratio for SCLB changed from 3.1 (-Nep4) to 1.52 (+Nep4, factor 2.0). SLN exhibited the strongest response to neprilysin expression, with a shift in ratio from 12.31 (-NEP) to 3.04 (+NEP, factor 4.0). The free CLIP-tag was considered as a fully soluble control (ratio: 0.18, Fig. 6C). In addition to expressing the full-length peptides together with the individual neprilysins, we also analyzed truncated forms of SCLA, SCLB, and SLN. In this regard, we expressed the predominant Nep4- or NEP-hydrolysis products identified above (Fig. 5) and evaluated their respective

localization in relation to the corresponding full-length peptides. All truncated peptides exhibited a considerably reduced membrane association (Fig. S6), with the extent being similar to the effects observed as a result of co-expressing the individual neprilysins along with the full-length peptides (Fig. 6). These results indicate that Nep4-mediated SCL cleavage and NEP-mediated SLN cleavage impair membrane localization of the respective peptides in a similar manner.

Nepilysin-mediated hydrolysis affects amount and oligomerization states of SERCA-inhibitory micropeptides in muscle tissue

In muscle cells of transgenic animals, reduced membrane localization in response to Nep4 overexpression was not observed for the *Drosophila* peptides (Figs. 6D, S7). However, in this tissue we detected species of higher molecular weight for both SCLA and SCLB that occurred in addition to the monomeric peptides (Fig. 6D). Corresponding constructs were stable in SDS-PAGE, thus probably representing SDS-resistant oligomers. Based on the apparent molecular masses (monomers: 17 kDa, oligomers: 68 kDa), tetrameric forms of the peptides are most likely. Of note, a similar resistance to denaturing conditions has also been confirmed for vertebrate PLN oligomers, with a pentameric form being predominant^{39, 40}. To our knowledge, this is the first indication on the ability of SCL peptides to oligomerize. Strikingly, for both peptides the high molecular weight species were largely absent in animals that overexpressed Nep4 in a muscle-specific manner (Fig. 6D, E), thus confirming *in vivo* relevance of the Nep4-mediated SCLA / SCLB cleavage and indicating that Nep4-mediated hydrolysis impairs the ability of both peptides to oligomerize. For SCLA, increased Nep4 expression also reduced the overall amount of the peptide in muscle cells by 56.9%, relative to animals with endogenous Nep4 expression, while overall SCLB levels were not significantly affected (Fig. 6E). The latter result was based on a tendency of monomeric SCLB to accumulate in animals with elevated Nep4 expression, thus compensating for the significant reduction in the amount of oligomeric SCLB and indicating a higher stability of Nep4-hydrolyzed SCLB, compared to hydrolyzed SCLA, in muscle tissue (Fig. 6D, E).

To further substantiate the indication that neprilysin-mediated SCL / SLN hydrolysis represents an evolutionarily conserved mechanism to regulate abundance and localization of the peptides, and thus SERCA activity, we analyzed the subcellular localization pattern of NEP and SERCA in human ventricular cardiomyocytes (Fig. S8). Both enzymes exhibited a highly similar localization, with the main signals being concentrated along the Z-discs of the muscle fibers (Fig. S8A'', arrow) and in membranes continuous with the nuclear membrane (Fig. S8A'', arrowhead). In control stainings lacking primary antibodies, no signal above background was observed (Fig. S8A'''). These data indicated colocalization of NEP and

SERCA in SR membranes of human cardiomyocytes, thus supporting the notion that neprilysin-mediated regulation of SERCA activity is relevant in humans and that the underlying molecular mechanisms may be comparable in flies and humans.

Discussion

While the principal mechanisms of muscle contraction in metazoa have been intensively studied, adaptive responses to variable physiological requirements are not entirely understood at the molecular level. However, SERCA is a major player involved in adaptation^{3, 4, 10, 36}. As known for vertebrates¹⁰, and more recently confirmed in insects¹¹, the activity of SERCA is controlled by SR membrane integral micropeptides that bind to the enzyme and modulate its activity. Well-characterized vertebrate peptides include PLN, SLN, MLN, and DWORF^{12, 13, 20, 21, 22}, while SCL represents a *Drosophila* ortholog of the SERCA-regulatory micropeptides¹¹. Based on the critical physiological relevance, vertebrate and fly loss-of-function mutants for these peptides exhibit compromised Ca²⁺ transients in heart cells concomitant with heart arrhythmia. In addition to the muscle-specific factors, endoregulin (ELN) and another-regulin (ALN) have been identified as SERCA-inhibiting micropeptides in non-muscle tissues, indicating a conserved mechanism for the control of intracellular Ca²⁺ dynamics in both muscle and non-muscle cell types³⁵. To date, no mechanism has been identified that directly regulates the turnover of any of the micropeptides within the SR membrane.

This study demonstrates that modulating the expression of the endopeptidase Nep4 significantly affects SERCA activity in *Drosophila*, thus establishing a correlation between neprilysin activity and the regulation of SERCA for the first time. A high physiological relevance is confirmed by the fact that altering *nep4* expression phenocopies characteristic effects of SCL knockout, including abnormal heart rhythmicity as well as impaired SERCA activity and SR Ca²⁺ load (Figs. 1, 2). By confirming Nep4-mediated hydrolysis of SERCA-regulatory SCL peptides (Figs. 5, S5), we provide evidence that neprilysin-mediated cleavage of these peptides is the mechanistic basis of the described phenotypes. The finding that the catalytically-active enzyme, and not the inactive variant, affected heart function and SERCA activity (Figs. 1, 2), supports this premise as it confirms aberrant enzymatic activity, and thus abnormal peptide hydrolysis, as a causative parameter.

Interestingly, we found that in S2 cells both, the *Drosophila* SCL peptides as well as human SLN exhibited a significantly reduced membrane anchoring ability as a result of co-expression of Nep4 or NEP, respectively (Fig. 6A-C). A similar effect was observed if the Nep4 / NEP hydrolysis products, identified in the *in vitro* cleavage assays (Fig. 5), were expressed in S2 cells. Again, Nep4-cleaved SCL as well as human NEP-cleaved SLN

exhibited a significantly reduced membrane localization, relative to the non-cleaved full-length peptides (Fig. S6). A milder relocalization effect was observed for truncated SCLA and SCLB, and a stronger was present with truncated SLN (Figs. 6, S6). Given the distinct cleavage products (Figs. 5, S6), the larger truncation of SLN (7 amino acids) in comparison to SCLA (2 amino acids) and SCLB (6 amino acids) may to some extent account for the individual effects. This possibility is supported by data confirming a similar degree of relocalization for human SLN and PLN in response to consecutive C-terminal truncation^{37, 41}, thus emphasizing the functional relevance of the corresponding C-termini.

In muscle tissue of transgenic animals, altered membrane localization in response to Nep4 overexpression was not observed for SCLA or SCLB. This was mainly due to the fact that, unlike the results in S2 cells, the peptide amounts detectable in the cytoplasmic fractions prepared from transgenic animals were very low, even if Nep4 was overexpressed. As a consequence, quantifying the ratio between soluble and membrane bound peptides was rather error-prone (Fig. 6D, S7). One explanation for this outcome could be an efficient degradation of the soluble Nep4-cleaved peptides in the cytoplasm of muscle cells, which may not occur that efficiently in S2 cells. Of note, instability and rapid intracellular degradation have already been reported for truncated forms of vertebrate PLN¹⁶ and SLN³⁷. However, a high *in vivo* relevance of the Nep4-mediated SCL cleavage was confirmed by the facts that muscle-specific overexpression of Nep4 significantly reduced the overall amount of SCLA in this tissue and, furthermore, largely abolished the formation of high molecular weight species of SCLA and SCLB, presumably representing peptide oligomers (Fig. 6D, E). While the reduced SCLA levels clearly indicate that Nep4 is required to control the amount of this peptide within the SR membrane, the reduced oligomerization observed for both SCLA and SCLB is equally remarkable, considering that oligomerization is also a well-known and physiologically highly relevant characteristic of vertebrate PLN¹⁰. Here, oligomerization represents a mechanism for storage of active PLN monomers, playing a key role in SERCA regulation^{42, 43}. Given our observation that SCL may also form oligomers (Fig. 6D, E), a similar mechanism could be present in *Drosophila*, with the Nep4 cleavage activity controlling both, the overall amount of the peptides, as well as the ratio between monomeric and oligomeric SCL. Of note, SCLA and SCLB oligomers were detected by SDS-PAGE, indicating high thermal stability and detergent resistant association. A similar resistance to denaturing conditions has also been reported for vertebrate PLN oligomers^{39, 40}.

Together with the data from S2 cells, these results indicate that i) Nep4 hydrolyzes SCLA and SCLB *in vivo*, ii) this cleavage event reduces membrane localization of the peptides as well as their ability to oligomerize, and iii) cleavage considerably reduces the overall amount of SCLA in muscles. In this regard, S2 cells may feature the principal molecular mechanism, while in muscle tissue, the highly adapted conditions result in a more complex regulation.

Here, especially the high abundance of SERCA may be crucial, which has been shown to affect the oligomeric structure of vertebrate PLN, with an increasing SERCA / PLN ratio causing depolymerization of pentameric PLN⁴⁴. Consistent with our results on the *Drosophila* SCL peptides, analyses on human PLN found i) a reduced membrane localization, ii) a reduced ability of the peptide to form oligomers, and iii) a reduced binding affinity to SERCA as a result of consecutive C-terminal truncation⁴¹. Thus, in addition to emphasizing the physiological relevance of the corresponding C-termini, these results corroborate the indication that amount and function of *Drosophila* and vertebrate SERCA-inhibitory micropeptides are regulated in a mechanistically similar manner.

Because interaction between the regulatory micropeptides and SERCA occurs within the SR membrane^{10, 11, 13}, it appears likely that loss of membrane localization represents the critical physiological event inactivating the peptides. This inactivation is presumably required to prevent the peptides from accumulating within the SR membrane and, eventually, from abnormally binding and inhibiting SERCA (Fig. 7). The fact that C-terminal truncation likewise affects membrane anchoring of human PLN⁴¹, human SLN^(37, Figs. 6, S6), and *Drosophila* SCL (Fig. 6, S6) indicates the presence of an evolutionarily conserved mechanism to control membrane association and general abundance of corresponding peptides.

Significantly, up to now no candidate enzyme that adequately catalyzes C-terminal cleavage *in vivo* has been identified in any organism. Our data indicate that Nep4 represents a corresponding factor in *Drosophila* and that the peptidase is necessary and sufficient to control the amount of SERCA-regulatory peptides within the SR membrane. Under *nep4* overexpression conditions, SCL peptides are excessively cleaved, while *nep4* knockdown results in peptide accumulation. As a result of both interventions, appropriate regulation of SERCA activity is impaired (Fig. 2), which eventually causes the observed phenotypes (Figs. 1, 2, 7).

In contrast to vertebrates that express multiple SERCA genes in a time- and tissue-specific manner^{4, 45}, in *Drosophila* only one corresponding gene is known (*CaP60A*,⁴⁶). Interestingly, this reduced complexity also applies to the SERCA-regulatory micropeptides. Currently, the only identified SERCA-regulatory micropeptides in *Drosophila* are SCLA and SCLB, with expression being confirmed in both cardiac and somatic muscle tissue¹¹. By contrast, vertebrate genomes contain at least four corresponding genes, each of them exhibiting specific expression patterns. While PLN and SLN are expressed in cardiac and slow skeletal muscle, MLN appears to be specific to all skeletal muscles^{12, 13, 20} and DWORF, the only SERCA-activating micropeptide identified to date, specific to heart and soleus²¹. This reciprocal expansion of SERCA and regulatory peptide family members during evolution suggests that the two families have coevolved as an effective and general mechanism to control Ca²⁺ handling in muscle cells. In this respect, the situation in *Drosophila*, with only

one SERCA and two micropeptide genes being present, would represent the phylogenetically ancient status, while a similar, yet more specialized regulation occurs in vertebrates. Our finding that altering *nep4* expression has similar effects in heart and body wall muscle cells supports this idea by indicating similar underlying physiologies in both contractile tissues (Fig. 1). Moreover, considering our data on human NEP (Figs. 5, 6, S6, S8), it appears likely that also the neprilysin-mediated regulation of micropeptide abundance is evolutionarily conserved. We could show that both human NEP and *Drosophila* Nep4 hydrolyze the luminal domain of human SLN with identical cleavage specificity (Fig. 5E, F). Furthermore, the effects on membrane anchoring were similar for truncated SCL and truncated SLN (Figs. 6A-C, S6), and also the localization pattern of NEP and SERCA in human ventricular cardiomyocytes (Fig. S8) was reminiscent of the corresponding pattern in the *Drosophila* heart (Figs. 3, 4, S1, S2). Interestingly, NEP expression has been reported to be elevated in cardiomyocytes of patients suffering from aortic valve stenosis or dilated cardiomyopathy⁴⁷. In that study, it was speculated that elevated NEP activity in these patient groups resulted in increased degradation of local bradykinin and ANP / BNP, and thus reduced protection from the progression of hypertrophy and fibrosis. However, in view of our data an alternative scenario may be more likely. We found that in human ventricular cardiomyocytes NEP localized in direct proximity to SERCA, which indicates colocalization in membranes of the SR (Fig. S8). Therefore, it is conceivable that the increased NEP expression results in increased cleavage of SLN and correspondingly enhanced SERCA activity and cardiomyocyte contractility. Thus, elevated NEP expression in aortic valve stenosis or dilated cardiomyopathy patients may represent a physiological response to restore cardiac ejection fraction and to ameliorate the effects of cardiac disease, rather than being causative.

While further research is necessary to assess these issues in detail, the present study introduces neprilysin activity as a novel and efficient regulator of SERCA. As SERCA is an important therapeutic target in myocardial disorders, our data can represent a valuable basis for the development of innovative therapies against predominant heart and muscle diseases.

Materials and Methods

Fly strains

The following *Drosophila* lines were used in this work. *w¹¹¹⁸* (RRID:BDSC_5905) was used as control strain. RRID:BDSC_59041 that expresses GFP fused to an ER / SR targeting signal from Cytochrome b5 under the control of UAS was applied as a control in pull-down assays. Driver lines were *mef2-Gal4* (RRID:BDSC_27390), *tinC-Gal4* (R. Bodmer, Sanford Burnham

Medical Research Institute, San Diego, CA, USA), and *nep4*-Gal4^{25,29}. UAS lines were UAS-Nep4A²⁵, UAS-Nep4A_{inact} (catalytically inactive form (E873Q),²⁵), UAS-FH::SCLA¹¹, and UAS-FH::SCLB¹¹. UAS-roGFP and UAS-Nep4::roGFP lines were established by cloning the *roGFP2*³³ or *nep4::roGFP2* coding sequence into the pUAST vector⁴⁸. The latter construct included a short in-frame spacer sequence (gcgggcgga) between the *nep4A* and *roGFP2* coding sequences. Resulting constructs were subjected to P-element-based transformation using commercial services (Best Gene Inc., CA, USA). Flies expressing GCaMP3 in a cardiac-specific manner (UAS-GCaMP3 / UAS-GCaMP3; *tinCΔ4*-Gal4, UAS-GCaMP3 / *tinCΔ4*-Gal4, UAS-GCaMP3,⁴⁹) were applied to measure Ca²⁺-transients in cardiomyocytes. Knockdown of *nep4* was achieved using line 100189 (KK library, Vienna *Drosophila* Resource Center [VDRC]). High *nep4*-specific knockdown efficiency of the respective hairpin was confirmed previously^{24, 25}. A second *nep4*-specific RNAi construct (line 16669, GD library, VDRC) did not significantly reduce *nep4* transcript levels²⁵. It was therefore excluded from further analysis.

Generation of expression constructs

For heterologous expression of Nep4B in *Sf21* cells, the *nep4B* coding sequence was fused to a C-terminal His-tag by appropriate primer design and cloned downstream of the polyhedrin promoter into a pFastBac Dual vector (Thermo Fisher Scientific, Waltham, MA, USA). To track transfection efficiency, an *eGFP* reporter gene was inserted into the same vector under the control of the p10 promoter. Generation of recombinant bacmids and transfection/infection was performed according to the Bac-to-Bac baculovirus expression system manual (Life Technologies, Carlsbad, CA, USA).

Plasmids for expression of CLIP-tagged peptides, human NEP or *Drosophila* Nep4 in S2 cells were generated based on an *E. coli* / *S. cerevisiae* / *D. melanogaster* triple-shuttle derivative of the pAc5.1/V5-His vector (Thermo Fisher Scientific) adapted for cloning by homologous recombination *in vivo*. The respective vector was constructed by *in vivo*-recombination in yeast, inserting *URA3* and a 2 μm sequence for selection and propagation, respectively, as described⁵⁰. Constructs expressing truncated peptides were generated using the Q5 Site-Directed Mutagenesis Kit (New England Biolabs, Ipswich, MA, USA) according to the manufacturer's instructions.

Motility and contraction analysis

Nep4 overexpression and knockdown was driven by *mef2*-Gal4. The driver line crossed to *w¹¹¹⁸* was used as a control. Movement and contraction assays were conducted as

previously described⁵¹. Briefly, wandering third instar larvae of each respective genotype were transferred onto glass petri dishes supplemented with millimeter paper. All movements were recorded with a standard video camera (Canon UC X10Hi, Canon, Tokyo, Japan). Movement speed was determined by calculating the distance covered in a continuous run of 10 s. The same run was used to count larval body contractions. Because increased Nep4 levels in muscle tissue affect body size²⁴, distance and speed were calculated in relation to animal size.

Analysis of cardiac function

For SOHA analysis, 1-week-old male flies were tranquilized on ice for 1 min, placed in a 60 mm petri dish containing a thin layer of Vaseline, and fixed by their spread wings with the ventral side up. Animals were then covered with artificial hemolymph solution containing 5 mM KCl, 8 mM MgCl₂, 2 mM CaCl₂, 108 mM NaCl, 1 mM NaH₂PO₄, 5 mM HEPES, 4 mM NaHCO₃, 10 mM trehalose, and 10 mM sucrose, pH 7.1⁵². For semi-intact heart preparations, the head as well as the ventral half of the thorax and abdomen and all abdominal internal organs, except for the dorsal vessel, were removed. After dissection, the preparation was allowed to rest for at least 10 min. Heartbeat recordings were evaluated as described previously^{23, 53}.

Measurements of Ca²⁺ transients were conducted as previously described^{54, 55}. Briefly, 1-week-old male flies were anesthetized with carbon dioxide, placed in a 60 mm petri dish containing Vaseline, and fixed with the ventral side up. The head and thorax were cut off to exclude neuronal influence on cardiac activity. The middle ventral region of the abdomen was opened and the internal organs were removed. Subsequently, the preparation was submerged in oxygenated artificial hemolymph solution. Ca²⁺ transients were recorded using a Carl Zeiss LSM 410 confocal microscope (Zeiss, Jena, Germany). GCaMP3 was excited at 488 nm with an Ar laser and the fluorescence signal was detected using a 505–530 nm band-pass detection filter. Changes in fluorescence of the conical chamber, localized in the first abdominal segment, were scanned, with an increase in fluorescence, followed by a decrease in fluorescence, reflecting the transient elevation of cytosolic [Ca²⁺] that precedes contraction. Recordings of Ca²⁺ transients were conducted for 25 seconds. Resulting images (1024 x 1024 pixel) were analyzed with ImageJ (National Institutes of Health, MD, USA) and LabChart software (AD Instruments, CO, USA).

Analyzed hearts were not paced and parameters were only compared under the premise that spontaneous heart rates of semi-intact preparations were not significantly different between the individual groups of flies. Ca²⁺ transient amplitudes were calculated according to the formula $F_{\max} - F_0 / F_0$ and depicted in arbitrary units of fluorescence. F_{\max} represents the

maximal fluorescence signal obtained during the systole, and F0 corresponds to the minimal fluorescence recorded during the diastolic period. This approach normalizes differences in indicator concentration between cells, thus providing a plausible method for comparing ratios between different samples / genotypes. Relaxation was measured by calculation of Tau constant (sec), based on the exponential decay of Ca^{2+} transients. For estimating the sarcoplasmic reticulum Ca^{2+} load, a caffeine pulse (10 mM) was applied to the perfusion media. This compound triggers the release of Ca^{2+} through the ryanodine receptor³⁰. The amplitudes of the caffeine-induced Ca^{2+} transient and the Ca^{2+} transients recorded during the 5 seconds preceding the caffeine pulse (pre-caffeine) were measured and Ca^{2+} load was expressed as the ratio between the caffeine-induced Ca^{2+} transient amplitude divided by the average of the corresponding pre-caffeine Ca^{2+} transient amplitudes. SERCA activity was calculated by subtracting the inverse of the rate constant of caffeine induced Ca^{2+} transient decay (Tau_{Caff}) from that of the pre-caffeine transients (Tau_{Ca}), $(1/\text{Tau}_{\text{Ca}} - 1/\text{Tau}_{\text{Caff}})$. In this regard, the rate constant of $[\text{Ca}^{2+}]_i$ decay during a caffeine-induced Ca^{2+} transient largely reflects the function of NCX, while both NCX and SERCA contribute to pre-caffeine $[\text{Ca}^{2+}]_i$ decay^{30, 56, 57, 58, 59, 60, 61, 62, 63}.

Cell culture, subcellular localization and fractionation

S2 cells were grown in Schneider's *Drosophila* medium (Pan Biotech, Aidenbach, Germany). Transfection was done in 6-well plates or 15 cm² flasks using TransFectin (BioRad, Hercules, CA, USA) according to the manufacturer's instructions. For co-transfection, total plasmid amounts were adjusted to a maximum of 3 µg. For immunostaining, cells were fixed in 4% formaldehyde in phosphate-buffered saline (PBS) for 20 min and rinsed three times with PBS. Subsequently, samples were treated with permeabilization/blocking solution (0.1% Triton X-100, 2% bovine serum albumin [BSA] in PBS) for 20 min and rinsed again three times with PBS. To exclude a possible cross-reaction of antibodies, cells were sequentially stained. In a first step, samples were incubated with anti-Calnexin antibodies (RRID:AB_2722011, 1:200) overnight at 4°C. Cells were washed with PBS (3x, 15 min each), blocked with ROTI ImmunoBlock (Roth, Karlsruhe, Germany) for 45 min, and incubated with secondary antibodies (RRID:AB_2534071, 1:200) diluted in ROTI ImmunoBlock for 90 min. Cells were washed as described before and incubated with anti-CLIP antibodies (RRID:AB_2827567, 1:100) and anti-Nep4/anti-NEP antibodies (anti-Nep4: RRID:AB_2569115, 1:500, monospecificity confirmed in²⁸; anti-NEP: human, ab256494, 1:100, Abcam). Following another washing step, cells were blocked again with ROTI ImmunoBlock and incubated with secondary antibodies (RRID:AB_2534074, 1:200; RRID:AB_2338084, 1:100). Finally, cells were washed again as described above and

mounted in Fluoromount-G (Thermo Fisher Scientific). Confocal images were captured with an LSM 800 microscope (Zeiss). For fractionation, 5 ml of transfected cells were harvested (300 x g, 3 min, room temperature [RT]) and labeled with 1 μ M CLIP-Cell TMR-Star (New England Biolabs) in 100 μ l PBS at 37 °C for 30 min. Excess substrate was washed out with PBS for 15 min. Afterwards, cells were resuspended in 500 μ l 0.5 M NaCl including protease inhibitor (Promega, Madison, WI, USA.) and lysed using a glass-teflon homogenizer. Homogenates were centrifuged to remove cell debris (500 x g, 5 min, 4 °C) and the resulting supernatant was subjected to ultracentrifugation (100.000 x g, 1 h, 4 °C). The soluble cytoplasmic fraction was collected and prepared for SDS-PAGE, while the pellet was resuspended in 250 μ l 0.5 M NaCl, using a 1 ml syringe with a 25 gauge needle. Following another ultracentrifugation step (100.000 x g, 45 min, 4 °C), the membrane-enriched pellet was resuspended again in the same buffer and prepared for SDS-PAGE. In-gel detection of CLIP-tagged constructs was done with a ChemiDoc MP Imaging System (BioRad). For quantification, pixel intensities were measured using Image Lab Software, Version 6.0.1 (BioRad).

For fractionation of tissue samples, transgenic 3rd instar larvae were frozen in liquid nitrogen and homogenized. Homogenates were resuspended in 120 μ l 0.5 M NaCl including protease inhibitor and centrifuged (10.000 x g, 15 min, 4 °C). The resulting supernatant was processed similar to the supernatant of S2 cells, yet 60 μ l were used for pellet resuspension after ultracentrifugation. Western blot based pixel intensities were quantified with a ChemiDoc MP Imaging System (BioRad) in combination with Image Lab Software, Version 6.0.1 (BioRad).

Enzymatic cleavage assay

Heterologous expression of Nep4B was performed in S₂21 cells (RRID:CVCL_0518) as described previously²⁴. Transfected and non-transfected S₂21 cells were cultured in 75 cm² flasks for 72 h and harvested by centrifugation (300 x g, 5 min). Subsequently, cells were resuspended in 5 ml binding buffer (50 mM NaH₂PO₄, pH 7.9, 300 mM NaCl) and lysed with a glass-teflon homogenizer. The resulting homogenates were centrifuged (10.000 x g, 10 min) and the supernatants were subjected to gravity-flow-based His-tag purification according to the manufacturer's instructions (Protino Ni-NTA agarose, Macherey-Nagel, Düren, Germany). To measure enzymatic activity, 3 μ l of Nep4B-containing (10 ng/ml, purified from *nep4B* transfected cells) and non-containing (from untransfected control cells) preparations were supplemented with 7 μ l (250 ng) of individual peptides. To measure activity of human NEP (transcript variant 1, D⁵³-W⁷⁵⁰, N-terminal His-tag fusion, Enzo Life Sciences, Farmingdale, NY, USA), 1 μ l (50 ng) of the enzyme was supplemented with 9 μ l (250 ng) of individual peptides. All dilutions were prepared in hydrolysis buffer (100 mM

NaCl, 50 mM Tris, pH 7.0). After 5 h of incubation (35 °C), 1 µl of each respective preparation was analyzed via mass spectrometry (see below). For measurements of untreated peptides, respective samples were diluted in hydrolysis buffer without addition of enzyme and processed as described above. Peptides were synthesized at JPT Peptide Technologies (Berlin, Germany) with more than 90% purity. Individual cleavage assays were repeated at least three times.

Pull-down assay

30 third instar larvae of each control genotype (*mef2-Gal4 > UAS-roGFP* or *mef2-Gal4 > UAS-GFP.ER*), as well as an equal weight of *mef2-Gal4 > UAS-Nep4A::roGFP* third instar larvae, were frozen in liquid nitrogen and homogenized. Homogenates were resuspended in 300 µl lysis buffer (150 mM NaCl, 50 mM Tris, 1 mM MgCl, 0.2% n-dodecyl-β-D-maltopyranoside [DDM]) and centrifuged (10.000 x g, 15 min). The resulting supernatants were incubated for 30 min at 4 °C with 50 µl of µMACS anti-GFP MicroBeads (Miltenyi Biotec, Auburn, CA, USA). Beads were immobilized in calibrated µ-columns (Miltenyi Biotec), which were equilibrated beforehand with 200 µl lysis buffer. After two washing steps using 200 µl lysis buffer, bound proteins were reduced by incubation in 50 µl reducing solution (10 mM dithiothreitol [DTT], 100 mM NH₄HCO₃) for 5 min at RT and additional 30 min at 38 °C, followed by two washing steps with 20 mM Tris-HCl (pH 7.5). Subsequently, bound proteins were alkylated by addition of 50 µl alkylation solution (54 mM Iodacetamid, 100 mM NH₄HCO₃) and incubation for 15 min in the dark. The columns were then washed twice with 100 µl digestion buffer (50 mM NH₄HCO₃, 5% acetonitrile), sealed, and incubated with 25 µl trypsin solution (0.01 µg trypsin / lysC in digestion buffer) overnight. Eluates were centrifuged (10.000 x g, 10 min) and subjected to mass spectrometry analysis (5 µl per sample). At least three independent biological replicates were analyzed for each genotype.

Mass spectrometry

Reversed-phase chromatography was performed using the UltiMate 3000 RSLCnano System (Thermo Fisher Scientific). Samples were loaded onto a trap column (Acclaim PepMap 100 C18, 5 µm, 0.1 mm x 20 mm, Thermo Fisher Scientific) and washed with loading buffer (0.1% TFA in H₂O) at a flow rate of 25 µl/min. The trap column was switched in line with a separation column (Acclaim PepMap 100 C18 2 µm, 0.075 mm x 150 mm, Thermo Fisher Scientific). Subsequently, bound peptides were eluted by changing the mixture of buffer A (99% water, 1% acetonitrile, 0.1% formic acid) and buffer B (80% acetonitrile, 20% water and 0.1% formic acid) from 100:0 to 20:80 within 60 min. The flow

rate was kept constant at 0.3 $\mu\text{l}/\text{min}$. Eluted compounds were directly electrosprayed through an EASY-Spray ion source (Thermo Fisher Scientific) into a Q Exactive Plus Orbitrap mass spectrometer (Thermo Fisher Scientific). Eluates were analyzed by measuring the masses of the intact molecules as well as the masses of the fragments, which were generated by higher-energy collisional dissociation (HCD) of the corresponding parent ion. For peptide cleavage assays, extracted ion chromatograms corresponding to the synthesized peptides or their respective proteolytic fragments were analyzed using FreeStyle Software (v1.3, Thermo Fisher Scientific). For analysis of pull down data, PEAKS Studio software (Version 10.6, Bioinformatics Solutions Inc., Waterloo, Canada), in combination with a *Drosophila*-specific SwissProt database (UP000000803, www.uniprot.org/proteomes/UP000000803) was used to determine peptide-specific amino acid sequences (parent mass error tolerance: 10 ppm; fragment mass error tolerance: 0.2 Da; enzyme: trypsin; max missed cleavages: 2; selected PTMs: carbamidomethylation, oxidation, phosphorylation). Label-free quantification was performed by comparing peptide and protein amounts of different groups according to established protocols⁶⁴, with each group consisting of at least three independent biological replicates. The protein list was controlled by FDR (threshold: 1%) and significance was calculated by PEAKS software (one-way ANOVA). Classification as possible interaction partner required $p < 0.01$, with quantification being based on at least two individual protein-specific peptides. The mass spectrometry proteomics data have been deposited to the ProteomeXchange Consortium via the PRIDE⁶⁵ partner repository (<http://www.ebi.ac.uk/pride>) with the dataset identifier PXD027738.

Immunohistochemistry and western blot

Animals were dissected on Sylgard plates (Sylgard 184 Elastomer Base and Curing Agent, Dow Corning, MI, USA), fixed in 3.7% formaldehyde in PBS for 1 h, rinsed three times in PBS, and transferred into 1.5 ml reaction cups. Subsequently, tissues were permeabilized in 1% Triton X-100 for 1 h, blocked in ROTI ImmunoBlock (45 min), and incubated with primary antibodies (overnight, 4 °C). Samples were washed in PBT (3x, 10 min each) and blocked again as described above. Secondary antibodies were applied for 90 min. For staining of human tissue, myocardial left ventricular heart slices (5 μm) were deparaffinized and rehydrated as previously described⁶⁶. Tissue permeabilization was done in 0.1 % Triton X-100 (15 min), followed by washing in PBS (3x) and blocking in 5% BSA. Primary antibodies were diluted in 5% BSA in PBS and incubated overnight. Sections were washed in 1% BSA in PBS (3x, 5 min each), followed by incubation with secondary antibodies (1 h, 4 °C). Finally, samples were washed as described above and mounted in Fluoromount-G. Primary antibodies used were: anti-Nep4 (RRID:AB_2569115, 1:200, monospecificity confirmed in²⁸),

anti-SERCA (1:500, *Drosophila*-specific, kind gift from Mani Ramaswami, monospecificity confirmed in ⁶⁷), anti-SERCA (human, ab219173, 1:100, Abcam, Cambridge, UK), anti-NEP (human, ab256494, 1:100, Abcam), anti-GFP (RRID:AB_889471, 1:500), anti-GFP (RRID:AB_305564, 1:2000), anti-GFP (RRID:AB_300798, 1:750), and anti-HA (RRID:AB_262051, 1:100). The secondary antibodies were anti-mouse-A647 (RRID:AB_2687948, 1:200), anti-mouse-Cy2 (RRID:AB_2307343, 1:100), anti-mouse-Cy3 (RRID:AB_2338680, 1:200), anti-rabbit-Cy2 (RRID:AB_2338021, 1:100), anti-rabbit-Cy3 (RRID:AB_2338000, 1:200), anti-rabbit-Dy550 (RRID:AB_10674190, 1:200), anti-goat-A488 (ab150141, Abcam, 1:150), and anti-chicken-A488 (RRID:AB_2340375, 1:100). For STED imaging, Star 488 (2-0102-006-7, Abberior, Göttingen, Germany), Star Orange (RRID:AB_2847853), and Star Red (RRID:AB_2620152) secondary antibodies were used. Confocal images were captured with an LSM5 Pascal confocal microscope (Zeiss). STED imaging was performed using a Leica TCS STED CW microscope (Leica Microsystems, Wetzlar, Germany).

Western blots were performed as described ²⁵. Primary antibodies were anti-Actin (RRID:AB_528068, 1:20), anti-Calnexin (RRID:AB_2722011, 1:500), and anti-SERCA (⁶⁷, 1:5000). Secondary antibodies were anti-mouse-alkaline phosphatase (AP) (RRID:AB_258091, 1:10.000) and anti-rabbit-alkaline phosphatase (RRID:AB_258446, 1:10.000). For quantification, pixel intensities of respective bands were measured using Image Lab Software, Version 6.0.1 (BioRad).

Protein orientation

Determination of Nep4 orientation in SR membranes was performed as described ³⁴. Briefly, dorsal muscles of Nep4::roGFP2-expressing third instar larvae were dissected as previously described ⁵³. As distinct from heart preparations, the dorsal vessel as well as the main tracheal branches were also removed. Preparations were placed with the ventral side down on an object slide and covered with PBS. Confocal images were captured with an inverse LSM Olympus IX81 (Zeiss) using excitation at 405 nm and 488 nm. After measuring an untreated steady state, the PBS was replaced by 0.5 mM diamide and the oxidized state was captured 1 min later. Subsequently, the diamide solution was replaced by 2 mM DTT and the reduced state was captured after 7 min of incubation. By calculating the ratio of the average 405 nm / 488 nm signal intensities and comparing the steady-state ratio with the corresponding oxidized and reduced states, the redox environment of Nep4::roGFP in the untreated muscles was deduced. As a control, cytoplasmic roGFP2 was analyzed analogously.

Statistical analysis

For statistical analysis of physiological heart parameters, cardiac Ca²⁺ transients, muscle performance, and Nep4 orientation in the SR membrane, one-way ANOVA followed by Dunnett's Multiple Comparison Test was used. ER / nuclear fluorescence ratios were statistically assessed by one-way ANOVA with subsequent Bonferroni's Multiple Comparison Test to allow for comparison between selected groups. Western blot quantifications and analyses on the effects of variable heart rates on Ca²⁺ flux parameters (Tab. S2) were statistically analyzed using a paired t-test (two-tailed) allowing pairing of related values from one individual replicate. For all tests, a p value < 0.05 was considered significant (*p < 0.05, **p < 0.01, ***p < 0.001). Except for the pull-down data, which were statistically analyzed and visualized with PEAKS Studio software, all other data were analyzed and visualized using GraphPad Prism 5 (Version 5.03, GraphPad Software Inc., San Diego, CA, USA).

Figures

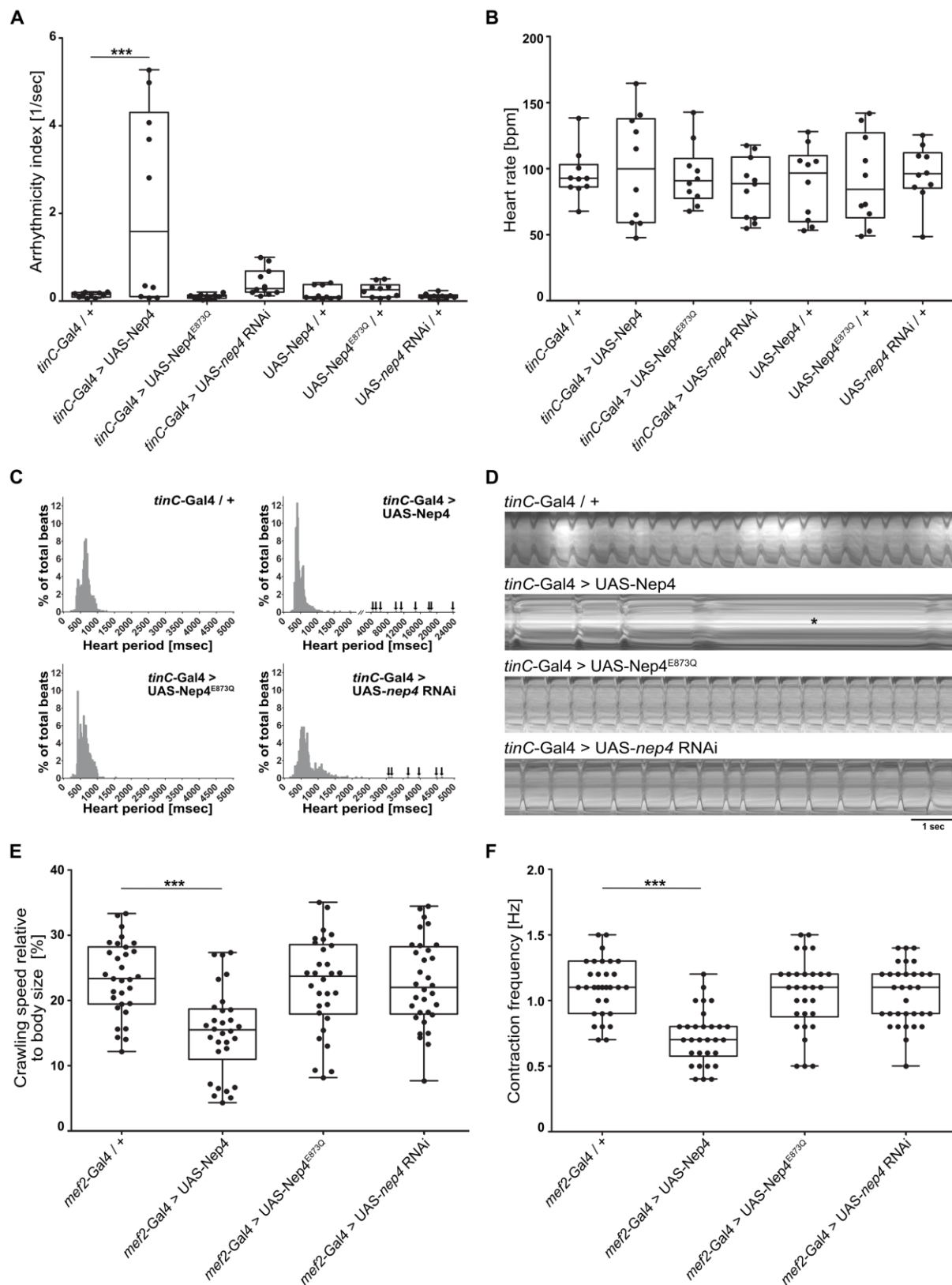


Figure 1

Nep4 activity is critical to heart and body wall muscle function. (A) Relative to control animals (*tinC-Gal4 / +*, $n = 10$), cardiomyocyte-specific overexpression of catalytically active *Nep4* (*tinC-Gal4 > UAS-Nep4*, $n = 10$) results in arrhythmia. Overexpression of inactive *Nep4* (*tinC-*

Gal4 > UAS-Nep4^{E873Q}, n = 10) or reduced expression of the peptidase (*tinC*-Gal4 > UAS-*nep4* RNAi, n = 11) do not significantly affect rhythmicity. UAS controls (UAS-Nep4, n = 10; UAS-Nep4^{E873Q}, n = 10; UAS-*nep4* RNAi, n = 10) lacking Gal4 expression are also without any effect. **(B)** Relative to control animals (*tinC*-Gal4 / +, n = 10), neither knockdown of *nep4* (*tinC*-Gal4 > UAS-*nep4* RNAi, n = 11) nor increased expression of active (*tinC*-Gal4 > UAS-Nep4, n = 10) or inactive Nep4 (*tinC*-Gal4 > UAS-Nep4^{E873Q}, n = 10) affect heart rate. **(C)** Combined histograms showing the distribution of heart periods (HP) from flies of the indicated genotypes. Cardiomyocyte-specific overexpression of catalytically active Nep4 (*tinC*-Gal4 > UAS-Nep4, n = 10 with 964 recorded beats) as well as reduced expression of the peptidase (*tinC*-Gal4 > UAS-*nep4* RNAi, n = 11 with 881 recorded beats) result in occurrence of abnormally long HPs (arrows). Control hearts (*tinC*-Gal4 / +, n = 10 with 897 recorded beats) or hearts overexpressing inactive Nep4 (*tinC*-Gal4 > UAS-Nep4^{E873Q}, n = 10 with 929 recorded beats) do not exhibit such impairments. **(D)** Representative 10 s M-mode traces depict heart contractions from flies of the indicated genotypes. Increased expression of catalytically active Nep4 (*tinC*-Gal4 > UAS-Nep4) causes arrhythmia with prolonged periods of diastolic heart arrest (asterisk). **(E)** Body wall muscle function is impaired by elevated Nep4 levels. Relative to control animals (*mef2*-Gal4 / +, n = 31), muscle-specific Nep4 overexpression (*mef2*-Gal4 > UAS-Nep4, n = 30) results in a decrease in crawling speed by 34%. Increased expression of catalytically inactive Nep4 (*mef2*-Gal4 > UAS-Nep4^{E873Q}, n = 30) or knockdown of the peptidase (*mef2*-Gal4 > UAS-*nep4* RNAi, n = 32) has no significant effect. To factor in the fact that elevated levels of Nep4 affect body size²⁴, the crawling speed [mm/sec] was calculated relative to the size of respective animals. **(F)** Relative to control animals (*mef2*-Gal4/+, median: 1.1 Hz, n = 31), muscle-specific Nep4 overexpression (*mef2*-Gal4 > UAS-Nep4, n = 30) results in decreased muscle contraction frequency (median: 0.7 Hz). Increased expression of catalytically inactive Nep4 (*mef2*-Gal4 > UAS-Nep4^{E873Q}, n = 30) or knockdown of the peptidase (*mef2*-Gal4 > UAS-*nep4* RNAi, n = 32) has no significant effect (median: 1.1 Hz and 1.1 Hz, respectively). Asterisks indicate statistically significant deviations from respective controls (p < 0.001, one-way ANOVA followed by Dunnett's Multiple Comparison Test). For all experiments, at least 10 individual animals were analyzed per genotype.

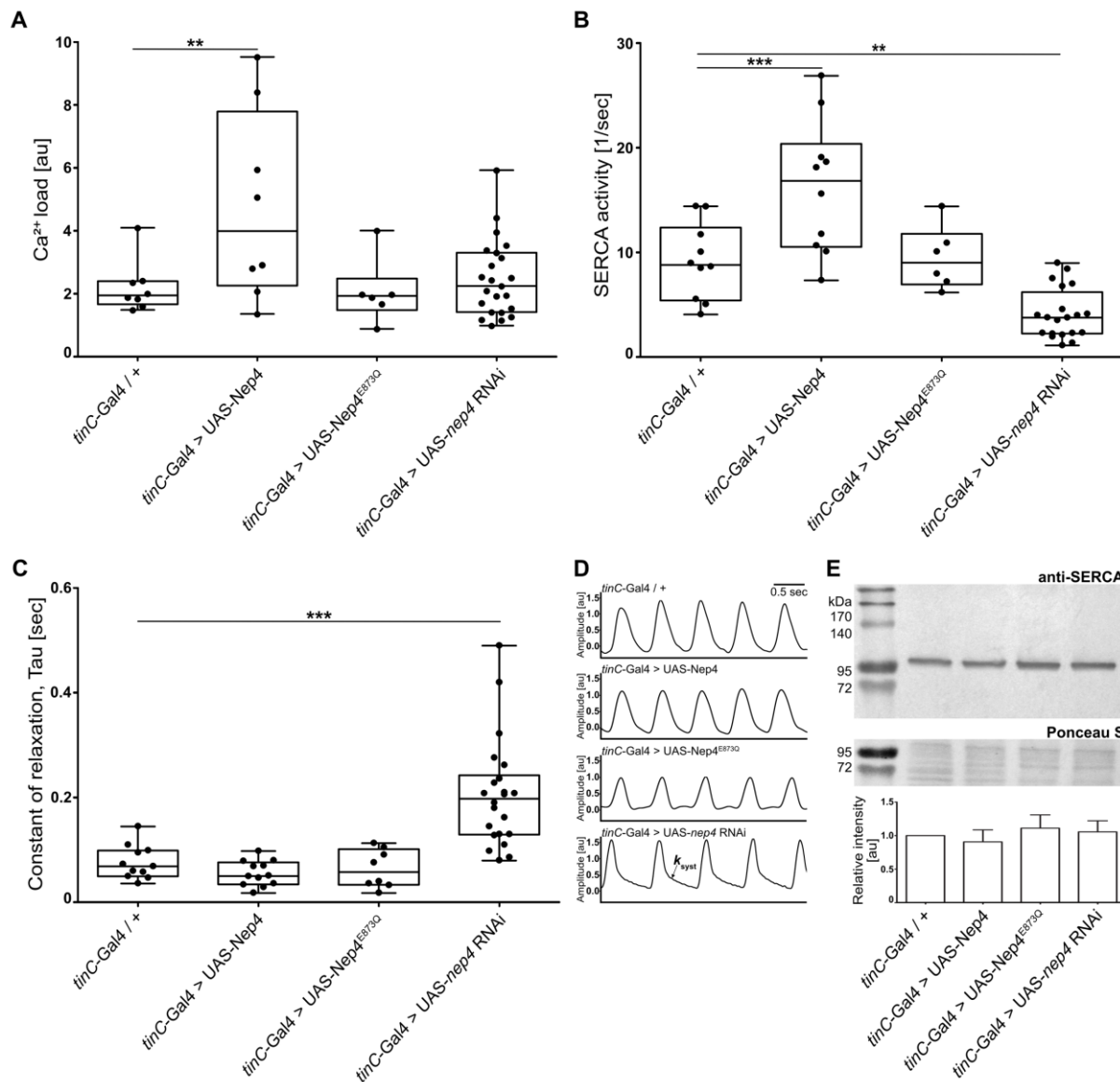


Figure 2

Cardiac Ca²⁺ homeostasis is affected by altered nep4 expression levels. **(A)** Relative to control animals (*tinC-Gal4 / +*, n = 8), sarcoplasmic reticulum Ca²⁺ load is increased by 105% in cardiomyocytes overexpressing active Nep4 (*tinC-Gal4 > UAS-Nep4*, n = 8). Overexpression of catalytically inactive Nep4 (*tinC-Gal4 > UAS-Nep4^{E873Q}*, n = 6) or knockdown of the peptidase (*tinC-Gal4 > UAS-nep4 RNAi*, n = 23) has no significant effect. **(B)** Relative to control animals (*tinC-Gal4 / +* n = 10), overexpression of active Nep4 (*tinC-Gal4 > UAS-Nep4*, n = 10) results in an increase in SERCA activity by 91%, while knockdown of the peptidase (*tinC-Gal4 > UAS-nep4 RNAi*, n = 20) reduces SERCA activity by 57%. Overexpression of catalytically inactive Nep4 (*tinC-Gal4 > UAS-Nep4^{E873Q}*, n = 6) has no significant effect. **(C)** The constant of relaxation (Tau) is only affected by knockdown of *nep4*. Relative to controls (*tinC-Gal4 / +*, n = 11), corresponding animals (*tinC-Gal4 > UAS-nep4 RNAi*, n = 22) exhibit a 2.9-fold increase in Tau. Overexpression of active (*tinC-Gal4 > UAS-Nep4*, n = 12) or inactive Nep4 (*tinC-Gal4 > UAS-Nep4^{E873Q}*, n = 8) has no

significant effects. Asterisks indicate statistically significant deviations from respective controls (** $p < 0.01$, *** $p < 0.001$, one-way ANOVA followed by Dunnett's Multiple Comparison Test). Each dot represents one analyzed animal. **(D)** Representative Ca^{2+} traces indicating the decay rate constant of the systolic Ca^{2+} transients (k_{syst}). Traces from 1 week old adult *Drosophila* hearts of the depicted genotypes are shown. **(E)** Representative western blot of total protein extracts isolated from adult flies of the indicated genotypes. For quantification, pixel intensity measurements were normalized to corresponding loading controls (Ponceau S). Resulting values are shown relative to the control (*tinC-Gal4 / +*). The lower panel depicts the mean values (+ SD) of three individual biological replicates. SERCA protein levels are not affected by altered *nep4* expression (paired t-test, two-tailed).

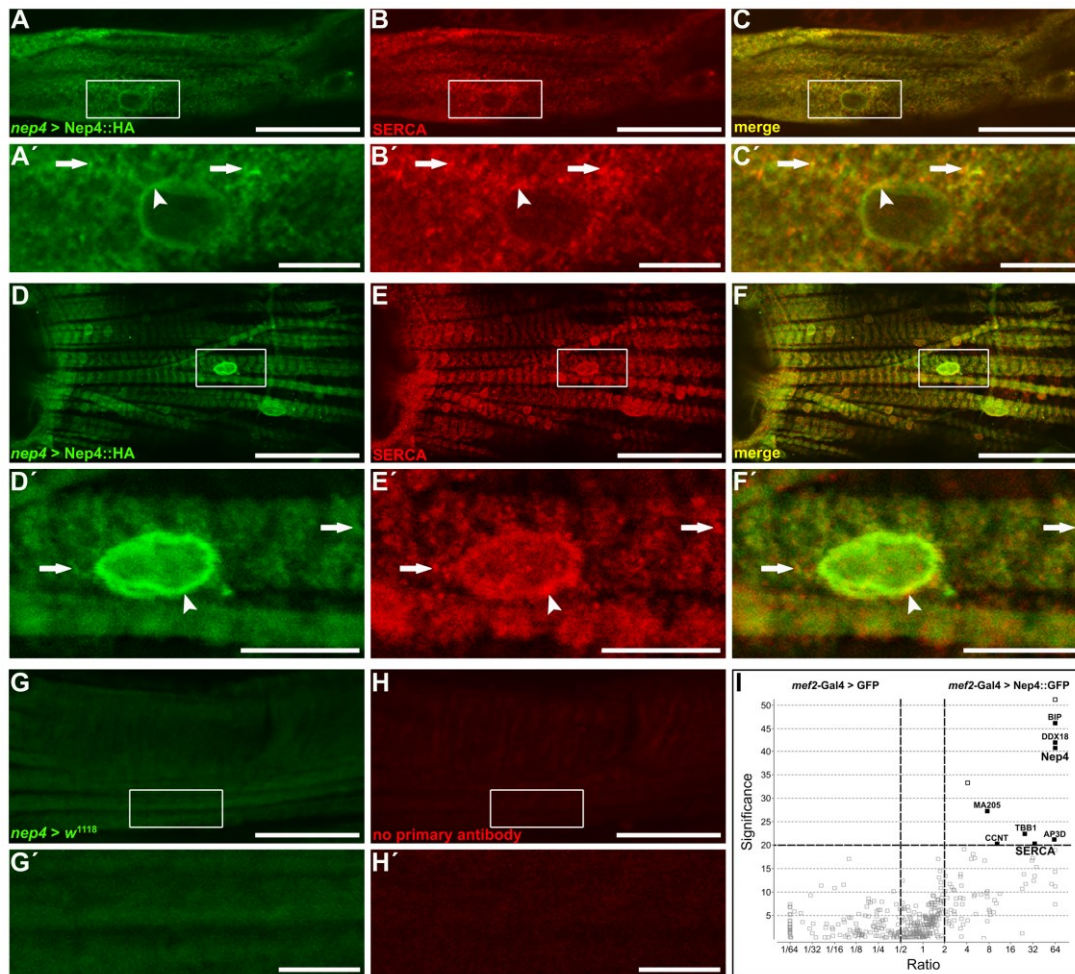


Figure 3

Nep4 partially colocalizes with *SERCA* in heart tissue. (**A, D**) *Nep4::HA* was expressed under the control of the native *nep4* enhancer and labeled with a monospecific anti-HA antibody (*nep4* > *Nep4::HA*). (**B, E**) *SERCA* was labeled with a monospecific antibody detecting the endogenous protein (*SERCA*). Optical slices of adult heart muscle fibers (**A-C**) or ventral longitudinal muscle fibers (**D-F**) are shown. Scale bars: 50 μ m; ventral view, anterior left. Boxes indicate areas of higher magnification, as depicted in (**A'-C'**) and (**D'-F', D''', E'''**). Scale bars: 10 μ m. *Nep4::HA* colocalizes with *SERCA* in membranes contiguous with the nuclear membrane (**C', F'**, arrowheads). In addition, both proteins partially colocalize in a punctate manner along the muscle fibers (**C', F'**, arrows). Control stainings lacking the UAS *Nep4::HA* construct (*nep4* > *w¹¹¹⁸*, **G, G'**) or primary *SERCA* antibodies (**H, H'**) do not exhibit any signal above background. (**I**) Volcano plot depicting the results of pull-down assays using *Nep4::GFP* as bait and free cytoplasmic *GFP* as control. Bait proteins were expressed in third instar larval muscle tissue. *SERCA* coprecipitates with *Nep4::GFP*. Data are based on three individual biological replicates. Open outlined squares depict proteins with quantification being based on only one detected peptide. Corresponding candidates were excluded from further analysis. A significance value of 20 corresponds to $p < 0.01$ (one-way ANOVA).

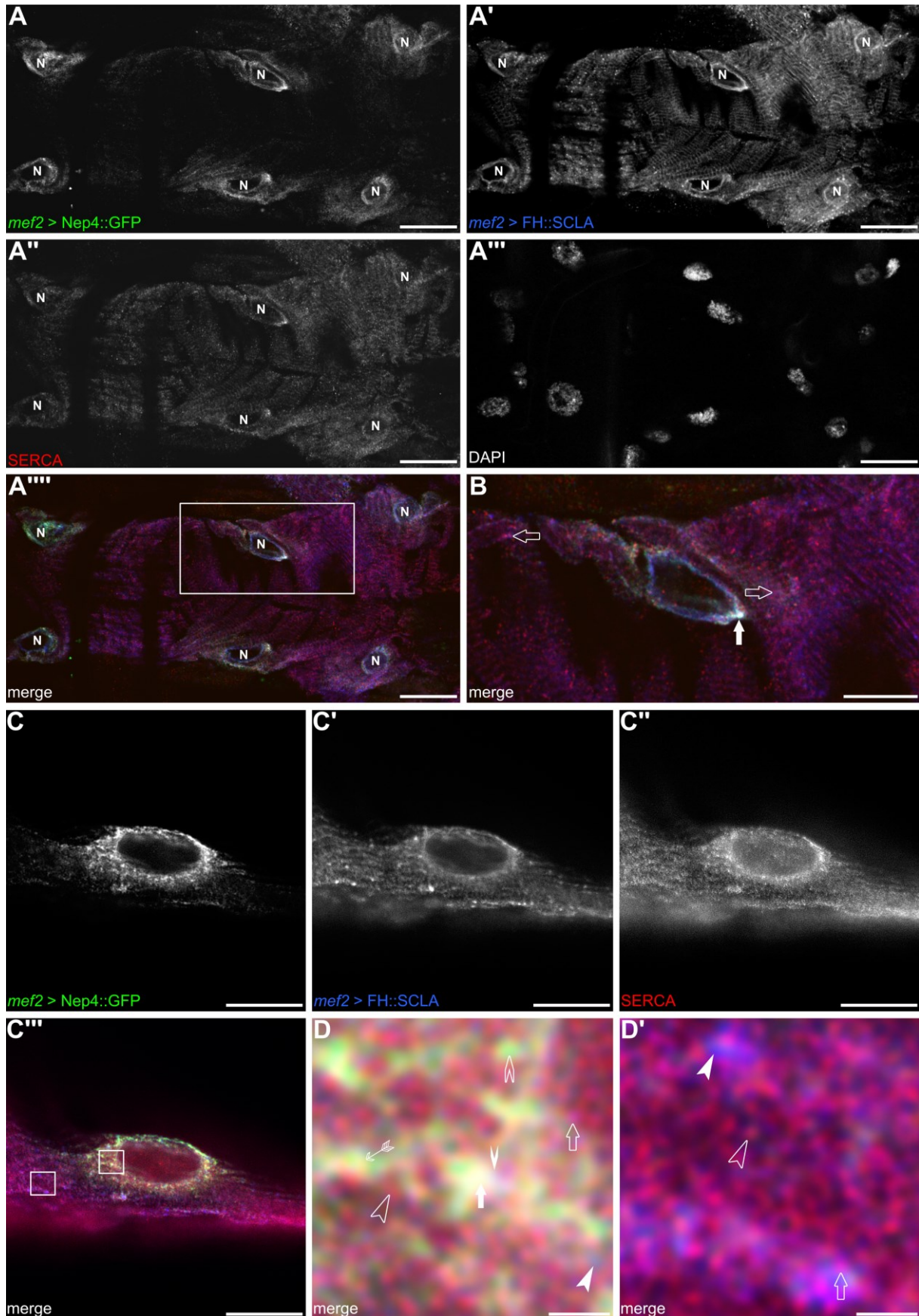


Figure 4

Nep4 partially colocalizes with Sarcolamban A. GFP-tagged Nep4 (*mef2* > Nep4::GFP, A, A''', B, C, C''', D, D') and FH-tagged Sarcolamban A (*mef2* > FH::SCLA, A', A''', B, C',

C''', **D**, **D'**) were expressed under the control of the muscle-specific *mef2* enhancer and labeled with monospecific antibodies against the GFP- or the FH-tag. SERCA was labeled with a monospecific antibody detecting the endogenous protein (SERCA, **A''**, **A''''**, **B**, **C''**, **C'''**, **D**, **D'**). DAPI was used as a nuclear marker (**A'''**). Optical slices of third instar larval heart tissue are shown. The box in **C'''** indicates an area of higher magnification as depicted in **(B)**. **(A-A''''**, **B)** Nep4, SERCA and SCLA signals colocalize predominantly around the nuclei (**B**, solid arrow). More distant from the nuclei, only SERCA and SCLA signals are visible (**B**, open arrows). Scale bars: 20 μm (**A-A''''**); 10 μm (**B**); ventral view, anterior left. **(C-D')** STED images of analogously stained cardiac tissue. Boxes in **C'''** indicate areas of higher magnification as depicted in **(D, D')**. Overlap between Nep4, SERCA, and SCLA signals is visible predominantly around the nucleus (**D**, solid arrow). Individual colocalization between SCLA and SERCA (**D**, open arrow), Nep4 and SERCA (**D**, feathered arrow), or Nep4 and SCLA (**D**, solid winged arrowhead) occurs occasionally. Individual signals of SERCA (**D**, open arrowhead), Nep4 (**D**, open winged arrowhead), and SCLA (**D**, solid arrowhead) are present as well. More distant from the nucleus, only SERCA and SCLA are detected, while Nep4 is largely absent (**D'**). For SERCA and SCLA, again a colocalizing portion (**D'**, open arrow) as well as individual SERCA (**D'**, open arrowhead) and SCLA signals (**D'**, solid arrowhead) are present. Scale bars: 10 μm (**C-C'''**); 1 μm (**D, D'**).

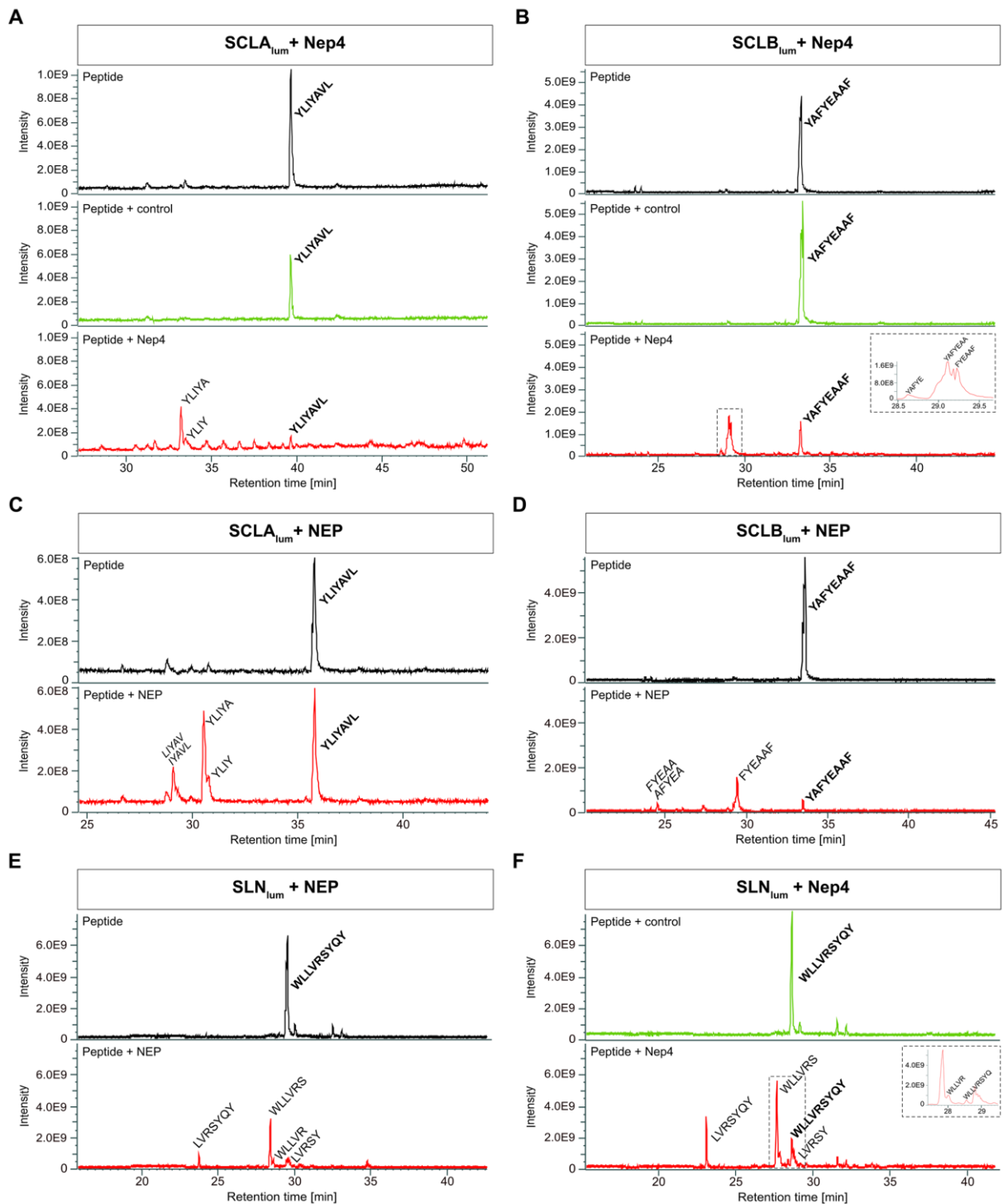


Figure 5

Nepriylsins hydrolyze the luminal domain of SERCA-inhibitory micropeptides. Depicted are total ion chromatograms of the luminal part of *Drosophila* Sarcolamban A (SCLA_{lum}, **A, C**), *Drosophila* Sarcolamban B (SCLB_{lum}, **B, D**), and human sarcolipin (SLN_{lum}, **E, F**). Full-length peptides (bold) are detected under all applied experimental conditions (peptide only, black chromatograms; peptide incubated with control preparation, green chromatograms; peptide incubated with purified enzyme, red chromatograms). Specific cleavage fragments are detected only after addition of enzyme. (**A**) Incubation of SCLA_{lum} (YLIYAVL) with *Drosophila*

Nep4 results in formation of YLIYA and YLIY fragments (red chromatogram). **(C)** The same fragments are generated by human neprilysin (NEP)-mediated hydrolysis of SCLA_{lum}. An additional peak corresponds to either *LIYAV* or *IYAVL*. **(B)** Incubation of SCLB_{lum} (**YAFYEAAF**) with *Drosophila* Nep4 results in formation of FYEAAF, YAFYEAA, and YAFYE fragments (red chromatogram). **(D)** Human NEP-mediated hydrolysis of SCLB_{lum} generates predominantly FYEAAF. In addition, minor amounts of *FYEAA* or *AFYEA* are produced. **(E)** Incubation of SLN_{lum} (**WLLVRSYQY**) with human NEP results in formation of WLLVRS, LVRSYQY, LVRSY, and WLLVR fragments (red chromatogram). **(F)** Incubation of SLN_{lum} (**WLLVRSYQY**) with *Drosophila* Nep4 results in formation of WLLVRS, LVRSYQY, and LVRSY fragments (red chromatogram). Insets depict areas of magnification indicated by the dashed boxes. Italicized fragments could not be assigned to one exclusive peptide sequence. Y-axes show absolute peak intensities, X-axes depict retention times. Individual cleavage assays were repeated at least three times.

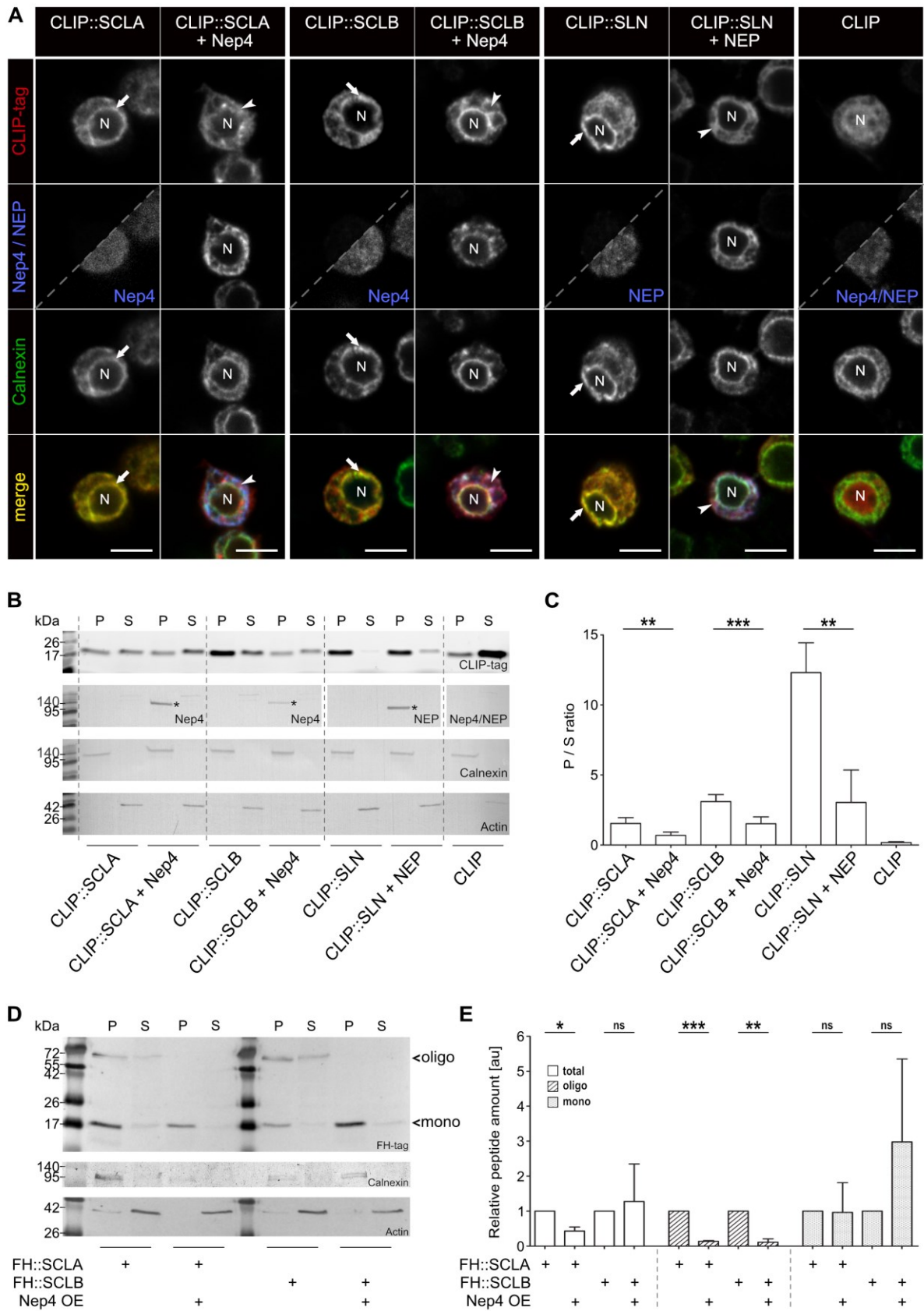


Figure 6

Nepilysin-hydrolyzed SERCA-inhibitory micropeptides exhibit reduced membrane anchoring.
(A) CLIP-tagged Sarcolamban A (SCLA), Sarcolamban B (SCLB), and Sarcolipin (SLN)

peptides were expressed in *Drosophila* S2 cells as full-length peptides (CLIP::SCLA; CLIP::SCLB; CLIP::SLN), either with or without co-expression of Nep4 (SCLA, SCLB) or human NEP (SLN). CLIP-tag and Nep4 or NEP were visualized by immunostainings as indicated. Split images are overexposed in the lower right part to confirm presence of cells. Anti-Calnexin antibodies were applied as ER membrane marker. Cells expressing the free CLIP-tag were used as a soluble control. While full-length SCL / SLN peptides mainly localize to the ER (arrows), co-expression of Nep4 or NEP results in reduced signal overlap of the peptides with the ER marker (arrowheads). Scale bars: 5 μ M. **(B)** Subcellular fractions of *Drosophila* S2 cells expressing the indicated CLIP-tagged SCL or SLN constructs, with or without co-expression of Nep4 or NEP, were analyzed by SDS-PAGE and subsequent fluorescent in-gel detection of CLIP-tagged fusions. Western blot analysis was performed with anti-Nep4 and anti-NEP antibodies, as indicated, to confirm peptidase expression (asterisks), and with anti-Calnexin antibodies (marker for ER membranes) and anti-Actin antibodies (cytosolic marker) to confirm identity of the individual fractions. Coomassie staining (CBB) was used as loading control. P = pellet (membrane-enriched); S = supernatant. **(C)** Peptide-specific ratios between membrane-enriched (P) and soluble (S) fractions were determined by pixel intensity measurements. The diagram depicts the resultant mean values (+ SD) of five individual biological replicates. Asterisks indicate statistically significant differences between the individual peptide-specific ratios (**p < 0.01, ***p < 0.001, paired t-test, two-tailed). Free CLIP-tag was used as a soluble control. **(D)** Subcellular fractions of *Drosophila* 3rd instar larvae expressing the indicated FH-tagged SCL constructs in a muscle-specific manner (*mef2-Gal4*), with or without co-expression of Nep4, were analyzed by Western blot. Peptides were detected with anti-HA antibodies. Actin signals were used for normalization. P = pellet (membrane-enriched); S = supernatant; mono = peptide monomer; oligo = peptide oligomer. **(E)** Relative amounts of peptide oligomers (oligo), peptide monomers (mono), and the sum of both (total) were determined by pixel intensity measurements. For each of the indicated SCL / Nep4 combinations, the combined signals from pellet and supernatant fractions, as depicted in **(D)**, were evaluated. Resultant data represent mean values (+ SD) of three individual biological replicates. Asterisks indicate statistically significant differences (*p < 0.05, **p < 0.01, paired t-test, two-tailed).

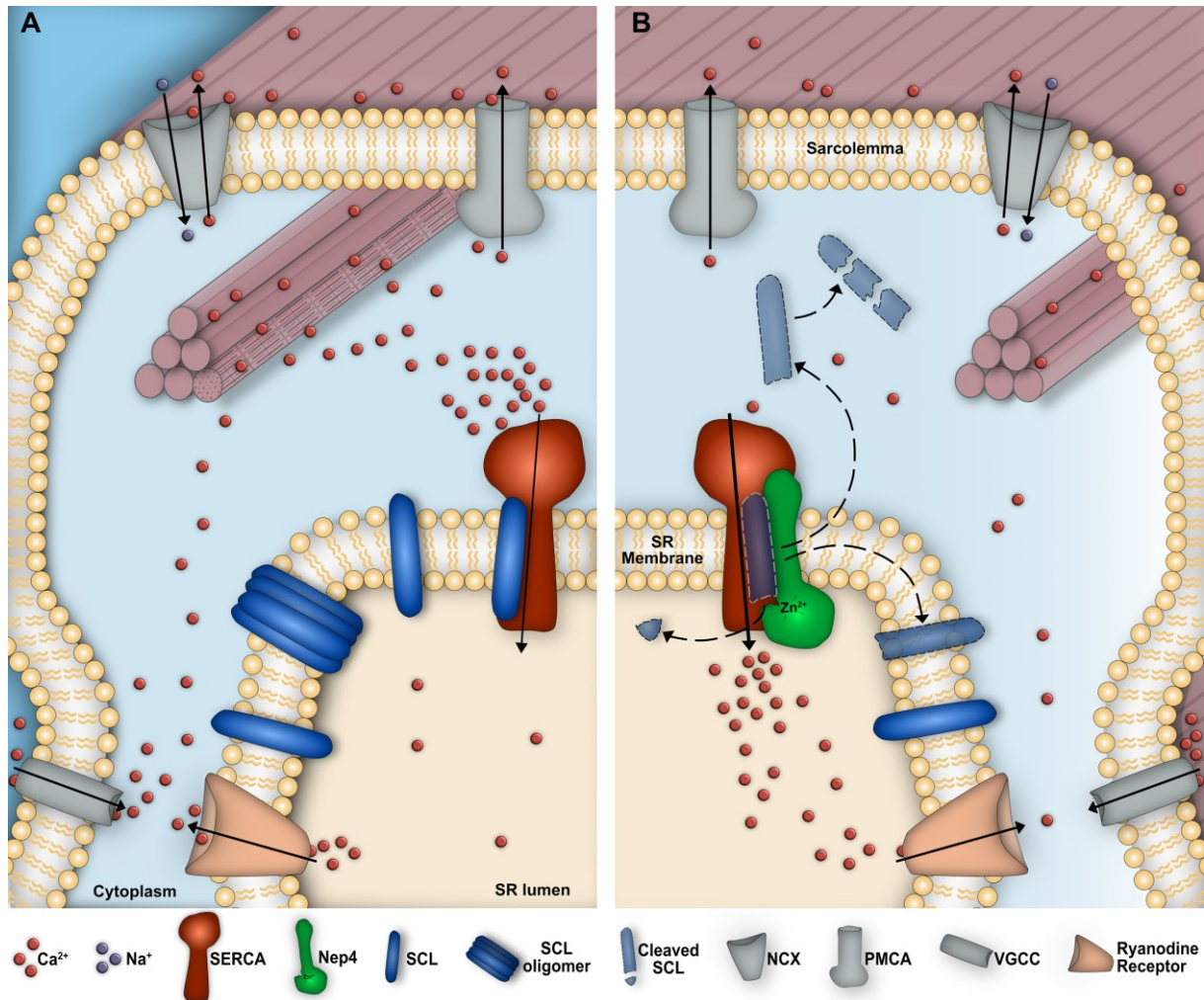


Figure 7

Nepilysin-mediated hydrolysis of SERCA-inhibitory micropeptides is essential to control SERCA activity

(A) Without Nep4, Sarcolamban (SCL) peptides occur in a monomeric and an oligomeric state and accumulate within the sarcoplasmic reticulum (SR) membrane, resulting in abnormal binding and inhibition of SERCA and a consequential reduction in the SERCA-mediated Ca²⁺ transport. (B) Nep4-mediated SCL hydrolysis reduces the ability of the peptides to oligomerize and releases them from the SR membrane, thus preventing SCL accumulation and excessive SERCA inhibition. Released peptides become degraded in the cytoplasm. VGCC: Voltage-gated L-type Ca²⁺ channel; RyR: Ryanodine receptor; NCX: Na⁺/Ca²⁺ exchanger; PMCA: Plasma membrane Ca²⁺ ATPase.

References

1. Hasenfuss G, Pieske B. Calcium cycling in congestive heart failure. *J Mol Cell Cardiol* **34**, 951-969 (2002).
2. Periasamy M, Bhupathy P, Babu GJ. Regulation of sarcoplasmic reticulum Ca²⁺ ATPase pump expression and its relevance to cardiac muscle physiology and pathology. *Cardiovasc Res* **77**, 265-273 (2008).
3. Gehrig SM, *et al.* Hsp72 preserves muscle function and slows progression of severe muscular dystrophy. *Nature* **484**, 394-398 (2012).
4. Periasamy M, Kalyanasundaram A. SERCA pump isoforms: their role in calcium transport and disease. *Muscle Nerve* **35**, 430-442 (2007).
5. Gorski PA, Ceholski DK, Hajjar RJ. Altered myocardial calcium cycling and energetics in heart failure--a rational approach for disease treatment. *Cell Metab* **21**, 183-194 (2015).
6. Kawase Y, Hajjar RJ. The cardiac sarcoplasmic/endoplasmic reticulum calcium ATPase: a potent target for cardiovascular diseases. *Nat Clin Pract Cardiovasc Med* **5**, 554-565 (2008).
7. Vazquez-Martinez O, Canedo-Merino R, Diaz-Munoz M, Riesgo-Escovar JR. Biochemical characterization, distribution and phylogenetic analysis of *Drosophila melanogaster* ryanodine and IP₃ receptors, and thapsigargin-sensitive Ca²⁺ ATPase. *J Cell Sci* **116**, 2483-2494 (2003).
8. Abraham DM, Wolf MJ. Disruption of sarcoendoplasmic reticulum calcium ATPase function in *Drosophila* leads to cardiac dysfunction. *PLoS One* **8**, e77785 (2013).
9. Sanyal S, Jennings T, Dowse H, Ramaswami M. Conditional mutations in SERCA, the Sarco-endoplasmic reticulum Ca²⁺-ATPase, alter heart rate and rhythmicity in *Drosophila*. *J Comp Physiol B* **176**, 253-263 (2006).
10. MacLennan DH, Kranias EG. Phospholamban: a crucial regulator of cardiac contractility. *Nat Rev Mol Cell Biol* **4**, 566-577 (2003).
11. Magny EG, *et al.* Conserved regulation of cardiac calcium uptake by peptides encoded in small open reading frames. *Science* **341**, 1116-1120 (2013).
12. Minamisawa S, *et al.* Chronic phospholamban-sarcoplasmic reticulum calcium ATPase interaction is the critical calcium cycling defect in dilated cardiomyopathy. *Cell* **99**, 313-322 (1999).
13. Minamisawa S, Wang Y, Chen J, Ishikawa Y, Chien KR, Matsuoka R. Atrial chamber-specific expression of sarcolipin is regulated during development and hypertrophic remodeling. *J Biol Chem* **278**, 9570-9575 (2003).
14. Asahi M, *et al.* Cardiac-specific overexpression of sarcolipin inhibits sarco(endo)plasmic reticulum Ca²⁺ ATPase (SERCA2a) activity and impairs cardiac function in mice. *Proc Natl Acad Sci U S A* **101**, 9199-9204 (2004).

15. Haghghi K, *et al.* A mutation in the human phospholamban gene, deleting arginine 14, results in lethal, hereditary cardiomyopathy. *Proc Natl Acad Sci U S A* **103**, 1388-1393 (2006).
16. Haghghi K, *et al.* Human phospholamban null results in lethal dilated cardiomyopathy revealing a critical difference between mouse and human. *J Clin Invest* **111**, 869-876 (2003).
17. Schmitt JP, *et al.* Dilated cardiomyopathy and heart failure caused by a mutation in phospholamban. *Science* **299**, 1410-1413 (2003).
18. Shanmugam M, *et al.* Ablation of phospholamban and sarcolipin results in cardiac hypertrophy and decreased cardiac contractility. *Cardiovasc Res* **89**, 353-361 (2011).
19. Uemura N, *et al.* Down-regulation of sarcolipin mRNA expression in chronic atrial fibrillation. *Eur J Clin Invest* **34**, 723-730 (2004).
20. Anderson DM, *et al.* A micropeptide encoded by a putative long noncoding RNA regulates muscle performance. *Cell* **160**, 595-606 (2015).
21. Nelson BR, *et al.* A peptide encoded by a transcript annotated as long noncoding RNA enhances SERCA activity in muscle. *Science* **351**, 271-275 (2016).
22. Fisher ME, *et al.* Dwarf open reading frame (DWORF) is a direct activator of the sarcoplasmic reticulum calcium pump SERCA. *Elife* **10**, (2021).
23. Fink M, *et al.* A new method for detection and quantification of heartbeat parameters in *Drosophila*, zebrafish, and embryonic mouse hearts. *Biotechniques* **46**, 101-113 (2009).
24. Hallier B, *et al.* *Drosophila* neprilysins control insulin signaling and food intake via cleavage of regulatory peptides. *Elife* **5**, (2016).
25. Panz M, Vitos-Faleato J, Jendretzki A, Heinisch JJ, Paululat A, Meyer H. A novel role for the non-catalytic intracellular domain of Neprilysins in muscle physiology. *Biol Cell* **104**, 553-568 (2012).
26. Hartley PS, Motamedchaboki K, Bodmer R, Ocorr K. SPARC-Dependent Cardiomyopathy in *Drosophila*. *Circ Cardiovasc Genet* **9**, 119-129 (2016).
27. Vaughan L, Marley R, Miellet S, Hartley PS. The impact of SPARC on age-related cardiac dysfunction and fibrosis in *Drosophila*. *Exp Gerontol* **109**, 59-66 (2018).
28. Meyer H, Panz M, Zmojdzian M, Jagla K, Paululat A. Neprilysin 4, a novel endopeptidase from *Drosophila melanogaster*, displays distinct substrate specificities and exceptional solubility states. *J Exp Biol* **212**, 3673-3683 (2009).
29. Meyer H, *et al.* *Drosophila* metalloproteases in development and differentiation: the role of ADAM proteins and their relatives. *Eur J Cell Biol* **90**, 770-778 (2011).
30. Diaz ME, Graham HK, O'Neill S C, Trafford AW, Eisner DA. The control of sarcoplasmic reticulum Ca content in cardiac muscle. *Cell Calcium* **38**, 391-396 (2005).

31. Diaz ME, Trafford AW, O'Neill SC, Eisner DA. Measurement of sarcoplasmic reticulum Ca²⁺ content and sarcolemmal Ca²⁺ fluxes in isolated rat ventricular myocytes during spontaneous Ca²⁺ release. *J Physiol* **501** (Pt 1), 3-16 (1997).
32. Lehmacher C, Abeln B, Paululat A. The ultrastructure of Drosophila heart cells. *Arthropod Struct Dev* **41**, 459-474 (2012).
33. Dooley CT, Dore TM, Hanson GT, Jackson WC, Remington SJ, Tsien RY. Imaging dynamic redox changes in mammalian cells with green fluorescent protein indicators. *J Biol Chem* **279**, 22284-22293 (2004).
34. Tsachaki M, Birk J, Egert A, Odermatt A. Determination of the topology of endoplasmic reticulum membrane proteins using redox-sensitive green-fluorescence protein fusions. *Biochim Biophys Acta* **1853**, 1672-1682 (2015).
35. Anderson DM, *et al.* Widespread control of calcium signaling by a family of SERCA-inhibiting micropeptides. *Sci Signal* **9**, ra119 (2016).
36. Payre F, Desplan C. RNA. Small peptides control heart activity. *Science* **351**, 226-227 (2016).
37. Gramolini AO, Kislinger T, Asahi M, Li W, Emili A, MacLennan DH. Sarcolipin retention in the endoplasmic reticulum depends on its C-terminal RSYQY sequence and its interaction with sarco(endo)plasmic Ca(2+)-ATPases. *Proc Natl Acad Sci U S A* **101**, 16807-16812 (2004).
38. Odermatt A, *et al.* Sarcolipin regulates the activity of SERCA1, the fast-twitch skeletal muscle sarcoplasmic reticulum Ca²⁺-ATPase. *J Biol Chem* **273**, 12360-12369 (1998).
39. Jones LR, Simmerman HK, Wilson WW, Gurd FR, Wegener AD. Purification and characterization of phospholamban from canine cardiac sarcoplasmic reticulum. *J Biol Chem* **260**, 7721-7730 (1985).
40. Robia SL, Flohr NC, Thomas DD. Phospholamban pentamer quaternary conformation determined by in-gel fluorescence anisotropy. *Biochemistry* **44**, 4302-4311 (2005).
41. Abrol N, *et al.* Phospholamban C-terminal residues are critical determinants of the structure and function of the calcium ATPase regulatory complex. *J Biol Chem* **289**, 25855-25866 (2014).
42. Kimura Y, Kurzydowski K, Tada M, MacLennan DH. Phospholamban inhibitory function is activated by depolymerization. *J Biol Chem* **272**, 15061-15064 (1997).
43. Robia SL, Campbell KS, Kelly EM, Hou Z, Winters DL, Thomas DD. Forster transfer recovery reveals that phospholamban exchanges slowly from pentamers but rapidly from the SERCA regulatory complex. *Circ Res* **101**, 1123-1129 (2007).
44. Reddy LG, Jones LR, Thomas DD. Depolymerization of phospholamban in the presence of calcium pump: a fluorescence energy transfer study. *Biochemistry* **38**, 3954-3962 (1999).
45. Misquitta CM, Sing A, Grover AK. Control of sarcoplasmic/endoplasmic-reticulum Ca²⁺ pump expression in cardiac and smooth muscle. *Biochem J* **338** (Pt 1), 167-173 (1999).

46. Magyar A, Bakos E, Varadi A. Structure and tissue-specific expression of the *Drosophila melanogaster* organellar-type Ca²⁺-ATPase gene. *Biochem J* **310** (Pt 3), 757-763 (1995).
47. Fielitz J, *et al.* Neutral endopeptidase is activated in cardiomyocytes in human aortic valve stenosis and heart failure. *Circulation* **105**, 286-289 (2002).
48. Brand AH, Perrimon N. Targeted gene expression as a means of altering cell fates and generating dominant phenotypes. *Development* **118**, 401-415 (1993).
49. Lin N, *et al.* A method to measure myocardial calcium handling in adult *Drosophila*. *Circ Res* **108**, 1306-1315 (2011).
50. Paululat A, Heinisch JJ. New yeast/*E. coli*/*Drosophila* triple shuttle vectors for efficient generation of *Drosophila* P element transformation constructs. *Gene* **511**, 300-305 (2012).
51. Post Y, Paululat A. Muscle Function Assessment Using a *Drosophila* Larvae Crawling Assay. *Bio-Protocol* **8**, (2018).
52. Vogler G, Ocorr K. Visualizing the beating heart in *Drosophila*. *J Vis Exp*, (2009).
53. Schiemann R, Lammers K, Janz M, Lohmann J, Paululat A, Meyer H. Identification and In Vivo Characterisation of Cardioactive Peptides in *Drosophila melanogaster*. *Int J Mol Sci* **20**, (2018).
54. Balcazar D, *et al.* SERCA is critical to control the Bowditch effect in the heart. *Sci Rep* **8**, 12447 (2018).
55. Santalla M, *et al.* Aging and CaMKII alter intracellular Ca²⁺ transients and heart rhythm in *Drosophila melanogaster*. *PLoS One* **9**, e101871 (2014).
56. Bassani JW, Bassani RA, Bers DM. Relaxation in rabbit and rat cardiac cells: species-dependent differences in cellular mechanisms. *J Physiol* **476**, 279-293 (1994).
57. Cheng J, *et al.* CaMKII inhibition in heart failure, beneficial, harmful, or both. *Am J Physiol Heart Circ Physiol* **302**, H1454-1465 (2012).
58. Diaz ME, Graham HK, Trafford AW. Enhanced sarcolemmal Ca²⁺ efflux reduces sarcoplasmic reticulum Ca²⁺ content and systolic Ca²⁺ in cardiac hypertrophy. *Cardiovasc Res* **62**, 538-547 (2004).
59. Fakuade FE, *et al.* Altered Atrial Cytosolic Calcium Handling Contributes to the Development of Postoperative Atrial Fibrillation. *Cardiovasc Res*, (2020).
60. Gao J, *et al.* Assessment of Sarcoplasmic Reticulum Calcium Reserve and Intracellular Diastolic Calcium Removal in Isolated Ventricular Cardiomyocytes. *J Vis Exp*, (2017).
61. Gomez IM, *et al.* Inhalation of marijuana affects *Drosophila* heart function. *Biol Open* **8**, (2019).
62. Mederle K, *et al.* The angiotensin receptor-associated protein Atrap is a stimulator of the cardiac Ca²⁺-ATPase SERCA2a. *Cardiovasc Res* **110**, 359-370 (2016).

63. Piacentino V, 3rd, *et al.* Cellular basis of abnormal calcium transients of failing human ventricular myocytes. *Circ Res* **92**, 651-658 (2003).
64. Lin H, He L, Ma B. A combinatorial approach to the peptide feature matching problem for label-free quantification. *Bioinformatics* **29**, 1768-1775 (2013).
65. Perez-Riverol Y, *et al.* The PRIDE database and related tools and resources in 2019: improving support for quantification data. *Nucleic Acids Res* **47**, D442-D450 (2019).
66. Brodehl A, *et al.* Functional characterization of the novel DES mutation p.L136P associated with dilated cardiomyopathy reveals a dominant filament assembly defect. *J Mol Cell Cardiol* **91**, 207-214 (2016).
67. Sanyal S, *et al.* Analysis of conditional paralytic mutants in *Drosophila* sarcoplasmic reticulum calcium ATPase reveals novel mechanisms for regulating membrane excitability. *Genetics* **169**, 737-750 (2005).

Acknowledgments

We thank Martina Biedermann and Mechthild Krabusch for excellent technical assistance with fly work; Masaki Fukata, Yuko Fukata, Hirokazu Ishii, Tomomi Nemoto, and Mikio Furuse for providing expertise on STED microscopy; Michael Stuke for contributing to the protein orientation assay; Matthew Wolf for providing transgenic GCaMP3 stocks; and Jose Pueyo-Marques for sharing transgenic Sarcolamban stocks. Anti-SERCA antibodies were kindly provided by Mani Ramaswami. We further acknowledge the Vienna *Drosophila* Resource Center (VDRC) and the Bloomington *Drosophila* Stock Center (BDSC, NIH P40OD018537) for providing fly stocks. This research was funded by the German Research Foundation (SFB 944: Physiology and Dynamics of Cellular Microcompartments) (HMe, AP), and by a stipend from the Hans Mühlenhoff Foundation (RS). We also acknowledge the support of the Open Access Publishing Fund of Osnabrück University. The use of human tissue from explanted hearts for research purposes was according to the convention of Helsinki and accepted by the local ethics committee (ethics commission of the faculty of the Ruhr University Bochum, located in Bad Oeynhausen, vote 21/2013). Informed consent was obtained from all participants.

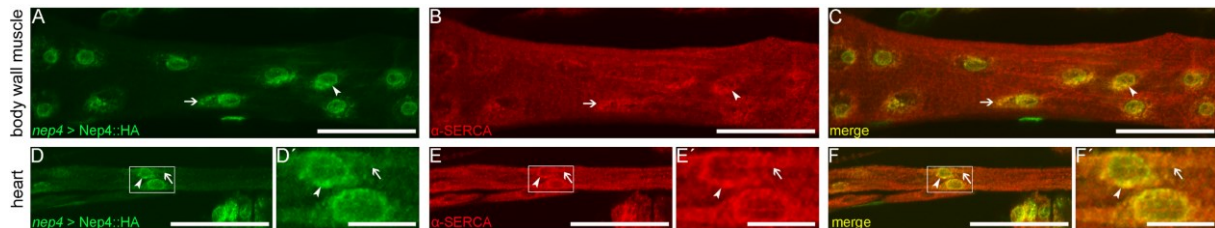
Author contributions

RS, AB, Acquisition of data, Analysis and interpretation of data, Drafting or revising the article; EC, PF, Acquisition of data, Drafting or revising the article; SW, JJH, HMi, AP, Analysis and interpretation of data, Drafting or revising the article; HMe, Conception and design, Acquisition of data, Analysis and interpretation of data, Drafting or revising the article

Competing Interests

The authors declare that they have no competing interests.

Supplementary Figures

**Figure S1**

Nep4 partially colocalizes with *SERCA* in third instar larval heart and body wall muscles. (A, D) *Nep4::HA* protein was expressed under the control of the native *nep4* enhancer and labeled with a monospecific antibody against the HA-tag (*nep4* > *Nep4::HA*). (B, E) *SERCA* was labeled with a monospecific antibody detecting the endogenous protein (*SERCA*). Optical projections of a third instar larval body wall muscle fiber (A-C) or heart tube (D-F) are shown. Scale bars: 50 μm ; ventral view, anterior left. Boxes indicate areas of higher magnification, as depicted in (D'-F'). Scale bars: 10 μm . *Nep4::HA* colocalizes with *SERCA* in membranes contiguous with the nuclear membrane (arrowheads). In addition, both proteins partially colocalize in a punctate manner along the muscle tissue (arrows).

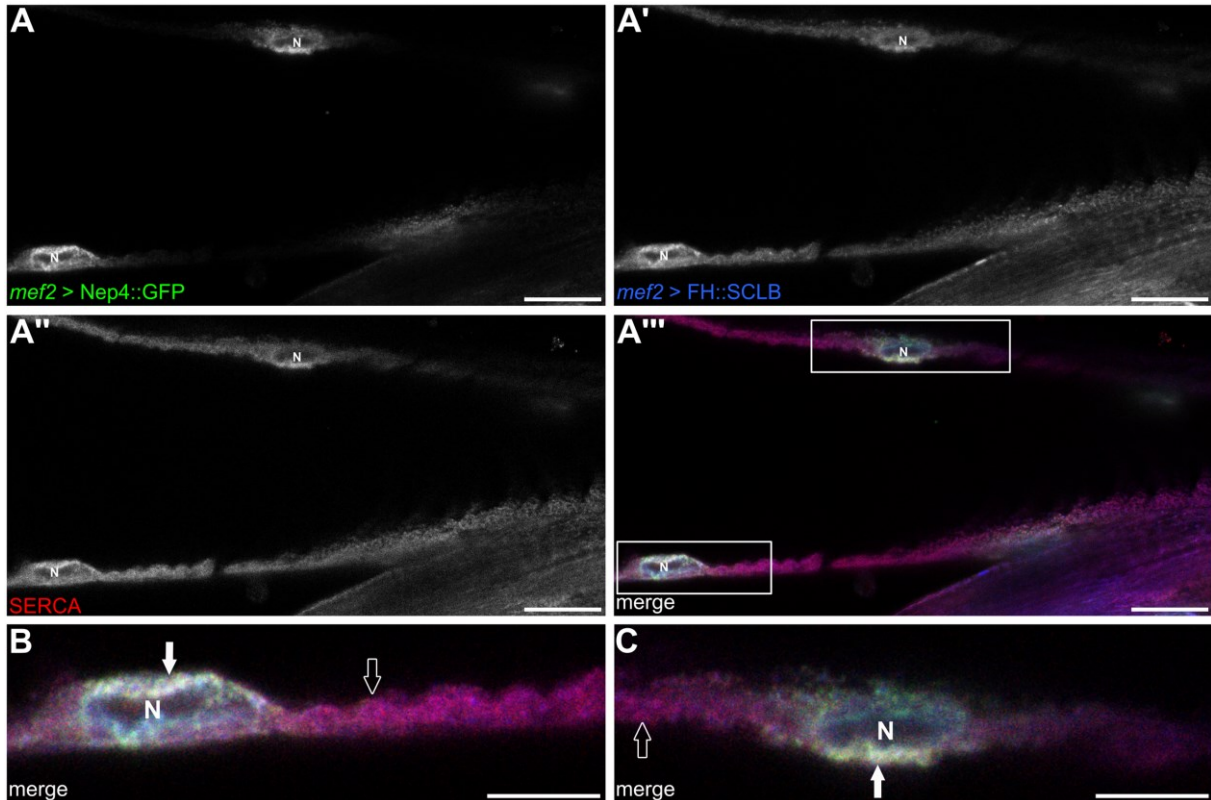


Figure S2

Nep4 partially colocalizes with Sarcolamban B in larval heart tissue. GFP-tagged Nep4 (*mef2* > *Nep4::GFP*, **A**) and FH-tagged Sarcolamban B (*mef2* > *FH::SCLB*, **A'**) were expressed under the control of the muscle-specific *mef2* enhancer and labeled with monospecific antibodies against the GFP- or the FH-tag, respectively. SERCA was labeled with a monospecific antibody detecting the endogenous protein (SERCA, **A''**). Colocalization of all three factors is visible around the nuclei (**B**, **C**, solid arrow). More distant from the nuclei, only SERCA and SCLB signals are present (**B**, **C**, open arrow). Confocal images of third instar larval heart tissue are shown. Scale bars: 20 μm ; ventral view, anterior left. Insets indicate areas of higher magnification as depicted in **B** and **C**. Scale bars: 10 μm .

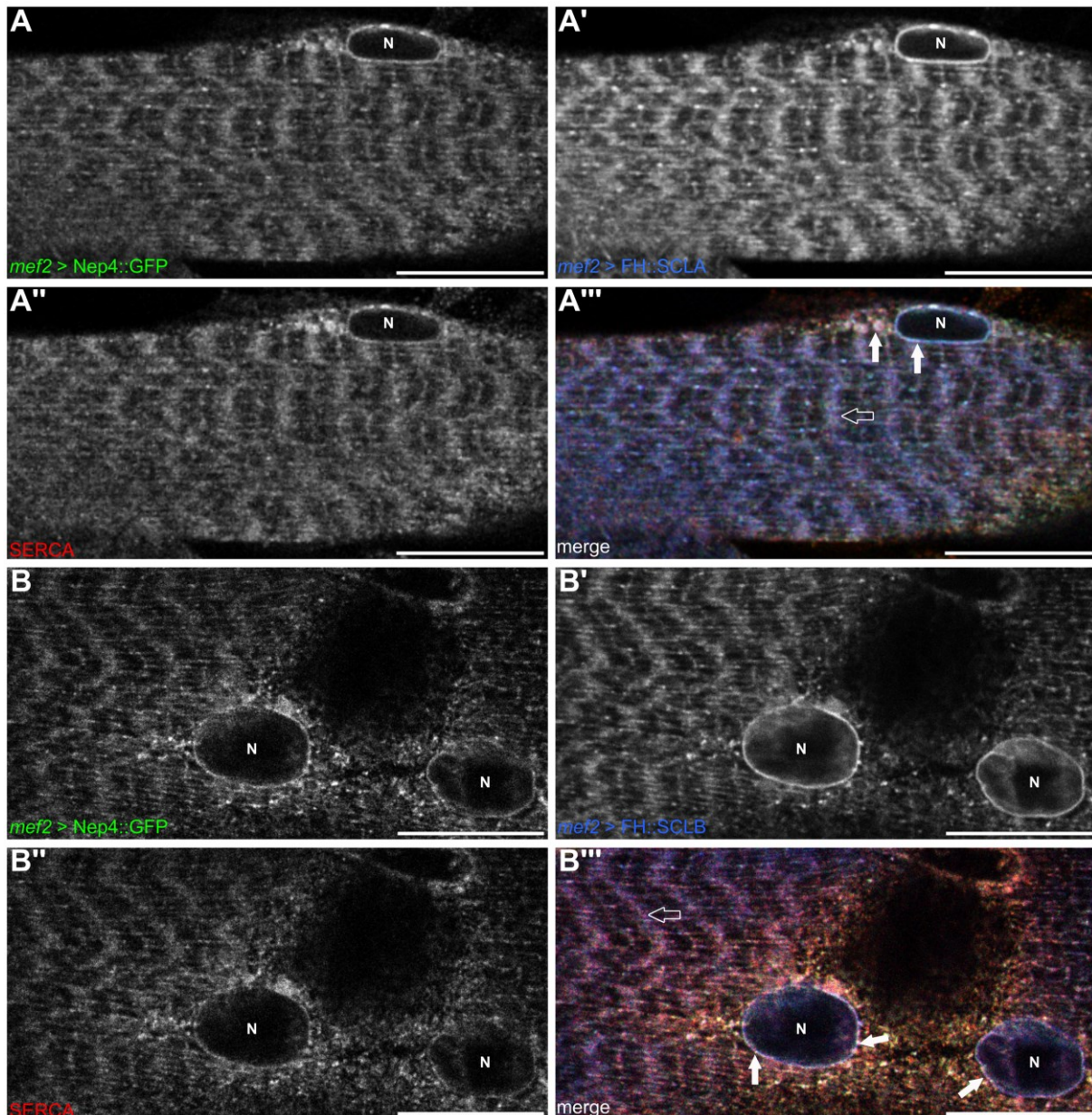
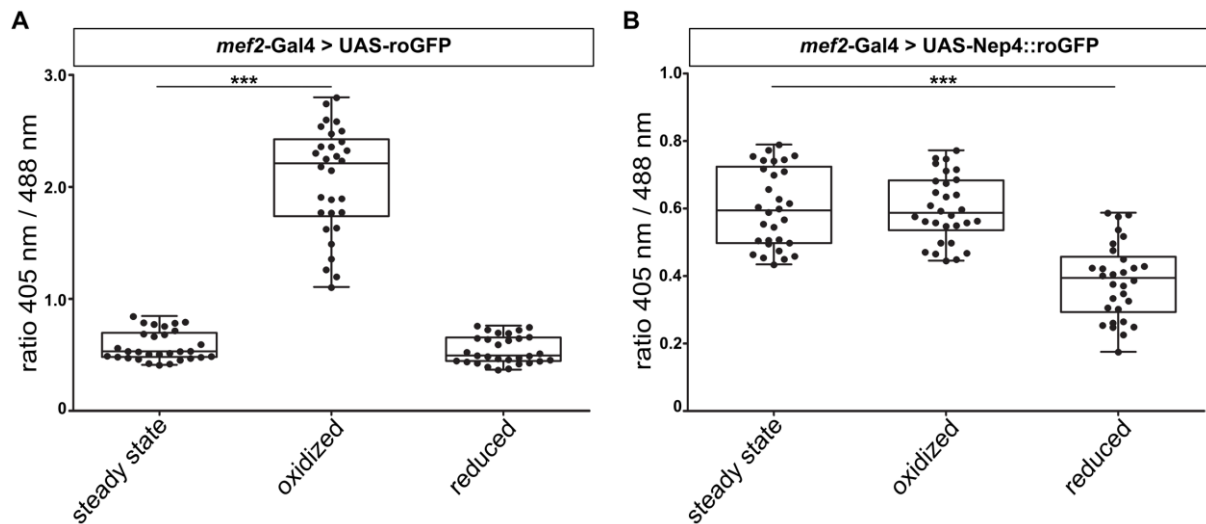


Figure S3

Nep4 partially colocalizes with Sarcolamban A and Sarcolamban B in larval body wall muscles. GFP-tagged *Nep4* (*mef2* > *Nep4::GFP*, **A**, **B**) and FH-tagged Sarcolamban A (*mef2* > *FH::SCLA*, **A'**) or Sarcolamban B (*mef2* > *FH::SCLB*, **B'**) were expressed under the control of the muscle-specific *mef2* enhancer and labeled with monospecific antibodies against the GFP- or the FH-tag, respectively. SERCA was labeled with a monospecific antibody detecting the endogenous protein (SERCA, **A''**, **B''**). Colocalization of *Nep4*, SCLA, and SERCA is visible around the nuclei (**A'''**, solid arrows). More distant from the nuclei, only SERCA and SCLA signals are present (**A'''**, open arrow). A similar localization pattern is apparent for *Nep4*, SCLB, and SERCA (**B'''**). Confocal images of third instar larval body wall muscles are shown. Scale bars: 20 μ m; ventral view, anterior left.

**Figure S4**

The C-terminus of Nep4 localizes to the SR lumen. A Nep4::roGFP fusion (*mef2-Gal4 > UAS-Nep4::roGFP*) was employed to determine the orientation of the protein within the SR membrane. Free roGFP was used as a control (*mef2-Gal4 > UAS-roGFP*). While the steady-state fluorescence intensity ratio (405 nm / 488 nm excitation) of free roGFP reflects reducing conditions (**A**), roGFP fused to the C-terminus of Nep4 exhibits a corresponding ratio that is characteristic for oxidizing conditions (**B**). For each experimental condition, 30 ROIs from three individual animals were analyzed (10 ROIs per animal). Asterisks indicate statistically significant deviations from respective controls ($p < 0.001$, one-way ANOVA followed by Dunnett's Multiple Comparison Test).

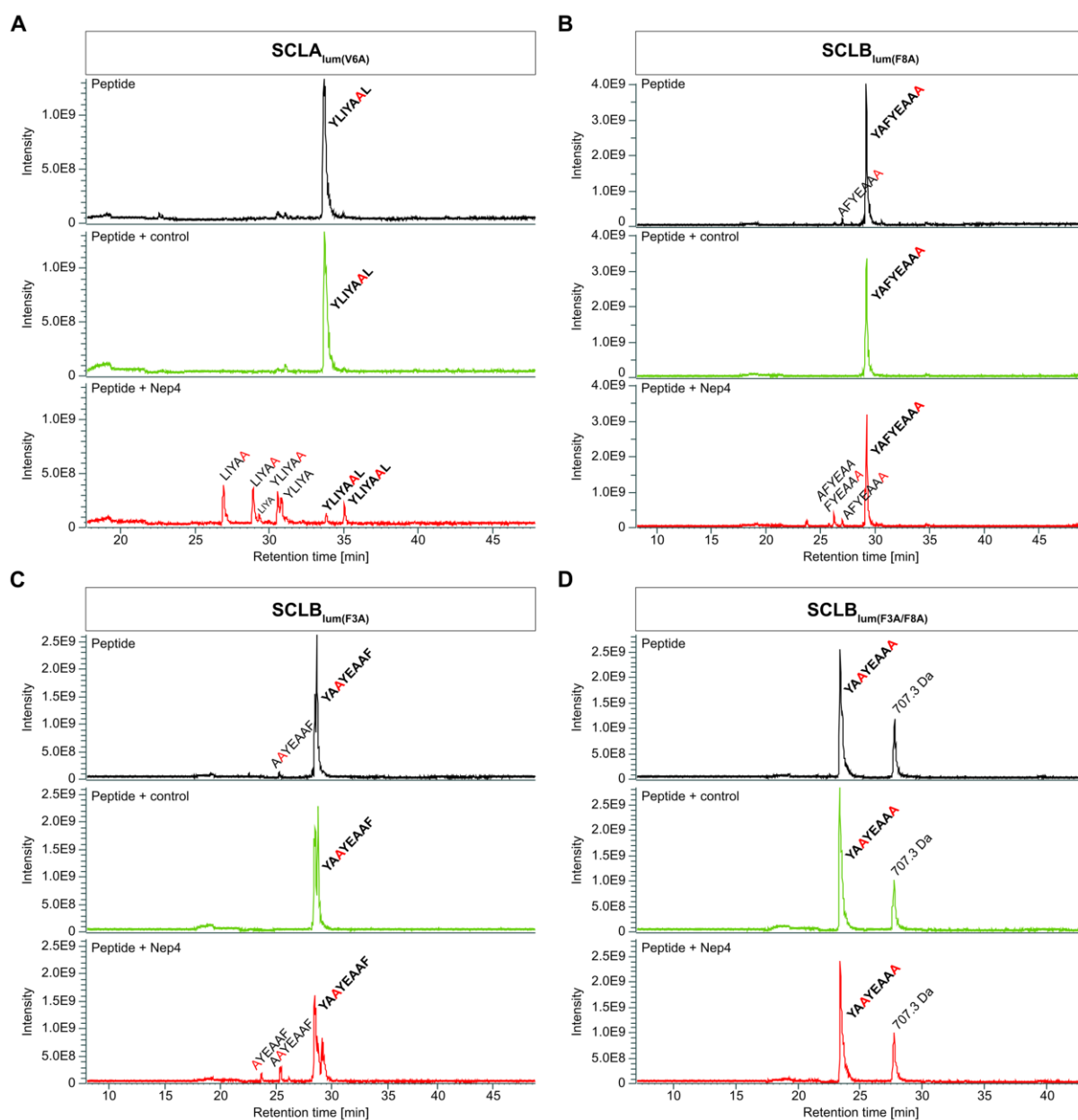


Figure S5

The amino acid at P1' is a critical determinant of the Nep4 cleavage specificity. Depicted are total ion chromatograms of mutated $SCLA_{lum}$ (**A**) and $SCLB_{lum}$ derivatives (**B-D**). Mutated residues are marked in red. Full-length peptides (bold) are detected under all applied experimental conditions (pure peptide, black chromatogram; peptide incubated with control preparation, green chromatogram; peptide incubated with purified Nep4, red chromatogram). Italicized fragments could not unambiguously be assigned to one distinct peptide sequence. (**A**) Substitution of Val-6 by Ala ($SCLA_{lum(V6A)}$, **YLIYAAL**) results in additional cleavage between Tyr-1 and Leu-2 as well as between Ala-6 and Leu-7, giving rise to the peptide fragments **LIYAA**, **LIYA** and **YLIYAA** (red chromatogram). (**B**) The $SCLB_{lum(F8A)}$ derivative (**YAFYEAAA**) is largely resistant to Nep4-mediated hydrolysis (red chromatogram). Aside from the full-length peptide, only minor amounts of a **AFYEAAA** cleavage product are

detected; a third peak of low amplitude corresponds to either *AFYEAA* or *FYEAAA* (See also Table S1). **(C)** The $\text{SCLB}_{\text{lum}(F3A)}$ derivative (*YAA^AYEAAF*) is largely resistant to Nep4-mediated hydrolysis (red chromatogram). Aside from the full-length peptide, only minor amounts of the fragments *AYEAAF* and *AA^AYEAAF* are detected, with the latter also being present in the untreated peptide sample (black chromatogram). **(D)** The $\text{SCLB}_{\text{lum}(F3A/F8A)}$ derivative (*YAA^AYEAAA*) is completely resistant to Nep4-mediated hydrolysis; no cleavage products are detected (red chromatogram). In addition to the full-length peptide (*YAA^AYEAAA*), under all three experimental conditions a non-assignable peak with a molecular mass of 707.3 Da is present. Y-axes show absolute peak intensities, X-axes depict retention times. Individual cleavage assays were repeated at least three times.

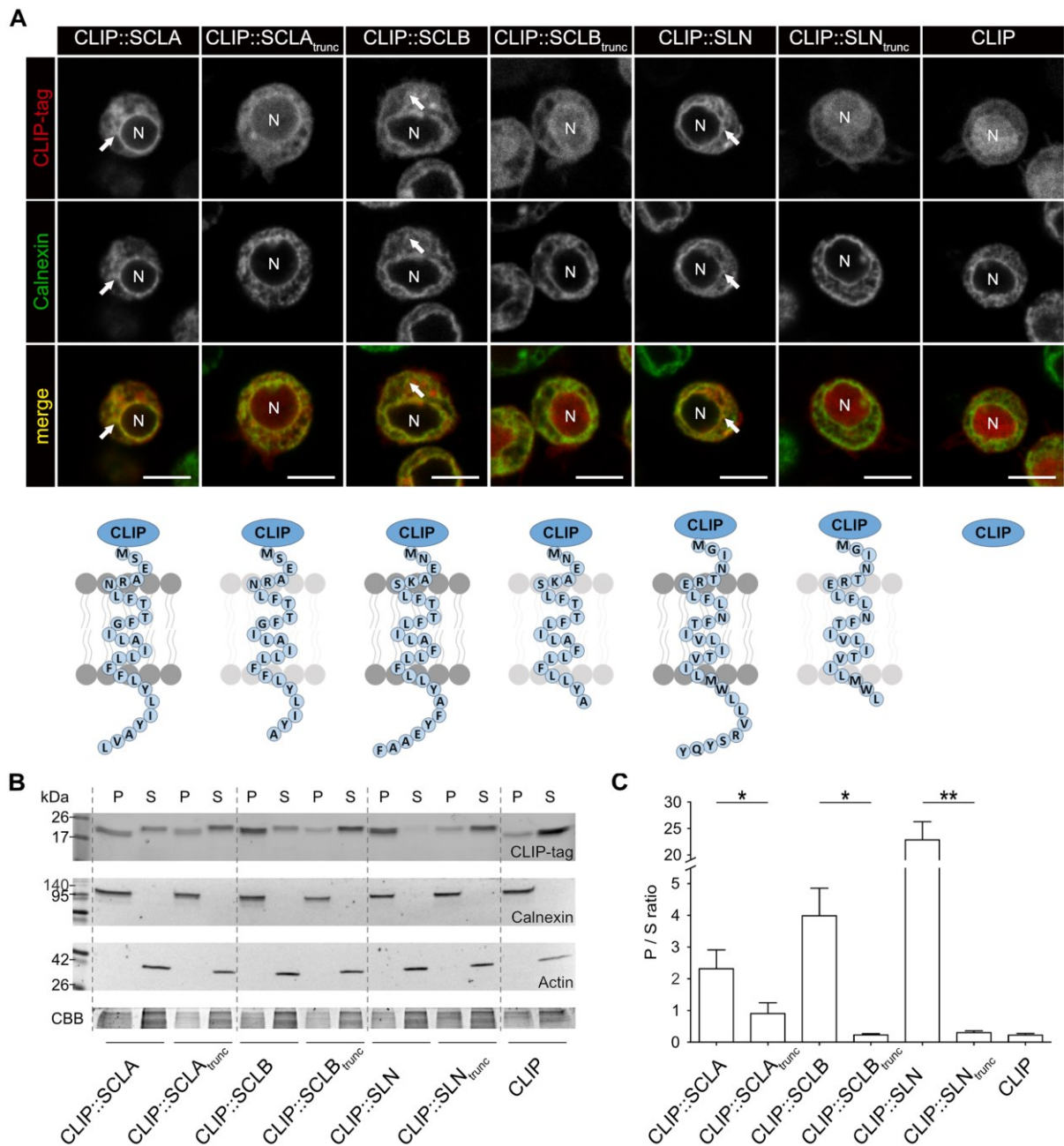
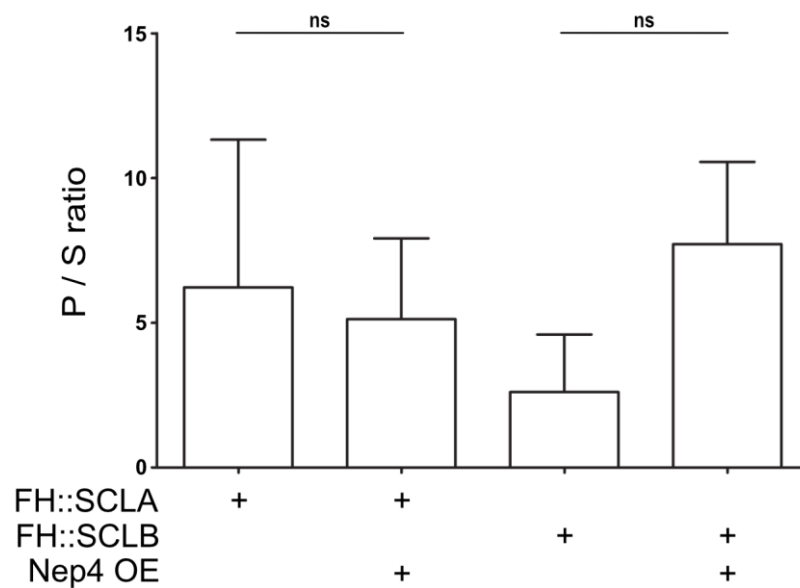


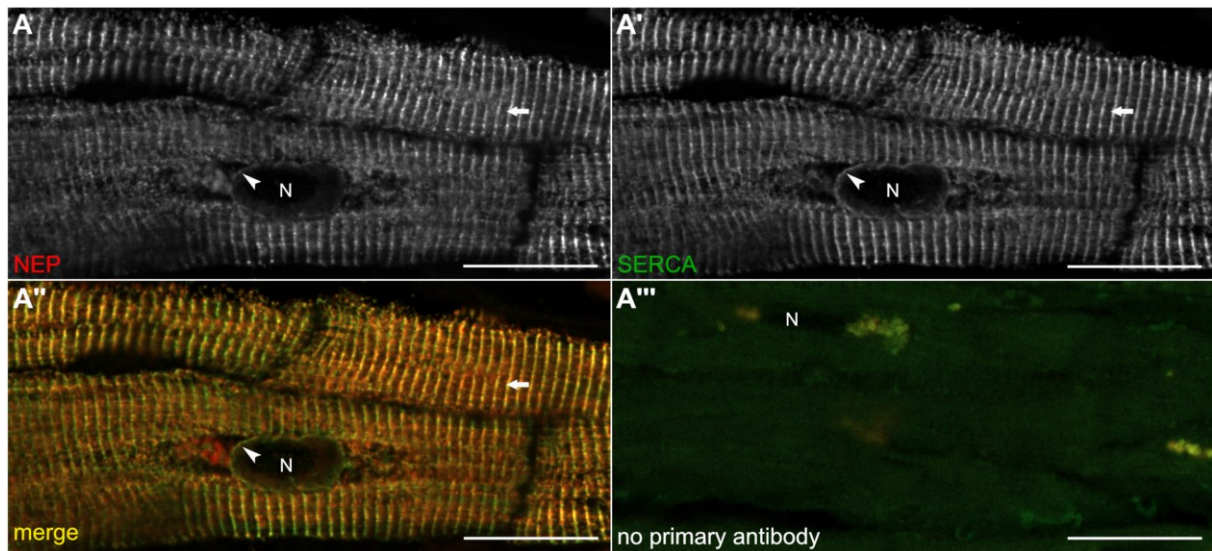
Figure S6

Truncated Sarcolamban and Sarcolipin peptides exhibit reduced membrane anchoring in S2 cells. (A) CLIP-tagged Sarcolamban A (SCLA), Sarcolamban B (SCLB), and Sarcolipin (SLN) were expressed in *Drosophila* S2 cells as full-length (CLIP::SCLA; CLIP::SCLB; CLIP::SLN) and C-terminally truncated constructs (CLIP::SCLA_{trunc}; CLIP::SCLB_{trunc}; CLIP::SLN_{trunc}). All constructs were labeled with CLIP-Cell TMR-Star substrate. Cells expressing the free CLIP-tag were used as a soluble control and anti-Calnexin antibodies (RRID:AB_2722011, 1:200) in combination with anti-mouse-A488 secondary antibodies (RRID:AB_2338845, 1:200) were used as ER marker. While full-length SCL / SLN peptides mainly localize to the ER (arrows), the corresponding truncated peptides accumulate in the nucleus (N). Scale bars: 5 μ m. The lower panel depicts schematics of the analyzed SCL / SLN constructs. (B) Subcellular

fractions of *Drosophila* S2 cells expressing the indicated CLIP-tagged SCL or SLN constructs were analyzed by SDS-PAGE and subsequent fluorescent in-gel detection of CLIP-tagged fusions. Western blot analysis was performed with anti-Calnexin antibodies (marker for ER membranes) and anti-Actin antibodies (cytosolic marker) to confirm identity of the individual fractions. Coomassie staining (CBB) was used as loading control. P = pellet (membrane-enriched); S = supernatant. (C) Peptide-specific ratios between membrane-enriched (P) and soluble (S) fractions were determined by pixel intensity measurements. Depicted are the resultant mean values (+ SD) of three individual biological replicates. Asterisks indicate statistically significant differences between the individual peptide-specific ratios (*p < 0.05, **p < 0.01, paired t-test, two-tailed). Free CLIP-tag (CLIP) was used as a soluble control.

**Fig. S7**

Overexpression of Nep4 does not significantly affect Sarcolamban A or Sarcolamban B membrane localization in third instar larval muscle tissue. Subcellular fractions of *Drosophila* 3rd instar larvae expressing the indicated SCL constructs, with or without co-expression of Nep4, were analyzed by Western blot. Peptide-specific ratios between membrane-enriched (P) and soluble (S) fractions were determined by pixel intensity measurements. Only the monomeric form of the peptides was considered. The diagram depicts the resultant mean values (+ SD) of three individual biological replicates. No statistically significant differences were observed.

**Fig. S8**

NEP and SERCA partially colocalize in human ventricular cardiomyocytes. (A) Human left ventricular cardiomyocytes were stained for NEP (A) and SERCA (A'). Overlapping signals are present along the Z-discs (A-A'', arrow) and in membranes continuous with nuclear membrane (A-A'', arrowhead). In the absence of primary antibodies, no signal above background is visible (A'''). Scale bars: 20 μm.

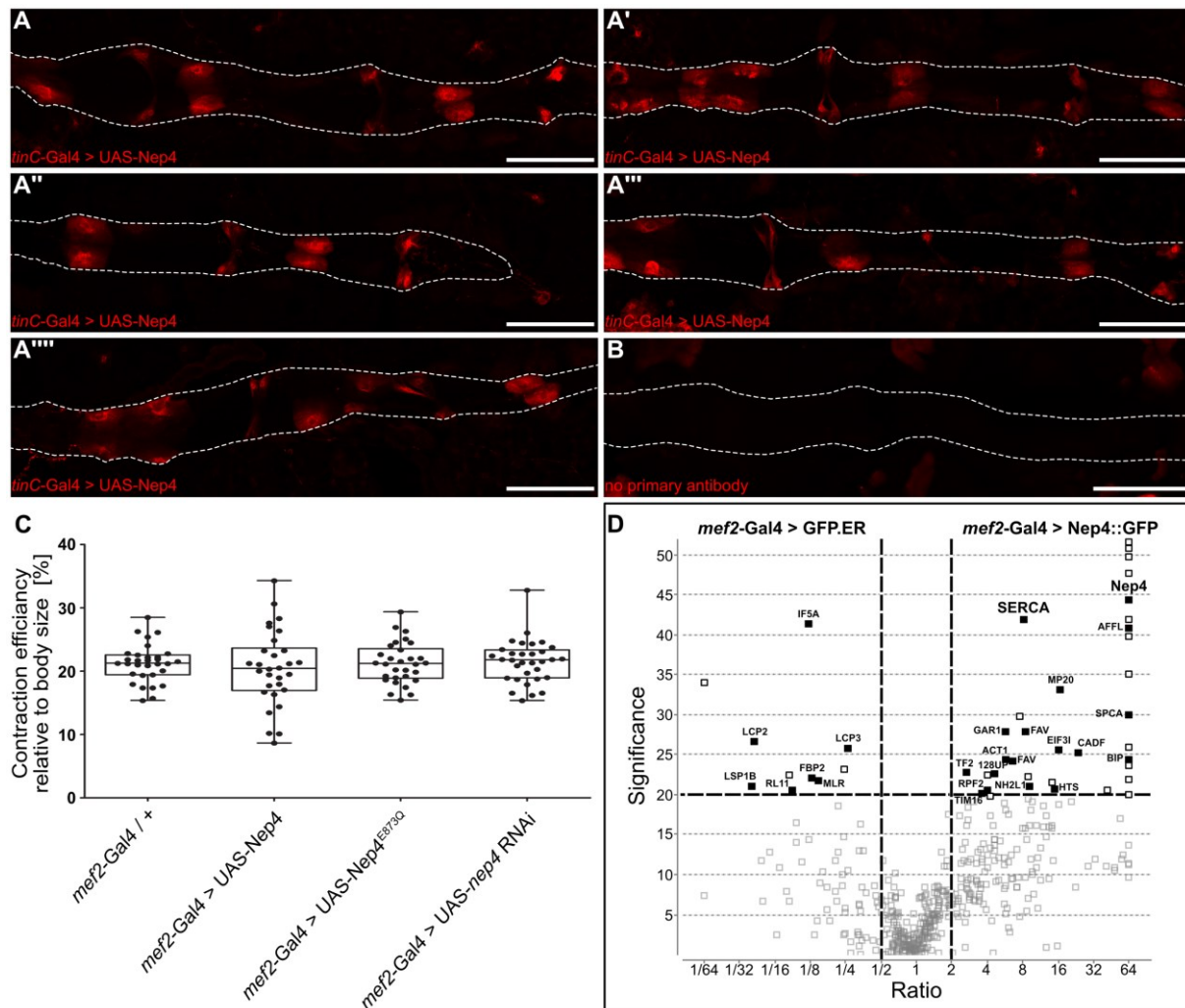


Fig. S9

Control data. (A-A''') Immunostainings of one week old adult males with heart-specific overexpression of Nep4 (*tinC-Gal4 > UAS-Nep4*) confirm similar Nep4 protein levels in the individual animals. Nep4 was detected with a monospecific antibody (RRID:AB_2569115). (B) Control stainings lacking primary antibodies do not exhibit any signal above background. Maximum projections of the heart chamber are shown; scale bars: 100 μ m; the heart tube is indicated by dashed lines; all images were captured under similar conditions.

(C) Contraction efficiency of third instar larval body wall muscles is not affected by increased Nep4 expression (*mef2-Gal4 > UAS-Nep4*, $n = 30$), knockdown of *nep4* (*mef2-Gal4 > UAS-nep4 RNAi*, $n = 32$) or increased expression of catalytically inactive Nep4 (*mef2-Gal4 > UAS-Nep4^{E873Q}*, $n = 30$), relative to control animals (*mef2-Gal4 / +*, $n = 31$). Contraction efficiency was calculated by normalizing the mean crawled distance per contraction to the body length of respective animals. Statistical significance was assessed by a one-way ANOVA followed by Dunnett's Multiple Comparison Test.

(D) Proteins coprecipitating with Nep4 were identified by pull down assays using total protein extracts of male third instar larvae expressing GFP-tagged Nep4 as bait (*mef2-Gal4 > Nep4::GFP*) and SR-luminal GFP (*mef2-Gal4 > GFP.ER*) as a control. SERCA significantly

coprecipitates with Nep4. Data are based on three individual biological replicates. Open outlined squares depict proteins with quantification being based on only one detected peptide. Corresponding candidates were excluded from further analyses. A significance value of 20 corresponds to $p < 0.01$ (one-way ANOVA).

Supplementary Tables

Table S1

Analyzed peptides and cleavage characteristics

Name	Sequence	Hydrolyzed by	Cleavage products	Cleavage position	Analyzed in
Sarcolamban A _{lum}	YLIYAVLa	Nep4	YLIYA YLIY	A/V Y/A	Fig. 5A
		NEP	YLIYA YLIY <i>LIYAV / IYAVLa</i>	A/V Y/A Y/L; V/L; L/I	Fig. 5C
Sarcolamban A _{lum} (V6A)	YLIYA ^A La	Nep4	YLIYA ^A YLIYA LIYA ^A LIYA	^A /L A/A Y/L; ^A /L Y/L; A/ ^A	Fig. S5A
Sarcolamban B _{lum}	YAFYEAAFa	Nep4	YAFYEAA FYEAFFa YAFYE	A/F A/F E/A	Fig. 5B
		NEP	FYEAAFa <i>FYEAA / AFYEA</i>	A/F A/F; Y/A; A/A	Fig. 5D
Sarcolamban B _{lum} (F8A)	YAFYEAA ^A a	Nep4	<i>AFYEAA / FYEAA^Aa</i>	^A /A; A/F	Fig. S5B
Sarcolamban B _{lum} (F3A)	Y ^A AYEAAFa	Nep4	^A YEAAFa	^A /A	Fig. S5C
Sarcolamban B _{lum} (F3A/F8A)	Y ^A AYEAAAa	n/a	n/a	n/a	Fig. S5D
Sarcolipin _{lum}	WLLVRSYQYa	Nep4	WLLVRSYQ LVRYSQYa WLLVRS WLLVR LVRYS	Q/Y L/L S/Y R/S L/L; Y/Q	Fig. 5F
		NEP	LVRYSQYa WLLVRS WLLVR LVRYS	L/L S/Y R/S L/L; Y/Q	Fig. 5E

Peptides analyzed for *Drosophila* Neprilysin 4 (Nep4) or human Neprilysin (NEP) mediated cleavage. Mutated residues are labelled in red; C-terminal amidation is indicated by an a. Italicized fragments could not be assigned to one unique peptide sequence.

Table S2

Variable beating frequencies do not affect Ca²⁺ flux parameters

Cardiac parameter	<i>tinC-Gal4 > UAS-nep4</i> RNAi; population	<i>tinC-Gal4 > UAS-nep4</i> RNAi; subgroup selected for slower heart rate	Significance values
Heart rate [bpm]	191.66 (SEM=12.41, n=22)	136.25 (SEM=10.56, n=9)	0,002
SR Ca ²⁺ load [au]	2.47 (SEM=0.25, n=22)	2.83 (SEM=0.50, n=9)	0,538
SERCA activity [1/sec]	4.11 (SEM=0.53, n=20)	3.40 (SEM=0.76, n=9)	0,564
Constant of relaxation, Tau [sec]	0.20 (SEM=0.02, n=22)	0.26 (SEM=0.04, n=9)	0,314

Depicted are Ca²⁺ flux parameters of *nep4* knockdown flies (*tinC-Gal4 > UAS-nep4* RNAi) and of a subgroup of *nep4* knockdown flies selected for slower heart rates. For this subgroup, all effects on SR Ca²⁺ load, SERCA activity, and Tau are consistent with the population data. n depicts the number of analyzed animals. Statistically significant differences are indicated in bold ($p < 0.05$, Students t-test (two-tailed)).

Supplementary Videos

Supplementary Videos 1-4

Overexpression and knockdown of nep4 affect heart rhythmicity

Representative heart recordings (30 sec) of adult animals of the following genotypes are shown: *tinC-Gal4 / +* (supplementary video 1); *tinC-Gal4 > UAS-Nep4* (supplementary video 2); *tinC-Gal4 > UAS-Nep4^{E873Q}* (supplementary video 3); *tinC-Gal4 > UAS-nep4* RNAi (supplementary video 4).

3 Discussion

The identification of signaling peptides and regulatory micropeptides continues to expand. While signaling peptides often represent switches for highly intricate pathways that rely on the precise orchestration of many different factors, membrane-located micropeptides usually modulate the activity of their specific interaction partner. In both cases, there is a need for regulatory mechanisms that target the biologically active peptides and are capable of terminating their respective actions. This work could characterize the neprilysin as an enzyme with promiscuous functionality based on broad substrate specificity and a variable subcellular localization (Figure 19). By cleavage of several extracellular peptides implicated in insulin signaling, the *Drosophila* neprilysin localizing to the cell surfaces serves as a central regulator of food intake, body size and weight, and development (2.1; 3.1). The complexity of the thereby affected pathways was further amplified by the finding that several of the signaling peptides also play a formerly unknown role in the modulation of heart functionality (2.2; 3.2). Neprilysin localizing at the SR membrane facilitates another functionality. In this compartment, the enzyme hydrolyzes SERCA-inhibitory micropeptides to ensure proper muscle contraction and heart functionality (2.4; 3.3).

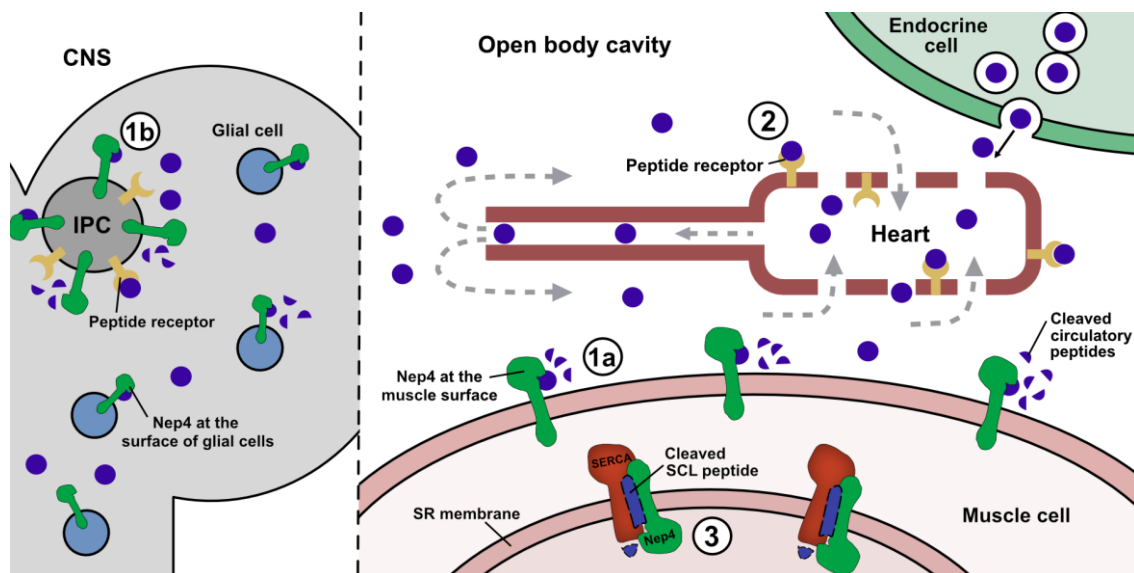


Figure 19 | Tissue-dependent subcellular localization of Nep4 is related to distinct functionalities of the enzyme. A simplified scheme summarizes the results of this thesis. (1) Regulation of insulin signaling is facilitated by Nep4 that localizes to the plasma membrane of muscle cells (1a), cardiomyocytes (not shown), or cells of the CNS (1b). At the CNS, Nep4 is present at the surface of IPCs and distinct glial cells. By the cleavage of signaling peptides circulating in the hemolymph produced by, for example, endocrine cells of the gut or fat body, activity of surface-located Nep4 prohibits peptide receptor activation, e.g., at IPCs. (2) Several peptides of the insulin signaling pathway additionally exert cardiomodulatory effects, probably via binding to receptors located at the surface of cardiomyocytes. (3) Nep4 also localizes to the SR membrane of body wall muscles and cardiomyocytes. The main project of this thesis identified the Nep4 as a critical regulator of SERCA activity. This functionality is based on the Nep4-mediated cleavage of SERCA-inhibitory SCL peptides. Only one IPC is shown for simplification. The depicted muscle cell also represents the cardiomyocytes of the heart. A highly deviant scale was applied to all structures to allow for the display of all functionalities.

3.1 Activity of Nep4 is critical to peptide homeostasis in insulin signaling

Insulin and insulin-like growth factor (IGF) signaling (IIS), including all involved molecular components, is evolutionary well-conserved. Nevertheless, mainly due to a reduced number of genes coding for peptide receptors and downstream signaling elements, invertebrates exhibit extenuated complexity of IIS compared to mammals (reviewed by Nässel and Zandawala, 2019). Furthermore, the open circulatory system of *Drosophila melanogaster* mediates the uncoupling of oxygen transport and distribution of metabolites, nutrients, and signaling molecules. This uncoupling allows the investigation of metabolic and cardiac dysfunctions that would be lethal in higher taxa with a closed cardiovascular system. Therefore, *Drosophila* has become a preferred model system to dissect various aspects of IIS and has already extensively contributed to our understanding of this signaling pathway (see section 1.1.1; reviewed in Rajan & Perrimon, 2013; Owusu-Ansah and Perrimon, 2014; Padmanabha and Baker 2014).

In the first project of this thesis, the role of *Drosophila* Neprilysin 4 (Nep4) in IIS was investigated. Examining the body size and weight of third instar larvae with tissue-specific overexpression or knockdown of the peptidase, it was apparent that muscle-specific overexpression of Nep4 leads to a severe reduction of both analyzed parameters (2.1, *Figure 1B*; Hallier et al., 2016). Furthermore, the knockdown of Nep4 in glial cells significantly reduces the body size and weight, whereby this effect can be rescued by ectopic expression of Nep4. An aberrant Nep4 expression also affects the development and life span (2.1, *Figure 1A*; Hallier et al., 2016). Both muscle-specific overexpression and knockdown of the peptidase result in enhanced embryonic lethality. Even though increased lethality of animals with elevated Nep4 levels in muscle tissue persists throughout development, the most substantial effect in the form of the complete lethality occurs in third instar larvae. On the contrary, reduced Nep4 expression is concomitant with a 100 % lethality during metamorphosis. Of note, animals with overexpression of catalytically inactive Nep4 (Panz et al., 2012) only exhibit increased lethality in the late larval development, probably due to overexpression of the intracellular domain. A previous study could show that this domain is critical to muscle integrity at this state, and overexpression of the cytoplasmic Nep4 domain is concomitant with a muscle degeneration phenotype (Panz et al., 2012). The fact that the elicited effects were restricted to overexpression of catalytically active Nep4 in the other stages, which is also true for the effects on body size and weight, renders the cleavage of so far unknown peptide substrates pivotal for proper development and growth. Since growth is closely related to metabolism, the metabolite composition of third instar larvae with reduced or enhanced Nep4 levels was analyzed via NMR metabolomics. Compared to control animals, larvae with elevated or diminished levels of the peptidase in muscle tissue exhibit distinct changes in metabolite composition (2.1, *Figure 2*; Hallier et al., 2016). These changes are related to impaired energy metabolism, like increased glucose levels or the reduction of NAD (Nicotinamide adenine dinucleotide).

According to affected energy metabolism, the food intake of larvae with aberrant Nep4 expression is significantly reduced (2.1, *Figure 3A*; Hallier et al., 2016). Since food intake is a process directly connected to insulin signaling and the production and release of insulin-like peptides (DILPs), *dilp1*, *dilp2*, *dilp3*, and *dilp5* expression levels were determined via qRT-PCR. Thereby, muscle-specific overexpression of Nep4 was shown to significantly reduce the expression of all *dilps*, an effect that was not elicited by overexpression of the inactive enzyme or the knockdown (2.1, *Figure 3B*; Hallier et al., 2016). Subsequently, the endogenous localization of the enzyme was investigated (2.1, *Figure 4*; Hallier et al., 2016).

On the one hand, the enzyme can be detected in muscle cells where it localizes to the cell surface and to intracellular membranes that were previously found to constitute the membranes of the sarcoplasmic reticulum (SR; Panz et al., 2012). On the other hand, Nep4 resides in CNS glial cells (2.1, *Figure 5*; Hallier et al., 2016) and at the plasma membrane of specific neurons: the IPCs (2.1, *Figure 6*; Hallier et al., 2016). Interestingly, these neurosecretory cells are responsible for producing and releasing of the DILP peptides (see also 1.1.1). Since the described metabolism-related phenotypes are based on the catalytic activity of Nep4 and the expression of *dilps* is predominately dependent on the binding of several peptides to their respective receptors at the surface of the IPCs, these peptides were tested as candidates for Nep4-mediated hydrolysis in an *in vitro* cleavage assay (2.1, *Figure 7*; Hallier et al., 2016). The candidates for this *in vitro* screen were chosen based on their proven relation to insulin signaling and food intake. Because steric conformation of the neprilysin binding pocket excludes substrates over ~3 kDa (see 1.1.2), considerably larger peptides were excluded from the screen. By incubation of 23 candidate peptides with purified Nep4B and subsequent analysis of cleavage products via mass spectrometry, 16 candidates were found to represent novel *in vitro* substrates of the peptidase (Table 2). On the contrary, the tested candidates hugin, neuropeptide F (NPF), proctolin, the short neuropeptide F species sNPF 3 and 4, tachykinin 3, and tachykinin 6 were resistant to Nep4-mediated hydrolysis (2.1, *Table 1*; Hallier et al., 2016). While cleavage of some peptides only occurs at one site (allatostatin A3; drosulfakinin 1; sNPF₁₁₋₁₁; tachykinin 4; tachykinin 5), most of the substrates are cleaved at several positions (Table 2). Some peptides even exhibit progressive C-terminal truncation if incubated with the peptidase (allatostatin A2, allatostatin A4, and leucokinin). However, no formation of cleavage products in preparations lacking the Nep4 renders the observed catalytic activity as specific. Indeed, neprilysins are typically characterized by their broad substrate specificity and promiscuous activity. Over 50 peptide substrates are, for example, known for the human NEP (reviewed, e.g., in Erdős and Skidgel, 1989; Bayes-Genis et al., 2016a). Therefore, the relatively broad specificity exhibited by Nep4 in this screen nicely reflects the commonly described neprilysin properties.

Table 2 | Identified Nep4 *in vitro* substrates implicated in insulin signaling and the regulation of food intake.

Nep4-mediated hydrolysis of the depicted peptides at the indicated cleavage sites results in the formation of several cleavage products. Respective cleavage positions are indicated (#). Via mass spectrometry detected peptide fragments are underlined. Data based on (2.1, *Table 1*; Hallier et al., 2016).

Peptide	Sequence	Scissile bonds	Cleavage products
Allatostatin A1	VERYAFGL _a	G#L F#G	<u>VERYAFG</u> #L VERYAF#GL _a
Allatostatin A2	LPVYNFGL _a	G#L F#G N#F	<u>LPVYNFG</u> #L _a <u>LPVYNF</u> #GL _a <u>LPVYN</u> #FGL _a
Allatostatin A3	SRPYSFGL _a	P#Y	SRP# <u>YSFGL</u> _a
Allatostatin A4	TTRPQPFNFGL _a	G#L N#F P#F	<u>TTRPQPFNF</u> #L _a <u>TTRPQPFN</u> #FGL _a <u>TTRPQP</u> #FNFGL _a
AKH	QLTFSPDW _a	L#T T#F	QL# <u>TFSPDW</u> _a QLT# <u>FSPDW</u> _a
Corazonin	QTFQYSRGWTN _a	T#F G#W	QT# <u>FQYSRGWTN</u> _a QTFQYSRG#WTN _a
DH ₃₁	TVDFGLARGYSGTQEA KHRMGLAAANFAGGP _a	G#Y; G#L G#Y	<u>TVDFGLARG</u> #YSGTQEA <u>KH</u> <u>RMG</u> #LAAANFAGGP _a <u>TVDFGLARG</u> #YSGTQEA <u>KH</u> RMGLAAANFAGGP _a
Drosulfakinin 1	FDDYGHMR _{Fa}	R#F	<u>FDDYGHMR</u> #F _a
Drosulfakinin 2	GGDDQFDDYGHMR _{Fa}	R#F Q#F	<u>GGDDQFDDYGHMR</u> #F _a GGDDQ# <u>FDDYGHMR</u> _{Fa}
Leucokinin	NSVVLGKKQRFHSW _{Ga}	S#W H#S R#F	<u>NSVVLGKKQRFHS</u> #W _{Ga} <u>NSVVLGKKQRFH</u> #SW _{Ga} <u>NSVVLGKKQR</u> #FHSW _{Ga}
sNPF ₁₋₁₁	AQRSPSLRLR _{Fa}	L#R	<u>AQRSPSLRL</u> #R _{Fa}
sNPF ₁₄₋₁₁ ; sNPF ₂₁₂₋₁₉	SPSLRLR _{Fa}	R#F S#L	SPSLRLR#F _a SPS# <u>LRLR</u> _{Fa}
Tachykinin 1	APTSSFIGM _{Ra}	G#M S#F	<u>APTSSFIG</u> #M _{Ra} APTSS# <u>FIGM</u> _{Ra}
Tachykinin 2	APLAFVGLR _a	P#L G#L A#F F#V	AP# <u>LAFVGLR</u> _a <u>APLAFVG</u> #L _{Ra} APLA# <u>FVGLR</u> _a <u>APLAF</u> #VGLR _a
Tachykinin 4	APVNSFVGM _{Ra}	G#M	<u>APVNSFVG</u> #M _{Ra}
Tachykinin 5	APNGFLGM _{Ra}	G#F	APNG# <u>FLGM</u> _{Ra}

Furthermore, it is also known that neprilysins prefer to cleave their substrates at the amino-terminal bond of hydrophobic residues (e.g., Gafford et al., 1983; Matsas et al., 1983; Hersh and Morihara, 1986; Tiraboschi et al., 1999; Oefner et al., 2000; Rose et al., 2002). This also applies to most of the observed cleavage sites in this screen since substrate hydrolysis preferably occurred at the amino bond of Phe and Leu or N-terminally of other hydrophobic residues. However, based on the many identified substrates and single cleavage events, it is hardly possible to deviate which cleavage event(s) accounts for the observed phenotypes related to impairments of IIS. In addition, the question remains which of the formed cleavage products are inactive. A possibility to

solve this is to test whether the formed fragments can still activate their respective receptors *in vitro* and *in vivo*.

Nevertheless, the result of increased Nep4-mediated cleavage of one or several peptides is the reduced *dilp* expression and related downstream effects of impaired IIS signaling, like the reduced body size and weight, a metabolic shift, and a decreased life span. These phenotypes of Nep4 overexpressing larvae correspond to known IPC ablation phenotypes, like elevated levels of circulating glucose or a reduced body size and body weight (Rulifson et al., 2002; Broughton et al., 2005). Accordingly, knockdown of the insulin-degrading enzyme (IDE) has the opposite effect, concomitant with a reduced hemolymph carbohydrate content and an increased body weight (Tsuda et al., 2010; Hyun and Hashimoto, 2011). However, unlike animals with IPC ablation or knockdown of the IDE, flies with aberrant Nep4 expression do not show advantageous effects like the extension of their life span. The reason could be that dissimilar to IPC ablation, the overexpression of Nep4 does not only affect IPCs and insulin signaling but could also interfere with other processes affected by the enhanced cleavage of the peptides (see section 3.2). In line with this, Nep4 was already shown to be important for muscle integrity (Panz et al., 2012). Furthermore, the additional muscle-specific occurrence of Nep4 at the SR even hints at another up to now unknown functionality of the enzyme that could be affected by the overexpression (Figure 19; see also section 3.3)

Dissection of the effects produced by the Nep4-mediated peptide cleavage is also bedeviled because the novel substrates act in a highly intricate network with partially overlapping or even opposing roles. Drosulfakinins and allatostatin A, for example, induce satiety respectively inhibit feeding (Hergarden et al., 2012; Söderberg et al., 2012; Chen et al., 2016), whereas other substrates like corazonin or sNPF species are positive regulators of insulin signaling and promote food intake (Lee et al., 2008; Hergarden et al., 2012). Moreover, the peptides do not all act on the same level but in a hierarchically organized way. Accordingly, the substrates can be divided into three groups. The first group of peptides bind to their specific receptors predominantly expressed by IPCs to directly induce *dilp* expression (e.g., sNPF, AKH). Peptides of the second group do not primarily bind to IPCs, but trigger peptide production at other neurosecretory cells (e.g., DH₃₁, allatostatin A). The thereby produced peptides then act on IPCs. The third group is relatively small and encompasses peptides produced by IPCs (drosulfakinins; Söderberg et al., 2012). As a representative of the first group, AKH is released by the AKH producing cells (APCs) of the corpora cardiaca (CC), and the production of the peptide is dependent on different factors, like the binding of AstA or the hemolymph glucose level (e.g., Kim and Rulifson, 2004; Hentze et al., 2015). Hence, the AKH level integrates several information sources and is also considered a “master regulator” (Galikova et al., 2015). Moreover, the AKH receptors are expressed at IPCs and in the fat body, where activation of AKHR is accomplished by mobilizing stored energy reserves (Bharucha et al., 2008). Like AKH, also sNPF and corazonin act as integrators of several information sources since their release from neurosecretory cells is, i.a., triggered by

DH₃₁ (e.g., Johnson et al., 2005; Lee et al., 2008; Veenstra et al., 2008). The fact that Nep4 is a regulator of peptides from all three described groups underlines the complexity of the overall regulatory mechanism.

Another interesting point is that Nep4 is expressed in muscle tissue but also in glial cells and the IPCs (2.1, *Figure 5-6*; Hallier et al., 2016). Since the body size and weight are affected in animals with muscle-specific Nep4 overexpression or glial cell-specific knockdown of the peptidase, both expression sites seem to play a physiologically relevant role. Strikingly, the glial cell-specific knockdown of the peptidase diminished growth, an effect not occurring upon muscle-specific reduced expression of Nep4. Based on this, one can deviate that the expression of Nep4 at the surface of glial cells is necessary for the regulation of peptide clearance at the CNS during larval development. Perhaps, the Nep4 present at the CNS can rescue the reduced peptide inactivation in animals exhibiting muscle-specific Nep4 knockdown. Of note, Nep4 is not only expressed in some glial cells of the CNS but also by IPCs (2.1, *Figure 6*; Hallier et al., 2016). Here, the functionality of the peptidase could be to cleave substrates prior to binding to their receptors on the IPCs, thereby ensuring efficient inhibition of receptor activation. Nevertheless, aberrant expression of the peptidase in a neuron-specific manner does not interfere with growth or development (2.1, *Figure 1*; Hallier et al., 2016). Another explanation for surface-located Nep4 appearance in different tissues could be a correlation of Nep4 expression with the occurrence of their primary hydrolysis target. In this context, the Nep4 at the muscle surfaces could be responsible for cleaving the fat body or gut-derived peptides, while Nep4 in the CNS could be essential to cleave neuropeptides circulating in the CNS (*Figure 19*). To further investigate this issue, it would be interesting to analyze *dilp* expression levels in flies with disturbed Nep4 levels in IPCs and glial cells.

Besides elevated glucose levels, the metabolomic analysis also showed that animals with muscle-specific overexpression exhibit reduced circulating levels of NAD and lactate, metabolites related to a process called aerobic glycolysis (2.1, *Figure 1*; Hallier et al., 2016). The aerobic glycolysis allows for rapid and extensive growth during the larval developmental stages, and impairment of this program leads to increased larval lethality (Tennessen et al., 2011; Tennessen et al., 2014). However, the relevance of aerobic glycolysis and many other distinct aspects of insulin signaling is restricted to the larval stage, where the animals feed a lot, and the DILPs primarily have to positively couple the nutrient uptake with systemic growth. In adults, insulin signaling is not that much adjusted to one main task but is rather critical for overall homeostasis. As a result, IIS in adult flies is even more complex and, therefore, less well-understood (reviewed by Nässel and Zandawala, 2019). One distinction between larval and adult IIS is, for example, that the IPCs of adults can sense hemolymph levels autonomously and are not reliant on the sensing activity of APCs (Park et al., 2014). Another difference is that the spatial expression pattern of gut-derived peptides like allatostatin A, DH₃₁, sNPF, or tachykinin is altered in adults compared to larvae (reviewed by Nässel and Zandawala,

2019). Because of such distinctions, it would be of great value to investigate if Nep4 is also a crucial regulator of IIS in adults and to further examine the causes for possible differences. Since muscle-specific overexpression and glial-specific knockdown of the peptidase result in larval lethality, alternatives for driving the expression need to be used to analyze adults.

In summary, Nep4 was found to be a crucial regulator of insulin signaling. By cleavage of peptides circulating in the hemolymph, the Nep4 localizing to the plasma membranes of different tissues controls food intake, larval growth, and development (Figure 19). However, the ongoing identification of novel peptides and peptide receptors and further characterization of the already known signaling circuits render our knowledge regarding IIS still incomplete (reviewed by Nässel and Zandawala, 2019). Based on the high relevance of the newly identified mechanism, it would be worth testing the new candidates regarding their susceptibility to neprilysin-mediated hydrolysis. Relevance is also underlined by the probably conserved role of neprilysins in IIS since recent data showed that NEP is a regulator of glucose metabolism in humans (reviewed by Packer, 2018; Esser and Zraika, 2019). Therefore, NEP inhibition even could be a possible target to treat patients with diabetes.

3.2 Identification of peptides with cardiomodulatory function

Many neuropeptides and peptide hormones do not exclusively act in one pathway but fulfill several functions in different contexts (e.g., reviewed in Schoofs et al., 2017; Nässel et al., 2019). This also applies to the peptides identified as novel Nep4 substrates in (2.1, Hallier et al., 2016). Since Nep4 localizes, i.a., to the *Drosophila* heart (see 2.4; Schiemann et al.) and, with corazonin, one of the insulin signaling-related substrates has a well-documented function in modulating the heartbeat of insects (Veenstra, 1989), the peptides were assessed for putative cardiomodulatory properties (2.2, Schiemann et al., 2018). In the first part of this study, the synthesized peptides were applied onto semi-intact larval heart preparations, and different heart parameters such as the heart rate with systolic and diastolic intervals, contraction strength (fractional shortening), and rhythmicity were examined via semi-automatic optical heartbeat analysis (SOHA; Fink et al., 2009) (2.2, *Figure 1, Figure 3, Figure 4*; Schiemann et al., 2018). 11 of the 19 tested candidates significantly altered one or more heart parameters upon application, whereby the exerted effects were quite distinct (Table 3). The peptides either exhibited inotropic (allatostatin A1, leucokinin) or chronotropic effects (allatostatin A2, corazonin, DH₃₁, proctolin, tachykinin1, tachykinin 3, tachykinin 4, and tachykinin 5). Remarkably, the heart rate acceleration due to reduced diastolic intervals was the most abundant effect among the chronotropic peptides.

Table 3 | *In vitro* effects of peptide application on different heart parameters. Listed are the individual effects upon application of the peptides at a concentration of 1×10^{-7} . Nomenclature indicates significance of the observed effects. (+ = increase, $p < 0.05$; ++ = increase, $p < 0.01$; +++ = increase, $p < 0.001$; - = decrease, $p < 0.05$; -- = decrease, $p < 0.01$; --- = decrease, $p < 0.001$; / = no significant effect; based on paired sample Student's t-test). \ominus indicates full arrest of heartbeat upon peptide application. HR (Heart Rate); DI (Diastolic interval), SI (Systolic Interval), FS (Fractional Shortening), AI (Arrhythmicity index). Data based on (2.3, Table 1; Schiemann et al., 2016).

Peptide	Sequence	HR	DI	SI	FS	AI
AKH	QLTFSPDWa	/	/	/	/	/
Allatostatin A1	VERYAFGLa	/	/	/	+	/
Allatostatin A2	LPVYNFGLa	/	-	+	/	/
Allatostatin A3	SRPYSFGLa	/	/	/	/	/
Allatostatin A4	TTRPQPFNFGLa	\ominus	\ominus	\ominus	\ominus	\ominus
Corazonin	QTFQYSRGWTNa	++	--	+	/	/
DH ₃₁	TVDFGLARGYSGTQEA KHRMGLAAANFAGGPa	+++	-	--	/	/
Drosulfakinin 1	FDDYGHMRFa	/	/	/	/	/
Drosulfakinin 2	GGDDQFDDYGHMRFa	/	/	/	/	/
Leucokinin	NSVVLGKKQRFHSWGa	/	/	/	+	/
Proctolin	RYLPT	+++	---	/	/	+
sNPF ₁₁₋₁₁	AQRSPSLRLRFa	/	/	/	/	/
sNPF ₁₄₋₁₁ sNPF ₂₁₂₋₁₉	SPSLRLRFa	/	/	/	/	/
Tachykinin 1	APTSSFIGMRa	+++	--	/	/	+
Tachykinin 2	APLAFVGLRa	/	/	/	/	/
Tachykinin 3	APTGF ^T GMRa	+	/	/	/	/
Tachykinin 4	APVNSFVGMRa	/	/	/	/	++
Tachykinin 5	APNGFLGMRa	+++	--	/	/	/
Tachykinin 6	AALSDSYDLRGKQQRf ADFNSKfVAVRa	/	/	/	/	/

Furthermore, one of the tested candidates, the allatostatin A4 peptide, triggered the complete yet reversible heartbeat arrest upon application.

Possible dose-dependencies of the identified cardioacceleratory peptides were tested by applying varying peptide concentrations. Surprisingly, though the progressive increase of applied peptide concentrations from 1×10^{-11} to 1×10^{-7} mainly was concomitant with more potent elicited effects, application of the highest peptide concentration of 1×10^{-5} resulted in all cases in a diminished response (2.2, Figure 2; Schiemann et al., 2018). In addition, the dose-response experiment revealed that Allatostatin A4 only leads to a cardiac arrest at a concentration of 1×10^{-7} .

To test whether the cardioacceleratory peptides exhibit physiological *in vivo* relevance regarding heartbeat regulation, their respective peptide precursor proteins were ubiquitously downregulated in third instar larvae. Subsequently, the heart parameters were analyzed by a newly developed software that allowed for the investigation of intact animals (HIRO; developed by Kay Lammers, Osnabrück University, Department of Zoology/Developmental biology). The downregulation of allatostatin A, corazonin, proctolin, and tachykinin protein precursors results in a significantly accelerated heart rate of intact *Drosophila* larvae. (2.2, *Figure 5*; Schiemann et al., 2018).

In summary, an *in vitro* screen for cardioactive peptides followed by the *in vivo* assessment of positive candidates revealed four peptides/peptide species that affect the heartbeat of *Drosophila* in a physiologically relevant manner. Of note, peptides identified in the *in vitro* screen were either exclusively chronotropic or inotropic. It is well-known that the peptides activate downstream signaling cascades by binding to G protein-coupled receptors (GPCRs; see sections 1.1 and 1.1.1). The fact that altered levels of these circulatory peptides affected the larval heart rate *in vitro* and *in vivo* in combination with the myogenic nature of the larval heart emphasizes the abundance of respective GPCRs at the surface of cardiomyocytes (*Figure 19*). Therefore, investigating GPCR localization at this tissue, for example via antibody staining, is recommended. Intriguingly, the activity of several GPCRs like the β -adrenergic receptor is crucial to heartbeat regulation in vertebrates (reviewed by Capote et al., 2015). The at first sight surprising result of the dose-response experiments also hints at the implication of GPCR receptors. As a common reaction to prolonged stimulation, GPCRs are internalized and distributed to the endomembrane system (e.g., reviewed in Hanyalogu and von Zastrow, 2008; Sorkin and von Zastrow, 2009; Drake et al., 2006; Calebiro and Godbole, 2018). Therefore, the efficient internalization of respective GPCRs could explain the decreased effects at high peptide concentrations. It would be interesting to determine the respective peptide receptors' threshold values by applying different peptide concentrations ranging between the identified threshold range of 1×10^{-7} to 1×10^{-5} .

However, the question remains about how the activation of respective GPCRs modulates the heartbeat. Even though different heart-modulatory effects have been reported for *Drosophila* peptides or peptide-related proteins, these effects' underlying molecular mechanism somewhat remains unclear (e.g., Nichols et al., 1999; Johnson et al., 2000; Liao et al., 2014; Ormerod et al., 2016). In this regard, it would be of high interest to further investigate the downstream signaling of GPCRs in the cardiac tissue.

3.3 Neprilysins control heart and muscle contraction via the inactivation of SERCA-inhibitory micropeptides

Neprilysin 4 is expressed in different cell types and tissues throughout the whole development of *Drosophila melanogaster*. Thereby, Nep4 enzymes of both somatic muscles and cardiac cells exhibit a particular distinction compared to the other tissues.

In addition to the typical ectoenzyme localization at the plasma membrane, Nep4 also resides at the membranes of the sarcoplasmic reticulum in muscle tissue (Panz et al., 2012; 2.1, *Figure 4*; Hallier et al., 2016). In the main project of the thesis, the functionality of Nep4 in this compartment was investigated.

Since the SR is closely related to muscle and heart performance (see section 1.2.3), different cardiac parameters were analyzed in adult flies with heart-specific aberrant expression of Nep4 (2.4, *Figure 1*; Schiemann et al.). Compared to control animals, flies with an elevated Nep4 level undergo extensive arrhythmias, including recurring heartbeat arrest (2.4, *Figure 1A, 1C-D*; Schiemann et al.). This phenotype relies on the enzyme's catalytic activity because overexpression of a catalytically inactive variant (Panz et al., 2012; 2.1, Hallier et al., 2016) does not affect heartbeat rhythmicity. The knockdown of Nep4 in cardiac cells leads to a slight increase of arrhythmia in the form of prolonged heart periods, though not in a statistically significant manner. Interestingly, in addition to the affected cardiac performance of adult animals, elevated Nep4 levels impair the functionality of larval muscles (2.4, *Figure 1E-F*; Schiemann et al.). Due to a reduced contraction frequency of body wall muscles, the crawling speed of larvae exhibiting Nep4 overexpression in muscle cells is significantly reduced. As the effects on the adult heart, the impairments in larvae rely on the catalytic activity of Nep4.

In many cases, impaired muscle functionality is related to aberrant Ca^{2+} cycling (1.2.2). Using the genetically encoded Ca^{2+} indicator GCaMP3 (Tian et al., 2009), different parameters of Ca^{2+} cycling were assessed in the heart tissue of animals with altered Nep4 levels. Interestingly, flies overexpressing catalytically active Nep4 exhibit an increased SR Ca^{2+} load (2.4, *Figure 2A*; Schiemann et al.). Usually, an increased SR Ca^{2+} load can be caused by impaired Ca^{2+} release via the RyR or by enhanced activity of SERCA, which is responsible for the transport of cytoplasmic Ca^{2+} into the SR and terminates the systolic phase (see 1.2.2; 1.2.3). Indeed, the increased Ca^{2+} uptake mediated by this enzyme was found to be causative of the high SR Ca^{2+} load in Nep4 overexpressing animals (2.4, *Figure 2B*; Schiemann et al.). Since some SERCA-interacting factors have been shown to decrease the expression level of the ATPase (e.g., Jiao et al., 2012), comparable expression levels of SERCA were proved via quantitative western blots for all genotypes (2.4, *Figure 2E*; Schiemann et al.). The knockdown of the peptidase slightly increases SR Ca^{2+} load and significantly reduces SERCA activity. Surprisingly, the constant of relaxation (τ) is only considerably affected in animals with reduced Nep4 levels (2.4, *Figure 2C-D*; Schiemann et al.). However, flies overexpressing catalytic active Nep4 tend towards τ reduction, even though this effect is not statistically significant. Since the single measurements for both elevated and reduced Nep4 expression display a high individual variance, the increase of measurements would probably be beneficial to clarify the picture. Nevertheless, the distinct effect of Nep4 overexpression or knockdown on SERCA activity indicates a functional relationship between the proteins.

To further investigate this relationship, subcellular localization of SERCA and Nep4 were examined in two kinds of *Drosophila* adult heart muscles: cardiomyocytes and ventral longitudinal muscles (VLMs). Nep4 and SERCA partially co-localize in both tissues, especially in the perinuclear membrane (2.4, *Figure 3A'-C'; D'-F'*; Schiemann et al.). The “NEST” (nuclear envelope biosynthesis) pathway could explain the accumulation of SR proteins at the perinuclear membrane. New SR proteins are translated at the rough ER constituting the perinuclear membrane and occasionally accumulate at this site before they reach their respective target SR location via transversely directed tubules (Ogata and Yamasaki, 1990; McFarland et al., 2010; Sleiman et al., 2015; He et al., 2020).

However, Nep4 and SERCA also co-localize at SR membranes of larval cardiac muscles and body wall muscles, indicating a conserved relationship between Nep4 and SERCA in all muscle tissues and stages (2.4, *Figure S1*; Schiemann et al.). Subsequent pull-down assays indeed revealed a direct interaction of Nep4 and SERCA (2.4, *Figure 3I*; Schiemann et al.). Since *Drosophila* SERCA is known to be inhibited by the binding of transmembrane SCL peptides (Magny et al., 2013; see section 1.2.4) and Nep4-mediated regulation of heart and muscle contraction relies on the catalytic activity of the peptidase, localization of all three factors was assessed (2.4, *Figure 4*; Schiemann et al.). Larvae with muscle-specific overexpression of Nep4 and SCLA (2.4, *Figure 4A-B, Figure S3A-A'*; Schiemann et al.) or SCLB (2.4, *Figure S2, Figure S3B-B'*; Schiemann et al.) exhibit partial co-localization of all three factors in cardiomyocytes and body wall muscles, especially at the perinuclear membrane. Furthermore, STED super-resolution microscopy of animals with Nep4/SCLA overexpression revealed more varying localization of the factors (2.4, *Figure 4C-D'*; Schiemann et al.). As indicated by the LSM-derived data, all three factors preferentially co-localize at the perinuclear membrane. Also, individual co-localization of SCLA and Nep4, SCLA and SERCA, and Nep4 and SERCA is apparent. In the more peripheral areas of the SR, SERCA and SCLA are the predominant factors.

Because the localization studies in combination with the co-immunoprecipitation of Nep4 and SERCA hinted towards a direct interaction of Nep4, SERCA, and the SCL peptides, *in vitro* cleavage assays were applied to test whether the SCLs represent substrates of the peptidase. Beforehand, the putative cleavage regions were determined by assessing the Nep4 orientation in the SR membrane using a redox-sensitive Nep4::roGFP fusion construct (Dooley et al., 2004; Tsachaki et al., 2015). Since the redox state of Nep4::roGFP corresponds to oxidizing conditions, the Nep4 C-terminus holding the catalytically active site localizes to the lumen of the SR in muscle tissue (2.4, *Figure S4*; Schiemann et al.). Based on this finding, it was conducted that cleavage of SCL peptides can only occur at their C-terminal residues protruding to the SR lumen. Therefore, the cleavage assays were performed with the synthesized C-terminal tails of SCLA (YLIYAVL, SCLA_{lum}) and SCLB (YAFYEAAF, SCLB_{lum}) (2.4; *Figure 5A-B*; Schiemann et al.). Due to the different used prediction methods, available predictions of either

transmembrane or luminal localization of the C-terminal residues of other regulin peptides vary. The predictions are, for example, based on TMHMM analyses, molecular dynamics simulations, solid-state NMR analyses, or crystal structures (e.g., Buffy et al., 2006; Anderson et al., 2016; Glaves et al., 2020; Gopinath et al., 2021; Rathod et al., 2021). Hence, how far the respective C-terminal residues protrude into the SR lumen remains unclear. Therefore, the synthesized peptides used in the cleavage assays were generously chosen to ensure representation of the whole C-Terminus. Both SCL_{lum} peptides were incubated with purified recombinant Nep4, and resulting cleavage products were analyzed by Orbitrap mass spectrometry. SCLA_{lum} and SCLB_{lum} were efficiently hydrolyzed, resulting in the formation of two, respectively, three specific cleavage products (Figure 20). All cleavage products were generated through the hydrolysis of the amino-terminal bond of the hydrophobic residues Val, Ala, or Phe. These cleavage sites correspond to the known neprilysin specificity, which was as well confirmed in the screen for novel insulin signaling-related peptide substrates (2.1, Hallier et al. 2016; Table 2). Of note, control preparations lacking Nep4 did not exhibit catalytic activity. Relevance of the hydrophobic C-terminal residues for cleavage susceptibility was further assessed in cleavage assays with peptides holding Ala substitutions for Val and Phe residues at hydrolysis sites.

Peptide	+Nep4	+NEP
SCLA_{lum} 		
SCLB_{lum} 		
SLN_{lum} 		

Figure 20 | Neprilysins hydrolyze SERCA-inhibitory peptides. Via orbitrap mass spectrometry detected peptide fragments are indicated in blue. Cleavage products that could not be assigned to a distinct sequence are marked in italics. The Nep4-mediated hydrolysis of SCLA_{lum} results in the formation of two distinct cleavage products. One of these cleavage products is also generated by the human neprilysin (NEP). NEP-dependent catalyzation of SCLA_{lum} furthermore gives rise to two other fragments, whereby one of which could not be assigned to a sequence based on its detected size. The SCLB_{lum} peptide gives rise to three cleavage fragments upon incubation with Nep4. One of these fragments is also generated by NEP, in addition to a further cleavage product. NEP also cleaves the vertebrate SLN_{lum} peptide at four different sites. The same cleavage products are formed as a result of Nep4-mediated hydrolysis. Furthermore, Nep4 also cleaves SLN_{lum} at the N-terminal bond of the C-terminal Val residue. Data are based on (2.4; Figure 5; Schiemann et al.).

In all cases, the substitutions altered or even inhibited Nep4-mediated catalysis of the peptides (2.4, *Figure S5*; Schiemann et al.).

To test if the found mechanistic relationship between SERCA-inhibitory peptides and neprilysin is evolutionary conserved, the *Drosophila* SCL peptides were examined for their susceptibility to cleavage through the human NEP. Strikingly, both peptides are efficiently hydrolyzed by the enzyme, indeed indicating evolutionary conservation. Possible conservation was also reconfirmed by the specific cleavage of the vertebrate sarcolipin peptide (SLN_{lum}; WLLVRSYQY) through *Drosophila* Nep4 and human NEP (2.4, *Figure 5F-D*; Schiemann et al.). The SLN peptide was chosen as a candidate because it exhibits extensive structural similarities to the SCL peptides, including a C-terminal tail (Anderson et al., 2016; Rathod et al., 2021). Both enzymes hydrolyzed the SLN_{lum} peptide with a high overlap of generated cleavage sites. Thus, it is shown for the first time that SERCA-regulatory micropeptides represent at least *in vitro* substrates of the neprilysin. In contrast to the rather variable N-Terminus (see *Figure 14*; section 1.2.4), the C-terminus is highly conserved among the regulins (Anderson et al., 2016; Rathod et al., 2021). Interestingly, the C-termini of SERCA-regulatory peptides are known to be critical for the peptide-mediated modulation of the ATPase activity. For phospholamban (PLN), it was shown that a single point mutation targeting a C-terminal Val residue (Val49Ala) is sufficient to interrupt PLN-dependent SERCA inhibition (Minamisawa et al., 1999; Abrol et al., 2014). Also, the inhibitory function of the SLN peptide relies on its C-terminal domain, and truncation leads to the loss of inhibitory function (Odermatt et al., 1998; Gramolini et al., 2004; Gorski et al., 2013). Strikingly, the SLN C-terminal RSYQY sequence transfer to a generic transmembrane helix generates a peptide with SLN-like SERCA-inhibitory properties (Gorski et al., 2013). Furthermore, the C-terminal addition of a FLAG-tag was reported to diminish SLN functionality (Odermatt et al., 1998). In line with this finding, adding a C-terminal GFP-tag to the SCL-peptides also severely interferes with their functionality and even interrupts co-immunoprecipitation with SERCA (Magny et al., 2013).

The SLN C-terminal domain was shown to interact with SERCA directly (e.g., Gramolini et al., 2004; Gorski et al., 2013; Sahoo et al., 2013; Glaves et al., 2020; Wang et al., 2021). This interaction mediates altered positioning of the peptide's transmembrane domain. As a result, the transmembrane domain can bind to the canonical inhibitory groove of the ATPase (Winther et al., 2013; Toyoshima et al., 2013; reviewed by Aguayo-Ortiz et al., 2020b; Rathod et al., 2021). Thereby, the SLN residues Tyr29 and Tyr31 are critical for the direct interaction of SERCA and the SLN C-terminus (Rathod et al., 2021; Hughes et al., 2007). In the conducted *in vitro* cleavage assay with the SLN_{lum} peptide, four of the five observed cleavage events produced by NEP led to the secession of both Tyr residues and one hydrolysis event cleaved at least the Tyr31 (*Figure 20*). Based on their hydrophobic and aromatic side chain, the Phe residues of SCLA could correspond to the Tyr residues of SLN. Therefore, it would be highly interesting to test if SCLB holding C-Terminal Phe/Ala substitutions can still interact with SERCA. Remarkably,

substituting both Phe residues render the peptide completely inaccessible for Nep4-mediated hydrolysis (2.4, *Figure S5D*; Schiemann et al.).

In essence, the C-terminal cleavage of SCL peptides by Nep4 localizing at SR membranes is likely to terminate SCL-dependent SERCA inhibition and is probably the explanation for the elevated SERCA activity in animals overexpressing Nep4 (*Figure 20*; *Figure 21*). However, the fate of inactivated peptides and the physiological significance of the identified mechanism was further examined in co-localization studies and biochemical subcellular fractionation assays performed by Annika Buhr (Osnabrück University, Department of Zoology/Developmental Biology). The co-expression of CLIP-tagged full-length SCLA, SCLB, and SLN peptides with Nep4 or human NEP enzymes in *Drosophila* S2 cells results in partial relocation of the peptides (2.4, *Figure 6A*; Schiemann et al.). Upon ectopic neprilysin expression, the abundance of peptides localizing to the cytoplasm or nucleoplasm instead of the cellular membranes significantly increases (2.4, *Figure 6B-C*; Schiemann et al.). The most substantial effect was apparent for the NEP-dependent relocation of SLN, whereas the Nep4-mediated shift of SCL peptides was more moderate. Interestingly, also C-terminally truncated SCL and SLN peptides, which correspond to the main generated peptide fragments of the cleavage assay, exhibit a reduced membrane localization (2.4, *Figure S6*; Schiemann et al.). Together, these results indicate the reduced membrane-anchoring of SCL and SLN peptides upon neprilysin-mediated cleavage of their C-Termini. A possible role of the C-Terminus in the peptide localization was already described for SLN (Gramolini et al., 2004; Wang et al., 2021). The conserved RSYQY sequence was found to mediate the ER/SR retention, and progressive truncation of the sequence was concomitant with mislocalization. Thereby, removing the Arg27 was critical for the loss of SR/ER localization, and further truncation, including the Leu24, finally results in the peptide's degradation (Gramolini et al., 2004). Enhanced degradation is also apparent in the PLN Leu39 premature stop mutation, which is associated with the development of dilated cardiomyopathy (Haghighi et al., 2003). Moreover, the PLN Val49 residue mutation also leads to decreased membrane anchoring, including mislocalization to the cytoplasm and nucleus (Abrol et al., 2014). Of note, the diminished SR retention of SLN can be rescued by analog expression of SERCA (Gramolini et al., 2004), which seems not to apply to PLN (Abrol et al., 2014).

Since the presence of SERCA appears to be an essential factor in the localization of the micropeptides, the subcellular localization of the peptides in somatic muscle tissue was analyzed. Even though collective overexpression of Nep4 and SCL peptides in larval body wall muscles did not lead to detectable relocation of the peptides (2.4, *Figure 6D-E*; *Figure S7*; Schiemann et al.), western blots of corresponding subcellular fractions revealed another effect. For both peptides, elevated Nep4 levels correlate with the reduced formation of peptide oligomers. In addition, it reduces the overall amount of SCLA in the muscle, an effect that could not be detected for SCLB (2.4, *Figure 6E*; Schiemann et al.).

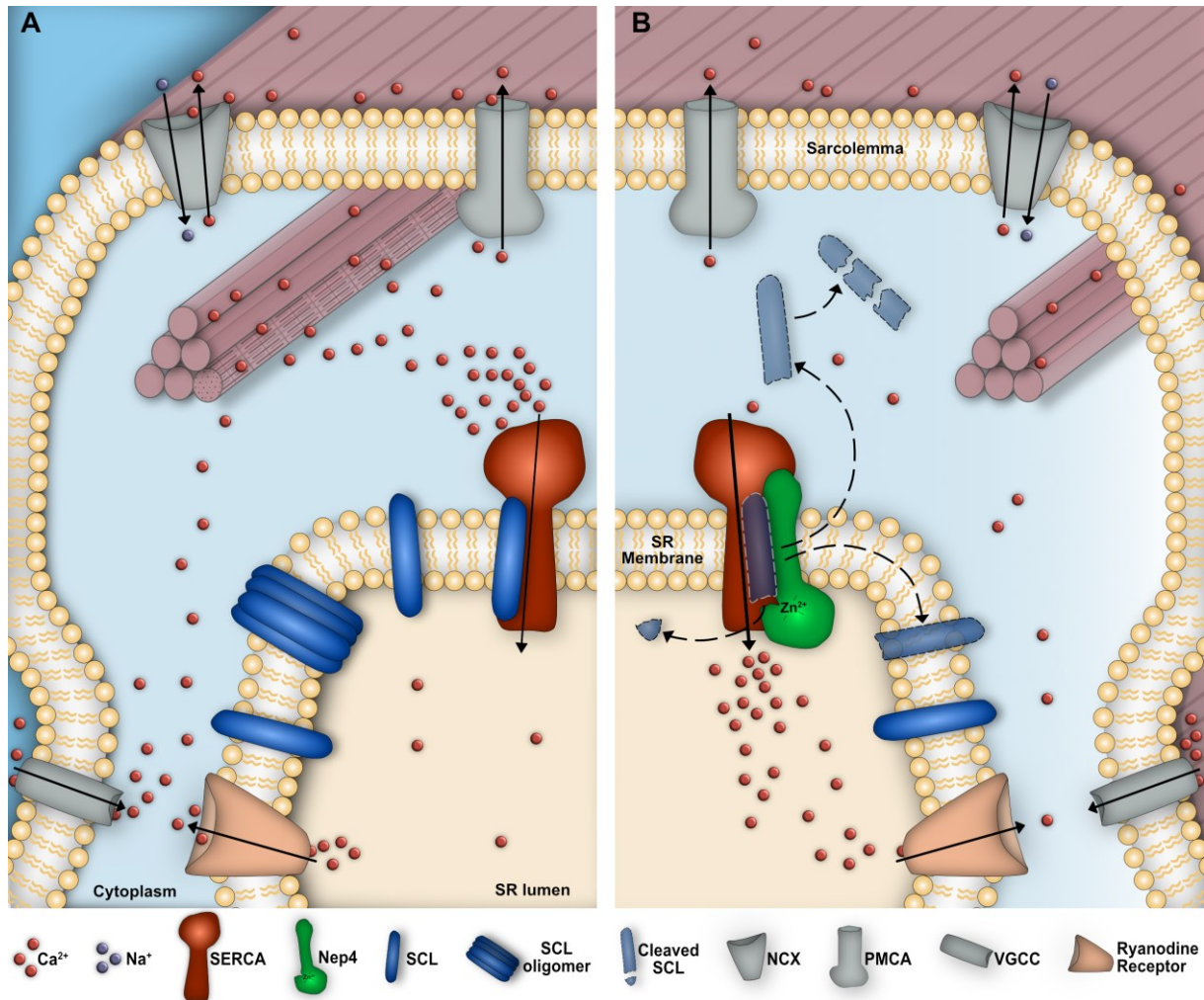


Figure 21 | Working model of Nep4-dependent regulation of muscle and heart contraction. (A) The influx of extracellular Ca^{2+} into a muscle cell via the VGCCs induces the opening of the RyRs localized at the SR membrane. As a result, the SR Ca^{2+} store is released into the cytoplasm, where the Ca^{2+} can interact with sarcomeric components to trigger muscle contraction. The transport of Ca^{2+} from the cytoplasm back into the SR lumen is primarily mediated by the action of SERCA and terminates the contraction phase. This process is modulated by SR-membrane integral SCL peptides that bind and inhibit the ATPase. The SCL peptides are organized as monomers or oligomers. (B) Upon Nep4 overexpression, the formation of SCL oligomers is prevented, and SERCA is hyperactive. These effects are based on excessive Nep4-mediated cleavage of the SCL C-termini. The cleaved peptides fail to inhibit SERCA activity, do not oligomerize, and tend to lose membrane anchoring, eventually followed by cytoplasmic degradation. Abbreviations: Voltage-gated calcium channel (VGCC); Ryanodine receptor (RyR); Sarcoplasmic reticulum (SR); Sarco/endoplasmic reticulum Ca^{2+} ATPase (SERCA); Sarcolamban (SCL); Neprilysin 4 (Nep4); $\text{Na}^{+}/\text{Ca}^{2+}$ exchanger (NCX); Plasma membrane Ca^{2+} ATPase (PMCA). Modified after (2.4, Schiemann et al.).

Based on the molecular weight of the apparent oligomers, it can be conducted that the peptides organize to some extent in tetramers at endogenous Nep4 expression levels. The tetramers exhibited stability in SDS-PAGE, as it was also shown for PLN pentamers (Jones et al., 1985; Simmerman et al., 1996; Robia et al., 2005). Remarkably, oligomeric states were additionally reported for SLN, the recently discovered regulins ELN, MLN, and DWORF, as well as some of the arthropod SCL peptides (Hellstern et al., 2001; Autry et al., 2011; Autry et al., 2020; Bak et al., 2020; Singh et al., 2019). However, all the peptides canonically bind to SERCA as monomers (Singh et al., 2019).

Because peptide cleavage assays and the relocalization studies suggest functional conservation of the neprilysin-mediated cleavage of SERCA-regulatory peptides, subcellular localization of NEP and SERCA was examined in human ventricular cardiomyocytes. Intriguingly, the proteins exhibit extensive co-localization along the Z-discs and perinuclear membranes of the cardiomyocytes (2.4, *Figure S8*; Schiemann et al.). Together with the previously mentioned results, this finding further indicates the evolutionary conservation of the novel regulatory mechanism from flies to humans.

In summary, *Drosophila* Neprilysin 4 is a crucial regulator of muscle contraction, a functionality mediated by the distinct localization of Nep4 at the SR membrane of muscle tissue (*Figure 19*; *Figure 21*). Proper control of heart and muscle contractions relies on the activity of SERCA that transports the cytosolic Ca^{2+} into the SR lumen to terminate the contraction phase. On the one hand, this process is regulated by the binding of inhibitory SCL peptides and probably fine-tuned through oligomerization of the peptides (*Figure 21A*). On the other hand, the peptide's ability to form oligomers and inhibit SERCA activity is diminished by the catalytic activity of Nep4 (*Figure 21B*). A hint regarding the importance of the endogenously expressed Nep4 in this process could be the observation that the muscle-specific Nep4 knockdown conducted in the first project revealed complete pupal lethality (2.1, *Figure 1A*; Hallier et al., 2016). Remarkably, though the animals succeed in metamorphosis, they fail to emerge the pupae at the end. The typical twitching-like movements of the legs prior to eclosure are also not apparent in these animals. It would be interesting to examine if the SERCA in these animals undergoes SCL-mediated superinhibition due to Nep4 absence. Based on this theory, the question remains why the cardiac Nep4 knockdown in adults or the muscle-specific knockdown in larvae does not significantly affect heart rhythmicity, respectively the crawling speed.

However, exerted effects of elevated Nep4 levels are more unambiguous than the knockdown effects, whereby the fate of the cleaved SCL peptides needs to be further investigated. For PLN, it was shown that the C-terminal truncation does not only diminish its SERCA-inhibitory functionality but also reduces the membrane anchoring and its ability to form oligomers (Abrol et al., 2014). Therefore, expression of the C-terminally mutated SCL and SLN peptides to test whether these peptides are still capable of binding SERCA, inhibiting the pumping action of the ATPase, and forming oligomers would be interesting. The results of this study could help to answer the still unsolved details of the identified mechanism. The finding that SERCA and Nep4 co-localize and co-immunoprecipitate suggests that cleavage of the SCL peptides occurs in their SERCA-bound state. Though this does not exclude cleavage events targeting unbound SCL, it emphasizes the possibility that the interaction of the peptides C-Terminus with SERCA at the SR lumen sterically enables the Nep4-mediated cleavage. Finally, it is not clear what happens to the peptides after hydrolysis. In contrast to the other regulins, SLN can stay associated with SERCA throughout the catalytic cycle (Sahoo et al., 2013). This specific feature is probably related to SLN's SERCA uncoupling

functionality related to thermogenesis. Strikingly, C-terminal truncation of SLN does not retrieve SLN from the SERCA binding pocket but reduces the uncoupling, as reported in a recent study (Wang et al., 2021).

The findings of this project further designate *Drosophila* as an amenable model system to investigate heart functionality and the molecular underpinnings of different cardiac diseases (reviewed by Taghli-Lamalle et al., 2016). In this line, the recent discovery of novel SERCA-regulatory micropeptides was first initiated by identifying the SCL peptides as modulators of *Drosophila* SERCA (Magny et al., 2013; reviewed in Payre and Desplan, 2016). However, the fact that both human regulins PLN and SLN have been related to cardiac misfunction (e.g., Uemura et al., 2004; Haghghi et al., 2006) emphasizes significance of the herein described mechanism of Nep4-mediated SCL inactivation from flies to humans.

4 References

- Abraham, D. M., & Wolf, M. J. (2013). Disruption of sarcoendoplasmic reticulum calcium ATPase function in *Drosophila* leads to cardiac dysfunction. *PloS one*, *8*(10), e77785.
- Abrol, N., Smolin, N., Armanious, G., Ceholski, D. K., Trieber, C. A., Young, H. S., & Robia, S. L. (2014). Phospholamban C-terminal residues are critical determinants of the structure and function of the calcium ATPase regulatory complex. *The Journal of biological chemistry*, *289*(37), 25855–25866.
- Adachi, T., Weisbrod, R. M., Pimentel, D. R., Ying, J., Sharov, V. S., Schöneich, C., & Cohen, R. A. (2004). S-Glutathiolation by peroxynitrite activates SERCA during arterial relaxation by nitric oxide. *Nature medicine*, *10*(11), 1200–1207. <https://doi.org/10.1038/nm1119>
- Agrawal, N., Delanoue, R., Mauri, A., Basco, D., Pasco, M., Thorens, B., & Léopold, P. (2016). The *Drosophila* TNF Eiger Is an Adipokine that Acts on Insulin-Producing Cells to Mediate Nutrient Response. *Cell metabolism*, *23*(4), 675–684.
- Aguayo-Ortiz, R., & Espinoza-Fonseca, L. M. (2020a). Linking Biochemical and Structural States of SERCA: Achievements, Challenges, and New Opportunities. *International journal of molecular sciences*, *21*(11), 4146.
- Aguayo-Ortiz, R., & Espinoza-Fonseca, L. M. (2020b). Atomistic Structure and Dynamics of the Ca²⁺-ATPase Bound to Phosphorylated Phospholamban. *International journal of molecular sciences*, *21*(19), 7261.
- Ahlquist R. P. (1948). A study of the adrenotropic receptors. *The American journal of physiology*, *153*(3), 586–600.
- Akaike, T., Du, N., Lu, G., Minamisawa, S., Wang, Y., & Ruan, H. (2017). A Sarcoplasmic Reticulum Localized Protein Phosphatase Regulates Phospholamban Phosphorylation and Promotes Ischemia Reperfusion Injury in the Heart. *JACC. Basic to translational science*, *2*(2), 160–180.
- Akin, B. L., Hurley, T. D., Chen, Z., & Jones, L. R. (2013). The structural basis for phospholamban inhibition of the calcium pump in sarcoplasmic reticulum. *The Journal of biological chemistry*, *288*(42), 30181–30191.
- Albers R. W. (1967). Biochemical aspects of active transport. *Annual review of biochemistry*, *36*, 727–756.
- Alford, R. F., Smolin, N., Young, H. S., Gray, J. J., & Robia, S. L. (2020). Protein docking and steered molecular dynamics suggest alternative phospholamban-binding sites on the SERCA calcium transporter. *The Journal of biological chemistry*, *295*(32), 11262–11274.
- Altshuler, I., Vaillant, J. J., Xu, S., & Cristescu, M. E. (2012). The evolutionary history of sarco(endo)plasmic calcium ATPase (SERCA). *PloS one*, *7*(12), e52617.
- Anderson, D. M., Anderson, K. M., Chang, C. L., Makarewich, C. A., Nelson, B. R., McAnally, J. R., Kasaragod, P., Shelton, J. M., Liou, J., Bassel-Duby, R., & Olson, E. N. (2015). A

- micropeptide encoded by a putative long noncoding RNA regulates muscle performance. *Cell*, 160(4), 595–606.
- Anderson, D. M., Makarewich, C. A., Anderson, K. M., Shelton, J. M., Bezprozvannaya, S., Bassel-Duby, R., & Olson, E. N. (2016). Widespread control of calcium signaling by a family of SERCA-inhibiting micropeptides. *Science signaling*, 9(457), ra119.
- Andrews, C., Xu, Y., Kirberger, M., & Yang, J. J. (2020). Structural Aspects and Prediction of Calmodulin-Binding Proteins. *International journal of molecular sciences*, 22(1), 308.
- Anger, M., Samuel, J. L., Marotte, F., Wuytack, F., Rappaport, L., & Lompré, A. M. (1993). The sarco(endo)plasmic reticulum Ca(2+)-ATPase mRNA isoform, SERCA 3, is expressed in endothelial and epithelial cells in various organs. *FEBS letters*, 334(1), 45–48.
- Antonova, Y., Arik, A. J., Moore, W., Riehle, M. A., & Brown, M. R. (2012). Insulin-like peptides: structure, signaling, and function. In *Insect endocrinology* (pp. 63-92).
- Apell H. J. (2003). Structure-function relationship in P-type ATPases--a biophysical approach. *Reviews of physiology, biochemistry and pharmacology*, 150, 1–35.
- Arvanitis, D. A., Vafiadaki, E., Fan, G. C., Mitton, B. A., Gregory, K. N., Del Monte, F., Kontrogianni-Konstantopoulos, A., Sanoudou, D., & Kranias, E. G. (2007). Histidine-rich Ca-binding protein interacts with sarcoplasmic reticulum Ca-ATPase. *American journal of physiology. Heart and circulatory physiology*, 293(3), H1581–H1589.
- Asahi, M., McKenna, E., Kurzydowski, K., Tada, M., & MacLennan, D. H. (2000). Physical interactions between phospholamban and sarco(endo)plasmic reticulum Ca²⁺-ATPases are dissociated by elevated Ca²⁺, but not by phospholamban phosphorylation, vanadate, or thapsigargin, and are enhanced by ATP. *The Journal of biological chemistry*, 275(20), 15034–15038.
- Asahi, M., Sugita, Y., Kurzydowski, K., De Leon, S., Tada, M., Toyoshima, C., & MacLennan, D. H. (2003). Sarcolipin regulates sarco(endo)plasmic reticulum Ca²⁺-ATPase (SERCA) by binding to transmembrane helices alone or in association with phospholamban. *Proceedings of the National Academy of Sciences of the United States of America*, 100(9), 5040–5045.
- Autry, J. M., & Jones, L. R. (1997). Functional Co-expression of the canine cardiac Ca²⁺ pump and phospholamban in *Spodoptera frugiperda* (Sf21) cells reveals new insights on ATPase regulation. *The Journal of biological chemistry*, 272(25), 15872–15880.
- Autry, J. M., Karim, C. B., Perumbakkam, S., Finno, C. J., McKenzie, E. C., Thomas, D. D., & Valberg, S. J. (2020). Sarcolipin Exhibits Abundant RNA Transcription and Minimal Protein Expression in Horse Gluteal Muscle. *Veterinary sciences*, 7(4), 178.
- Autry, J. M., Rubin, J. E., Pietrini, S. D., Winters, D. L., Robia, S. L., & Thomas, D. D. (2011). Oligomeric interactions of sarcolipin and the Ca-ATPase. *The Journal of biological chemistry*, 286(36), 31697–31706.
- Autry, J. M., Thomas, D. D., & Espinoza-Fonseca, L. M. (2016). Sarcolipin Promotes Uncoupling of the SERCA Ca²⁺ Pump by Inducing a Structural Rearrangement in the Energy-Transduction Domain. *Biochemistry*, 55(44), 6083–6086.

- Babu, G. J., Bhupathy, P., Carnes, C. A., Billman, G. E., & Periasamy, M. (2007). Differential expression of sarcolipin protein during muscle development and cardiac pathophysiology. *Journal of molecular and cellular cardiology*, *43*(2), 215–222.
- Bai, H., Kang, P., & Tatar, M. (2012). Drosophila insulin-like peptide-6 (dilp6) expression from fat body extends lifespan and represses secretion of Drosophila insulin-like peptide-2 from the brain. *Aging cell*, *11*(6), 978–985.
- Bak, J. J., Aguayo-Ortiz, R., Khan, M. B., Robia, S. L., Lemieux, M. J., Espinoza-Fonseca, L. M., & Young, H. S. (2020). Sarcolambans are phospholamban-and sarcolipin-like regulators of the sarcoplasmic reticulum calcium pump SERCA. *bioRxiv*.
- Bal, N. C., Maurya, S. K., Sopariwala, D. H., Sahoo, S. K., Gupta, S. C., Shaikh, S. A., Pant, M., Rowland, L. A., Bombardier, E., Goonasekera, S. A., Tupling, A. R., Molkentin, J. D., & Periasamy, M. (2012). Sarcolipin is a newly identified regulator of muscle-based thermogenesis in mammals. *Nature medicine*, *18*(10), 1575–1579.
- Barone, V., Randazzo, D., Del Re, V., Sorrentino, V., & Rossi, D. (2015). Organization of junctional sarcoplasmic reticulum proteins in skeletal muscle fibers. *Journal of muscle research and cell motility*, *36*(6), 501–515.
- Bataillé, L., Frendo, J. L., & Vincent, A. (2015). Hox control of Drosophila larval anatomy; The Alary and Thoracic Alary-Related Muscles. *Mechanisms of development*, *138 Pt 2*, 170–176.
- Bayes-Genis, A., Barallat, J., & Richards, A. M. (2016a). A Test in Context: Nephilysin: Function, Inhibition, and Biomarker. *Journal of the American College of Cardiology*, *68*(6), 639–653.
- Bayes-Genis, A., Morant-Talamante, N., & Lupón, J. (2016b). Nephilysin and Natriuretic Peptide Regulation in Heart Failure. *Current heart failure reports*, *13*(4), 151–157.
- Bednářová, A., Kodrík, D., & Krishnan, N. (2013). Unique roles of glucagon and glucagon-like peptides: Parallels in understanding the functions of adipokinetic hormones in stress responses in insects. *Comparative biochemistry and physiology. Part A, Molecular & integrative physiology*, *164*(1), 91–100.
- Beghi, S., Cavaliere, F., & Buschini, A. (2020). Gene polymorphisms in calcium-calmodulin pathway: Focus on cardiovascular disease. *Mutation research. Reviews in mutation research*, *786*, 108325.
- Ben-Johny, M., & Yue, D. T. (2014). Calmodulin regulation (calmodulation) of voltage-gated calcium channels. *The Journal of general physiology*, *143*(6), 679–692.
- Berridge, M. J., Bootman, M. D., & Roderick, H. L. (2003). Calcium signalling: dynamics, homeostasis and remodelling. *Nature reviews. Molecular cell biology*, *4*(7), 517–529.
- Bers D. M. (2002). Cardiac excitation-contraction coupling. *Nature*, *415*(6868), 198–205.
- Bers D. M. (2008). Calcium cycling and signaling in cardiac myocytes. *Annual review of physiology*, *70*, 23–49.
- Bharucha, K. N., Tarr, P., & Zipursky, S. L. (2008). A glucagon-like endocrine pathway in Drosophila modulates both lipid and carbohydrate homeostasis. *The Journal of experimental biology*, *211*(Pt 19), 3103–3110.

- Bhupathy, P., Babu, G. J., & Periasamy, M. (2007). Sarcolipin and phospholamban as regulators of cardiac sarcoplasmic reticulum Ca^{2+} ATPase. *Journal of molecular and cellular cardiology*, *42*(5), 903–911.
- Bhupathy, P., Babu, G. J., Ito, M., & Periasamy, M. (2009). Threonine-5 at the N-terminus can modulate sarcolipin function in cardiac myocytes. *Journal of molecular and cellular cardiology*, *47*(5), 723–729.
- Bidwell, P., Blackwell, D. J., Hou, Z., Zima, A. V., & Robia, S. L. (2011). Phospholamban binds with differential affinity to calcium pump conformers. *The Journal of biological chemistry*, *286*(40), 35044–35050.
- Birse, R. T., Söderberg, J. A., Luo, J., Winther, A. M., & Nässel, D. R. (2011). Regulation of insulin-producing cells in the adult *Drosophila* brain via the tachykinin peptide receptor DTKR. *The Journal of experimental biology*, *214*(Pt 24), 4201–4208.
- Bjarnadóttir, T. K., Gloriam, D. E., Hellstrand, S. H., Kristiansson, H., Fredriksson, R., & Schiöth, H. B. (2006). Comprehensive repertoire and phylogenetic analysis of the G protein-coupled receptors in human and mouse. *Genomics*, *88*(3), 263–273.
- Bland, N. D., Pinney, J. W., Thomas, J. E., Turner, A. J., & Isaac, R. E. (2008). Bioinformatic analysis of the neprilysin (M13) family of peptidases reveals complex evolutionary and functional relationships. *BMC evolutionary biology*, *8*, 16.
- Blaustein, M. P., & Lederer, W. J. (1999). Sodium/calcium exchange: its physiological implications. *Physiological reviews*, *79*(3), 763–854.
- Bobe, R., Bredoux, R., Corvazier, E., Andersen, J. P., Clausen, J. D., Dode, L., Kovács, T., & Enouf, J. (2004). Identification, expression, function, and localization of a novel (sixth) isoform of the human sarco/endoplasmic reticulum Ca^{2+} ATPase 3 gene. *The Journal of biological chemistry*, *279*(23), 24297–24306.
- Bobe, R., Bredoux, R., Wuytack, F., Quarek, R., Kovács, T., Papp, B., Corvazier, E., Magnier, C., & Enouf, J. (1994). The rat platelet 97-kDa Ca^{2+} ATPase isoform is the sarcoendoplasmic reticulum Ca^{2+} ATPase 3 protein. *The Journal of biological chemistry*, *269*(2), 1417–1424.
- Bodmer, R., & Frasch, M. (2010). Development and aging of the *Drosophila* heart. In *Heart Development and Regeneration*, Academic Press. 47-86.
- Bokník, P., Unkel, C., Kirchhefer, U., Kleideiter, U., Klein-Wiele, O., Knapp, J., Linck, B., Lüss, H., Müller, F. U., Schmitz, W., Vahlensieck, U., Zimmermann, N., Jones, L. R., & Neumann, J. (1999). Regional expression of phospholamban in the human heart. *Cardiovascular research*, *43*(1), 67–76.
- Borson D. B. (1991). Roles of neutral endopeptidase in airways. *The American journal of physiology*, *260*(4 Pt 1), L212–L225.
- Brandl, C. J., deLeon, S., Martin, D. R., & MacLennan, D. H. (1987). Adult forms of the Ca^{2+} ATPase of sarcoplasmic reticulum. Expression in developing skeletal muscle. *The Journal of biological chemistry*, *262*(8), 3768–3774.

- Brandl, C. J., Green, N. M., Korczak, B., & MacLennan, D. H. (1986). Two Ca²⁺ ATPase genes: homologies and mechanistic implications of deduced amino acid sequences. *Cell*, *44*(4), 597–607.
- Brini, M., & Carafoli, E. (2009). Calcium pumps in health and disease. *Physiological reviews*, *89*(4), 1341–1378.
- Brody I. A. (1969). Muscle contracture induced by exercise. A syndrome attributable to decreased relaxing factor. *The New England journal of medicine*, *281*(4), 187–192.
- Brody, T., & Cravchik, A. (2000). Drosophila melanogaster G protein-coupled receptors. *The Journal of cell biology*, *150*(2), F83–F88.
- Broggiolo, W., Stocker, H., Ikeya, T., Rintelen, F., Fernandez, R., & Hafen, E. (2001). An evolutionarily conserved function of the Drosophila insulin receptor and insulin-like peptides in growth control. *Current biology : CB*, *11*(4), 213–221.
- Broughton, S. J., Piper, M. D., Ikeya, T., Bass, T. M., Jacobson, J., Drieger, Y., Martinez, P., Hafen, E., Withers, D. J., Leever, S. J., & Partridge, L. (2005). Longer lifespan, altered metabolism, and stress resistance in Drosophila from ablation of cells making insulin-like ligands. *Proceedings of the National Academy of Sciences of the United States of America*, *102*(8), 3105–3110.
- Bublitz, M., Musgaard, M., Poulsen, H., Thøgersen, L., Olesen, C., Schiøtt, B., Morth, J. P., Møller, J. V., & Nissen, P. (2013). Ion pathways in the sarcoplasmic reticulum Ca²⁺-ATPase. *The Journal of biological chemistry*, *288*(15), 10759–10765.
- Buffy, J. J., Buck-Koehntop, B. A., Porcelli, F., Traaseth, N. J., Thomas, D. D., & Veglia, G. (2006). Defining the intramembrane binding mechanism of sarcolipin to calcium ATPase using solution NMR spectroscopy. *Journal of molecular biology*, *358*(2), 420–429.
- Bullard, B., & Pastore, A. (2019). Through thick and thin: dual regulation of insect flight muscle and cardiac muscle compared. *Journal of muscle research and cell motility*, *40*(2), 99–110.
- Burbaum, L., Schneider, J., Scholze, S., Böttcher, R. T., Baumeister, W., Schwille, P., Plitzko, J. M., & Jasnin, M. (2021). Molecular-scale visualization of sarcomere contraction within native cardiomyocytes. *Nature communications*, *12*(1), 4086. <https://doi.org/10.1038/s41467-021-24049-0>
- Burk, S. E., Lytton, J., MacLennan, D. H., & Shull, G. E. (1989). cDNA cloning, functional expression, and mRNA tissue distribution of a third organellar Ca²⁺ pump. *The Journal of biological chemistry*, *264*(31), 18561–18568.
- Calderón, J. C., Bolaños, P., & Caputo, C. (2014). The excitation-contraction coupling mechanism in skeletal muscle. *Biophysical reviews*, *6*(1), 133–160.
- Calebiro, D., & Godbole, A. (2018). Internalization of G-protein-coupled receptors: Implication in receptor function, physiology and diseases. *Best practice & research. Clinical endocrinology & metabolism*, *32*(2), 83–91.
- Campbell, A. M., Kessler, P. D., & Fambrough, D. M. (1992). The alternative carboxyl termini of avian cardiac and brain sarcoplasmic reticulum/endoplasmic reticulum Ca(2+)-ATPases are on opposite sides of the membrane. *The Journal of biological chemistry*, *267*(13), 9321–9325.

- Campbell, K. B., & Chandra, M. (2006). Functions of stretch activation in heart muscle. *The Journal of general physiology*, *127*(2), 89–94.
- Campbell, K. L., & Dicke, A. A. (2018). Sarcolipin Makes Heat, but Is It Adaptive Thermogenesis?. *Frontiers in physiology*, *9*, 714.
- Cantilina, T., Sagara, Y., Inesi, G., & Jones, L. R. (1993). Comparative studies of cardiac and skeletal sarcoplasmic reticulum ATPases. Effect of a phospholamban antibody on enzyme activation by Ca²⁺. *The Journal of biological chemistry*, *268*(23), 17018–17025.
- Capote, L. A., Mendez Perez, R., & Lymperopoulos, A. (2015). GPCR signaling and cardiac function. *European journal of pharmacology*, *763*(Pt B), 143–148.
- Carafoli E. (2002). Calcium signaling: a tale for all seasons. *Proceedings of the National Academy of Sciences of the United States of America*, *99*(3), 1115–1122.
- Carafoli, E., & Krebs, J. (2016). Why Calcium? How Calcium Became the Best Communicator. *The Journal of biological chemistry*, *291*(40), 20849–20857.
- Catalucci, D., Latronico, M., Ceci, M., Rusconi, F., Young, H. S., Gallo, P., Santonastasi, M., Bellacosa, A., Brown, J. H., & Condorelli, G. (2009). Akt increases sarcoplasmic reticulum Ca²⁺ cycling by direct phosphorylation of phospholamban at Thr17. *The Journal of biological chemistry*, *284*(41), 28180–28187.
- Ceholski, D. K., Trieber, C. A., Holmes, C. F., & Young, H. S. (2012). Lethal, hereditary mutants of phospholamban elude phosphorylation by protein kinase A. *The Journal of biological chemistry*, *287*(32), 26596–26605.
- Chandrasekera, P. C., Kargacin, M. E., Deans, J. P., & Lytton, J. (2009). Determination of apparent calcium affinity for endogenously expressed human sarco(endo)plasmic reticulum calcium-ATPase isoform SERCA3. *American journal of physiology. Cell physiology*, *296*(5), C1105–C1114.
- Chemaly, E. R., Troncone, L., & Lebeche, D. (2018). SERCA control of cell death and survival. *Cell calcium*, *69*, 46–61.
- Chen, Z., Akin, B. L., & Jones, L. R. (2007). Mechanism of reversal of phospholamban inhibition of the cardiac Ca²⁺-ATPase by protein kinase A and by anti-phospholamban monoclonal antibody 2D12. *The Journal of biological chemistry*, *282*(29), 20968–20976.
- Cheng, W., Altafaj, X., Ronjat, M., & Coronado, R. (2005). Interaction between the dihydropyridine receptor Ca²⁺ channel beta-subunit and ryanodine receptor type 1 strengthens excitation-contraction coupling. *Proceedings of the National Academy of Sciences of the United States of America*, *102*(52), 19225–19230.
- Cheung W. Y. (1970). Cyclic 3',5'-nucleotide phosphodiesterase. Demonstration of an activator. *Biochemical and biophysical research communications*, *38*(3), 533–538.
- Chorna, T., & Hasan, G. (2012). The genetics of calcium signaling in *Drosophila melanogaster*. *Biochimica et biophysica acta*, *1820*(8), 1269–1282.
- Chowański, S., Walkowiak-Nowicka, K., Winkiel, M., Marciniak, P., Urbański, A., & Pacholska-Bogalska, J. (2021). Insulin-Like Peptides and Cross-Talk With Other Factors in the Regulation of Insect Metabolism. *Frontiers in physiology*, *12*, 701203.

- Chu, G., Li, L., Sato, Y., Harrer, J. M., Kadambi, V. J., Hoit, B. D., Bers, D. M., & Kranias, E. G. (1998). Pentameric assembly of phospholamban facilitates inhibition of cardiac function in vivo. *The Journal of biological chemistry*, *273*(50), 33674–33680.
- Clancy, D. J., Gems, D., Harshman, L. G., Oldham, S., Stocker, H., Hafen, E., Leivers, S. J., & Partridge, L. (2001). Extension of life-span by loss of CHICO, a Drosophila insulin receptor substrate protein. *Science (New York, N.Y.)*, *292*(5514), 104–106.
- Clapham D. E. (2007). Calcium signaling. *Cell*, *131*(6), 1047–1058.
- Clark, K. A., McElhinny, A. S., Beckerle, M. C., & Gregorio, C. C. (2002). Striated muscle cytoarchitecture: an intricate web of form and function. *Annual review of cell and developmental biology*, *18*, 637–706.
- Clausen, J. D., & Andersen, J. P. (2010). Glutamate 90 at the luminal ion gate of sarcoplasmic reticulum Ca²⁺-ATPase is critical for Ca(2+) binding on both sides of the membrane. *The Journal of biological chemistry*, *285*(27), 20780–20792.
- Collet C. (2009). Excitation-contraction coupling in skeletal muscle fibers from adult domestic honeybee. *Pflugers Archiv : European journal of physiology*, *458*(3), 601–612.
- Colombani, J., Andersen, D. S., & Léopold, P. (2012). Secreted peptide Dilp8 coordinates Drosophila tissue growth with developmental timing. *Science (New York, N.Y.)*, *336*(6081), 582–585.
- Copley, R. R., Schultz, J., Ponting, C. P., & Bork, P. (1999). Protein families in multicellular organisms. *Current opinion in structural biology*, *9*(3), 408–415.
- Cornea, R. L., Jones, L. R., Autry, J. M., & Thomas, D. D. (1997). Mutation and phosphorylation change the oligomeric structure of phospholamban in lipid bilayers. *Biochemistry*, *36*(10), 2960–2967.
- Curtis, N. J., Ringo, J. M., & Dowse, H. B. (1999). Morphology of the pupal heart, adult heart, and associated tissues in the fruit fly, Drosophila melanogaster. *Journal of morphology*, *240*(3), 225–235.
- Dally, S., Bredoux, R., Corvazier, E., Andersen, J. P., Clausen, J. D., Dode, L., Fanchaouy, M., Gelebart, P., Monceau, V., Del Monte, F., Gwathmey, J. K., Hajjar, R., Chaabane, C., Bobe, R., Raies, A., & Enouf, J. (2006). Ca²⁺-ATPases in non-failing and failing heart: evidence for a novel cardiac sarco/endoplasmic reticulum Ca²⁺-ATPase 2 isoform (SERCA2c). *The Biochemical journal*, *395*(2), 249–258.
- Das, D., Aradhya, R., Ashoka, D., & Inamdar, M. (2008). Post-embryonic pericardial cells of Drosophila are required for overcoming toxic stress but not for cardiac function or adult development. *Cell and tissue research*, *331*(2), 565–570.
- de Meis, L., Arruda, A. P., & Carvalho, D. P. (2005). Role of sarco/endoplasmic reticulum Ca(2+)-ATPase in thermogenesis. *Bioscience reports*, *25*(3-4), 181–190.
- de Meis, L., Bianconi, M. L., & Suzano, V. A. (1997). Control of energy fluxes by the sarcoplasmic reticulum Ca²⁺-ATPase: ATP hydrolysis, ATP synthesis and heat production. *FEBS letters*, *406*(1-2), 201–204.

- de Meis, L., Martins, O. B., & Alves, E. W. (1980). Role of water, hydrogen ion, and temperature on the synthesis of adenosine triphosphate by the sarcoplasmic reticulum adenosine triphosphatase in the absence of a calcium ion gradient. *Biochemistry*, *19*(18), 4252–4261.
- de Mendonça, R. L., Beck, E., Rumjanek, F. D., & Goffeau, A. (1995). Cloning and characterization of a putative calcium-transporting ATPase gene from *Schistosoma mansoni*. *Molecular and biochemical parasitology*, *72*(1-2), 129–139.
- Dehnen, L., Janz, M., Verma, J. K., Psathaki, O. E., Langemeyer, L., Fröhlich, F., Heinisch, J. J., Meyer, H., Ungermann, C., & Paululat, A. (2020). A trimeric metazoan Rab7 GEF complex is crucial for endocytosis and scavenger function. *Journal of cell science*, *133*(13), jcs247080.
- Delanoue, R., Meschi, E., Agrawal, N., Mauri, A., Tsatskis, Y., McNeill, H., & Léopold, P. (2016). *Drosophila* insulin release is triggered by adipose Stunted ligand to brain Methuselah receptor. *Science (New York, N.Y.)*, *353*(6307), 1553–1556.
- des Georges, A., Clarke, O. B., Zalk, R., Yuan, Q., Condon, K. J., Grassucci, R. A., Hendrickson, W. A., Marks, A. R., & Frank, J. (2016). Structural Basis for Gating and Activation of RyR1. *Cell*, *167*(1), 145–157.e17.
- Desai-Shah, M., Papoy, A. R., Ward, M., & Cooper, R. L. (2010). Roles of the Sarcoplasmic/Endoplasmic reticulum Ca²⁺-ATPase, plasma membrane Ca²⁺-ATPase and Na⁺/Ca²⁺ exchanger in regulation of heart rate in larval *Drosophila*. *The Open Physiology Journal*, *3*(1).
- Devault, A., Nault, C., Zollinger, M., Fournie-Zaluski, M. C., Roques, B. P., Crine, P., & Boileau, G. (1988). Expression of neutral endopeptidase (enkephalinase) in heterologous COS-1 cells. Characterization of the recombinant enzyme and evidence for a glutamic acid residue at the active site. *The Journal of biological chemistry*, *263*(8), 4033–4040.
- Dhitavat, J., Fairclough, R. J., Hovnanian, A., & Burge, S. M. (2004). Calcium pumps and keratinocytes: lessons from Darier's disease and Hailey-Hailey disease. *The British journal of dermatology*, *150*(5), 821–828.
- Docherty, K. F., Vaduganathan, M., Solomon, S. D., & McMurray, J. (2020). Sacubitril/Valsartan: Nephilysin Inhibition 5 Years After PARADIGM-HF. *JACC. Heart failure*, *8*(10), 800–810.
- Dode, L., De Greef, C., Mountian, I., Attard, M., Town, M. M., Casteels, R., & Wuytack, F. (1998). Structure of the human sarco/endoplasmic reticulum Ca²⁺-ATPase 3 gene. Promoter analysis and alternative splicing of the SERCA3 pre-mRNA. *The Journal of biological chemistry*, *273*(22), 13982–13994.
- Dooley, C. T., Dore, T. M., Hanson, G. T., Jackson, W. C., Remington, S. J., & Tsien, R. Y. (2004). Imaging dynamic redox changes in mammalian cells with green fluorescent protein indicators. *The Journal of biological chemistry*, *279*(21), 22284–22293.
- Dowling, J. J., Lawlor, M. W., & Dirksen, R. T. (2014). Triadopathies: an emerging class of skeletal muscle diseases. *Neurotherapeutics : the journal of the American Society for Experimental NeuroTherapeutics*, *11*(4), 773–785.
- Downes, G. B., & Gautam, N. (1999). The G protein subunit gene families. *Genomics*, *62*(3), 544–552.

- Dowse, H., Ringo, J., Power, J., Johnson, E., Kinney, K., & White, L. (1995). A congenital heart defect in *Drosophila* caused by an action-potential mutation. *Journal of neurogenetics*, *10*(3), 153–168.
- Drake, M. T., Shenoy, S. K., & Lefkowitz, R. J. (2006). Trafficking of G protein-coupled receptors. *Circulation research*, *99*(6), 570–582.
- Drechsler, M., Schmidt, A. C., Meyer, H., & Paululat, A. (2013). The conserved ADAMTS-like protein lonely heart mediates matrix formation and cardiac tissue integrity. *PLoS genetics*, *9*(7), e1003616.
- Dulcis, D., & Levine, R. B. (2003). Innervation of the heart of the adult fruit fly, *Drosophila melanogaster*. *The Journal of comparative neurology*, *465*(4), 560–578.
- Dulcis, D., & Levine, R. B. (2005). Glutamatergic innervation of the heart initiates retrograde contractions in adult *Drosophila melanogaster*. *The Journal of neuroscience : the official journal of the Society for Neuroscience*, *25*(2), 271–280.
- Dulhunty, A. F., Wei-LaPierre, L., Casarotto, M. G., & Beard, N. A. (2017). Core skeletal muscle ryanodine receptor calcium release complex. *Clinical and experimental pharmacology & physiology*, *44*(1), 3–12.
- Dunham, E. T., & Glynn, I. M. (1961). Adenosinetriphosphatase activity and the active movements of alkali metal ions. *The Journal of physiology*, *156*(2), 274–293.
- Dux, L., & Martonosi, A. (1983). Two-dimensional arrays of proteins in sarcoplasmic reticulum and purified Ca²⁺-ATPase vesicles treated with vanadate. *The Journal of biological chemistry*, *258*(4), 2599–2603.
- Dyla, M., Kjærgaard, M., Poulsen, H., & Nissen, P. (2020). Structure and Mechanism of P-Type ATPase Ion Pumps. *Annual review of biochemistry*, *89*, 583–603.
- Dyla, M., Terry, D. S., Kjaergaard, M., Sørensen, T. L., Lauwring Andersen, J., Andersen, J. P., Rohde Knudsen, C., Altman, R. B., Nissen, P., & Blanchard, S. C. (2017). Dynamics of P-type ATPase transport revealed by single-molecule FRET. *Nature*, *551*(7680), 346–351.
- Ebashi S. (1961). Calcium binding activity of vesicular relaxing factor. *Journal de chirurgie*, *82*, 236–244.
- Ebashi, S., & Lipmann, F. (1962). Adenosine triphosphate-linked concentration of calcium ions in a particulate fraction of rabbit muscle. *The Journal of cell biology*, *14*(3), 389–400.
- Edwards, J. N., Cully, T. R., Shannon, T. R., Stephenson, D. G., & Launikonis, B. S. (2012). Longitudinal and transversal propagation of excitation along the tubular system of rat fast-twitch muscle fibres studied by high speed confocal microscopy. *The Journal of physiology*, *590*(3), 475–492.
- Ehler, E., & Gautel, M. (2008). The sarcomere and sarcomerogenesis. *Advances in experimental medicine and biology*, *642*, 1–14.
- Eisner, D. A., Caldwell, J. L., Kistamás, K., & Trafford, A. W. (2017). Calcium and Excitation-Contraction Coupling in the Heart. *Circulation research*, *121*(2), 181–195.
- Endo M. (2009). Calcium-induced calcium release in skeletal muscle. *Physiological reviews*, *89*(4), 1153–1176.

- Endo, M., Tanaka, M., & Ogawa, Y. (1970). Calcium induced release of calcium from the sarcoplasmic reticulum of skinned skeletal muscle fibres. *Nature*, *228*(5266), 34–36.
- Erdős, E. G., & Skidgel, R. A. (1989). Neutral endopeptidase 24.11 (enkephalinase) and related regulators of peptide hormones. *FASEB journal : official publication of the Federation of American Societies for Experimental Biology*, *3*(2), 145–151.
- Escalante, R., & Sastre, L. (1993). Similar alternative splicing events generate two sarcoplasmic or endoplasmic reticulum Ca-ATPase isoforms in the crustacean *Artemia franciscana* and in vertebrates. *The Journal of biological chemistry*, *268*(19), 14090–14095.
- Escalante, R., & Sastre, L. (1994). Structure of *Artemia franciscana* sarco/endoplasmic reticulum Ca-ATPase gene. *The Journal of biological chemistry*, *269*(17), 13005–13012.
- Espinoza-Fonseca, L. M., Autry, J. M., & Thomas, D. D. (2015). Sarcolipin and phospholamban inhibit the calcium pump by populating a similar metal ion-free intermediate state. *Biochemical and biophysical research communications*, *463*(1-2), 37–41.
- Esser, N., & Zraika, S. (2019). Nephilysin inhibition: a new therapeutic option for type 2 diabetes?. *Diabetologia*, *62*(7), 1113–1122.
- Fabiato, A., & Fabiato, F. (1972). Excitation-contraction coupling of isolated cardiac fibers with disrupted or closed sarcolemmas. Calcium-dependent cyclic and tonic contractions. *Circulation research*, *31*(3), 293–307.
- Fabiato, A., & Fabiato, F. (1978). Calcium-induced release of calcium from the sarcoplasmic reticulum of skinned cells from adult human, dog, cat, rabbit, rat, and frog hearts and from fetal and new-born rat ventricles. *Annals of the New York Academy of Sciences*, *307*, 491–522.
- Fajardo, V. A., Bombardier, E., Vigna, C., Devji, T., Bloemberg, D., Gamu, D., Gramolini, A. O., Quadrilatero, J., & Tupling, A. R. (2013). Co-expression of SERCA isoforms, phospholamban and sarcolipin in human skeletal muscle fibers. *PloS one*, *8*(12), e84304.
- Feng, R., Zhou, X., Zhang, W., Pu, T., Sun, Y., Yang, R., Wang, D., Zhang, X., Gao, Y., Cai, Z., Liang, Y., Yu, Q., Wu, Y., Lei, X., Liang, Z., Jones, O., Wang, L., Xu, M., Sun, Y., Isaacs, W. B., ... Xu, X. (2019). Dynamics expression of *DmFKBP12/Calstabin* during embryonic early development of *Drosophila melanogaster*. *Cell & bioscience*, *9*, 8.
- Fernandez, R., Tabarini, D., Azpiazu, N., Frasch, M., & Schlessinger, J. (1995). The *Drosophila* insulin receptor homolog: a gene essential for embryonic development encodes two receptor isoforms with different signaling potential. *The EMBO journal*, *14*(14), 3373–3384.
- Fernández-de Gortari, E., & Espinoza-Fonseca, L. M. (2018). Structural basis for relief of phospholamban-mediated inhibition of the sarcoplasmic reticulum Ca²⁺-ATPase at saturating Ca²⁺ conditions. *The Journal of biological chemistry*, *293*(32), 12405–12414.
- Fink, M., Callol-Massot, C., Chu, A., Ruiz-Lozano, P., Izpisua Belmonte, J. C., Giles, W., Bodmer, R., & Ocorr, K. (2009). A new method for detection and quantification of heartbeat parameters in *Drosophila*, zebrafish, and embryonic mouse hearts. *BioTechniques*, *46*(2), 101–113.
- Fisher, M. E., Bovo, E., Aguayo-Ortiz, R., Cho, E. E., Pribadi, M. P., Dalton, M. P., Rathod, N., Lemieux, M. J., Espinoza-Fonseca, L. M., Robia, S. L., Zima, A. V., & Young, H. S. (2021).

- Dwarf open reading frame (DWORF) is a direct activator of the sarcoplasmic reticulum calcium pump SERCA. *eLife*, *10*, e65545.
- Fleischer, S., Ogunbunmi, E. M., Dixon, M. C., & Fleer, E. A. (1985). Localization of Ca²⁺ release channels with ryanodine in junctional terminal cisternae of sarcoplasmic reticulum of fast skeletal muscle. *Proceedings of the National Academy of Sciences of the United States of America*, *82*(21), 7256–7259.
- Foggia, L., & Hovnanian, A. (2004). Calcium pump disorders of the skin. *American journal of medical genetics. Part C, Seminars in medical genetics*, *131C*(1), 20–31.
- Ford, L. E., & Podolsky, R. J. (1970). Regenerative calcium release within muscle cells. *Science (New York, N.Y.)*, *167*(3914), 58–59.
- Franzini-Armstrong, C., & Porter, K. R. (1964). Sarcolemmal invaginations constituting the T system in fish muscle fibers. *The Journal of cell biology*, *22*(3), 675–696.
- Franzini-Armstrong, C., Protasi, F., & Ramesh, V. (1999). Shape, size, and distribution of Ca(2+) release units and couplons in skeletal and cardiac muscles. *Biophysical journal*, *77*(3), 1528–1539.
- Fruen, B. R., Bardy, J. M., Byrem, T. M., Strasburg, G. M., & Louis, C. F. (2000). Differential Ca(2+) sensitivity of skeletal and cardiac muscle ryanodine receptors in the presence of calmodulin. *American journal of physiology. Cell physiology*, *279*(3), C724–C733.
- Gabella G. (1984). Structural apparatus for force transmission in smooth muscles. *Physiological reviews*, *64*(2), 455–477.
- Gafford, J. T., Skidgel, R. A., Erdös, E. G., & Hersh, L. B. (1983). Human kidney "enkephalinase", a neutral metalloendopeptidase that cleaves active peptides. *Biochemistry*, *22*(13), 3265–3271.
- Gáliková, M., Diesner, M., Klepsatel, P., Hehlert, P., Xu, Y., Bickmeyer, I., Predel, R., & Kühnlein, R. P. (2015). Energy Homeostasis Control in Drosophila Adipokinetic Hormone Mutants. *Genetics*, *201*(2), 665–683.
- Gamu, D., Bombardier, E., Smith, I. C., Fajardo, V. A., & Tupling, A. R. (2014). Sarcolipin provides a novel muscle-based mechanism for adaptive thermogenesis. *Exercise and sport sciences reviews*, *42*(3), 136–142.
- Garelli, A., Gontijo, A. M., Miguela, V., Caparros, E., & Dominguez, M. (2012). Imaginal discs secrete insulin-like peptide 8 to mediate plasticity of growth and maturation. *Science (New York, N.Y.)*, *336*(6081), 579–582.
- Geeves M. A. (1991). The dynamics of actin and myosin association and the crossbridge model of muscle contraction. *The Biochemical journal*, *274* (Pt 1)(Pt 1), 1–14.
- Gélébart, P., Martin, V., Enouf, J., & Papp, B. (2003). Identification of a new SERCA2 splice variant regulated during monocytic differentiation. *Biochemical and biophysical research communications*, *303*(2), 676–684.
- George, C. H., Jundi, H., Thomas, N. L., Fry, D. L., & Lai, F. A. (2007). Ryanodine receptors and ventricular arrhythmias: emerging trends in mutations, mechanisms and therapies. *Journal of molecular and cellular cardiology*, *42*(1), 34–50.

- George, S. G., & Kenny, J. (1973). Studies on the enzymology of purified preparations of brush border from rabbit kidney. *The Biochemical journal*, *134*(1), 43–57.
- Geske, J. B., Ommen, S. R., & Gersh, B. J. (2018). Hypertrophic Cardiomyopathy: Clinical Update. *JACC. Heart failure*, *6*(5), 364–375.
- Geurts, M., Clausen, J. D., Arnou, B., Montigny, C., Lenoir, G., Corey, R. A., Jaxel, C., Møller, J. V., Nissen, P., Andersen, J. P., le Maire, M., & Bublitz, M. (2020). The SERCA residue Glu340 mediates interdomain communication that guides Ca²⁺ transport. *Proceedings of the National Academy of Sciences of the United States of America*, *117*(49), 31114–31122.
- Glaves, J. P., Primeau, J. O., Espinoza-Fonseca, L. M., Lemieux, M. J., & Young, H. S. (2019). The Phospholamban Pentamer Alters Function of the Sarcoplasmic Reticulum Calcium Pump SERCA. *Biophysical journal*, *116*(4), 633–647. <https://doi.org/10.1016/j.bpj.2019.01.013>
- Glaves, J. P., Primeau, J. O., Gorski, P. A., Espinoza-Fonseca, L. M., Lemieux, M. J., & Young, H. S. (2020). Interaction of a Sarcolipin Pentamer and Monomer with the Sarcoplasmic Reticulum Calcium Pump, SERCA. *Biophysical journal*, *118*(2), 518–531.
- Glaves, J. P., Trieber, C. A., Ceholski, D. K., Stokes, D. L., & Young, H. S. (2011). Phosphorylation and mutation of phospholamban alter physical interactions with the sarcoplasmic reticulum calcium pump. *Journal of molecular biology*, *405*(3), 707–723.
- Goldstein, M. A., & Burdette, W. J. (1971). Striated visceral muscle of drosophila melanogaster. *Journal of morphology*, *134*(3), 315–334.
- Gong, D., Chi, X., Wei, J., Zhou, G., Huang, G., Zhang, L., Wang, R., Lei, J., Chen, S., & Yan, N. (2019). Modulation of cardiac ryanodine receptor 2 by calmodulin. *Nature*, *572*(7769), 347–351.
- Goody R. S. (2003). The missing link in the muscle cross-bridge cycle. *Nature structural biology*, *10*(10), 773–775.
- Gopinath, T., Weber, D., Wang, S., Larsen, E., & Veglia, G. (2021). Solid-State NMR of Membrane Proteins in Lipid Bilayers: To Spin or Not To Spin?. *Accounts of chemical research*, *54*(6), 1430–1439.
- Gorski, P. A., Ceholski, D. K., & Hajjar, R. J. (2015a). Altered myocardial calcium cycling and energetics in heart failure--a rational approach for disease treatment. *Cell metabolism*, *21*(2), 183–194.
- Gorski, P. A., Glaves, J. P., Vangheluwe, P., & Young, H. S. (2013). Sarco(endo)plasmic reticulum calcium ATPase (SERCA) inhibition by sarcolipin is encoded in its luminal tail. *The Journal of biological chemistry*, *288*(12), 8456–8467.
- Gorski, P. A., Trieber, C. A., Ashrafi, G., & Young, H. S. (2015b). Regulation of the sarcoplasmic reticulum calcium pump by divergent phospholamban isoforms in zebrafish. *The Journal of biological chemistry*, *290*(11), 6777–6788.
- Gorski, P. A., Trieber, C. A., Larivière, E., Schuermans, M., Wuytack, F., Young, H. S., & Vangheluwe, P. (2012). Transmembrane helix 11 is a genuine regulator of the endoplasmic reticulum Ca²⁺ pump and acts as a functional parallel of β -subunit on α -Na⁺,K⁺-ATPase. *The Journal of biological chemistry*, *287*(24), 19876–19885.

- Gramolini, A. O., Kislinger, T., Asahi, M., Li, W., Emili, A., & MacLennan, D. H. (2004). Sarcolipin retention in the endoplasmic reticulum depends on its C-terminal RSYQY sequence and its interaction with sarco(endo)plasmic Ca²⁺-ATPases. *Proceedings of the National Academy of Sciences of the United States of America*, *101*(48), 16807–16812.
- Gramolini, A. O., Trivieri, M. G., Oudit, G. Y., Kislinger, T., Li, W., Patel, M. M., Emili, A., Kranias, E. G., Backx, P. H., & MacLennan, D. H. (2006). Cardiac-specific overexpression of sarcolipin in phospholamban null mice impairs myocyte function that is restored by phosphorylation. *Proceedings of the National Academy of Sciences of the United States of America*, *103*(7), 2446–2451.
- Green, H. J., Ballantyne, C. S., MacDougall, J. D., Tarnopolsky, M. A., & Schertzer, J. D. (2003). Adaptations in human muscle sarcoplasmic reticulum to prolonged submaximal training. *Journal of applied physiology (Bethesda, Md. : 1985)*, *94*(5), 2034–2042.
- Grewal S. S. (2009). Insulin/TOR signaling in growth and homeostasis: a view from the fly world. *The international journal of biochemistry & cell biology*, *41*(5), 1006–1010.
- Grönke, S., Clarke, D. F., Broughton, S., Andrews, T. D., & Partridge, L. (2010). Molecular evolution and functional characterization of *Drosophila* insulin-like peptides. *PLoS genetics*, *6*(2), e1000857.
- Grote Beverborg, N., Später, D., Knöll, R., Hidalgo, A., Yeh, S. T., Elbeck, Z., Silljé, H., Eijgenraam, T. R., Siga, H., Zurek, M., Palmér, M., Pehrsson, S., Albery, T., Bomer, N., Hoes, M. F., Boogerd, C. J., Frisk, M., van Rooij, E., Damle, S., Louch, W. E., ... van der Meer, P. (2021). Phospholamban antisense oligonucleotides improve cardiac function in murine cardiomyopathy. *Nature communications*, *12*(1), 5180.
- Gunteski-Hamblin, A. M., Greeb, J., & Shull, G. E. (1988). A novel Ca²⁺ pump expressed in brain, kidney, and stomach is encoded by an alternative transcript of the slow-twitch muscle sarcoplasmic reticulum Ca-ATPase gene. Identification of cDNAs encoding Ca²⁺ and other cation-transporting ATPases using an oligonucleotide probe derived from the ATP-binding site. *The Journal of biological chemistry*, *263*(29), 15032–15040.
- Guo, J., Bian, Y., Bai, R., Li, H., Fu, M., & Xiao, C. (2013). Globular adiponectin attenuates myocardial ischemia/reperfusion injury by upregulating endoplasmic reticulum Ca²⁺-ATPase activity and inhibiting endoplasmic reticulum stress. *Journal of cardiovascular pharmacology*, *62*(2), 143–153.
- Gurha, P., Abreu-Goodger, C., Wang, T., Ramirez, M. O., Drumond, A. L., van Dongen, S., Chen, Y., Bartonicek, N., Enright, A. J., Lee, B., Kelm, R. J., Jr, Reddy, A. K., Taffet, G. E., Bradley, A., Wehrens, X. H., Entman, M. L., & Rodriguez, A. (2012). Targeted deletion of microRNA-22 promotes stress-induced cardiac dilation and contractile dysfunction. *Circulation*, *125*(22), 2751–2761.
- Gustavsson, M., Verardi, R., Mullen, D. G., Mote, K. R., Traaseth, N. J., Gopinath, T., & Veglia, G. (2013). Allosteric regulation of SERCA by phosphorylation-mediated conformational shift of phospholamban. *Proceedings of the National Academy of Sciences of the United States of America*, *110*(43), 17338–17343.
- Györke, S., Stevens, S. C., & Terentyev, D. (2009). Cardiac calsequestrin: quest inside the SR. *The Journal of physiology*, *587*(Pt 13), 3091–3094.

- Haghighi, K., Kolokathis, F., Gramolini, A. O., Waggoner, J. R., Pater, L., Lynch, R. A., Fan, G. C., Tsiapras, D., Parekh, R. R., Dorn, G. W., 2nd, MacLennan, D. H., Kremastinos, D. T., & Kranias, E. G. (2006). A mutation in the human phospholamban gene, deleting arginine 14, results in lethal, hereditary cardiomyopathy. *Proceedings of the National Academy of Sciences of the United States of America*, *103*(5), 1388–1393.
- Haghighi, K., Kolokathis, F., Pater, L., Lynch, R. A., Asahi, M., Gramolini, A. O., Fan, G. C., Tsiapras, D., Hahn, H. S., Adamopoulos, S., Liggett, S. B., Dorn, G. W., 2nd, MacLennan, D. H., Kremastinos, D. T., & Kranias, E. G. (2003). Human phospholamban null results in lethal dilated cardiomyopathy revealing a critical difference between mouse and human. *The Journal of clinical investigation*, *111*(6), 869–876.
- Hallier, B., Schiemann, R., Cordes, E., Vitos-Faleato, J., Walter, S., Heinisch, J. J., Malmendal, A., Paululat, A., & Meyer, H. (2016). *Drosophila* neprilysins control insulin signaling and food intake via cleavage of regulatory peptides. *eLife*, *5*, e19430.
- Hanlon, C. D., & Andrew, D. J. (2015). Outside-in signaling--a brief review of GPCR signaling with a focus on the *Drosophila* GPCR family. *Journal of cell science*, *128*(19), 3533–3542.
- Hanson J. (1957). The structure of the smooth muscle fibres in the body wall of the earth worm. *The Journal of biophysical and biochemical cytology*, *3*(1), 111–122.
- Hanson, J., & Huxley, H. E. (1953). Structural basis of the cross-striations in muscle. *Nature*, *172*(4377), 530–532.
- Hanyaloglu, A. C., & von Zastrow, M. (2008). Regulation of GPCRs by endocytic membrane trafficking and its potential implications. *Annual review of pharmacology and toxicology*, *48*, 537–568.
- Harris, K. P., & Littleton, J. T. (2015). Transmission, Development, and Plasticity of Synapses. *Genetics*, *201*(2), 345–375.
- Hartford, C., & Lal, A. (2020). When Long Noncoding Becomes Protein Coding. *Molecular and cellular biology*, *40*(6), e00528-19.
- Hartong, R., Wang, N., Kurokawa, R., Lazar, M. A., Glass, C. K., Apriletti, J. W., & Dillmann, W. H. (1994). Delineation of three different thyroid hormone-response elements in promoter of rat sarcoplasmic reticulum Ca²⁺-ATPase gene. Demonstration that retinoid X receptor binds 5' to thyroid hormone receptor in response element 1. *The Journal of biological chemistry*, *269*(17), 13021–13029.
- Hasenfuss, G., & Pieske, B. (2002). Calcium cycling in congestive heart failure. *Journal of molecular and cellular cardiology*, *34*(8), 951–969.
- Hasselbach, W., & Makinose, M. (1961). The calcium pump of the "relaxing granules" of muscle and its dependence on ATP-splitting. *Biochemische Zeitschrift*, *333*, 518-528.
- Hasselbach, W., & Makinose, M. (1963). On the mechanism of calcium transport across the membrane of the sarcoplasmic reticulum. *Biochemische Zeitschrift*, *339*, 94-111.
- He Xl, Chow Dc, Martick, M. M., & Garcia, K. C. (2001). Allosteric activation of a spring-loaded natriuretic peptide receptor dimer by hormone. *Science (New York, N.Y.)*, *293*(5535), 1657–1662.

- He, W., Huang, D., Guo, S., Wang, D., Guo, J., Cala, S. E., & Chen, Z. (2020). Association with SERCA2a directs phospholamban trafficking to sarcoplasmic reticulum from a nuclear envelope pool. *Journal of molecular and cellular cardiology*, *143*, 107–119.
- Hellstern, S., Pegoraro, S., Karim, C. B., Lustig, A., Thomas, D. D., Moroder, L., & Engel, J. (2001). Sarcoplipin, the shorter homologue of phospholamban, forms oligomeric structures in detergent micelles and in liposomes. *The Journal of biological chemistry*, *276*(33), 30845–30852.
- Helmstädter, M., & Simons, M. (2017). Using *Drosophila* nephrocytes in genetic kidney disease. *Cell and tissue research*, *369*(1), 119–126.
- Hentze, J. L., Carlsson, M. A., Kondo, S., Nässel, D. R., & Rewitz, K. F. (2015). The Neuropeptide Allatostatin A Regulates Metabolism and Feeding Decisions in *Drosophila*. *Scientific reports*, *5*, 11680.
- Hergarden, A. C., Tayler, T. D., & Anderson, D. J. (2012). Allatostatin-A neurons inhibit feeding behavior in adult *Drosophila*. *Proceedings of the National Academy of Sciences of the United States of America*, *109*(10), 3967–3972.
- Hernández-Ochoa, E. O., Pratt, S., Lovering, R. M., & Schneider, M. F. (2016). Critical Role of Intracellular RyR1 Calcium Release Channels in Skeletal Muscle Function and Disease. *Frontiers in physiology*, *6*, 420.
- Hersh, L. B., & Morihara, K. (1986). Comparison of the subsite specificity of the mammalian neutral endopeptidase 24.11 (enkephalinase) to the bacterial neutral endopeptidase thermolysin. *The Journal of biological chemistry*, *261*(14), 6433–6437.
- Hilgemann D. W. (2020). Control of cardiac contraction by sodium: Promises, reckonings, and new beginnings. *Cell calcium*, *85*, 102129.
- Hilger, D., Masureel, M., & Kobilka, B. K. (2018). Structure and dynamics of GPCR signaling complexes. *Nature structural & molecular biology*, *25*(1), 4–12.
- Hofmann, S. L., Topham, M., Hsieh, C. L., & Francke, U. (1991). cDNA and genomic cloning of HRC, a human sarcoplasmic reticulum protein, and localization of the gene to human chromosome 19 and mouse chromosome 7. *Genomics*, *9*(4), 656–669.
- Hovnanian A. (2007). SERCA pumps and human diseases. *Sub-cellular biochemistry*, *45*, 337–363.
- Hoyle G. (1969). Comparative aspects of muscle. *Annual review of physiology*, *31*, 43–84.
- Hsu, I. U., Linsley, J. W., Reid, L. E., Hume, R. I., Leflein, A., & Kuwada, J. Y. (2020). Dstac Regulates Excitation-Contraction Coupling in *Drosophila* Body Wall Muscles. *Frontiers in physiology*, *11*, 573723.
- Huang, B., Wang, S., Qin, D., Boutjdir, M., & El-Sherif, N. (1999). Diminished basal phosphorylation level of phospholamban in the postinfarction remodeled rat ventricle: role of beta-adrenergic pathway, G(i) protein, phosphodiesterase, and phosphatases. *Circulation research*, *85*(9), 848–855.
- Hughes, E., Clayton, J. C., Kitmitto, A., Esmann, M., & Middleton, D. A. (2007). Solid-state NMR and functional measurements indicate that the conserved tyrosine residues of sarcoplipin are

- involved directly in the inhibition of SERCA1. *The Journal of biological chemistry*, 282(36), 26603–26613.
- Huxley H. E. (1969). The mechanism of muscular contraction. *Science (New York, N.Y.)*, 164(3886), 1356–1365.
- Huxley, A. F., & Niedergerke, R. (1954). Structural changes in muscle during contraction; interference microscopy of living muscle fibres. *Nature*, 173(4412), 971–973.
- Huxley, H., & Hanson, J. (1954). Changes in the cross-striations of muscle during contraction and stretch and their structural interpretation. *Nature*, 173(4412), 973–976.
- Hwang, J. H., Zorzato, F., Clarke, N. F., & Treves, S. (2012). Mapping domains and mutations on the skeletal muscle ryanodine receptor channel. *Trends in molecular medicine*, 18(11), 644–657.
- Hynes, T. R., Block, S. M., White, B. T., & Spudich, J. A. (1987). Movement of myosin fragments in vitro: domains involved in force production. *Cell*, 48(6), 953–963.
- Hyun, J., & Hashimoto, C. (2011). Physiological effects of manipulating the level of insulin-degrading enzyme in insulin-producing cells of *Drosophila*. *Fly*, 5(1), 53–57.
- Ikemoto, N., Bhatnagar, G. M., Nagy, B., & Gergely, J. (1972). Interaction of divalent cations with the 55,000-dalton protein component of the sarcoplasmic reticulum. Studies of fluorescence and circular dichroism. *The Journal of biological chemistry*, 247(23), 7835–7837.
- Ikeya, T., Galic, M., Belawat, P., Nairz, K., & Hafen, E. (2002). Nutrient-dependent expression of insulin-like peptides from neuroendocrine cells in the CNS contributes to growth regulation in *Drosophila*. *Current biology : CB*, 12(15), 1293–1300.
- Ikura, M., & Ames, J. B. (2006). Genetic polymorphism and protein conformational plasticity in the calmodulin superfamily: two ways to promote multifunctionality. *Proceedings of the National Academy of Sciences of the United States of America*, 103(5), 1159–1164.
- Inesi, G., & Tadini-Buoninsegni, F. (2014). Ca(2+)/H (+) exchange, lumenal Ca(2+) release and Ca (2+)/ATP coupling ratios in the sarcoplasmic reticulum ATPase. *Journal of cell communication and signaling*, 8(1), 5–11.
- Inesi, G., Ma, H., Lewis, D., & Xu, C. (2004). Ca²⁺ occlusion and gating function of Glu309 in the ADP-fluoroaluminate analog of the Ca²⁺-ATPase phosphoenzyme intermediate. *The Journal of biological chemistry*, 279(30), 31629–31637.
- Inoue, M., Sakuta, N., Watanabe, S., Zhang, Y., Yoshikaie, K., Tanaka, Y., Ushioda, R., Kato, Y., Takagi, J., Tsukazaki, T., Nagata, K., & Inaba, K. (2019). Structural Basis of Sarco/Endoplasmic Reticulum Ca²⁺-ATPase 2b Regulation via Transmembrane Helix Interplay. *Cell reports*, 27(4), 1221–1230.e3.
- Inui, M., Saito, A., & Fleischer, S. (1987). Isolation of the ryanodine receptor from cardiac sarcoplasmic reticulum and identity with the feet structures. *The Journal of biological chemistry*, 262(32), 15637–15642.
- Irving M. (2017). Regulation of Contraction by the Thick Filaments in Skeletal Muscle. *Biophysical journal*, 113(12), 2579–2594.

- Itskov, P. M., & Ribeiro, C. (2013). The dilemmas of the gourmet fly: the molecular and neuronal mechanisms of feeding and nutrient decision making in *Drosophila*. *Frontiers in neuroscience*, *7*, 12.
- Ivy, J. R., Drechsler, M., Catterson, J. H., Bodmer, R., Ocorr, K., Paululat, A., & Hartley, P. S. (2015). *Klf15* Is Critical for the Development and Differentiation of *Drosophila* Nephrocytes. *PLoS one*, *10*(8), e0134620.
- James, P., Inui, M., Tada, M., Chiesi, M., & Carafoli, E. (1989). Nature and site of phospholamban regulation of the Ca²⁺ pump of sarcoplasmic reticulum. *Nature*, *342*(6245), 90–92.
- Jan, L. Y., & Jan, Y. N. (1976a). L-glutamate as an excitatory transmitter at the *Drosophila* larval neuromuscular junction. *The Journal of physiology*, *262*(1), 215–236.
- Jan, L. Y., & Jan, Y. N. (1976b). Properties of the larval neuromuscular junction in *Drosophila melanogaster*. *The Journal of physiology*, *262*(1), 189–214.
- Jensen, A. M., Sørensen, T. L., Olesen, C., Møller, J. V., & Nissen, P. (2006). Modulatory and catalytic modes of ATP binding by the calcium pump. *The EMBO journal*, *25*(11), 2305–2314.
- Jiao, Q., Takeshima, H., Ishikawa, Y., & Minamisawa, S. (2012). Sarcalumenin plays a critical role in age-related cardiac dysfunction due to decreases in SERCA2a expression and activity. *Cell calcium*, *51*(1), 31–39.
- Johnson, E. C., Shafer, O. T., Trigg, J. S., Park, J., Schooley, D. A., Dow, J. A., & Taghert, P. H. (2005). A novel diuretic hormone receptor in *Drosophila*: evidence for conservation of CGRP signaling. *The Journal of experimental biology*, *208*(Pt 7), 1239–1246.
- Johnson, E., Ringo, J., & Dowse, H. (1997). Modulation of *Drosophila* heartbeat by neurotransmitters. *Journal of comparative physiology. B, Biochemical, systemic, and environmental physiology*, *167*(2), 89–97.
- Johnson, E., Ringo, J., & Dowse, H. (2000). Native and heterologous neuropeptides are cardioactive in *Drosophila melanogaster*. *Journal of insect physiology*, *46*(8), 1229–1236.
- Johnson, E., Ringo, J., Bray, N., & Dowse, H. (1998). Genetic and pharmacological identification of ion channels central to the *Drosophila* cardiac pacemaker. *Journal of neurogenetics*, *12*(1), 1–24.
- Johnson, E., Sherry, T., Ringo, J., & Dowse, H. (2002). Modulation of the cardiac pacemaker of *Drosophila*: cellular mechanisms. *Journal of comparative physiology. B, Biochemical, systemic, and environmental physiology*, *172*(3), 227–236.
- Jones, L. R., Simmerman, H. K., Wilson, W. W., Gurd, F. R., & Wegener, A. D. (1985). Purification and characterization of phospholamban from canine cardiac sarcoplasmic reticulum. *The Journal of biological chemistry*, *260*(12), 7721–7730.
- Jorgensen P. L. (1975). Purification and characterization of (Na⁺, K⁺)-ATPase. V. Conformational changes in the enzyme Transitions between the Na-form and the K-form studied with tryptic digestion as a tool. *Biochimica et biophysica acta*, *401*(3), 399–415.
- Jorgensen, W. K., & Rice, M. J. (1983). Superextension and supercontraction in locust ovipositor muscles. *Journal of Insect Physiology*, *29*(5), 437–448.

- Jungbluth, H., Treves, S., Zorzato, F., Sarkozy, A., Ochala, J., Sewry, C., Phadke, R., Gautel, M., & Muntoni, F. (2018). Congenital myopathies: disorders of excitation-contraction coupling and muscle contraction. *Nature reviews. Neurology*, *14*(3), 151–167.
- Kahn, A. J., & Sandow, A. (1950). The potentiation of muscular contraction by the nitrate-ion. *Science (New York, N.Y.)*, *112*(2918), 647–649.
- Kakiuchi, S., & Yamazaki, R. (1970). Calcium dependent phosphodiesterase activity and its activating factor (PAF) from brain studies on cyclic 3',5'-nucleotide phosphodiesterase (3). *Biochemical and biophysical research communications*, *41*(5), 1104–1110.
- Kamp, T. J., & Hell, J. W. (2000). Regulation of cardiac L-type calcium channels by protein kinase A and protein kinase C. *Circulation research*, *87*(12), 1095–1102.
- Kapan, N., Lushchak, O. V., Luo, J., & Nässel, D. R. (2012). Identified peptidergic neurons in the Drosophila brain regulate insulin-producing cells, stress responses and metabolism by coexpressed short neuropeptide F and corazonin. *Cellular and molecular life sciences: CMLS*, *69*(23), 4051–4066.
- Karim, C. B., Zhang, Z., Howard, E. C., Torgersen, K. D., & Thomas, D. D. (2006). Phosphorylation-dependent conformational switch in spin-labeled phospholamban bound to SERCA. *Journal of molecular biology*, *358*(4), 1032–1040.
- Karlsen, J. L., & Bublitz, M. (2016). How to Compare, Analyze, and Morph Between Crystal Structures of Different Conformations: The P-Type ATPase Example. *Methods in molecular biology (Clifton, N.J.)*, *1377*, 523–539.
- Karpati, G., Charuk, J., Carpenter, S., Jablecki, C., & Holland, P. (1986). Myopathy caused by a deficiency of Ca²⁺-adenosine triphosphatase in sarcoplasmic reticulum (Brody's disease). *Annals of neurology*, *20*(1), 38–49.
- Katz A. M. (1998). Discovery of phospholamban. A personal history. *Annals of the New York Academy of Sciences*, *853*, 9–19.
- Kawamoto, R. M., Brunschwig, J. P., Kim, K. C., & Caswell, A. H. (1986). Isolation, characterization, and localization of the spanning protein from skeletal muscle triads. *The Journal of cell biology*, *103*(4), 1405–1414.
- Kerr, M. A., & Kenny, A. J. (1974a). The purification and specificity of a neutral endopeptidase from rabbit kidney brush border. *The Biochemical journal*, *137*(3), 477–488.
- Kerr, M. A., & Kenny, A. J. (1974b). The molecular weight and properties of a neutral metallo-endopeptidase from rabbit kidney brush border. *The Biochemical journal*, *137*(3), 489–495.
- Khananshvili D. (2014). Sodium-calcium exchangers (NCX): molecular hallmarks underlying the tissue-specific and systemic functions. *Pflugers Archiv: European journal of physiology*, *466*(1), 43–60.
- Kho, C., Lee, A., Jeong, D., Oh, J. G., Chaanine, A. H., Kizana, E., Park, W. J., & Hajjar, R. J. (2011). SUMO1-dependent modulation of SERCA2a in heart failure. *Nature*, *477*(7366), 601–605.
- Kim, J., & Neufeld, T. P. (2015). Dietary sugar promotes systemic TOR activation in Drosophila through AKH-dependent selective secretion of Dilp3. *Nature communications*, *6*, 6846.

- Kim, S. K., & Rulifson, E. J. (2004). Conserved mechanisms of glucose sensing and regulation by *Drosophila corpora cardiaca* cells. *Nature*, *431*(7006), 316–320.
- Kimura, T., Nakamori, M., Lueck, J. D., Pouliquin, P., Aoike, F., Fujimura, H., Dirksen, R. T., Takahashi, M. P., Dulhunty, A. F., & Sakoda, S. (2005). Altered mRNA splicing of the skeletal muscle ryanodine receptor and sarcoplasmic/endoplasmic reticulum Ca²⁺-ATPase in myotonic dystrophy type 1. *Human molecular genetics*, *14*(15), 2189–2200.
- Kimura, Y., Kurzydowski, K., Tada, M., & MacLennan, D. H. (1997). Phospholamban inhibitory function is activated by depolymerization. *The Journal of biological chemistry*, *272*(24), 15061–15064.
- Kimura, Y., Otsu, K., Nishida, K., Kuzuya, T., & Tada, M. (1994). Thyroid hormone enhances Ca²⁺ pumping activity of the cardiac sarcoplasmic reticulum by increasing Ca²⁺ ATPase and decreasing phospholamban expression. *Journal of molecular and cellular cardiology*, *26*(9), 1145–1154.
- Kirchberger, M. A., Tada, M., & Katz, A. M. (1975). Phospholamban: a regulatory protein of the cardiac sarcoplasmic reticulum. *Recent advances in studies on cardiac structure and metabolism*, *5*, 103–115.
- Kirchberger, M. A., & Antonetz, T. (1982). Calmodulin-mediated regulation of calcium transport and (Ca²⁺ + Mg²⁺)-activated ATPase activity in isolated cardiac sarcoplasmic reticulum. *The Journal of biological chemistry*, *257*(10), 5685–5691.
- Kirchberger, M. A., Tada, M., Repke, D. I., & Katz, A. M. (1972). Cyclic adenosine 3',5'-monophosphate-dependent protein kinase stimulation of calcium uptake by canine cardiac microsomes. *Journal of molecular and cellular cardiology*, *4*(6), 673–680.
- Kiss, E., Jakab, G., Kranias, E. G., & Edes, I. (1994). Thyroid hormone-induced alterations in phospholamban protein expression. Regulatory effects on sarcoplasmic reticulum Ca²⁺ transport and myocardial relaxation. *Circulation research*, *75*(2), 245–251.
- Klapper R. (2000). The longitudinal visceral musculature of *Drosophila melanogaster* persists through metamorphosis. *Mechanisms of development*, *95*(1-2), 47–54.
- Klapper, R., Heuser, S., Strasser, T., & Janning, W. (2001). A new approach reveals syncytia within the visceral musculature of *Drosophila melanogaster*. *Development (Cambridge, England)*, *128*(13), 2517–2524.
- Klapper, R., Stute, C., Schomaker, O., Strasser, T., Janning, W., Renkawitz-Pohl, R., & Holz, A. (2002). The formation of syncytia within the visceral musculature of the *Drosophila* midgut is dependent on *duf*, *sns* and *mbc*. *Mechanisms of development*, *110*(1-2), 85–96.
- Knollmann B. C. (2009). New roles of calsequestrin and triadin in cardiac muscle. *The Journal of physiology*, *587*(Pt 13), 3081–3087.
- Kobayashi, C., Kobayashi, S., Orii, H., Watanabe, K., & Agata, K. (1998). Identification of two distinct muscles in the planarian *Dugesia japonica* by their expression of myosin heavy chain genes. *Zoological science*, *15*(6), 861-869.

- Kobayashi, T., Kurebayashi, N., & Murayama, T. (2021). The Ryanodine Receptor as a Sensor for Intracellular Environments in Muscles. *International journal of molecular sciences*, *22*(19), 10795.
- Kokkonen, J. O., Kuoppala, A., Saarinen, J., Lindstedt, K. A., & Kovanen, P. T. (1999). Kallidin- and bradykinin-degrading pathways in human heart: degradation of kallidin by aminopeptidase M-like activity and bradykinin by neutral endopeptidase. *Circulation*, *99*(15), 1984–1990.
- Korczak, B., Zarain-Herzberg, A., Brandl, C. J., Ingles, C. J., Green, N. M., & MacLennan, D. H. (1988). Structure of the rabbit fast-twitch skeletal muscle Ca²⁺-ATPase gene. *The Journal of biological chemistry*, *263*(10), 4813–4819.
- Kranias E. G. (1985). Regulation of calcium transport by protein phosphatase activity associated with cardiac sarcoplasmic reticulum. *The Journal of biological chemistry*, *260*(20), 11006–11010.
- Kranias, E. G., & Hajjar, R. J. (2012). Modulation of cardiac contractility by the phospholamban/SERCA2a regulatome. *Circulation research*, *110*(12), 1646–1660.
- Kranias, E. G., & Solaro, R. J. (1982). Phosphorylation of troponin I and phospholamban during catecholamine stimulation of rabbit heart. *Nature*, *298*(5870), 182–184.
- Kréneisz, O., Chen, X., Fridell, Y. W., & Mulkey, D. K. (2010). Glucose increases activity and Ca²⁺ in insulin-producing cells of adult *Drosophila*. *Neuroreport*, *21*(17), 1116–1120.
- Kubo, M., Mitsuda, Y., Takagi, M., & Imanaka, T. (1992). Alteration of specific activity and stability of thermostable neutral protease by site-directed mutagenesis. *Applied and environmental microbiology*, *58*(11), 3779–3783.
- Kühlbrandt W. (2004). Biology, structure and mechanism of P-type ATPases. *Nature reviews. Molecular cell biology*, *5*(4), 282–295.
- Kumarswamy, R., Lyon, A. R., Volkmann, I., Mills, A. M., Bretthauer, J., Pahuja, A., Geers-Knörr, C., Kraft, T., Hajjar, R. J., Macleod, K. T., Harding, S. E., & Thum, T. (2012). SERCA2a gene therapy restores microRNA-1 expression in heart failure via an Akt/FoxO3A-dependent pathway. *European heart journal*, *33*(9), 1067–1075
- Kuo, I. Y., & Ehrlich, B. E. (2015). Signaling in muscle contraction. *Cold Spring Harbor perspectives in biology*, *7*(2), a006023.
- Kushnir, A., Wajsberg, B., & Marks, A. R. (2018). Ryanodine receptor dysfunction in human disorders. *Biochimica et biophysica acta. Molecular cell research*, *1865*(11 Pt B), 1687–1697.
- Kute, P. M., Soukarieh, O., Tjeldnes, H., Trégouët, D. A., & Valen, E. (2022). Small Open Reading Frames, How to Find Them and Determine Their Function. *Frontiers in genetics*, *12*, 796060.
- Kwak, S. J., Hong, S. H., Bajracharya, R., Yang, S. Y., Lee, K. S., & Yu, K. (2013). *Drosophila* adiponectin receptor in insulin producing cells regulates glucose and lipid metabolism by controlling insulin secretion. *PloS one*, *8*(7), e68641.
- LaBeau, E. M., Trujillo, D. L., & Cripps, R. M. (2009). Bithorax complex genes control alary muscle patterning along the cardiac tube of *Drosophila*. *Mechanisms of development*, *126*(5-6), 478–486.

- Lamb G. D. (2000). Excitation-contraction coupling in skeletal muscle: comparisons with cardiac muscle. *Clinical and experimental pharmacology & physiology*, *27*(3), 216–224.
- Lammers, K., Abeln, B., Hüsken, M., Lehmacher, C., Psathaki, O. E., Alcorta, E., Meyer, H., & Paululat, A. (2017). Formation and function of intracardiac valve cells in the *Drosophila* heart. *The Journal of experimental biology*, *220*(Pt 10), 1852–1863.
- Lanner, J. T., Georgiou, D. K., Joshi, A. D., & Hamilton, S. L. (2010). Ryanodine receptors: structure, expression, molecular details, and function in calcium release. *Cold Spring Harbor perspectives in biology*, *2*(11), a003996.
- Leberer, E., Timms, B. G., Campbell, K. P., & MacLennan, D. H. (1990). Purification, calcium binding properties, and ultrastructural localization of the 53,000- and 160,000 (sarcalumenin)-dalton glycoproteins of the sarcoplasmic reticulum. *The Journal of biological chemistry*, *265*(17), 10118–10124.
- Lee, H. H., Zaffran, S., & Frasch, M. (2006). Development of the larval visceral musculature. In *Muscle development in Drosophila* (pp. 62-78). Springer, New York, NY.
- Lee, K. S., Kwon, O. Y., Lee, J. H., Kwon, K., Min, K. J., Jung, S. A., Kim, A. K., You, K. H., Tatar, M., & Yu, K. (2008). *Drosophila* short neuropeptide F signalling regulates growth by ERK-mediated insulin signalling. *Nature cell biology*, *10*(4), 468–475.
- Leenhardt, A., Denjoy, I., & Guicheney, P. (2012). Catecholaminergic polymorphic ventricular tachycardia. *Circulation. Arrhythmia and electrophysiology*, *5*(5), 1044–1052.
- Lefkowitz R. J. (2013). A brief history of G-protein coupled receptors (Nobel Lecture). *Angewandte Chemie (International ed. in English)*, *52*(25), 6366–6378.
- Lehmacher, C., Abeln, B., & Paululat, A. (2012). The ultrastructure of *Drosophila* heart cells. *Arthropod structure & development*, *41*(5), 459–474.
- Lehman, W., Hatch, V., Korman, V., Rosol, M., Thomas, L., Maytum, R., Geeves, M. A., Van Eyk, J. E., Tobacman, L. S., & Craig, R. (2000). Tropomyosin and actin isoforms modulate the localization of tropomyosin strands on actin filaments. *Journal of molecular biology*, *302*(3), 593–606.
- Lemke, S. B., & Schnorrer, F. (2017). Mechanical forces during muscle development. *Mechanisms of development*, *144*(Pt A), 92–101.
- Lenz, C., Williamson, M., Hansen, G. N., & Grimmelikhuijzen, C. J. (2001). Identification of four *Drosophila* allatostatins as the cognate ligands for the *Drosophila* orphan receptor DAR-2. *Biochemical and biophysical research communications*, *286*(5), 1117–1122.
- Letarte, M., Vera, S., Tran, R., Addis, J. B., Onizuka, R. J., Quackenbush, E. J., Jongeneel, C. V., & McInnes, R. R. (1988). Common acute lymphocytic leukemia antigen is identical to neutral endopeptidase. *The Journal of experimental medicine*, *168*(4), 1247–1253.
- Lewis, D., Pilankatta, R., Inesi, G., Bartolommei, G., Moncelli, M. R., & Tadini-Buoninsegni, F. (2012). Distinctive features of catalytic and transport mechanisms in mammalian sarcoplasmic reticulum Ca²⁺ ATPase (SERCA) and Cu⁺ (ATP7A/B) ATPases. *The Journal of biological chemistry*, *287*(39), 32717–32727.

- Li, L., Desantiago, J., Chu, G., Kranias, E. G., & Bers, D. M. (2000). Phosphorylation of phospholamban and troponin I in beta-adrenergic-induced acceleration of cardiac relaxation. *American journal of physiology. Heart and circulatory physiology*, *278*(3), H769–H779.
- Liao, F. T., Chang, C. Y., Su, M. T., & Kuo, W. C. (2014). Necessity of angiotensin-converting enzyme-related gene for cardiac functions and longevity of *Drosophila melanogaster* assessed by optical coherence tomography. *Journal of biomedical optics*, *19*(1), 011014.
- Lin, Q., Zhao, G., Fang, X., Peng, X., Tang, H., Wang, H., Jing, R., Liu, J., Lederer, W. J., Chen, J., & Ouyang, K. (2016). IP₃ receptors regulate vascular smooth muscle contractility and hypertension. *JCI insight*, *1*(17), e89402.
- Liu, N., Li, T., Wang, Y., & Liu, S. (2021). G-Protein Coupled Receptors (GPCRs) in Insects-A Potential Target for New Insecticide Development. *Molecules (Basel, Switzerland)*, *26*(10), 2993.
- Lu, F., & Pu, W. T. (2020). The architecture and function of cardiac dyads. *Biophysical reviews*, *12*(4), 1007–1017.
- Luo, J., Lushchak, O. V., Goergen, P., Williams, M. J., & Nässel, D. R. (2014). *Drosophila* insulin-producing cells are differentially modulated by serotonin and octopamine receptors and affect social behavior. *PloS one*, *9*(6), e99732.
- Lymn, R. W., & Taylor, E. W. (1971). Mechanism of adenosine triphosphate hydrolysis by actomyosin. *Biochemistry*, *10*(25), 4617–4624.
- Lytton, J., & MacLennan, D. H. (1988). Molecular cloning of cDNAs from human kidney coding for two alternatively spliced products of the cardiac Ca²⁺-ATPase gene. *The Journal of biological chemistry*, *263*(29), 15024–15031.
- Lytton, J., Zarain-Herzberg, A., Periasamy, M., & MacLennan, D. H. (1989). Molecular cloning of the mammalian smooth muscle sarco(endo)plasmic reticulum Ca²⁺-ATPase. *The Journal of biological chemistry*, *264*(12), 7059–7065.
- MacDougall, L. K., Jones, L. R., & Cohen, P. (1991). Identification of the major protein phosphatases in mammalian cardiac muscle which dephosphorylate phospholamban. *European journal of biochemistry*, *196*(3), 725–734.
- MacLennan D. H. (1974). Isolation of proteins of the sarcoplasmic reticulum. *Methods in enzymology*, *32*, 291–302.
- MacLennan, D. H., & Kranias, E. G. (2003). Phospholamban: a crucial regulator of cardiac contractility. *Nature reviews. Molecular cell biology*, *4*(7), 566–577.
- MacLennan, D. H., & Wong, P. T. (1971). Isolation of a calcium-sequestering protein from sarcoplasmic reticulum. *Proceedings of the National Academy of Sciences of the United States of America*, *68*(6), 1231–1235.
- MacLennan, D. H., Brandl, C. J., Korczak, B., & Green, N. M. (1985). Amino-acid sequence of a Ca²⁺ + Mg²⁺-dependent ATPase from rabbit muscle sarcoplasmic reticulum, deduced from its complementary DNA sequence. *Nature*, *316*(6030), 696–700.

- Magny, E. G., Pueyo, J. I., Pearl, F. M., Cespedes, M. A., Niven, J. E., Bishop, S. A., & Couso, J. P. (2013). Conserved regulation of cardiac calcium uptake by peptides encoded in small open reading frames. *Science (New York, N.Y.)*, *341*(6150), 1116–1120.
- Magyar, A., & Váradi, A. (1990). Molecular cloning and chromosomal localization of a sarco/endoplasmic reticulum-type Ca²⁺-ATPase of *Drosophila melanogaster*. *Biochemical and biophysical research communications*, *173*(3), 872–877.
- Magyar, A., Bakos, E., & Váradi, A. (1995). Structure and tissue-specific expression of the *Drosophila melanogaster* organellar-type Ca(2+)-ATPase gene. *The Biochemical journal*, *310* (Pt 3)(Pt 3), 757–763.
- Makarewich C. A. (2020). The hidden world of membrane microproteins. *Experimental cell research*, *388*(2), 111853.
- Makarewich, C. A., & Olson, E. N. (2017). Mining for Micropeptides. *Trends in cell biology*, *27*(9), 685–696.
- Makarewich, C. A., Munir, A. Z., Schiattarella, G. G., Bezprozvannaya, S., Raguimova, O. N., Cho, E. E., Vidal, A. H., Robia, S. L., Bassel-Duby, R., & Olson, E. N. (2018). The DWORF micropeptide enhances contractility and prevents heart failure in a mouse model of dilated cardiomyopathy. *eLife*, *7*, e38319.
- Makinose, M., & Hasselbach, W. (1971). ATP synthesis by the reverse of the sarcoplasmic calcium pump. *FEBS letters*, *12*(5), 271–272.
- Malfoy, B., Swerts, J. P., Guyon, A., Roques, B. P., & Schwartz, J. C. (1978). High-affinity enkephalin-degrading peptidase in brain is increased after morphine. *Nature*, *276*(5687), 523–526.
- Mall, S., Broadbridge, R., Harrison, S. L., Gore, M. G., Lee, A. G., & East, J. M. (2006). The presence of sarcolipin results in increased heat production by Ca(2+)-ATPase. *The Journal of biological chemistry*, *281*(48), 36597–36602.
- Martin, V., Bredoux, R., Corvazier, E., Van Gorp, R., Kovacs, T., Gelebart, P., & Enouf, J. (2002). Three novel sarco/endoplasmic reticulum Ca²⁺-ATPase (SERCA) 3 isoforms. Expression, regulation, and function of the membranes of the SERCA3 family. *The Journal of biological chemistry*, *277*(27), 24442–24452.
- Marty I. (2015). Triadin regulation of the ryanodine receptor complex. *The Journal of physiology*, *593*(15), 3261–3266.
- Marty, I., Robert, M., Villaz, M., De Jongh, K., Lai, Y., Catterall, W. A., & Ronjat, M. (1994). Biochemical evidence for a complex involving dihydropyridine receptor and ryanodine receptor in triad junctions of skeletal muscle. *Proceedings of the National Academy of Sciences of the United States of America*, *91*(6), 2270–2274.
- Matsas, R., Fulcher, I. S., Kenny, A. J., & Turner, A. J. (1983). Substance P and [Leu]enkephalin are hydrolyzed by an enzyme in pig caudate synaptic membranes that is identical with the endopeptidase of kidney microvilli. *Proceedings of the National Academy of Sciences of the United States of America*, *80*(10), 3111–3115.

- Mattiazzi, A., & Kranias, E. G. (2014). The role of CaMKII regulation of phospholamban activity in heart disease. *Frontiers in pharmacology*, 5, 5.
- Maurya, S. K., & Periasamy, M. (2015). Sarcolipin is a novel regulator of muscle metabolism and obesity. *Pharmacological research*, 102, 270–275.
- Maurya, S. K., Bal, N. C., Sopariwala, D. H., Pant, M., Rowland, L. A., Shaikh, S. A., & Periasamy, M. (2015). Sarcolipin Is a Key Determinant of the Basal Metabolic Rate, and Its Overexpression Enhances Energy Expenditure and Resistance against Diet-induced Obesity. *The Journal of biological chemistry*, 290(17), 10840–10849.
- McFarland, T. P., Milstein, M. L., & Cala, S. E. (2010). Rough endoplasmic reticulum to junctional sarcoplasmic reticulum trafficking of calsequestrin in adult cardiomyocytes. *Journal of molecular and cellular cardiology*, 49(4), 556–564.
- McMurray, J. J., Packer, M., Desai, A. S., Gong, J., Lefkowitz, M. P., Rizkala, A. R., Rouleau, J. L., Shi, V. C., Solomon, S. D., Swedberg, K., Zile, M. R., & PARADIGM-HF Investigators and Committees (2014). Angiotensin-neprilysin inhibition versus enalapril in heart failure. *The New England journal of medicine*, 371(11), 993–1004.
- Medioni, C., Sénatore, S., Salmand, P. A., Lalevée, N., Perrin, L., & Sémériva, M. (2009). The fabulous destiny of the *Drosophila* heart. *Current opinion in genetics & development*, 19(5), 518–525.
- Meissner G. (2017). The structural basis of ryanodine receptor ion channel function. *The Journal of general physiology*, 149(12), 1065–1089.
- Menon, K. P., Carrillo, R. A., & Zinn, K. (2013). Development and plasticity of the *Drosophila* larval neuromuscular junction. *Wiley interdisciplinary reviews. Developmental biology*, 2(5), 647–670.
- Meyer, H., Buhr, A., Callaerts, P., Schiemann, R., Wolfner, M. F., & Marygold, S. J. (2021). Identification and bioinformatic analysis of neprilysin and neprilysin-like metalloendopeptidases in *Drosophila melanogaster*. *microPublication biology*, 2021, 10.17912
- Meyer, H., Panz, M., Albrecht, S., Drechsler, M., Wang, S., Hüsken, M., Lehmacher, C., & Paululat, A. (2011). *Drosophila* metalloproteases in development and differentiation: the role of ADAM proteins and their relatives. *European journal of cell biology*, 90(9), 770–778.
- Meyer, H., Panz, M., Zmojdzian, M., Jagla, K., & Paululat, A. (2009). Neprilysin 4, a novel endopeptidase from *Drosophila melanogaster*, displays distinct substrate specificities and exceptional solubility states. *The Journal of experimental biology*, 212(Pt 22), 3673–3683.
- Michelangeli, F., & East, J. M. (2011). A diversity of SERCA Ca²⁺ pump inhibitors. *Biochemical Society transactions*, 39(3), 789–797.
- Miguel-Aliaga, I., Thor, S., & Gould, A. P. (2008). Postmitotic specification of *Drosophila* insulinergic neurons from pioneer neurons. *PLoS biology*, 6(3), e58.
- Miller, A. (1950). The internal anatomy and histology of the imago of *Drosophila melanogaster*. *The biology of Drosophila*, 421-534.
- Minamisawa, S., Hoshijima, M., Chu, G., Ward, C. A., Frank, K., Gu, Y., Martone, M. E., Wang, Y., Ross, J., Jr, Kranias, E. G., Giles, W. R., & Chien, K. R. (1999). Chronic phospholamban-

- sarcoplasmic reticulum calcium ATPase interaction is the critical calcium cycling defect in dilated cardiomyopathy. *Cell*, *99*(3), 313–322.
- Minamisawa, S., Wang, Y., Chen, J., Ishikawa, Y., Chien, K. R., & Matsuoka, R. (2003). Atrial chamber-specific expression of sarcolipin is regulated during development and hypertrophic remodeling. *The Journal of biological chemistry*, *278*(11), 9570–9575.
- Mitchell, R. D., Saito, A., Palade, P., & Fleischer, S. (1983). Morphology of isolated triads. *The Journal of cell biology*, *96*(4), 1017–1029.
- Molina, M. R., & Cripps, R. M. (2001). Ostia, the inflow tracts of the *Drosophila* heart, develop from a genetically distinct subset of cardiac cells. *Mechanisms of development*, *109*(1), 51–59.
- Møller, J. V., Olesen, C., Winther, A. M., & Nissen, P. (2010). The sarcoplasmic Ca²⁺-ATPase: design of a perfect chemi-osmotic pump. *Quarterly reviews of biophysics*, *43*(4), 501–566.
- Monier, B., Astier, M., Sémériva, M., & Perrin, L. (2005). Steroid-dependent modification of Hox function drives myocyte reprogramming in the *Drosophila* heart. *Development (Cambridge, England)*, *132*(23), 5283–5293.
- Morissette, M. P., Susser, S. E., Stammers, A. N., O'Hara, K. A., Gardiner, P. F., Sheppard, P., Moffatt, T. L., & Duhamel, T. A. (2014). Differential regulation of the fiber type-specific gene expression of the sarcoplasmic reticulum calcium-ATPase isoforms induced by exercise training. *Journal of applied physiology (Bethesda, Md. : 1985)*, *117*(5), 544–555.
- Moss, S., Subramanian, V., & Acharya, K. R. (2018). High resolution crystal structure of substrate-free human neprilysin. *Journal of structural biology*, *204*(1), 19–25.
- Moss, S., Subramanian, V., & Acharya, K. R. (2020). Crystal structure of peptide-bound neprilysin reveals key binding interactions. *FEBS letters*, *594*(2), 327–336.
- Movsesian, M. A., Nishikawa, M., & Adelstein, R. S. (1984). Phosphorylation of phospholamban by calcium-activated, phospholipid-dependent protein kinase. Stimulation of cardiac sarcoplasmic reticulum calcium uptake. *The Journal of biological chemistry*, *259*(13), 8029–8032.
- Nagai, R., Zarain-Herzberg, A., Brandl, C. J., Fujii, J., Tada, M., MacLennan, D. H., Alpert, N. R., & Periasamy, M. (1989). Regulation of myocardial Ca²⁺-ATPase and phospholamban mRNA expression in response to pressure overload and thyroid hormone. *Proceedings of the National Academy of Sciences of the United States of America*, *86*(8), 2966–2970.
- Nässel, D. R., & Vanden Broeck, J. (2016). Insulin/IGF signaling in *Drosophila* and other insects: factors that regulate production, release and post-release action of the insulin-like peptides. *Cellular and molecular life sciences : CMLS*, *73*(2), 271–290.
- Nässel, D. R., & Winther, A. M. (2010). *Drosophila* neuropeptides in regulation of physiology and behavior. *Progress in neurobiology*, *92*(1), 42–104.
- Nässel, D. R., & Zandawala, M. (2019). Recent advances in neuropeptide signaling in *Drosophila*, from genes to physiology and behavior. *Progress in neurobiology*, *179*, 101607.
- Nässel, D. R., Kubrak, O. I., Liu, Y., Luo, J., & Lushchak, O. V. (2013). Factors that regulate insulin producing cells and their output in *Drosophila*. *Frontiers in physiology*, *4*, 252.

- Nässel, D. R., Liu, Y., & Luo, J. (2015). Insulin/IGF signaling and its regulation in *Drosophila*. *General and comparative endocrinology*, *221*, 255–266.
- Nef, H. M., Möllmann, H., Troidl, C., Kostin, S., Voss, S., Hilpert, P., Behrens, C. B., Rolf, A., Rixe, J., Weber, M., Hamm, C. W., & Elsässer, A. (2009). Abnormalities in intracellular Ca²⁺ regulation contribute to the pathomechanism of Tako-Tsubo cardiomyopathy. *European heart journal*, *30*(17), 2155–2164.
- Nelson, B. R., Makarewich, C. A., Anderson, D. M., Winders, B. R., Troupes, C. D., Wu, F., Reese, A. L., McAnally, J. R., Chen, X., Kavalali, E. T., Cannon, S. C., Houser, S. R., Bassel-Duby, R., & Olson, E. N. (2016). A peptide encoded by a transcript annotated as long noncoding RNA enhances SERCA activity in muscle. *Science (New York, N.Y.)*, *351*(6270), 271–275.
- Nichols, R., McCormick, J., Cohen, M., Howe, E., Jean, C., Paisley, K., & Rosario, C. (1999). Differential processing of neuropeptides influences *Drosophila* heart rate. *Journal of neurogenetics*, *13*(1-2), 89–104.
- Novelli, A., Valente, E. M., Bernardini, L., Ceccarini, C., Sinibaldi, L., Caputo, V., Cavalli, P., & Dallapiccola, B. (2004). Autosomal dominant Brody disease cosegregates with a chromosomal (2;7)(p11.2;p12.1) translocation in an Italian family. *European journal of human genetics : EJHG*, *12*(7), 579–583.
- Noyes, B. E., Katz, F. N., & Schaffer, M. H. (1995). Identification and expression of the *Drosophila* adipokinetic hormone gene. *Molecular and cellular endocrinology*, *109*(2), 133–141.
- Odermatt, A., Becker, S., Khanna, V. K., Kurzydowski, K., Leisner, E., Pette, D., & MacLennan, D. H. (1998). Sarcolipin regulates the activity of SERCA1, the fast-twitch skeletal muscle sarcoplasmic reticulum Ca²⁺-ATPase. *The Journal of biological chemistry*, *273*(20), 12360–12369.
- Odermatt, A., Taschner, P. E., Khanna, V. K., Busch, H. F., Karpati, G., Jablecki, C. K., Breuning, M. H., & MacLennan, D. H. (1996). Mutations in the gene-encoding SERCA1, the fast-twitch skeletal muscle sarcoplasmic reticulum Ca²⁺ ATPase, are associated with Brody disease. *Nature genetics*, *14*(2), 191–194.
- Odermatt, A., Taschner, P. E., Scherer, S. W., Beatty, B., Khanna, V. K., Cornblath, D. R., Chaudhry, V., Yee, W. C., Schrank, B., Karpati, G., Breuning, M. H., Knoers, N., & MacLennan, D. H. (1997). Characterization of the gene encoding human sarcolipin (SLN), a proteolipid associated with SERCA1: absence of structural mutations in five patients with Brody disease. *Genomics*, *45*(3), 541–553.
- Oefner, C., D'Arcy, A., Hennig, M., Winkler, F. K., & Dale, G. E. (2000). Structure of human neutral endopeptidase (Neprilysin) complexed with phosphoramidon. *Journal of molecular biology*, *296*(2), 341–349.
- Oefner, C., Pierau, S., Schulz, H., & Dale, G. E. (2007). Structural studies of a bifunctional inhibitor of neprilysin and DPP-IV. *Acta crystallographica. Section D, Biological crystallography*, *63*(Pt 9), 975–981.
- Oefner, C., Roques, B. P., Fournie-Zaluski, M. C., & Dale, G. E. (2004). Structural analysis of neprilysin with various specific and potent inhibitors. *Acta crystallographica. Section D, Biological crystallography*, *60*(Pt 2), 392–396.

- Ogata, T., & Yamasaki, Y. (1990). High-resolution scanning electron microscopic studies on the three-dimensional structure of the transverse-axial tubular system, sarcoplasmic reticulum and intercalated disc of the rat myocardium. *The Anatomical record*, *228*(3), 277–287.
- Ohsako, T., Shirakami, M., Oiwa, K., Ibaraki, K., Karr, T. L., Tomaru, M., Sanuki, R., & Takano-Shimizu-Kouno, T. (2021). The *Drosophila* Neprilysin 4 gene is essential for sperm function following sperm transfer to females. *Genes & genetic systems*, *96*(4), 177–186.
- Okamoto, N., & Yamanaka, N. (2015). Nutrition-dependent control of insect development by insulin-like peptides. *Current opinion in insect science*, *11*, 21–30.
- Okamoto, N., Yamanaka, N., Yagi, Y., Nishida, Y., Kataoka, H., O'Connor, M. B., & Mizoguchi, A. (2009). A fat body-derived IGF-like peptide regulates postfeeding growth in *Drosophila*. *Developmental cell*, *17*(6), 885–891.
- Oldham, W. M., & Hamm, H. E. (2008). Heterotrimeric G protein activation by G-protein-coupled receptors. *Nature reviews. Molecular cell biology*, *9*(1), 60–71.
- Olesen, C., Picard, M., Winther, A. M., Gyruup, C., Morth, J. P., Oxvig, C., Møller, J. V., & Nissen, P. (2007). The structural basis of calcium transport by the calcium pump. *Nature*, *450*(7172), 1036–1042.
- Olesen, C., Sørensen, T. L., Nielsen, R. C., Møller, J. V., & Nissen, P. (2004). Dephosphorylation of the calcium pump coupled to counterion occlusion. *Science (New York, N.Y.)*, *306*(5705), 2251–2255.
- Ormerod, K. G., LePine, O. K., Bhutta, M. S., Jung, J., Tattersall, G. J., & Mercier, A. J. (2016). Characterizing the physiological and behavioral roles of proctolin in *Drosophila melanogaster*. *Journal of neurophysiology*, *115*(1), 568–580.
- Ormerod, K. G., Scibelli, A. E., & Littleton, J. T. (2020). Excitation-contraction coupling and its relation to synaptic dysfunction in *Drosophila*. *bioRxiv*.
- Osborne, M. P. (1967). Supercontraction in the muscles of the blowfly larva: an ultrastructural study. *Journal of Insect Physiology*, *13*(10), 1471–1482.
- Oulès, B., Del Prete, D., Greco, B., Zhang, X., Lauritzen, I., Sevalle, J., Moreno, S., Paterlini-Bréchet, P., Trebak, M., Checler, F., Benfenati, F., & Chami, M. (2012). Ryanodine receptor blockade reduces amyloid- β load and memory impairments in Tg2576 mouse model of Alzheimer disease. *The Journal of neuroscience : the official journal of the Society for Neuroscience*, *32*(34), 11820–11834.
- Owusu-Ansah, E., & Perrimon, N. (2014). Modeling metabolic homeostasis and nutrient sensing in *Drosophila*: implications for aging and metabolic diseases. *Disease models & mechanisms*, *7*(3), 343–350.
- Packer M. (2018). Augmentation of glucagon-like peptide-1 receptor signalling by neprilysin inhibition: potential implications for patients with heart failure. *European journal of heart failure*, *20*(6), 973–977.
- Padmanabha, D., & Baker, K. D. (2014). *Drosophila* gains traction as a repurposed tool to investigate metabolism. *Trends in endocrinology and metabolism: TEM*, *25*(10), 518–527.

- Pagliaro, L., Marchesini, M., & Roti, G. (2021). Targeting oncogenic Notch signaling with SERCA inhibitors. *Journal of hematology & oncology*, *14*(1), 8.
- Palmgren, M. G., & Nissen, P. (2011). P-type ATPases. *Annual review of biophysics*, *40*, 243–266.
- Paniagua, R., Royuela, M., García-Anchuelo, R. M., & Fraile, B. (1996). Ultrastructure of invertebrate muscle cell types. *Histology and histopathology*, *11*(1), 181–201.
- Pankow, K., Schwiebs, A., Becker, M., Siems, W. E., Krause, G., & Walther, T. (2009). Structural substrate conditions required for neutral endopeptidase-mediated natriuretic Peptide degradation. *Journal of molecular biology*, *393*(2), 496–503.
- Panz, M., Vitos-Faleato, J., Jendretzki, A., Heinisch, J. J., Paululat, A., & Meyer, H. (2012). A novel role for the non-catalytic intracellular domain of Neprilysins in muscle physiology. *Biology of the cell*, *104*(9), 553–568.
- Park, C. S., Chen, S., Lee, H., Cha, H., Oh, J. G., Hong, S., Han, P., Ginsburg, K. S., Jin, S., Park, I., Singh, V. P., Wang, H. S., Franzini-Armstrong, C., Park, W. J., Bers, D. M., Kranias, E. G., Cho, C., & Kim, D. H. (2013). Targeted ablation of the histidine-rich Ca(2+)-binding protein (HRC) gene is associated with abnormal SR Ca(2+)-cycling and severe pathology under pressure-overload stress. *Basic research in cardiology*, *108*(3), 344.
- Park, H., Park, I. Y., Kim, E., Youn, B., Fields, K., Dunker, A. K., & Kang, C. (2004). Comparing skeletal and cardiac calsequestrin structures and their calcium binding: a proposed mechanism for coupled calcium binding and protein polymerization. *The Journal of biological chemistry*, *279*(17), 18026–18033.
- Park, S., Alfa, R. W., Topper, S. M., Kim, G. E., Kockel, L., & Kim, S. K. (2014). A genetic strategy to measure circulating Drosophila insulin reveals genes regulating insulin production and secretion. *PLoS genetics*, *10*(8), e1004555.
- Payre, F., & Desplan, C. (2016). RNA. Small peptides control heart activity. *Science (New York, N.Y.)*, *351*(6270), 226–227.
- Peachey L. D. (1965). The sarcoplasmic reticulum and transverse tubules of the frog's sartorius. *The Journal of cell biology*, *25*(3), 209–231.
- Peinelt, C., & Apell, H. J. (2002). Kinetics of the Ca(2+), H(+), and Mg(2+) interaction with the ion-binding sites of the SR Ca-ATPase. *Biophysical journal*, *82*(1 Pt 1), 170–181.
- Periasamy, M., & Kalyanasundaram, A. (2007). SERCA pump isoforms: their role in calcium transport and disease. *Muscle & nerve*, *35*(4), 430–442.
- Periasamy, M., Maurya, S. K., Sahoo, S. K., Singh, S., Sahoo, S. K., Reis, F., & Bal, N. C. (2017). Role of SERCA Pump in Muscle Thermogenesis and Metabolism. *Comprehensive Physiology*, *7*(3), 879–890.
- Periz, G., & Fortini, M. E. (1999). Ca(2+)-ATPase function is required for intracellular trafficking of the Notch receptor in Drosophila. *The EMBO journal*, *18*(21), 5983–5993.
- Perz-Edwards, R. J., Irving, T. C., Baumann, B. A., Gore, D., Hutchinson, D. C., Kržič, U., Porter, R. L., Ward, A. B., & Reedy, M. K. (2011). X-ray diffraction evidence for myosin-troponin connections and tropomyosin movement during stretch activation of insect flight

- muscle. *Proceedings of the National Academy of Sciences of the United States of America*, 108(1), 120–125.
- Peterson, B. Z., DeMaria, C. D., & Yue, D. T. (1999). Calmodulin is the Ca²⁺ sensor for Ca²⁺-dependent inactivation of L-type calcium channels. *Neuron*, 22(3), 549–558.
- Pfleger, J., Gresham, K., & Koch, W. J. (2019). G protein-coupled receptor kinases as therapeutic targets in the heart. *Nature reviews. Cardiology*, 16(10), 612–622.
- Philipson, K. D., & Nicoll, D. A. (2000). Sodium-calcium exchange: a molecular perspective. *Annual review of physiology*, 62, 111–133.
- Plesch B. (1977). An ultrastructural study of the musculature of the pond snail *Lymnaea stagnalis* (l.). *Cell and tissue research*, 180(3), 317–340.
- Poch, E., Leach, S., Snape, S., Cacic, T., MacLennan, D. H., & Lytton, J. (1998). Functional characterization of alternatively spliced human SERCA3 transcripts. *The American journal of physiology*, 275(6), C1449–C1458.
- Pool, A. H., & Scott, K. (2014). Feeding regulation in *Drosophila*. *Current opinion in neurobiology*, 29, 57–63.
- Poovathumkadavil, P., & Jagla, K. (2020). Genetic Control of Muscle Diversification and Homeostasis: Insights from *Drosophila*. *Cells*, 9(6), 1543.
- Porter, K. R., & Palade, G. E. (1957). Studies on the endoplasmic reticulum. III. Its form and distribution in striated muscle cells. *The Journal of biophysical and biochemical cytology*, 3(2), 269–300.
- Pospich, S., Sweeney, H. L., Houdusse, A., & Raunser, S. (2021). High-resolution structures of the actomyosin-V complex in three nucleotide states provide insights into the force generation mechanism. *eLife*, 10, e73724.
- Post, R. L., Hegyvary, C., & Kume, S. (1972). Activation by adenosine triphosphate in the phosphorylation kinetics of sodium and potassium ion transport adenosine triphosphatase. *The Journal of biological chemistry*, 247(20), 6530–6540.
- Post, R. L., Kume, S., Tobin, T., Orcutt, B., & Sen, A. K. (1969). Flexibility of an active center in sodium-plus-potassium adenosine triphosphatase. *The Journal of general physiology*, 54(1), 306–326.
- Primeau, J. O., Armanious, G. P., Fisher, M. E., & Young, H. S. (2018). The SarcoEndoplasmic Reticulum Calcium ATPase. *Sub-cellular biochemistry*, 87, 229–258.
- Pringle J. W. (1949). The excitation and contraction of the flight muscles of insects. *The Journal of physiology*, 108(2), 226–232.
- Raguimova, O. N., Aguayo-Ortiz, R., Robia, S. L., & Espinoza-Fonseca, L. M. (2020). Dynamics-Driven Allostery Underlies Ca²⁺-Mediated Release of SERCA Inhibition by Phospholamban. *Biophysical journal*, 119(9), 1917–1926.
- Raguimova, O. N., Smolin, N., Bovo, E., Bhayani, S., Autry, J. M., Zima, A. V., & Robia, S. L. (2018). Redistribution of SERCA calcium pump conformers during intracellular calcium signaling. *The Journal of biological chemistry*, 293(28), 10843–10856.

- Rajan, A., & Perrimon, N. (2012). *Drosophila* cytokine unpaired 2 regulates physiological homeostasis by remotely controlling insulin secretion. *Cell*, *151*(1), 123–137.
- Rajan, A., & Perrimon, N. (2013). Of flies and men: insights on organismal metabolism from fruit flies. *BMC biology*, *11*, 38.
- Rathod, N., Bak, J. J., Primeau, J. O., Fisher, M. E., Espinoza-Fonseca, L. M., Lemieux, M. J., & Young, H. S. (2021). Nothing Regular about the Regulins: Distinct Functional Properties of SERCA Transmembrane Peptide Regulatory Subunits. *International journal of molecular sciences*, *22*(16), 8891.
- Reconditi, M., Caremani, M., Pinzauti, F., Powers, J. D., Narayanan, T., Stienen, G. J., Linari, M., Lombardi, V., & Piazzesi, G. (2017). Myosin filament activation in the heart is tuned to the mechanical task. *Proceedings of the National Academy of Sciences of the United States of America*, *114*(12), 3240–3245.
- Reddish, F. N., Miller, C. L., Gorkhali, R., & Yang, J. J. (2017). Calcium Dynamics Mediated by the Endoplasmic/Sarcoplasmic Reticulum and Related Diseases. *International journal of molecular sciences*, *18*(5), 1024.
- Reddy, L. G., Jones, L. R., Cala, S. E., O'Brian, J. J., Tatulian, S. A., & Stokes, D. L. (1995). Functional reconstitution of recombinant phospholamban with rabbit skeletal Ca(2+)-ATPase. *The Journal of biological chemistry*, *270*(16), 9390–9397.
- Reddy, U. V., Weber, D. K., Wang, S., Larsen, E. K., Gopinath, T., De Simone, A., Robia, S., & Veglia, G. (2022). A kink in DWORF helical structure controls the activation of the sarcoplasmic reticulum Ca²⁺-ATPase. *Structure (London, England : 1993)*, *30*(3), 360–370.e6. <https://doi.org/10.1016/j.str.2021.11.003>
- Ren, G. R., Hauser, F., Rewitz, K. F., Kondo, S., Engelbrecht, A. F., Didriksen, A. K., Schjøtt, S. R., Sembach, F. E., Li, S., Søgaard, K. C., Søndergaard, L., & Grimmelikhuijzen, C. J. (2015). CCHamide-2 Is an Orexigenic Brain-Gut Peptide in *Drosophila*. *PloS one*, *10*(7), e0133017. <https://doi.org/10.1371/journal.pone.0133017>
- Reuter, H., & Seitz, N. (1968). The dependence of calcium efflux from cardiac muscle on temperature and external ion composition. *The Journal of physiology*, *195*(2), 451–470.
- Ringer S. (1882). Concerning the Influence exerted by each of the Constituents of the Blood on the Contraction of the Ventricle. *The Journal of physiology*, *3*(5-6), 380–393.
- Ringer S. (1883). A further Contribution regarding the influence of the different Constituents of the Blood on the Contraction of the Heart. *The Journal of physiology*, *4*(1), 29–42.3.
- Ríos E. (2018). Calcium-induced release of calcium in muscle: 50 years of work and the emerging consensus. *The Journal of general physiology*, *150*(4), 521–537.
- Ríos, E., Figueroa, L., Manno, C., Kraeva, N., & Riazi, S. (2015). The couplonopathies: A comparative approach to a class of diseases of skeletal and cardiac muscle. *The Journal of general physiology*, *145*(6), 459–474.
- Rizki T.M.(1978). The circulatory system and associated cells and tissues. In *The Genetics and Biology of Drosophila*. Volume 2b, pp. 397–452.

- Robert-Paganin, J., Pylypenko, O., Kikuti, C., Sweeney, H. L., & Houdusse, A. (2020). Force Generation by Myosin Motors: A Structural Perspective. *Chemical reviews*, *120*(1), 5–35. <https://doi.org/10.1021/acs.chemrev.9b00264>
- Robia, S. L., Flohr, N. C., & Thomas, D. D. (2005). Phospholamban pentamer quaternary conformation determined by in-gel fluorescence anisotropy. *Biochemistry*, *44*(11), 4302–4311.
- Rodney, G. G., Williams, B. Y., Strasburg, G. M., Beckingham, K., & Hamilton, S. L. (2000). Regulation of RYR1 activity by Ca(2+) and calmodulin. *Biochemistry*, *39*(26), 7807–7812.
- Rohrer, D., & Dillmann, W. H. (1988). Thyroid hormone markedly increases the mRNA coding for sarcoplasmic reticulum Ca²⁺-ATPase in the rat heart. *The Journal of biological chemistry*, *263*(15), 6941–6944.
- Root, C. M., Ko, K. I., Jafari, A., & Wang, J. W. (2011). Presynaptic facilitation by neuropeptide signaling mediates odor-driven food search. *Cell*, *145*(1), 133–144.
- Roques, B. P., Fournié-Zaluski, M. C., Soroca, E., Lecomte, J. M., Malfroy, B., Llorens, C., & Schwartz, J. C. (1980). The enkephalinase inhibitor thiorphan shows antinociceptive activity in mice. *Nature*, *288*(5788), 286–288.
- Rose, C., Voisin, S., Gros, C., Schwartz, J. C., & Ouimet, T. (2002). Cell-specific activity of neprilysin 2 isoforms and enzymic specificity compared with neprilysin. *The Biochemical journal*, *363*(Pt 3), 697–705.
- Rossi, A. E., & Dirksen, R. T. (2006). Sarcoplasmic reticulum: the dynamic calcium governor of muscle. *Muscle & nerve*, *33*(6), 715–731.
- Rossi, D., Barone, V., Giacomello, E., Cusimano, V., & Sorrentino, V. (2008). The sarcoplasmic reticulum: an organized patchwork of specialized domains. *Traffic (Copenhagen, Denmark)*, *9*(7), 1044–1049.
- Roti, G., Carlton, A., Ross, K. N., Markstein, M., Pajcini, K., Su, A. H., Perrimon, N., Pear, W. S., Kung, A. L., Blacklow, S. C., Aster, J. C., & Stegmaier, K. (2013). Complementary genomic screens identify SERCA as a therapeutic target in NOTCH1 mutated cancer. *Cancer cell*, *23*(3), 390–405.
- Rotstein, B., & Paululat, A. (2016). On the Morphology of the Drosophila Heart. *Journal of cardiovascular development and disease*, *3*(2), 15.
- Rotstein, B., Post, Y., Reinhardt, M., Lammers, K., Buhr, A., Heinisch, J. J., Meyer, H., & Paululat, A. (2018). Distinct domains in the matricellular protein Lonely heart are crucial for cardiac extracellular matrix formation and heart function in *Drosophila*. *The Journal of biological chemistry*, *293*(20), 7864–7879.
- Rowland, L. A., Bal, N. C., Kozak, L. P., & Periasamy, M. (2015). Uncoupling Protein 1 and Sarcolipin Are Required to Maintain Optimal Thermogenesis, and Loss of Both Systems Compromises Survival of Mice under Cold Stress. *The Journal of biological chemistry*, *290*(19), 12282–12289.
- Royer, L., & Ríos, E. (2009). Deconstructing calsequestrin. Complex buffering in the calcium store of skeletal muscle. *The Journal of physiology*, *587*(Pt 13), 3101–3111.

- Royuela, M., Fraile, B., Arenas, M. I., & Paniagua, R. (2000). Characterization of several invertebrate muscle cell types: a comparison with vertebrate muscles. *Microscopy research and technique*, *48*(2), 107–115.
- Rüegg J. C. (2016). Wilhelm Hasselbach: a personal tribute. *Journal of muscle research and cell motility*, *37*(4-5), 149–151.
- Rugendorff, A., Younossi-Hartenstein, A., & Hartenstein, V. (1994). Embryonic origin and differentiation of the *Drosophila* heart. *Roux's archives of developmental biology: the official organ of the EDBO*, *203*(5), 266–280.
- Rulifson, E. J., Kim, S. K., & Nusse, R. (2002). Ablation of insulin-producing neurons in flies: growth and diabetic phenotypes. *Science (New York, N.Y.)*, *296*(5570), 1118–1120.
- Sahoo, S. K., & Kim, D. H. (2008). Calumenin interacts with SERCA2 in rat cardiac sarcoplasmic reticulum. *Molecules and cells*, *26*(3), 265–269.
- Sahoo, S. K., Kim, T., Kang, G. B., Lee, J. G., Eom, S. H., & Kim, D. H. (2009). Characterization of calumenin-SERCA2 interaction in mouse cardiac sarcoplasmic reticulum. *The Journal of biological chemistry*, *284*(45), 31109–31121.
- Sahoo, S. K., Shaikh, S. A., Sopariwala, D. H., Bal, N. C., & Periasamy, M. (2013). Sarcolipin protein interaction with sarco(endo)plasmic reticulum Ca²⁺ ATPase (SERCA) is distinct from phospholamban protein, and only sarcolipin can promote uncoupling of the SERCA pump. *The Journal of biological chemistry*, *288*(10), 6881–6889.
- Sakuntabhai, A., Ruiz-Perez, V., Carter, S., Jacobsen, N., Burge, S., Monk, S., Smith, M., Munro, C. S., O'Donovan, M., Craddock, N., Kucherlapati, R., Rees, J. L., Owen, M., Lathrop, G. M., Monaco, A. P., Strachan, T., & Hovnanian, A. (1999). Mutations in ATP2A2, encoding a Ca²⁺ pump, cause Darier disease. *Nature genetics*, *21*(3), 271–277.
- Sanders, K. M., & Koh, S. D. (2007). Stretch-activated conductances in smooth muscles. *Current topics in membranes*, *59*, 511–540.
- Sandow A. (1952). Excitation-contraction coupling in muscular response. *The Yale journal of biology and medicine*, *25*(3), 176–201.
- Sanfelice, D., Sanz-Hernández, M., de Simone, A., Bullard, B., & Pastore, A. (2016). Toward Understanding the Molecular Bases of Stretch Activation: A functional comparison of the two Troponin C isoforms of lethocerus. *The Journal of biological chemistry*, *291*(31), 16090–16099.
- Sano, H., Nakamura, A., Texada, M. J., Truman, J. W., Ishimoto, H., Kamikouchi, A., Nibu, Y., Kume, K., Ida, T., & Kojima, M. (2015). The Nutrient-Responsive Hormone CCHamide-2 Controls Growth by Regulating Insulin-like Peptides in the Brain of *Drosophila melanogaster*. *PLoS genetics*, *11*(5), e1005209.
- Santulli, G., Lewis, D., des Georges, A., Marks, A. R., & Frank, J. (2018). Ryanodine Receptor Structure and Function in Health and Disease. *Sub-cellular biochemistry*, *87*, 329–352.
- Santulli, G., Pagano, G., Sardu, C., Xie, W., Reiken, S., D'Ascia, S. L., Cannone, M., Marziliano, N., Trimarco, B., Guise, T. A., Lacampagne, A., & Marks, A. R. (2015). Calcium release channel RyR2 regulates insulin release and glucose homeostasis. *The Journal of clinical investigation*, *125*(11), 4316.

- Sanyal, S., Consoulas, C., Kuromi, H., Basole, A., Mukai, L., Kidokoro, Y., Krishnan, K. S., & Ramaswami, M. (2005). Analysis of conditional paralytic mutants in *Drosophila* sarco-endoplasmic reticulum calcium ATPase reveals novel mechanisms for regulating membrane excitability. *Genetics*, *169*(2), 737–750.
- Sanyal, S., Jennings, T., Dowse, H., & Ramaswami, M. (2006). Conditional mutations in SERCA, the Sarco-endoplasmic reticulum Ca²⁺-ATPase, alter heart rate and rhythmicity in *Drosophila*. *Journal of comparative physiology. B, Biochemical, systemic, and environmental physiology*, *176*(3), 253–263.
- Schaffer, M. H., Noyes, B. E., Slaughter, C. A., Thorne, G. C., & Gaskell, S. J. (1990). The fruitfly *Drosophila melanogaster* contains a novel charged adipokinetic-hormone-family peptide. *The Biochemical journal*, *269*(2), 315–320.
- Schatzmann H. J. (1966). ATP-dependent Ca⁺⁺-extrusion from human red cells. *Experientia*, *22*(6), 364–365.
- Schaub, C., März, J., Reim, I., & Frasch, M. (2015). Org-1-dependent lineage reprogramming generates the ventral longitudinal musculature of the *Drosophila* heart. *Current biology: CB*, *25*(4), 488–494.
- Schiaffino, S., & Reggiani, C. (2011). Fiber types in mammalian skeletal muscles. *Physiological reviews*, *91*(4), 1447–1531.
- Schiemann, R., Buhr, A., Cordes, E., Walter, S., Heinisch, J. J., Ferrero, P., Milting, H., Paululat, A., and Meyer, H. (2022). Neprilysins regulate muscle contraction and heart function via cleavage of SERCA-inhibitory micropeptides. *Nature communications*, *13*(1):4420
- Schiemann, R., Lammers, K., Janz, M., Lohmann, J., Paululat, A., & Meyer, H. (2018). Identification and In Vivo Characterisation of Cardioactive Peptides in *Drosophila melanogaster*. *International journal of molecular sciences*, *20*(1), 2.
- Schmitt, J. P., Kamisago, M., Asahi, M., Li, G. H., Ahmad, F., Mende, U., Kranias, E. G., MacLennan, D. H., Seidman, J. G., & Seidman, C. E. (2003). Dilated cardiomyopathy and heart failure caused by a mutation in phospholamban. *Science (New York, N.Y.)*, *299*(5611), 1410–1413.
- Schnorrer, F., & Dickson, B. J. (2004). Muscle building; mechanisms of myotube guidance and attachment site selection. *Developmental cell*, *7*(1), 9–20.
- Schoofs, L., De Loof, A., & Van Hiel, M. B. (2017). Neuropeptides as Regulators of Behavior in Insects. *Annual review of entomology*, *62*, 35–52.
- Schweitzer, R., Zelzer, E., & Volk, T. (2010). Connecting muscles to tendons: tendons and musculoskeletal development in flies and vertebrates. *Development (Cambridge, England)*, *137*(17), 2807–2817.
- Schwinger, R. H., Münch, G., Bölck, B., Karczewski, P., Krause, E. G., & Erdmann, E. (1999). Reduced Ca²⁺-sensitivity of SERCA 2a in failing human myocardium due to reduced serin-16 phospholamban phosphorylation. *Journal of molecular and cellular cardiology*, *31*(3), 479–491.

- Scriven, D. R., Dan, P., & Moore, E. D. (2000). Distribution of proteins implicated in excitation-contraction coupling in rat ventricular myocytes. *Biophysical journal*, *79*(5), 2682–2691.
- Seiler, S., Wegener, A. D., Whang, D. D., Hathaway, D. R., & Jones, L. R. (1984). High molecular weight proteins in cardiac and skeletal muscle junctional sarcoplasmic reticulum vesicles bind calmodulin, are phosphorylated, and are degraded by Ca²⁺-activated protease. *The Journal of biological chemistry*, *259*(13), 8550–8557.
- Sellin, J., Albrecht, S., Kölsch, V., & Paululat, A. (2006). Dynamics of heart differentiation, visualized utilizing heart enhancer elements of the *Drosophila melanogaster* bHLH transcription factor Hand. *Gene expression patterns: GEP*, *6*(4), 360–375.
- Shafiq S. A. (1963). Electron microscopic studies on the indirect flight muscles of *Drosophila melanogaster*. II. Differentiation of myofibrils. *The Journal of cell biology*, *17*(2), 363–373.
- Shah, A. P., Nongthomba, U., Kelly Tanaka, K. K., Denton, M. L., Meadows, S. M., Bancroft, N., Molina, M. R., & Cripps, R. M. (2011). Cardiac remodeling in *Drosophila* arises from changes in actin gene expression and from a contribution of lymph gland-like cells to the heart musculature. *Mechanisms of development*, *128*(3-4), 222–233.
- Sharma, U., Cozier, G. E., Sturrock, E. D., & Acharya, K. R. (2020). Molecular Basis for Omapatrilat and Sampatrilat Binding to Neprilysin-Implications for Dual Inhibitor Design with Angiotensin-Converting Enzyme. *Journal of medicinal chemistry*, *63*(10), 5488–5500.
- Shattock, M. J., Ottolia, M., Bers, D. M., Blaustein, M. P., Boguslavskiy, A., Bossuyt, J., Bridge, J. H., Chen-Izu, Y., Clancy, C. E., Edwards, A., Goldhaber, J., Kaplan, J., Lingrel, J. B., Pavlovic, D., Philipson, K., Sipido, K. R., & Xie, Z. J. (2015). Na⁺/Ca²⁺ exchange and Na⁺/K⁺-ATPase in the heart. *The Journal of physiology*, *593*(6), 1361–1382.
- Simmerman, H. K., Collins, J. H., Theibert, J. L., Wegener, A. D., & Jones, L. R. (1986). Sequence analysis of phospholamban. Identification of phosphorylation sites and two major structural domains. *The Journal of biological chemistry*, *261*(28), 13333–13341.
- Simmerman, H. K., Kobayashi, Y. M., Autry, J. M., & Jones, L. R. (1996). A leucine zipper stabilizes the pentameric membrane domain of phospholamban and forms a coiled-coil pore structure. *The Journal of biological chemistry*, *271*(10), 5941–5946.
- Simon, M. I., Strathmann, M. P., & Gautam, N. (1991). Diversity of G proteins in signal transduction. *Science (New York, N.Y.)*, *252*(5007), 802–808.
- Singh, D. R., Dalton, M. P., Cho, E. E., Pribadi, M. P., Zak, T. J., Šeflová, J., Makarewich, C. A., Olson, E. N., & Robia, S. L. (2019). Newly Discovered Micropeptide Regulators of SERCA Form Oligomers but Bind to the Pump as Monomers. *Journal of molecular biology*, *431*(22), 4429–4443.
- Singh, J., Burrell, L. M., Cherif, M., Squire, I. B., Clark, A. L., & Lang, C. C. (2017). Sacubitril/valsartan: beyond natriuretic peptides. *Heart (British Cardiac Society)*, *103*(20), 1569–1577.
- Sitnik, J. L., Francis, C., Hens, K., Huybrechts, R., Wolfner, M. F., & Callaerts, P. (2014). Neprilysins: an evolutionarily conserved family of metalloproteases that play important roles in reproduction in *Drosophila*. *Genetics*, *196*(3), 781–797.

- Siviter, R. J., Coast, G. M., Winther, A. M., Nachman, R. J., Taylor, C. A., Shirras, A. D., Coates, D., Isaac, R. E., & Nässel, D. R. (2000). Expression and functional characterization of a *Drosophila* neuropeptide precursor with homology to mammalian preprotachykinin A. *The Journal of biological chemistry*, *275*(30), 23273–23280.
- Skidgel, R. A., Engelbrecht, S., Johnson, A. R., & Erdös, E. G. (1984). Hydrolysis of substance p and neurotensin by converting enzyme and neutral endopeptidase. *Peptides*, *5*(4), 769–776.
- Skou J. C. (1957). The influence of some cations on an adenosine triphosphatase from peripheral nerves. *Biochimica et biophysica acta*, *23*(2), 394–401.
- Slaidina, M., Delanoue, R., Gronke, S., Partridge, L., & Léopold, P. (2009). A *Drosophila* insulin-like peptide promotes growth during nonfeeding states. *Developmental cell*, *17*(6), 874–884.
- Sleiman, N. H., McFarland, T. P., Jones, L. R., & Cala, S. E. (2015). Transitions of protein traffic from cardiac ER to junctional SR. *Journal of molecular and cellular cardiology*, *81*, 34–45.
- Smith D. S. (1966). The structure of intersegmental muscle fibers in an insect, *Periplaneta americana* L. *The Journal of cell biology*, *29*(3), 449–459.
- Smith, I. C., Bombardier, E., Vigna, C., & Tupling, A. R. (2013). ATP consumption by sarcoplasmic reticulum Ca²⁺ pumps accounts for 40-50% of resting metabolic rate in mouse fast and slow twitch skeletal muscle. *PloS one*, *8*(7), e68924.
- Smith, Q. M., Inchingolo, A. V., Mihailescu, M. D., Dai, H., & Kad, N. M. (2021). Single-molecule imaging reveals the concerted release of myosin from regulated thin filaments. *eLife*, *10*, e69184.
- Smith, W. S., Broadbridge, R., East, J. M., & Lee, A. G. (2002). Sarcolipin uncouples hydrolysis of ATP from accumulation of Ca²⁺ by the Ca²⁺-ATPase of skeletal-muscle sarcoplasmic reticulum. *The Biochemical journal*, *361*(Pt 2), 277–286.
- Söderberg, J. A., Carlsson, M. A., & Nässel, D. R. (2012). Insulin-Producing Cells in the *Drosophila* Brain also Express Satiety-Inducing Cholecystokinin-Like Peptide, Drosulfakinin. *Frontiers in endocrinology*, *3*, 109.
- Soler, C., Laddada, L., & Jagla, K. (2016). Coordinated Development of Muscles and Tendon-Like Structures: Early Interactions in the *Drosophila* Leg. *Frontiers in physiology*, *7*, 22.
- Sørensen, T. L., Møller, J. V., & Nissen, P. (2004). Phosphoryl transfer and calcium ion occlusion in the calcium pump. *Science (New York, N.Y.)*, *304*(5677), 1672–1675.
- Sorkin, A., & von Zastrow, M. (2009). Endocytosis and signalling: intertwining molecular networks. *Nature reviews. Molecular cell biology*, *10*(9), 609–622.
- Sorrentino V. (2011). Sarcoplasmic reticulum: structural determinants and protein dynamics. *The international journal of biochemistry & cell biology*, *43*(8), 1075–1078.
- Spudich J. A. (2001). The myosin swinging cross-bridge model. *Nature reviews. Molecular cell biology*, *2*(5), 387–392.
- Stammers, A. N., Susser, S. E., Hamm, N. C., Hlynsky, M. W., Kimber, D. E., Kehler, D. S., & Duhamel, T. A. (2015). The regulation of sarco(endo)plasmic reticulum calcium-ATPases (SERCA). *Canadian journal of physiology and pharmacology*, *93*(10), 843–854.

- Staubli, F., Jorgensen, T. J., Cazzamali, G., Williamson, M., Lenz, C., Sondergaard, L., Roepstorff, P., & Grimmelikhuijzen, C. J. (2002). Molecular identification of the insect adipokinetic hormone receptors. *Proceedings of the National Academy of Sciences of the United States of America*, *99*(6), 3446–3451.
- Steenart, N. A., Ganim, J. R., Di Salvo, J., & Kranias, E. G. (1992). The phospholamban phosphatase associated with cardiac sarcoplasmic reticulum is a type 1 enzyme. *Archives of biochemistry and biophysics*, *293*(1), 17–24.
- Steiger G. J. (1971). Stretch activation and myogenic oscillation of isolated contractile structures of heart muscle. *Pflugers Archiv: European journal of physiology*, *330*(4), 347–361.
- Steinmetz, P. R., Kraus, J. E., Larroux, C., Hammel, J. U., Amon-Hassenzahl, A., Houliston, E., Wörheide, G., Nickel, M., Degnan, B. M., & Technau, U. (2012). Independent evolution of striated muscles in cnidarians and bilaterians. *Nature*, *487*(7406), 231–234.
- Stewart, T. A., Yapa, K. T., & Monteith, G. R. (2015). Altered calcium signaling in cancer cells. *Biochimica et biophysica acta*, *1848*(10 Pt B), 2502–2511.
- Stokes, D. L., Pomfret, A. J., Rice, W. J., Glaves, J. P., & Young, H. S. (2006). Interactions between Ca²⁺-ATPase and the pentameric form of phospholamban in two-dimensional co-crystals. *Biophysical journal*, *90*(11), 4213–4223.
- Stroik, D. R., Ceholski, D. K., Bidwell, P. A., Mleczko, J., Thanel, P. F., Kamdar, F., Autry, J. M., Cornea, R. L., & Thomas, D. D. (2020). Viral expression of a SERCA2a-activating PLB mutant improves calcium cycling and synchronicity in dilated cardiomyopathic hiPSC-CMs. *Journal of molecular and cellular cardiology*, *138*, 59–65.
- Sugita, Y., Miyashita, N., Yoda, T., Ikeguchi, M., & Toyoshima, C. (2006). Structural changes in the cytoplasmic domain of phospholamban by phosphorylation at Ser16: a molecular dynamics study. *Biochemistry*, *45*(39), 11752–11761.
- Sulbarán, G., Alamo, L., Pinto, A., Márquez, G., Méndez, F., Padrón, R., & Craig, R. (2015). An invertebrate smooth muscle with striated muscle myosin filaments. *Proceedings of the National Academy of Sciences of the United States of America*, *112*(42), E5660–E5668.
- Syme, D. A., & Josephson, R. K. (2002). How to build fast muscles: synchronous and asynchronous designs. *Integrative and comparative biology*, *42*(4), 762–770.
- Szegedi, C., Sárközi, S., Herzog, A., Jóna, I., & Varsányi, M. (1999). Calsequestrin: more than 'only' a luminal Ca²⁺ buffer inside the sarcoplasmic reticulum. *The Biochemical journal*, *337* (Pt 1)(Pt 1), 19–22.
- Tada, M., Kirchberger, M. A., & Katz, A. M. (1975). Phosphorylation of a 22,000-dalton component of the cardiac sarcoplasmic reticulum by adenosine 3':5'-monophosphate-dependent protein kinase. *The Journal of biological chemistry*, *250*(7), 2640–2647.
- Tada, M., Kirchberger, M. A., Repke, D. I., & Katz, A. M. (1974). The stimulation of calcium transport in cardiac sarcoplasmic reticulum by adenosine 3':5'-monophosphate-dependent protein kinase. *The Journal of biological chemistry*, *249*(19), 6174–6180.

- Taghli-Lamalle, O., Plantié, E., & Jagla, K. (2016). *Drosophila* in the Heart of Understanding Cardiac Diseases: Modeling Channelopathies and Cardiomyopathies in the Fruitfly. *Journal of cardiovascular development and disease*, 3(1), 7.
- Takekura, H., & Franzini-Armstrong, C. (2002). The structure of Ca²⁺ release units in arthropod body muscle indicates an indirect mechanism for excitation-contraction coupling. *Biophysical journal*, 83(5), 2742–2753.
- Takeshima H. (2002). Intracellular Ca²⁺ store in embryonic cardiac myocytes. *Frontiers in bioscience : a journal and virtual library*, 7, d1642–d1652.
- Takeshima, H., Komazaki, S., Nishi, M., Iino, M., & Kangawa, K. (2000). Junctophilins: a novel family of junctional membrane complex proteins. *Molecular cell*, 6(1), 11–22.
- Talla, E., de Mendonça, R. L., Degand, I., Goffeau, A., & Ghislain, M. (1998). Schistosoma mansoni Ca²⁺-ATPase SMA2 restores viability to yeast Ca²⁺-ATPase-deficient strains and functions in calcineurin-mediated Ca²⁺ tolerance. *The Journal of biological chemistry*, 273(43), 27831–27840.
- Tatar, M., Kopelman, A., Epstein, D., Tu, M. P., Yin, C. M., & Garofalo, R. S. (2001). A mutant *Drosophila* insulin receptor homolog that extends life-span and impairs neuroendocrine function. *Science (New York, N.Y.)*, 292(5514), 107–110.
- Taylor, M. V. (2006). Comparison of muscle development in *Drosophila* and vertebrates. In *Muscle development in Drosophila* (pp. 169-203). Springer, New York, NY.
- Teleman A. A. (2009). Molecular mechanisms of metabolic regulation by insulin in *Drosophila*. *The Biochemical journal*, 425(1), 13–26.
- Tennessen, J. M., Baker, K. D., Lam, G., Evans, J., & Thummel, C. S. (2011). The *Drosophila* estrogen-related receptor directs a metabolic switch that supports developmental growth. *Cell metabolism*, 13(2), 139–148.
- Tennessen, J. M., Bertagnolli, N. M., Evans, J., Sieber, M. H., Cox, J., & Thummel, C. S. (2014). Coordinated metabolic transitions during *Drosophila* embryogenesis and the onset of aerobic glycolysis. *G3 (Bethesda, Md.)*, 4(5), 839–850.
- Thierfelder, L., Watkins, H., MacRae, C., Lamas, R., McKenna, W., Vosberg, H. P., Seidman, J. G., & Seidman, C. E. (1994). Alpha-tropomyosin and cardiac troponin T mutations cause familial hypertrophic cardiomyopathy: a disease of the sarcomere. *Cell*, 77(5), 701–712.
- Thomas, D. D., Reddy, L. G., Karim, C. B., Li, M., Cornea, R., Autry, J. M., Jones, L. R., & Stamm, J. (1998). Direct spectroscopic detection of molecular dynamics and interactions of the calcium pump and phospholamban. *Annals of the New York Academy of Sciences*, 853, 186–194.
- Tian, L., Hires, S. A., Mao, T., Huber, D., Chiappe, M. E., Chalasani, S. H., Petreanu, L., Akerboom, J., McKinney, S. A., Schreiter, E. R., Bargmann, C. I., Jayaraman, V., Svoboda, K., & Looger, L. L. (2009). Imaging neural activity in worms, flies and mice with improved GCaMP calcium indicators. *Nature methods*, 6(12), 875–881.

- Tiraboschi, G., Jullian, N., They, V., Antonczak, S., Fournie-Zaluski, M. C., & Roques, B. P. (1999). A three-dimensional construction of the active site (region 507-749) of human neutral endopeptidase (EC.3.4.24.11). *Protein engineering*, *12*(2), 141–149.
- Titus, E. W., Deiter, F. H., Shi, C., Wojciak, J., Scheinman, M., Jura, N., & Deo, R. C. (2020). The structure of a calsequestrin filament reveals mechanisms of familial arrhythmia. *Nature structural & molecular biology*, *27*(12), 1142–1151.
- Toyoshima, C., & Cornelius, F. (2013). New crystal structures of PII-type ATPases: excitement continues. *Current opinion in structural biology*, *23*(4), 507–514.
- Toyoshima, C., & Nomura, H. (2002). Structural changes in the calcium pump accompanying the dissociation of calcium. *Nature*, *418*(6898), 605–611.
- Toyoshima, C., & Mizutani, T. (2004). Crystal structure of the calcium pump with a bound ATP analogue. *Nature*, *430*(6999), 529–535. <https://doi.org/10.1038/nature02680>
- Toyoshima, C., Asahi, M., Sugita, Y., Khanna, R., Tsuda, T., & MacLennan, D. H. (2003). Modeling of the inhibitory interaction of phospholamban with the Ca²⁺ ATPase. *Proceedings of the National Academy of Sciences of the United States of America*, *100*(2), 467–472.
- Toyoshima, C., Iwasawa, S., Ogawa, H., Hirata, A., Tsueda, J., & Inesi, G. (2013). Crystal structures of the calcium pump and sarcolipin in the Mg²⁺-bound E1 state. *Nature*, *495*(7440), 260–264.
- Toyoshima, C., Nakasako, M., Nomura, H., & Ogawa, H. (2000). Crystal structure of the calcium pump of sarcoplasmic reticulum at 2.6 Å resolution. *Nature*, *405*(6787), 647–655.
- Toyoshima, C., Nomura, H., & Tsuda, T. (2004). Lumenal gating mechanism revealed in calcium pump crystal structures with phosphate analogues. *Nature*, *432*(7015), 361–368.
- Toyoshima, C., Yonekura, S., Tsueda, J., & Iwasawa, S. (2011). Trinitrophenyl derivatives bind differently from parent adenine nucleotides to Ca²⁺-ATPase in the absence of Ca²⁺. *Proceedings of the National Academy of Sciences of the United States of America*, *108*(5), 1833–1838.
- Traaseth, N. J., Shi, L., Verardi, R., Mullen, D. G., Barany, G., & Veglia, G. (2009). Structure and topology of monomeric phospholamban in lipid membranes determined by a hybrid solution and solid-state NMR approach. *Proceedings of the National Academy of Sciences of the United States of America*, *106*(25), 10165–10170.
- Trejosiewicz, L. K., Malizia, G., Oakes, J., Losowsky, M. S., & Janossy, G. (1985). Expression of the common acute lymphoblastic leukaemia antigen (CALLA gp100) in the brush border of normal jejunum and jejunum of patients with coeliac disease. *Journal of clinical pathology*, *38*(9), 1002–1006. <https://doi.org/10.1136/jcp.38.9.1002>
- Treves, S., Jungbluth, H., Muntoni, F., & Zorzato, F. (2008). Congenital muscle disorders with cores: the ryanodine receptor calcium channel paradigm. *Current opinion in pharmacology*, *8*(3), 319–326.
- Trieber, C. A., Afara, M., & Young, H. S. (2009). Effects of phospholamban transmembrane mutants on the calcium affinity, maximal activity, and cooperativity of the sarcoplasmic reticulum calcium pump. *Biochemistry*, *48*(39), 9287–9296.

- Trieber, C. A., Douglas, J. L., Afara, M., & Young, H. S. (2005). The effects of mutation on the regulatory properties of phospholamban in co-reconstituted membranes. *Biochemistry*, *44*(9), 3289–3297.
- Tripathy, A., Xu, L., Mann, G., & Meissner, G. (1995). Calmodulin activation and inhibition of skeletal muscle Ca²⁺ release channel (ryanodine receptor). *Biophysical journal*, *69*(1), 106–119.
- Tsachaki, M., Birk, J., Egert, A., & Odermatt, A. (2015). Determination of the topology of endoplasmic reticulum membrane proteins using redox-sensitive green-fluorescence protein fusions. *Biochimica et biophysica acta*, *1853*(7), 1672–1682.
- Tsuda, M., Kobayashi, T., Matsuo, T., & Aigaki, T. (2010). Insulin-degrading enzyme antagonizes insulin-dependent tissue growth and Abeta-induced neurotoxicity in *Drosophila*. *FEBS letters*, *584*(13), 2916–2920.
- Turner, A. J., Isaac, R. E., & Coates, D. (2001). The neprilysin (NEP) family of zinc metalloendopeptidases: genomics and function. *BioEssays : news and reviews in molecular, cellular and developmental biology*, *23*(3), 261–269.
- Turrel, O., Lampin-Saint-Amaux, A., Pr eat, T., & Goguel, V. (2016). *Drosophila* Neprilysins Are Involved in Middle-Term and Long-Term Memory. *The Journal of neuroscience : the official journal of the Society for Neuroscience*, *36*(37), 9535–9546.
- Uemura, N., Ohkusa, T., Hamano, K., Nakagome, M., Hori, H., Shimizu, M., Matsuzaki, M., Mochizuki, S., Minamisawa, S., & Ishikawa, Y. (2004). Down-regulation of sarcolipin mRNA expression in chronic atrial fibrillation. *European journal of clinical investigation*, *34*(11), 723–730.
- Van Hiel, M. B., Vandersmissen, H. P., Proost, P., & Vanden Broeck, J. (2015). Cloning, constitutive activity and expression profiling of two receptors related to relaxin receptors in *Drosophila melanogaster*. *Peptides*, *68*, 83–90.
- van Tuyl, M., Blommaert, P. E., de Boer, P. A., Wert, S. E., Ruijter, J. M., Islam, S., Schnitzer, J., Ellison, A. R., Tibboel, D., Moorman, A. F., & Lamers, W. H. (2004). Prenatal exposure to thyroid hormone is necessary for normal postnatal development of murine heart and lungs. *Developmental biology*, *272*(1), 104–117.
- Vandecaetsbeek, I., Vangheluwe, P., Raeymaekers, L., Wuytack, F., & Vanoevelen, J. (2011). The Ca²⁺ pumps of the endoplasmic reticulum and Golgi apparatus. *Cold Spring Harbor perspectives in biology*, *3*(5), a004184.
- Vanden Broeck J. (2001). Neuropeptides and their precursors in the fruitfly, *Drosophila melanogaster*. *Peptides*, *22*(2), 241–254.
- Vangheluwe, P., Schuermans, M., Z ador, E., Waelkens, E., Raeymaekers, L., & Wuytack, F. (2005). Sarcolipin and phospholamban mRNA and protein expression in cardiac and skeletal muscle of different species. *The Biochemical journal*, *389*(Pt 1), 151–159.
- V aradi, A., Gilmore-Heber, M., & Benz, E. J., Jr (1989). Amplification of the phosphorylation site-ATP-binding site cDNA fragment of the Na⁺,K⁺-ATPase and the Ca²⁺-ATPase of *Drosophila melanogaster* by polymerase chain reaction. *FEBS letters*, *258*(2), 203–207.

- Veenstra J. A. (1989). Isolation and structure of corazonin, a cardioactive peptide from the American cockroach. *FEBS letters*, *250*(2), 231–234.
- Veenstra, J. A., & Ida, T. (2014). More Drosophila enteroendocrine peptides: Orcokinin B and the CCHamides 1 and 2. *Cell and tissue research*, *357*(3), 607–621.
- Veenstra, J. A., Agricola, H. J., & Sellami, A. (2008). Regulatory peptides in fruit fly midgut. *Cell and tissue research*, *334*(3), 499–516.
- Verardi, R., Shi, L., Traaseth, N. J., Walsh, N., & Veglia, G. (2011). Structural topology of phospholamban pentamer in lipid bilayers by a hybrid solution and solid-state NMR method. *Proceedings of the National Academy of Sciences of the United States of America*, *108*(22), 9101–9106.
- Verboomen, H., Wuytack, F., De Smedt, H., Himpens, B., & Casteels, R. (1992). Functional difference between SERCA2a and SERCA2b Ca²⁺ pumps and their modulation by phospholamban. *The Biochemical journal*, *286* (Pt 2)(Pt 2), 591–595.
- Verboomen, H., Wuytack, F., Van den Bosch, L., Mertens, L., & Casteels, R. (1994). The functional importance of the extreme C-terminal tail in the gene 2 organellar Ca(2+)-transport ATPase (SERCA2a/b). *The Biochemical journal*, *303* (Pt 3)(Pt 3), 979–984.
- Vibert, P., Craig, R., & Lehman, W. (1997). Steric-model for activation of muscle thin filaments. *Journal of molecular biology*, *266*(1), 8–14.
- Vigoreaux, J. O. (2006). Molecular basis of muscle structure. In *Muscle development in Drosophila* (pp. 143-156). Springer, New York, NY.
- Volk T. (1999). Singling out Drosophila tendon cells: a dialogue between two distinct cell types. *Trends in genetics : TIG*, *15*(11), 448–453.
- Volk, T., Wang, S., Rotstein, B., & Paululat, A. (2014). Matricellular proteins in development: perspectives from the Drosophila heart. *Matrix biology : journal of the International Society for Matrix Biology*, *37*, 162–166.
- Wahlquist, C., Jeong, D., Rojas-Muñoz, A., Kho, C., Lee, A., Mitsuyama, S., van Mil, A., Park, W. J., Sluijter, J. P., Doevendans, P. A., Hajjar, R. J., & Mercola, M. (2014). Inhibition of miR-25 improves cardiac contractility in the failing heart. *Nature*, *508*(7497), 531–535.
- Wang, Q., Paskevicius, T., Filbert, A., Qin, W., Kim, H. J., Chen, X. Z., Tang, J., Dacks, J. B., Agellon, L. B., & Michalak, M. (2020). Phylogenetic and biochemical analysis of calsequestrin structure and association of its variants with cardiac disorders. *Scientific reports*, *10*(1), 18115.
- Wang, S., Gopinath, T., Larsen, E. K., Weber, D. K., Walker, C., Uddigiri, V. R., Mote, K. R., Sahoo, S. K., Periasamy, M., & Veglia, G. (2021). Structural basis for sarcolipin's regulation of muscle thermogenesis by the sarcoplasmic reticulum Ca²⁺-ATPase. *Science advances*, *7*(48), eabi7154.
- Wang, W., Qiao, Y., & Li, Z. (2018). New Insights into Modes of GPCR Activation. *Trends in pharmacological sciences*, *39*(4), 367–386.
- Wang, Z., Grange, M., Wagner, T., Kho, A. L., Gautel, M., & Raunser, S. (2021). The molecular basis for sarcomere organization in vertebrate skeletal muscle. *Cell*, *184*(8), 2135–2150.e13.

- Waning, D. L., Mohammad, K. S., Reiken, S., Xie, W., Andersson, D. C., John, S., Chiechi, A., Wright, L. E., Umanskaya, A., Niewolna, M., Trivedi, T., Charkhzarrin, S., Khatiwada, P., Wronska, A., Haynes, A., Benassi, M. S., Witzmann, F. A., Zhen, G., Wang, X., Cao, X., ... Guise, T. A. (2015). Excess TGF- β mediates muscle weakness associated with bone metastases in mice. *Nature medicine*, *21*(11), 1262–1271.
- Wasserthal L. T. (2007). Drosophila flies combine periodic heartbeat reversal with a circulation in the anterior body mediated by a newly discovered anterior pair of ostial valves and 'venous' channels. *The Journal of experimental biology*, *210*(Pt 21), 3707–3719.
- Wawrzynow, A., Theibert, J. L., Murphy, C., Jona, I., Martonosi, A., & Collins, J. H. (1992). Sarcoplipin, the "proteolipid" of skeletal muscle sarcoplasmic reticulum, is a unique, amphipathic, 31-residue peptide. *Archives of biochemistry and biophysics*, *298*(2), 620–623.
- Weavers, H., Prieto-Sánchez, S., Grawe, F., Garcia-López, A., Artero, R., Wilsch-Bräuninger, M., Ruiz-Gómez, M., Skaer, H., & Denholm, B. (2009). The insect nephrocyte is a podocyte-like cell with a filtration slit diaphragm. *Nature*, *457*(7227), 322–326.
- Weber, A., & Herz, R. (1961). Requirement for calcium in the synaeresis of myofibrils. *Biochemical and Biophysical Research Communications*, *6*(5), 364–368.
- Weber, A., Herz, R., & Reiss, I. (1963). On the mechanism of the relaxing effect of fragmented sarcoplasmic reticulum. *The Journal of general physiology*, *46*(4), 679–702.
- Whyteside, A. R., & Turner, A. J. (2008). Human neprilysin-2 (NEP2) and NEP display distinct subcellular localisations and substrate preferences. *FEBS letters*, *582*(16), 2382–2386.
- Winther, A. M., Bublitz, M., Karlsen, J. L., Møller, J. V., Hansen, J. B., Nissen, P., & Buch-Pedersen, M. J. (2013). The sarcoplipin-bound calcium pump stabilizes calcium sites exposed to the cytoplasm. *Nature*, *495*(7440), 265–269.
- Wisløff, U., Loennechen, J. P., Currie, S., Smith, G. L., & Ellingsen, Ø. (2002). Aerobic exercise reduces cardiomyocyte hypertrophy and increases contractility, Ca²⁺ sensitivity and SERCA-2 in rat after myocardial infarction. *Cardiovascular research*, *54*(1), 162–174.
- Wittmann, T., Lohse, M. J., & Schmitt, J. P. (2015). Phospholamban pentamers attenuate PKA-dependent phosphorylation of monomers. *Journal of molecular and cellular cardiology*, *80*, 90–97.
- Woo, J. S., Jeong, S. Y., Park, J. H., Choi, J. H., & Lee, E. H. (2020). Calsequestrin: a well-known but curious protein in skeletal muscle. *Experimental & molecular medicine*, *52*(12), 1908–1925.
- Wray, S., & Burdyga, T. (2010). Sarcoplasmic reticulum function in smooth muscle. *Physiological reviews*, *90*(1), 113–178.
- Wu, K. D., Lee, W. S., Wey, J., Bungard, D., & Lytton, J. (1995). Localization and quantification of endoplasmic reticulum Ca(2+)-ATPase isoform transcripts. *The American journal of physiology*, *269*(3 Pt 1), C775–C784.
- Wu, M., & Sato, T. N. (2008). On the mechanics of cardiac function of Drosophila embryo. *PLoS one*, *3*(12), e4045.

- Wu, S., Liu, J., Reedy, M. C., Tregear, R. T., Winkler, H., Franzini-Armstrong, C., Sasaki, H., Lucaveche, C., Goldman, Y. E., Reedy, M. K., & Taylor, K. A. (2010). Electron tomography of cryofixed, isometrically contracting insect flight muscle reveals novel actin-myosin interactions. *PLoS one*, *5*(9), e12643.
- Wuytack, F., Papp, B., Verboomen, H., Raeymaekers, L., Dode, L., Bobe, R., Enouf, J., Bokkala, S., Authi, K. S., & Casteels, R. (1994). A sarco/endoplasmic reticulum Ca²⁺-ATPase 3-type Ca²⁺ pump is expressed in platelets, in lymphoid cells, and in mast cells. *The Journal of biological chemistry*, *269*(2), 1410–1416.
- Yabe, D., Nakamura, T., Kanazawa, N., Tashiro, K., & Honjo, T. (1997). Calumenin, a Ca²⁺-binding protein retained in the endoplasmic reticulum with a novel carboxyl-terminal sequence, HDEF. *The Journal of biological chemistry*, *272*(29), 18232–18239.
- Yang, C. H., Belawat, P., Hafen, E., Jan, L. Y., & Jan, Y. N. (2008). Drosophila egg-laying site selection as a system to study simple decision-making processes. *Science (New York, N.Y.)*, *319*(5870), 1679–1683.
- Yap, K. L., Kim, J., Truong, K., Sherman, M., Yuan, T., & Ikura, M. (2000). Calmodulin target database. *Journal of structural and functional genomics*, *1*(1), 8–14.
- Yoon, J. G., & Stay, B. (1995). Immunocytochemical localization of *Diploptera punctata* allatostatin-like peptide in *Drosophila melanogaster*. *The Journal of comparative neurology*, *363*(3), 475–488.
- Yurgel, M. E., Kakad, P., Zandawala, M., Nässel, D. R., Godenschwege, T. A., & Keene, A. C. (2019). A single pair of leucokinin neurons are modulated by feeding state and regulate sleep-metabolism interactions. *PLoS biology*, *17*(2), e2006409.
- Zaffran, S., Astier, M., Gratecos, D., Guillen, A., & Sémériva, M. (1995). Cellular interactions during heart morphogenesis in the *Drosophila* embryo. *Biology of the cell*, *84*(1-2), 13–24.
- Zalk, R., & Marks, A. R. (2017). Ca²⁺ Release Channels Join the 'Resolution Revolution'. *Trends in biochemical sciences*, *42*(7), 543–555.
- Zandawala, M., Yurgel, M. E., Texada, M. J., Liao, S., Rewitz, K. F., Keene, A. C., & Nässel, D. R. (2018). Modulation of *Drosophila* post-feeding physiology and behavior by the neuropeptide leucokinin. *PLoS genetics*, *14*(11), e1007767.
- Zarain-Herzberg, A., & Alvarez-Fernández, G. (2002). Sarco(endo)plasmic reticulum Ca²⁺-ATPase-2 gene: structure and transcriptional regulation of the human gene. *TheScientificWorldJournal*, *2*, 1469–1483.
- Zarain-Herzberg, A., García-Rivas, G., & Estrada-Avilés, R. (2014). Regulation of SERCA pumps expression in diabetes. *Cell calcium*, *56*(5), 302–310.
- Zarain-Herzberg, A., Marques, J., Sukovich, D., & Periasamy, M. (1994). Thyroid hormone receptor modulates the expression of the rabbit cardiac sarco (endo) plasmic reticulum Ca²⁺-ATPase gene. *The Journal of biological chemistry*, *269*(2), 1460–1467.
- Zeitouni, B., Sénatore, S., Séverac, D., Aknin, C., Sémériva, M., & Perrin, L. (2007). Signalling pathways involved in adult heart formation revealed by gene expression profiling in *Drosophila*. *PLoS genetics*, *3*(10), 1907–1921.

- Zhang, L., Kelley, J., Schmeisser, G., Kobayashi, Y. M., & Jones, L. R. (1997). Complex formation between junctin, triadin, calsequestrin, and the ryanodine receptor. Proteins of the cardiac junctional sarcoplasmic reticulum membrane. *The Journal of biological chemistry*, *272*(37), 23389–23397.
- Zhang, Y., Fujii, J., Phillips, M. S., Chen, H. S., Karpati, G., Yee, W. C., Schrank, B., Cornblath, D. R., Boylan, K. B., & MacLennan, D. H. (1995). Characterization of cDNA and genomic DNA encoding SERCA1, the Ca(2+)-ATPase of human fast-twitch skeletal muscle sarcoplasmic reticulum, and its elimination as a candidate gene for Brody disease. *Genomics*, *30*(3), 415–424.
- Zhao, G., Qiu, Y., Zhang, H. M., & Yang, D. (2019). Intercalated discs: cellular adhesion and signaling in heart health and diseases. *Heart failure reviews*, *24*(1), 115–132.
- Zheng, J., Yancey, D. M., Ahmed, M. I., Wei, C. C., Powell, P. C., Shanmugam, M., ... & Dell'Italia, L. J. (2014). Increased sarcolipin expression and adrenergic drive in humans with preserved left ventricular ejection fraction and chronic isolated mitral regurgitation. *Circulation: Heart Failure*, *7*(1), 194-202.
- Zwaal, R. R., Van Baelen, K., Groenen, J. T., van Geel, A., Rottiers, V., Kaletta, T., Dode, L., Raeymaekers, L., Wuytack, F., & Bogaert, T. (2001). The sarco-endoplasmic reticulum Ca²⁺ ATPase is required for development and muscle function in *Caenorhabditis elegans*. *The Journal of biological chemistry*, *276*(47), 43557–43563.

5 Appendix

5.1 Abbreviations

Å	Angstrom
aa	Amino acid
AC	Adenylyl cyclase
A-domain	Actuator domain
ADP	Adenosindiphosphat
AI	Arrhythmicity index
AKH	Adipokinetic hormone
AKHR	Adipokinetic hormone receptor
Akt/PKB	Protein kinase B
ALN	Another-regulin
AP	Action potential
APC	AKH producing cell
ARVD2	Arrhythmogenic right ventricular dysplasia type 2
AstA	Allatostatin A
ATP	Adenosintriphosphat
[Ca ²⁺]	Cytosolic Ca ²⁺ concentration
CALLA	Common acute lymphoblastic leukemia antigen
CaM	Calmodulin
CaMK	Ca ²⁺ -calmodulin-dependent protein kinase
CaMKII	Calcium/calmodulin-dependent protein kinase II
cAMP	Cyclic adenosine monophosphate
CaP60A	<i>Drosophila</i> SERCA
CASQ	Calsequestrin
CC	Corpora cardiaca
CCD	Central core disease
CICR	Calcium-induced calcium release
CNM	Centronuclear myopathy
CNP	C-type natriuretic peptide
CNS	Central nervous system
CPVT	Catecholaminergic polymorphic ventricular tachycardia
CRC	Ca ²⁺ release complex
CRU	Ca ²⁺ release unit
C-Terminus	Carboxy-Terminus
DAG	Diacylglycerol
DCM	Dilated cardiomyopathy
DH ₃₁	Diuretic hormone 31
DHPR	Dihydropyridin receptor
DI	Diastolic interval
DICR	Depolarization-induced Ca ²⁺ release
DILP	<i>Drosophila</i> insulin-like peptide
dInR	<i>Drosophila</i> insulin receptor
dLgr3	<i>Drosophila</i> Leucine-rich repeat-containing G protein-coupled receptor 3
DLM	Dorsal longitudinal muscles
DNA	Desoxyribonukleinsäure
DVM	Dorsoventral muscles
DWORF	Dwarf open reading frame
e.g.	For example
ECC	Excitation-contraction coupling

ECD	Extracellular domain
ECM	Extracellular matrix
ELN	Endoregulin
EM	Electron microscopy
ER	Endoplasmic reticulum
ERK	Extracellular signal-regulated kinase
<i>et al.</i>	And others
FS	Fractional shortening
G protein	Guanine nucleotide-binding protein
GDP	Guanosine diphosphate
GFP	Green fluorescent protein
Golgi	Golgi apparatus
GPCR	G protein-coupled receptor
GTP	Guanosine triphosphate
HA	Hemagglutinin
HAX-1	HS-1 associated protein X-1
HR	Heart rate
HF	Heart failure
HRC	Histidine-rich calcium-binding protein
Hsp20	Heat shock protein 20
i.a.	inter alia
I-1	Inhibitor-1
ICD	Intracellular domain
IDE	Insulin degrading enzyme
IFMs	Indirect flight muscle
IGF	Insulin-like growth factor
IIS	Insulin and insulin-like growth factor signaling
Ins(1,4,5)P3	Inositol-1,4,5-trisphosphate
IP ₃ R	Inositol 1, 4, 5-trisphosphate receptor
IPC	Insulin-producing cell
JP45	Junctophilin
jSR	Junctional sarcoplasmic reticulum
K _{Ca}	Affinity for calcium
L-SR	Longitudinal sarcoplasmic reticulum
LSM	Laser scanning microscopy
LTCC	L-type calcium channels
MAPK	mitogen-activated protein kinase
MH	Malignant hyperthermia
MLCK	Myosin light-chain kinase
MLN	Myoregulin
MmD	Multi-minicore disease
MME	Membrane metalloendopeptidase
MTJs	Myotendinous junctions
Na ⁺ /K ⁺ -ATPase	Sodium-potassium ATPase
nAChRs	Nicotinic acetylcholine receptors
NAD	Nicotinamide adenine dinucleotide
NCX	Na ⁺ /Ca ²⁺ exchanger
N-domain	Nucleotide-binding domain
NE	Noradrenaline
Nep	Neprilysin
NEP	Neutral endopeptidase
Nep4	Neprilysin 4
NEST	Nuclear envelope biosynthesis pathway
NH ₂	Amide group
NMJ	Neuromuscular junctions
NMR	Nuclear magnetic resonance

NPF	Neuropeptide F
N-Terminus	Amino-Terminus
PDB	Protein Data Bank
PDF	Pigment Dispersing Factor
Pi	Inorganic phosphate
PI3K	Phosphatidylinositol-3-kinase
PKA	Protein kinase A
PKB/Akt	Protein kinase B
PLC β	Phospholipase C β
PLN	Phospholamban
PMCA	Plasma membrane Ca ²⁺ ATPase
PP1	Protein phosphatase 1
PP2Ce	Protein phosphatase 2Ce
PtdIns(4,5)P2	Phosphatidylinositol-4,5-bisphosphate
PTM	Post-translational modification
qRT-PCR	Quantitative reverse transcription PCR
Rho	Rho GTPase
RhoGEF	Rho guanine nucleotide exchange factor protein
RNA	Ribonucleic acid
RyR	Ryanodine receptor
RyR1-RM	RyR1-related myopathies
SA	Stretch activation
SCL	Sarcolamban
SCLA	Sarcolamban A
SCLB	Sarcolamban B
S-domain	Support domain
SERCA	Sarco/endoplasmic reticulum Ca ²⁺ ATPase
smORF/sORF	Small open reading frames
sNPF	Short neuropeptide F
SOHA	Semi-automatic optical heartbeat analysis
SR	Sarcoplasmic reticulum
STED microscopy	Stimulated emission depletion microscopy
SUMO-1	Small ubiquitin-related modifier
SI	Systolic interlal
T-domain	Transport domain
TM	Transmembrane
TMD	Transmembrane Domain
Tn-C	Troponin receptor subunit
Tn-I	Troponin inhibitory subunit
Tn-T	Troponin tropomyosin-binding/thin filament-anchoring troponin subunits
TOR	Target of rapamycin
TRITC	Tetramethylrhodamine
T-tubule	Transverse tubule
UPD2	Unpaired-2
VGCC	Voltage-gated calcium channel
VLM	Ventral longitudinal muscles
V _{max}	Maximal activity
X-ray	X-radiation

5.2 Proteinogenic amino acids and SI units

SI units:

Symbol	Name	SI prefix
M	Mega	10^6
k	Kilo	10^3
h	Hekto	10^2
da	Deka	10^1
d	Dezi	10^{-1}
c	Zenti	10^{-2}
m	Milli	10^{-3}
μ	Mikro	10^{-6}
n	Nano	10^{-9}
p	Piko	10^{-12}
f	Femto	10^{-15}

Proteinogenic amino acids:

Amino acid	Abbreviaton	
	Three letter code	One letter code
Alanin	Ala	A
Arginin	Arg	R
Asparagin	Asn	N
Aspartat	Asp	D
Cystein	Cys	C
Glutamat	Glu	E
Glutamin	Gln	Q
Glycin	Gly	G
Histidin	His	H
Isoleucin	Ile	I
Leucin	Leu	L
Lysin	Lys	K
Methionin	Met	M
Phenylalanin	Phe	F
Prolin	Pro	P
Serin	Ser	S
Threonin	Thr	T
Tryptophan	Trp	W
Tyrosin	Tyr	Y
Valin	Val	V

5.3 Index of figures and tables

Index of figures:

Figure	Title	Page
1	Maturation and processing of neuropeptides and peptide hormones	5
2	GPCR-dependent activation of intracellular signaling pathways	7
3	Factors regulating <i>dilp</i> expression at the IPCs of <i>Drosophila</i> larvae	10
4	The extracellular domain of human NEP is critical for catalytic activity	12
5	Nep4A exhibits a dual subcellular localization in <i>Drosophila</i> muscles	14
6	The sarcomere is the basic contractile unit of muscles	16
7	Muscle tissues present in <i>Drosophila</i>	18
8	Ca ²⁺ cycling in vertebrate cardiomyocytes	22
9	Sarcomere shortening is Ca ²⁺ - and ATP-dependent	24
10	Triadic junctions of skeletal muscles	28
11	The sarcoplasmic reticulum is subdivided into junctional and longitudinal domains	29
12	Functional domains of SERCA	31
13	Catalytic mechanism of SERCA-mediated Ca ²⁺ transport	32
14	Comparison of SERCA-inhibitory peptides	38
15	Phospholamban is phosphorylated through the β -adrenergic pathway	40
16	Interaction of SLN and SERCA	42
17	Comparison of SERCA-modulating effects exerted by PLN and SLN	43
18	Insect SCL peptides modulate muscle contraction by inhibiting SERCA activity	46
19	Tissue-dependent subcellular localization of Nep4 is related to distinct functionalities of the enzyme	146
20	Nepriylsins hydrolyze SERCA-inhibitory peptides	157
21	Working model of Nep4-dependent regulation of muscle and heart contraction	160

Index of tables:

Table	Title	Page
1	SERCA genes and isoforms present in vertebrates	34
2	Identified Nep4 <i>in vitro</i> substrates implicated in insulin signaling and the regulation of food intake	149
3	<i>In vitro</i> effects of peptide application on different heart parameters	153

5.4 Publications

Hallier, B., Schiemann, R., Cordes, E., Vitos-Faleato, J., Walter, S., Heinisch, J. J., Malmendal, A., Paululat, A., and Meyer, H. (2016). *Drosophila* neprilysins control insulin signaling and food intake via cleavage of regulatory peptides. *eLife*, 5, e19430. doi: 10.7554/eLife.19430. PMID: 27919317; PMCID: PMC5140268.

Schiemann, R., Lammers, K., Janz, M., Lohmann, J., Paululat, A., and Meyer, H. (2018). Identification and In Vivo Characterisation of Cardioactive Peptides in *Drosophila melanogaster*. *International journal of molecular sciences*, 20(1), 2. doi: 10.3390/ijms20010002. PMID: 30577424; PMCID: PMC6337577.

Meyer, H., Buhr, A., Callaerts, P., Schiemann, R., Wolfner, M. F., and Marygold, S. J. (2021). Identification and bioinformatic analysis of neprilysin and neprilysin-like metalloendopeptidases in *Drosophila melanogaster*. *microPublication biology*, vol 2021. doi: 10.17912/micropub.biology.000410. PMID: 34189422; PMCID: PMC8223033.

Accepted manuscripts:

Schiemann, R. and Meyer, H. (2022). Neprilysin 4. Chapter in „Rawlings - Vol. 1 - Handbook of Proteolytic Enzymes: Metallopeptidases, 4th Edition”, ISBN: 9780128235874

Santalla, M., García, A., Schiemann, R., Paululat, A., Mattiazzi, A., Valverde, C., Hernández, G., Meyer, H., Ferrero, P. Interplay between SERCA, 4E-BP and eIF4-E in the *Drosophila* heart (Accepted for publication in PLOS ONE)

Manuscripts in revision:

Schiemann, R., Buhr, A., Cordes, E., Walter, S., Heinisch, J. J., Ferrero, P., Milting, H., Paululat, A., and Meyer, H. Neprilysins regulate muscle contraction and heart function via cleavage of SERCA-inhibitory micropeptides. (Manuscript in revision at Nature communications)

Updated status 29.07.22: The revised and adapted manuscript was published by Nature communications:

Schiemann, R., Buhr, A., Cordes, E., Walter, S., Heinisch, J. J., Ferrero, P., Milting, H., Paululat, A., and Meyer, H. (2022). Neprilysins regulate muscle contraction and heart function via cleavage of SERCA-inhibitory micropeptides. *Nature communications*, 13(1):4420. doi: 10.1038/s41467-022-31974-1. PMID: 35906206; PMCID: PMC9338278.

5.5 Overview of work contributions

Publication/ Manuscript	Figure/ Table	Contribution
2.1, Hallier et al., 2016	General	Acquisition of data, analysis and interpretation of data, drafting and revising the article
	Figure 1	Acquisition of data (together with Benjamin Hallier)
	Figure 7	Acquisition of data, analysis and interpretation of data, drafting of the figure
	Table 1	Acquisition of data, analysis and interpretation of data, drafting of the table
2.2, Schiemann et al., 2018	General	Conceiving and design of experiments, acquisition of data, analysis of data, drafting and revising the article
	Figure 1	Acquisition of data (together with Maren Janz and Jana Lohmann), analysis and interpretation of data, drafting of the figure
	Figure 2	Acquisition of data (together with Maren Janz), analysis and interpretation of data, drafting of the figure
	Figure 3	Acquisition of data (together with Maren Janz and Jana Lohmann), analysis and interpretation of data, drafting of the figure
	Figure 4	Acquisition of data (together with Maren Janz and Jana Lohmann), analysis and interpretation of data, drafting of the figure
	Figure 5	Acquisition of data (together with Kay Lammers), analysis and interpretation of data, drafting of the figure
	Table 1	Acquisition of data (together with Maren Janz and Jana Lohmann), analysis and interpretation of data, drafting of the table
	Table 2	Drafting of the table
	Table S1	Acquisition of data (together with Maren Janz and Jana Lohmann), analysis and interpretation of data, drafting of the table
	Table S2	Acquisition of data (together with Kay Lammers), analysis and interpretation of data, drafting of the table
2.3, Schiemann and Meyer, 2022	General	Analysis and interpretation of data, drafting and revising the article
	Figure 1	Drafting of the figure
	Table 1	Acquisition of data (data are partially derived from Meyer et al., 2009), analysis and interpretation of data, drafting of the table
	Table 2	Drafting of the table
2.4, Schiemann et al.	General	Acquisition of data, analysis and interpretation of data, drafting and revising the article
	Figure 1	Acquisition of data (A-D: together with Mirko Hüsken; E-F: together with Marc Hellmann), analysis and interpretation of data, drafting of the figure
	Figure 2	A-D: Analysis and interpretation of data, drafting of the figure E: Acquisition of data, analysis and interpretation of data, drafting of the figure
	Figure 3	I: Acquisition of data, analysis and interpretation of data, drafting of the figure
	Figure 4	A-B: Acquisition of data, analysis and interpretation of data, drafting of the figure C-D: Sample preparation

	Figure 5	Acquisition of data, analysis and interpretation of data, drafting of the figure
	Figure 7	Drafting of the figure
	Figure S2	Acquisition of data, analysis and interpretation of data, drafting of the figure
	Figure S3	Acquisition of data, analysis and interpretation of data, drafting of the figure
	Figure S4	Acquisition of data (together with Michael Stuke), analysis and interpretation of data, drafting of the figure
	Figure S5	Acquisition of data, analysis and interpretation of data, drafting of the figure
	Figure S8	Acquisition of data (sample preparation was partially done by Sandra Ratnavadivel), analysis and interpretation of data, drafting of the figure
	Figure S9	Acquisition of data, analysis and interpretation of data, drafting of the figure
	Table S1	Acquisition of data, analysis and interpretation of data, drafting of the table
	Table S2	Analysis and interpretation of data, drafting of the table

5.6 Fellowships and awards

Awards:

09.03.2017: Hans Mühlhoff-Förderpreis 2017

Fellowships:

01.02.2017-31.01.2017: PhD Fellowship granted by the “Integrated research training group” (IRTG) of the SFB944, Osnabrück University

01.12.2017-30.06.2019 Fellow of the Hans Mühlhoff-Stiftung Osnabrück

6 DVD index

Folder/File	File name	Description
PhD Thesis Ronja Schiemann	PhD Thesis Ronja Thea Schiemann	PDF file of this thesis
Publications	Hallier et al 2016	PDF file of (2.1, Hallier et al., 2016)
	Schiemann et al 2018	PDF file of (2.2, Schiemann et al., 2018)
	Schiemann and Meyer 2022	PDF file of (2.3, Schiemann and Meyer, 2022)
	Meyer et al. 2021	PDF file
	Schiemann et al manuscript	PDF file of (2.4, Schiemann et al.)
	Santalla et al manuscript	PDF file
Supplementary data Schiemann et al 2018	Figure S1	TIF file
	Table S1	Excel file
	Table S2	Excel file
Supplementary data Schiemann et al manuscript	Supplementary data Schiemann et al manuscript	PDF file
	Supplementary Video 1	AVI file
	Supplementary Video 2	AVI file
	Supplementary Video 3	AVI file
	Supplementary Video 4	AVI file
Figures Thesis Ronja Schiemann	Figures 1-21	TIF files
Tables Thesis Ronja Schiemann	Tables 1-3	PDF files

7 Curriculum vitae

Name Ronja Thea Schiemann
Date of birth 15.05.1990
Place of birth Hamburg

Academic education

05/2015-04/2022 Ph.D. student at the division of Zoology/Developmental Biology under the supervision of Dr. Heiko Harten

12/2014 **Master's degree (M.Sc.)**
Date of examination: 08.12.2014; Grade: 1.2
Master's Thesis at the Department of Zoology/Developmental Biology, Osnabrück University, under the supervision of Dr. Heiko Harten

10/2012-12/2014 Master studies at Osnabrück University
Study course: Biosciences with specialization in cell- and molecular biology

10/2012 **Bachelor's degree (B.Sc.)**
Date of examination: 05.10.2012; Grade: 2,0
Bachelor's Thesis at the Department of Developmental Biology, Hamburg University, under the supervision of Dr. René Lorbiecke

10/2008-10/2012 Bachelor studies at Hamburg University
Study course: Biology

School education

06/2008 **General qualification for university entrance**
Date of examination: 30.06.2008
Abitur at the Lessing-Gymnasium Hamburg-Harburg

2002-2008 Lessing -Gymnasium Hamburg-Harburg

8 Erklärung über die Eigenständigkeit der erbrachten wissenschaftlichen Leistung

Ich erkläre hiermit, dass ich die vorliegende Arbeit ohne unzulässige Hilfe Dritter und ohne Benutzung anderer als der angegebenen Hilfsmittel angefertigt habe. Die aus anderen Quellen direkt oder indirekt übernommenen Daten und Konzepte sind unter Angabe der Quelle gekennzeichnet. Bei der Auswahl und Auswertung folgenden Materials haben mir die nachstehend aufgeführten Personen in der jeweils beschriebenen Weise entgeltlich / unentgeltlich geholfen.

- Dr. Benjamin Hallier bei der Durchführung der Experimente für Abbildung 1 in (2.1, Hallier et al., 2016).
- Dr. Stefan Walter (Universität Osnabrück) bei der Durchführung von massenspektrometrischen Messungen für (2.1, Hallier et al., 2016) und (2.4, Schiemann et al.).
- Dr. Paola Ferrero (Universität La Plata, Argentinien) für die Zurverfügungstellung der Rohdaten für die Abbildung 2A-D in (2.4, Schiemann et al.).
- Kay Lammers bei der Durchführung der *in vivo* Herzmessungen für die Abbildung 5 in (2.2, Schiemann et al., 2018).
- Maren Janz bei der Durchführung der *in vitro* Herzmessungen für die Abbildungen 1-4 in (2.4, Schiemann et al. 2018) im Rahmen ihrer Masterarbeit.
- Jana Lohmann bei der Durchführung der *in vitro* Herzmessungen für die Abbildungen 1, 3 und 4 in (2.2, Schiemann et al. 2018) im Rahmen ihrer Masterarbeit.
- Michael Stuke bei der Erstellung der UAS-Nep4::roGFP und UAS-roGFP-Konstrukte verwendet in der Abbildung S4 in (2.4, Schiemann et al.) im Rahmen seiner Masterarbeit.
- Marc Hellmann bei der Durchführung der larvalen crawling assays für die Abbildung 1E-F in (2.4, Schiemann et al.) im Rahmen seiner Masterarbeit.
- Dr. Mirko Hüsken bei der Durchführung der *in vitro* Herzmessungen für die Abbildungen 1A-D in (2.4, Schiemann et al. 2018) im Rahmen seiner Dissertation
- Sandra Ratnavadivel (Herz- und Diabeteszentrum NRW, Bad Oeynhausen) Bad Oeynhausen) für die Bereitstellung und Vorbereitung der Herzgewebeproben für die Abbildung S8 in (2.4, Schiemann et al.) im Rahmen ihrer Dissertation

Weitere Personen waren an der inhaltlichen materiellen Erstellung der vorliegenden Arbeit nicht beteiligt. Insbesondere habe ich hierfür nicht die entgeltliche Hilfe von

Vermittlungs- bzw. Beratungsdiensten (Promotionsberater oder andere Personen) in Anspruch genommen. Niemand hat von mir unmittelbar oder mittelbar geldwerte Leistungen für Arbeiten erhalten, die im Zusammenhang mit dem Inhalt der vorgelegten Dissertation stehen.

Die Arbeit wurde bisher weder im In- noch im Ausland in gleicher oder ähnlicher Form einer anderen Prüfungsbehörde vorgelegt.

Osnabrück, 6. October 2022

(Ort, Datum)

(Unterschrift)

9 Erklärung über frühere etwaige Promotionsversuche

gem. § 8 Abs. 2 Buchstabe g der Promotionsordnung der Fachbereiche Physik, Biologie/Chemie und Mathematik/Informatik der Universität Osnabrück

Hiermit bestätige ich, dass die vorzulegende Dissertation bisher weder im In- noch im Ausland in gleicher oder ähnlicher Form einer anderen Prüfungsbehörde vorgelegt wurde.

Ort, Datum

Unterschrift

10 Danksagung

Zuerst möchte ich an dieser Stelle meinem Erstprüfer und Doktorvater Dr. Heiko Harten für die großartige Betreuung während meiner Promotionszeit bedanken. Es war toll, an einem so spannenden Projekt arbeiten zu dürfen und ich werde diese Zeit sehr vermissen. Egal, mit welchen wissenschaftlichen Problemen ich ihn aufgesucht habe, ich habe sein Büro immer zuversichtlich, und mit neuen Denkanstößen versehen, verlassen. Prof. Dr. Achim Paululat möchte ich einerseits für die Übernahme des Zweitgutachtens danken, darüber hinaus natürlich auch für die Aufnahme in die Arbeitsgruppe. Die vielen Gespräche auch zum wissenschaftlichen “Drumherum” waren eine Bereicherung. Dr. Stefan Walter gilt mein Dank sowohl für die Bereiterklärung, Teil meiner Prüfungskommission zu sein, als auch für die Betreuung und Beratung bei der Durchführung der massenspektrometrischen Experimente.

Desweiteren danke ich Herrn Prof. Dr. Hendrik Milting für die Bereitschaft, meiner Prüfungskommission anzugehören.

Natürlich gilt mein Dankeschön der gesamten Arbeitsgruppe Zoologie/Entwicklungsbiologie, die mir ein wunderbares Arbeitsumfeld geboten hat. Ich danke Martina Biedermann, Mechthild Krabusch, Eva Cordes, Werner Mangerich und Kerstin Etzold für all die Unterstützung, die ich erfahren durfte. Lydia Reckers gebührt mein Dank für die ganze organisatorische Hilfe. Ob als Sekretärin unserer Arbeitsgruppe, oder als Ansprechpartnerin im SFB-Büro, auf ihre tatkräftige Unterstützung konnte ich mich immer verlassen. Ich möchte außerdem den von mir betreuten Studenten Maren Janz, Michael Stuke, Jana Lohmann, Franziska Schweitzer und Marc Hellmann für ihren Einsatz und ihre Mitarbeit am Neprilysin-Projekt danken. Ein ganz besonderer Dank gilt der “alten” Doktorandengarde. Benni, Lena, Kay und Nena, unsere gemeinsame Zeit bedeutet mir unglaublich viel und die Eindrücke der vielen Erlebnisse, die wir auch abseits der Uni miteinander teilen durften, sind für mich nicht in Worte zu fassen. Es macht mich glücklich, euch während unserer gemeinsamen Zeit in der Zoologie als Freunde gewonnen zu haben.

Natürlich möchte ich auch der “neuen” Generation danken. Marcel, Maren, Nora, Annika, Christian, und Jonas, es war schön mit euch zusammenzuarbeiten. Ein großes Dankeschön geht an Annika Buhr, die mit mir das Neprilysin-Projekt weiterverfolgt hat und hoffentlich noch den einen oder anderen Durchbruch erzielen wird!

Zu guter Letzt möchte ich mich noch einmal insbesondere bei Maren und Lena für ihre Freundschaft und ihren Rückhalt in einer für mich manchmal nicht ganz einfachen Zeit bedanken: Danke!